INCORPORATION OF ZWITTERIONIC MONOMERS INTO WATERBORNE POLYMER DISPERSIONS

SUMI MURALI NAIR

SUPERVISORS: PROF. RADMILA TOMOVSKA

DR. AMAIA AGIRRE

Chemical Engineering Group

University of the Basque Country UPV/EHU

Donostia-San Sebastian

2023

Amma, Achan, Chechi

Acknowledgements

Let's face it, the acknowledgment section is the part everyone flips to first, even before checking out the fancy title of this PhD. This PhD might have turned me into a bona fide scientist and a chemistry witch (or at least, I hope it did!), it also had its say who I am today therefore, it's only fair to extend my heartfelt gratitude to the wonderful people who've left their mark during these research years and helped shape the person I am now. Thank you all sincerely!

My supervisors, Radmila Tomovska and Amaia Agirre, have my heartfelt gratitude for granting me the opportunity to pursue this PhD. Their enduring patience, unwavering guidance, and steadfast support have been the pillars upon which this work stands. I am genuinely thankful for their belief in me and this endeavor. Prof Radmila, I consider myself incredibly fortunate to have had the privilege of undertaking this journey under your exceptional mentorship. Your open-door policy for discussions, your willingness to make time for me even in the busiest of days, and your ability to balance kindness and firmness have left an indelible mark on my journey. Amaia, you have taught me more than just the methods of conducting experiments or the intricacies of research. Over these four years, you have been a consistent source of support in this thesis. Your continuous presence in the lab provided a great sense of reassurance and your availability anytime for questions and guidance has made a world of difference. I have taken away not just academic knowledge but also valuable life lessons from both of you, and I genuinely thank you from the depths of my heart. Ви благодарам многу, eskerrik asko.

I would like to take a moment to extend my gratitude to the other professors in the group —Txema, María, Joserra, Nick, Your willingness to share your knowledge, engage in enlightening scientific

discussions, and offer assistance whenever needed has been invaluable and a big shout-out to Inés for being incredibly nice and kind – you're a true gem!

I would like to offer my sincere thanks to the collaborative efforts of Professor Thomas Schaefer's group. Their contribution has been invaluable. I am also grateful to Dr. Lourdes Irusta and Alba González for their technical support in FT-IR and permeability measurements. Additionally, I extend my appreciation to Sgiker Services, Maite Miranda, and Dr. Ana Martínez for providing TEM images, and to Dr. Loli Martin for the AFM images. Your assistance has been instrumental in this research journey.

I would like to express my deep appreciation to Dr. Odair Araujo and Dr. Jorge Moniz for their generous offer that allowed me to commence an internship journey at Synthomer. Additionally, I extend my gratitude to the other outstanding members of the company, particularly Rita and Artur, for their invaluable support in the paint application laboratory. Rui, my breakfast buddy, those quiet morning chats were a soothing start to the day and Jaime, my Sintra-sidekick, you're a lifesaver for giving me a roof over my head. Our daily journeys to the company, where we spun our conversations in a delightful blend of Portuguese and Spanglish, were an absolute hoot! I genuinely enjoyed every moment. Muito obrigado to all of you awesome folks!

To my polymat comrades, those who are still around and to those who have moved on to new adventures, thank you for being part of my journey. I deeply value the memories we have shared. Whether it's our coffee gatherings, night outs, adventurous expeditions, each experience has been truly special. Thank you for being a part of my journey. Hanging out with you lot is like a constant reminder to stay healthy and active.

I also wish to express my gratitude for the financial support provided by the Industrial Liaison Program in Polymerization in Dispersed Media.

I want to pour out my gratitude to my friends, whether they are close enough for a high-five or far away enough for a virtual hug and they definitely know who they are. In moments of joy and in times of need, you have been there with comforting words, understanding smiles, and a listening ear.

To my friends who are just a stone's throw away, You all are like my personal heart compass – always pointing me in the direction of caffeine emergencies or an impromptu "let's hang out ASAP" moment, especially if it means feasting on something delicious together. Thanks for being my partners in adventure, culinary escapades, and for patiently listening to and bearing with me, all while offering the most hilariously unconventional yet well-intentioned wisdom.

To my long distance pals, I owe my sanity to your insane calls, outrageous antics, and chali sessions (a must-see in the Malayalam urban dictionary) that could rival any live stand-up comedy act have been a constant source of joy. Our virtual gatherings felt like a weekly prescription for comedy therapy, and I am certain we have set our own records for the most snorts induced by laughter during a call. Thank you!

I owe an immeasurable debt of gratitude to my parents and sister. They are the very foundation upon which my life has been built, the nurturing roots that have allowed me to grow and flourish.

Closing with a touch of Snoop Dogg's style, I would like to give a shout-out to myself, showin' some self-love and appreciation.

Sumi

Table of Contents

Chapter 1. Introduction

While nature and human progress intertwine on our planet, there is always a need of exploration and discovery. Within this world of investigation, we delve in the field of waterborne polymers for coating application, one of the important topics that holds the key to more environmental polymer materials. Therefore, the adoption of waterborne coatings by producers and consumers reflects a commitment to preserve our planet.

The global coatings market has remarkable growth, reaching a value of USD 146.54 billion in 2018 and projected to expand to USD 236.11 billion by 2026.[1] This substantial market size underscores the significant demand and economic impact of coatings across various industries. Traditionally, coatings have been predominantly available as solutions in organic solvents.[2,3] However, in recent years; there has been a notable shift towards waterborne coatings. While solvent borne coatings often offer superior mechanical and water resistance properties, emit considerable amounts of volatile organic compounds (VOCs), such as acetone, ethyl acetate, and aliphatic hydrocarbons. These VOCs not only possess strong odors and toxicity, but also contribute to the greenhouse effect, exacerbating global warming. Consequently, governmental regulations have become more stringent in terms of VOC emissions.[4,5]

In response to these environmental concerns, the coatings industry has explored greener alternatives, leading to the increased popularity of waterborne coatings. Waterborne coatings use water as the continuous phase, resulting in formulations with lower VOC content or even VOC free formulations. This shift towards waterborne coatings offers several advantages, including reduced costs, easier handling and safer processes. The demand for waterborne coatings has particularly surged in sectors such as automotive, construction, and furniture, driven by the increasing need for eco-friendly and low-toxicity alternatives.

Emulsion polymerization stands as the predominant technique for the production of waterborne polymers where the product is a polymer particle in size from 50 to 1000 nanometers dispersion, also known as latex.[6] This process is highly versatile and offers several advantages over other polymerization techniques, including the ability to produce polymers with well-defined particle size and morphology, high molar mass, and uniformity owing to radical compartmentalization possibility during monomer polymerization within the polymer particles.[7, 8]

Emulsion polymerization is an heterogeneous free-radical polymerization process and a typical recipe usually includes monomers (50 – 55 wt%), deionized water (45 wt%), initiators (0.5 wt% based on monomers-wbm) and surfactants (0.5 – 3% wbm) but additional components such as, crosslinking agents (0 – 0.5% wbm) and chain transfer agents (0 – 1 wt% wbm) may be presented, depending on the desired properties. At the beginning of the process, the monomers are dispersed in an aqueous solution of surfactant above the critical micellar concentration (cmc). Due to the excess of surfactant employed, some of the surfactant is adsorbed on the monomer droplets, stabilizing them and the rest forms aggregates (micelles) in the aqueous media. Such emulsion is made of large monomer droplets (1-10 μm) and the mentioned micelles, which due to hydrophobic core are monomer swollen. The polymerization starts in such system after heating at reaction temperature and addition of suitable initiator. The process can be performed either in batch, where all the components are mixed and enclosed in the reactor or in semi-continuous way, in which monomers and/or the other components are fed in the reactor during the polymerization process. The typical mechanism of emulsion polymerization is given in Figure 1.1.

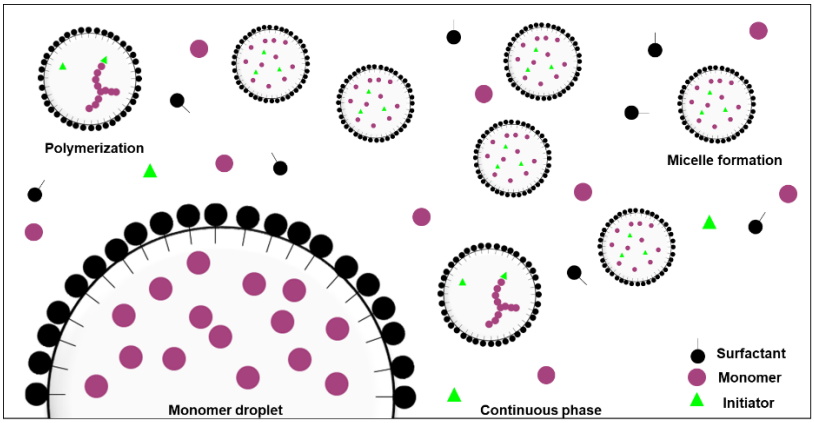

Figure 1.1. Schematic representation of emulsion polymerization.

In a batch polymerization process, three intervals can be differentiated. Polymer particles are nucleated in Interval I. Since most of the initiators are water-soluble, the radicals are mainly formed in the aqueous phase. However, these radicals are too hydrophilic to be able to directly enter into the monomer droplets (organic phase). Furthermore, due to the relatively large monomer droplets (1-10 μm) with respect to the monomer swollen micelles (10-20 μm), the surface area of the micelles is about three orders of magnitude higher than that of the monomer droplets, therefore, the entry of the radical into micelles is expected. The particles can be formed either by homogeneous or heterogeneous (micellar) nucleation. Homogeneous nucleation[9] is the predominant mechanism when employing monomers of relatively high water solubility as for examples methyl methacrylate (MMA) (1.5 g/100 g of water) and vinyl acetate (VAc) (2.5 g/100 g of water). The radicals arising from the initiator located in the aqueous media react with the monomer presented in the aqueous phase leading to the formation of oligoradicals. When these oligoradicals grow above the length at which they are not soluble in water anymore they precipitate[10] and become stabilized by the surfactant presented in the aqueous media.[11,12] The new species formed by this process are polymer particles, nucleated by homogeneous nucleation. On the other hand, if the solubility of the monomer employed is very low as in the case of styrene (St)

(0.045g/100 g of water), the predominant nucleation mechanism is heterogeneous (micellar). In a similar manner as in the previous case, the radicals created from the initiator in the aqueous media react with the monomer presented in the aqueous phase forming oligoradicals. When these oligoradicals become sufficiently hydrophobic, they can enter either in the micelles (creating polymer particles by micellar or heterogeneous nucleation) or in the existing polymer particles. Regardless of the nucleation mechanism, the newly formed particles are very small and suffer a tremendous increase in surface area upon polymer particle growth. Micelles tend to disappear as they are destroyed to provide surfactant to both, the increasing surface area of the growing polymer particles and the oligoradicals that precipitate in the aqueous media and because they become polymer particles by the oligoradical entry. Thus, during Interval I, the number of particles as well as the polymerization rate increase with reaction time. The end of Interval I is considered when all the micelles have been disappeared. In Interval II, polymer particles and monomer droplets coexist. As the polymerization proceeds the size of the polymer particles increase significantly. The monomer required for the polymerization diffuses from the monomer droplets through the aqueous phase to the polymer particles, and for very low water solubility monomers this can be challenging. In this stage, the number of particles (unless particle coagulation occurs) maintains constant and the polymerization rate may be consider constant. End of Interval II is marked by disappearance of monomer droplets. When Interval III starts, there are only polymer particles swelled with monomer in the reaction system. The monomer concentration decreases during Interval III continuously and as the number of polymer particles is kept constant (unless coagulation occurs) the polymerization rate decreases. These three intervals can be clearly distinguished when working under batch conditions, however, when the polymerization is carried out in semi-continuous or continuous mode the different stages cannot be distinguished since the processes occur simultaneously. Batch emulsion polymerization reactions are usually quite exothermic and the heat removal might be challenging when working in large scale, therefore, the priority processing mode in industry is the semi-continuous emulsion polymerization. Besides the safety reasons, semi-

continuous mode provides control on the polymer composition due the possibility to control the concentration of monomers, surfactant and initiator in the reactor. Moreover, this process design offers the potential for creating more intricate particle morphologies, such as core-shell particles, when properly designed and controlled.[13,14]

As already explained, surfactants play a critical role in emulsion polymerization. They are instrumental in particle nucleation; they colloidally stabilize the system during the polymerization reaction and maintain the stability during storage and transport, as well as in formulated products. Therefore, selecting the right surfactants holds great significance in the production of latexes with suitable particle size distribution and stability, tailored for specific applications. These surfactants can be categorized either as ionic or non-ionic[15-17] depending on the presence or absence of an ionic charge on the hydrophilic group.

Ionic surfactants are classified according to the nature of their charge in: i) anionic, when the hydrophilic group has a negative charge; ii) cationic, when the hydrophilic group has a positive charge; and iii) zwitterionic, when both positive and negative charges are in the same molecule.

Colloidal stability of ionically-stabilized polymer particles is determined by the balance between two opposing forces: electrostatic repulsion between oppositely charged particles and attractive Van der Waals forces. When colloids approach each other, their electrical double layer (EDL) maximizes the repulsion, but this force weakens beyond the EDL, while simultaneously, attractive forces increase. The heightened concentration of ions in the medium (resulting from the presence of salts) reduces the thickness of the electrostatic double layer (EDL) through interactions with its constituent ions. This compression often leads to coagulation due to the increased attractive forces among particles. The heightened sensitivity to electrolytes and the limited freeze-thaw stability of ionically stabilized latexes, among other drawbacks, pose challenges for their independent use in industrial applications.

On the other hand, non-ionic surfactants possess a combination of uncharged hydrophilic and hydrophobic groups, rendering them highly effective in wetting, spreading, and serving as surfactants and foaming agents. Unlike ionic surfactants that rely on electrostatic repulsion to get stability, non-ionic surfactants achieve stabilization through steric hindrance.

The advantages of non-ionic surfactants over their ionic counterparts lie in their reduced toxicity, increased resistance to electrolytes, and improved tolerance to pH variations and freeze-thaw cycles. However, non-ionic surfactants are generally less efficient in particle nucleation.[18] To overcome this limitation, a common practice in industry involves utilizing mixtures of ionic and non-ionic surfactants. Regardless of the type of surfactant, conventional surfactants are not chemically bonded to the polymer particles but they are physically adsorbed on the polymer particles and consequently, they bring some undesired effects on product properties. The extent of the problem is dependent on many factors, such as the chemical nature of the surfactant and the polymer matrix, the molar mass, diffusion ability and film casting conditions.[19] Due to the weak hydrophobic interaction between the surfactant and the polymer particle, the surfactant can be desorbed from the polymer particle and this can cause a reduction of the latex stability[20,21] especially under high shear, freezing and high ionic strength conditions.

Furthermore, during film formation process from waterborne dispersions stabilized with conventional surfactant, the surfactant migrates[22] either to the film-surface and changes the gloss properties of the film or to the film-substrate interface and reduces the adhesion between the film and the substrate. [23-26] In addition, if the chemical structure of the surfactant and the polymer matrix are compatible, the surfactant may dissolve throughout the matrix and make a plasticizing effect that deteriorates the mechanical properties of the film. On the contrary, if they are not compatible, surfactant molecules may aggregate forming hydrophilic pockets within the polymer matrix, which increases the water sensitivity of the films.[27,28] The migration of the surfactant during film formation can be mitigated by the use of

polymeric surfactants[29] nevertheless, they are not very efficient for particle nucleation during the polymerization process.[30]

Because of these drawbacks, some alternatives were developed, including the use of reactive surfactants and the use of surfactant-free emulsion polymerization[31-33] where the colloidal stability is achieved by the use of functional monomers or initiators.

Reactive surfactants usually combine a surface-active moiety with an initiating moiety (inisurf)[31,34] with a transfer agent moiety (transurf)[35] or with a monomer moiety (surfmer or polymerizable surfactant).[36] Due to their ability to chemically bond with polymer particles during the polymerization process, migration and desorption issues are prevented.[36] Although in principle, they all work well binding covalently to the particle, these systems have their own disadvantages. In case of using insurf or transurf, when colloidal stability is adjusted by varying their contents, polymerization rate and molar mass distribution are affected importantly.[37] Surfmers or polymerizable surfactants seem to be the most promising option. Surfmers maintain the essential amphiphilic structure of conventional surfactants, so they can adsorb onto the polymer particles but in contrast to conventional surfactants, surfmers bear a C=C double bond in their structure and therefore, they can copolymerize with the monomers during the polymerization process. As a result, the surfmer remains covalently bonded to the polymer particles preventing desorption or migration during storage of the latex or film formation process. Aguirreurreta et al.[38] found that the use of polymerizable surfactants (specifically Latemul PD-104 and Sipomer Pam-200) in an acrylic system lead to a reduction in the whitening of the film. This reduction was related to the integration of these surfactants into the polymer structure itself.

However, for decent performance, the surfmers should copolymerize with the monomers. Therefore, the reactivity ratios of the surfmers should be adapted to particular monomer system, turning their performance to be system dependent.

On the other hand, initiator or functional monomers can be also be used to provide colloidal stability of surfactant-free emulsion polymerization system. The polymer particles obtained are free of surfactant and with narrow molar mass distribution, usually used as calibration standards for various instruments such as electron microscopes and light scattering equipments and as model system for the fundamental research on coagulation, flocculation and optical, electro, kinetic and rheological properties of the colloids.[39-42]

These particles possess a clean surface and exhibit excellent surface chemical properties, including adhesion and water resistance.[43-45] The method has become commonly used to prepare latexes with narrow particle size distribution ranging from 100 nm to 5 μm.[46] However, producing high solids content latexes with particles in the size range of 10 nm to 100 nm remains challenging. This is primarily due to the strong tendency of small particles to coagulate when present in concentrated dispersions.

In surfactant-free emulsion polymerization, the initiators stabilize the colloidal particles by leaving charged fragments around the particles.[47] Thus, stabilization is achieved through electrostatic repulsion.[43,48-51] Potassium persulfate (KPS),[48,52] and 2,2-azobis(2-amidinopropane)dihydrochloride (V-50),[53,54] can be given as examples of anionic and cationic initiators, respectively. Nevertheless, it has been also reported the use of non-ionic initiators in surfactant-free emulsion polymerization that provide steric stabilization as for example polyethylene glycol-azo initiators (PEGA types).[55]

The main limitations of the use of initiators to provide stability in surfactant-free emulsion polymerization are that the reactions are performed at low solids content (around 10 wt%), that the final particle size is quite high (0.4-1 μm) and that the initiator amount cannot be varied without affecting the molar mass and reaction kinetics.[56,57]

The other alternative that involves the use of functional monomers have become a highly promising strategy for the synthesis of surfactant-free emulsion polymers, providing numerous advantages including enhanced colloidal stability and improved mechanical properties.[58-62] The functional

monomers are incorporated usually in 1-10 wt% with respect to the main monomers, the most commonly used functional groups are carboxylates,[63-66] sulfates,[67] amines,[68] and sulfonates.[64,69-74] However, there are also examples of the use of phosphate or phosphonate functional monomers in surfactant-free emulsion polymerization. Penta (propylene glycol) methacrylate phosphate was employed in surfactant-free seeded semi-continuous emulsion polymerization of methyl methacrylate/n-butyl acrylate/acrylic acid (MMA/n-BA/AA) but, surfactant was used in the seed synthesis.[75] Furthermore, phosphonate monomers have been incorporated into emulsion formulations to impart special properties such as improved substrate adhesion and anticorrosion characteristics.[38]

Nevertheless, most of these functional monomers present certain limitations. The stability provided by carboxylic acids is restricted by the pH of the medium.[64,76] For instance, pKa value of acrylic acid and methacrylic acid is 4.25 and 4.66, respectively. Therefore, when the pH is above the pKa of the acid, carboxylic groups become deprotonated, which leads to strong electrostatic repulsion between particles. However, at low pH values, they lose their ionic character and become practically useless for stabilization. Therefore, in these systems, either a buffer or a base is added to adjust the pH. On the other hand, since amines form positive charges around the polymer particles and most surfaces are negatively charged, their applications are limited. With respect to sulfates, they are subject to hydrolysis so they leave uncharged hydroxyl groups in place, which can further oxidize to carboxyls depending on the nature of the –OH group formed.[67]

Among the above mentioned functional groups, sulfonate that combines a very low pKa with high stability over a wide range of temperature and pH is the most attractive functional group . Sulfonate monomers are also extensively used in free radical polymerization[73,77,78] and controlled radical polymerization (CRP) and also for the production of sulfonated ionomers.[2,79]

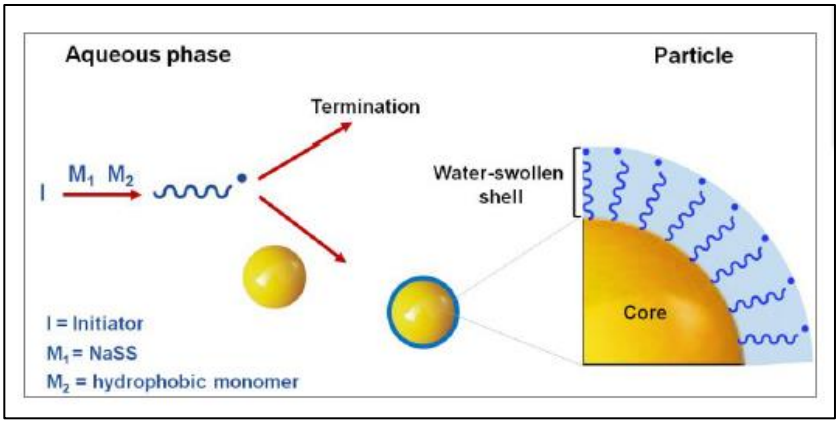

Figure 1.2. Schematic representation of polymerization of NaSS, in the aqueous phase and the surface of the polymer particles (PhD thesis of Sevilay Bilgin, UPV/EHU).[80]

Recently, Bilgin et al.[81] developed surfactant-free high solids content (60%) MMA/n-BA nanoparticle dispersions using sodium styrene sulfonate (NaSS) ionic monomer. This monomer was a prospering candidate due to its low pKa value (pKa=1)[82] which allows stabilization in wide range of pH and exhibit exceptional stability towards hydrolysis, oxidation, thermal degradation and also coagulation at extreme pH-s and temperatures. According to the authors, the critical issue for successful emulsifier-free polymerization is the high water solubility of NaSS, which usually enable creation of high quantity of water-soluble species. Thus, for stabilization of high solids content polymer dispersions it is necessary to have high chemical incorporation of NaSS onto the polymer particles, simultaneously decreasing the amount of water-soluble species. Bilgin and coworkers investigated the effect of functionalities and water solubility of co-monomers on the incorporation of NaSS onto MMA/n-BA particles, reporting that the presence of small amount of water-soluble co-monomer is determining for high incorporation.[81] They as well studied the effect of initiator type on the NaSS incorporation[72] and it was found that water-soluble initiator that forms hydrophobic radicals in aqueous phase able to immediately enter into polymer particles are suitable for high incorporation (Figure 1.2.). The effect of NaSS concentration on

the incorporation of NaSS onto the polymer particles was also studied [61] and the results showed that a higher concentration than 0.5% NaSS is required in order to reach stable latexes. The increase in NaSS concentration extended the incorporation of NaSS onto polymer particles. Furthermore, the waterborne polymers synthesized using NaSS displayed better performance than polymers stabilized with conventional surfactant, probably due to the lack of migration of surface-active species in these films. The incorporation of NaSS in the polymeric films resulted in a remarkable improvement in their mechanical properties. However, as the concentration of NaSS increased, an unintended consequence emerged with increased water uptake. This was attributed to the presence of water-soluble oligomers. Consequently, the excessive water uptake compromised the integrity of the polymer film.

This discovery holds significant importance and calls for further investigation and consideration in the development of waterborne coatings for practical applications. In line with this, Argaiz et al.[62,83] introduced both anionic and cationic functional monomers into polymer particles, aiming to establish interactions between individual particles within the polymer films. The formation of complexes through ionic bonds was particularly intriguing due to the high energy required to break a single bond. The main objective of their study was to induce inter-chain or inter-particle ionic complexation in polymer dispersions, aiming to enhance the production of waterborne coatings and investigate its effects on the final performance of the polymer film. They successfully mitigated the high water sensitivity of the films and enhanced mechanical properties by implementing ionic inter-particle complexation. In their research, waterborne dispersions stabilized by 1,4-diazabicyclo[2.2.2]octane (DABCO) cationic monomer and NaSS anionic monomer were synthesized without the use of surfactants.[84]

In light of the comprehensive research conducted in this field, it is evident that the incorporation of functional monomers in various studies has yielded positive outcomes, enhancing the latex stability and polymer films properties. Motivated by these issues, it was thought that the use of zwitterionic

monomers (ZMs) eventually can provide simultaneously both, colloidal stabilization and enhanced film properties.

ZMs encompass the same number of anionic and cationic moieties within the molecule thus, present an overall neutral charge. The presence of high-density ion pairs makes ZM highly hydrophilic[85] once incorporated into hydrophobic chains, they can create in situ colloidal stabilizing species, able to produce stable latexes. Unlike conventional polyelectrolytes, the addition of salts to aqueous solutions of zwitterionic polymers enhances their solubility and solution viscosity.[86] In the absence of salts, zwitterionic polymers experience electrostatic interactions between their chains. These interactions govern the polymer's conformation, causing it to collapse.[87] Addition of salts in zwitterionic polymers will screen out electrostatic interactions of intra- and inter-zwitterionic chains and break ionic pairs, thus causing the extension and dissociation of polymer chains (Figure 1.3)

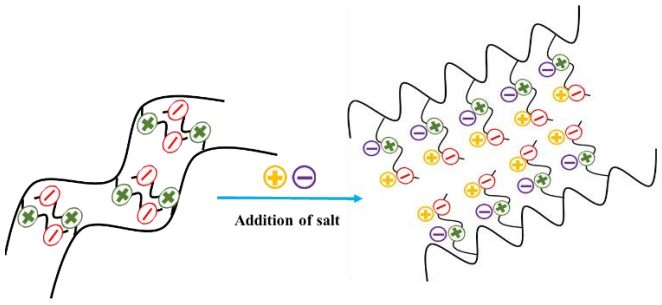

Figure 1.3. Anti-polyelectrolyte effect, zwitterionic polymer chains before and after salt addition.

The cationic group presented in the ZMs in most of the cases arises from a quaternary ammonium[88-90] however, there are also ZMs containing protonated amino[91] and pyridine groups.[92,93] ZMs are usually classified into three main groups based on their ionic nature, carboxybetaines (CB), sulfobetaines (SB), and phosphobetaines (PC). Figure 1.4 represents the most commonly used and commercially available zwittterionic monomers with different anionic groups. The densely clustered zwitterionic groups

possess the ability to establish a potent hydration layer through electrostatic interaction that avoids the adsorption of the protein due to the strong steric hydration repulsive forces. This layer effectively prevents non-specific protein adhesion and foreign body reactions.[94]

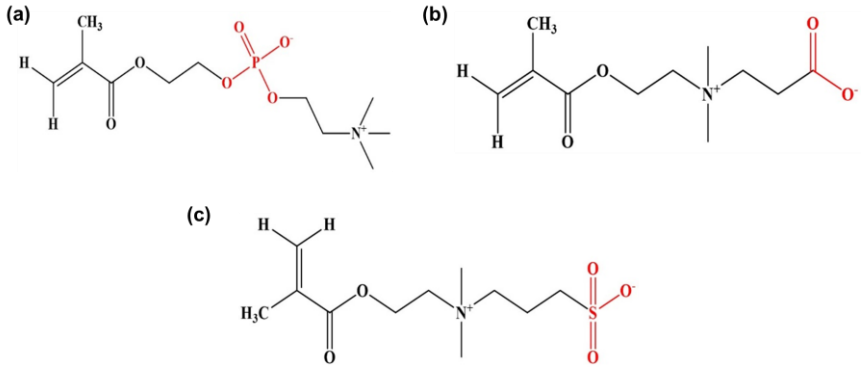

Figure 1.4. Chemical structure of the most widely employed and commercially available zwitterionic monomers (a) 2-(methacryloxy) ethyl 2-(trimethylammonio)ethyl phosphate,(b) 3-[[2-(methacryloxy)ethyl]dimethylammonio] propionate and (c) 2-(methacryloyloxy)ethyl]dimethyl-(3-sulfopropyl)ammonium hydroxide.

Polymer materials based on PC are known for their biocompatibility[95,96] resistance to protein and bacterial adsorption[97,98] and exceptional aqueous solubility that remains unaffected by changes in temperature or salt concentration.[99] Nevertheless, the synthesis procedure of phosphobetaine monomers, such as 2-methacryloyloxyethyl phosphoryl choline (MPC), is complex with associated high expense.[100] On the other hand, SB materials are generally easy to synthesize with low expense, displays an upper critical solution behavior and salt-responsive solubility due to the intra- and inter-polymer electrostatic interactions of the pendant SB zwitterions. These interactions can be disrupted by the addition of salt or by increasing the solution temperature, leading to changes in solubility behavior.[101,102] This unique characteristic of SB's aqueous solubility has sparked widespread investigation for the synthesis of materials that demonstrate responsive assembly in water and at interfaces.[103-105] The CB has

been studied intensively for structural and chemical properties due to its several advantages such as structural versatility, ease of synthesis, possibility of functionalization, ultra-low biofouling property and biocompatibility.[106-108]

Nevertheless, besides the nature of the anionic and cationic group, slight structural variations in zwitterionic monomers, such as changes in carbon spacer length (CSL) between both charges[109] pendant groups, and functional groups, can yield substantial differences in their properties.

Vaisocherova et al.[110] studied the effect of intercharge separation on the antifouling properties of zwitterionic poly (carboxybetaine acrylamide) in blood plasma and serum. The results revealed that the longer spacer group leads to a higher level of nonspecific protein adsorption.

Gauthier and coworkers[111] synthesized four different sulfobetaine methacrylate monomers in order to vary systematically the spacer length between the charged groups and the bulkiness of the monomer by changing the length of the quaternary ammonium functionality as can be seen in Figure 1.5. Then they used these ZMs to copolymerize them separately with n-BA and 2-ethoxyethyl acrylate in solution polymerization and evaluate the reactivity ratios for the copolymers. They found that in general, the more hydrophobic the sulfobetaine methacrylate the lower its reactivity towards the acrylate monomer. In a further work, they studied the ion aggregation behavior of these copolymers by dynamic mechanical analysis.[112] The results showed that by increasing the ZM content the storage modulus increased suggesting a higher degree of ionic crosslinking between ZM moieties. However, the increase was less pronounced for more hydrophobic (SPEE and SPEB) ZMs, probably due to the increased bulkiness hindering the aggregation of these sulfobetaine moieties. Quite surprisingly, the intercharge separation in the sulfobetaine moiety did not present any effect on the viscose-elastic properties.

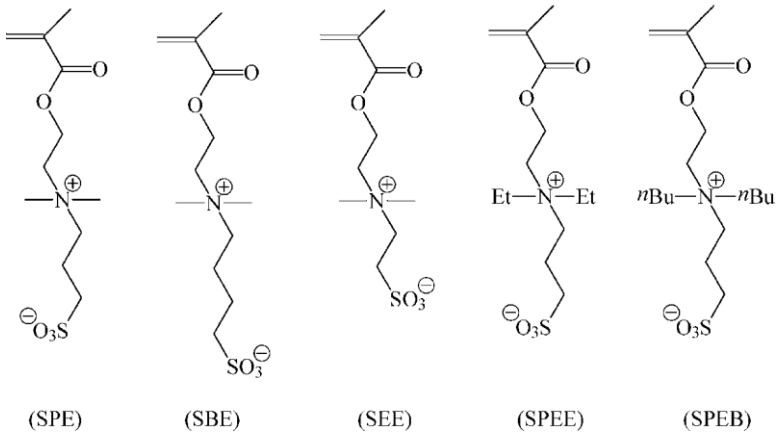

Figure 1.5. Sulfobetaine monomers used in the work of Gauthier et al .[111,112]

Besides the distance between the charged groups in sulfobetaines, the functional group present in the ZM plays also an important role, since it can affect the potential of the ammonium site for binding anions. As a consequence, depending on the functional group the strength of the interactions between the ZM moieties might be different affecting the polymer properties as for instance the upper critical temperature.[114]

Even though, the zwitterionic polymers are known since 1950s,[114] most of them have been homo or co-polymerized in solution for bio-applications. ZMs have hardly been co-polymerized in emulsion polymerization or used for colloidal stabilization of waterborne dispersions, because of very high hydrophilicity, making the copolymerization in emulsion very challenging.

Blom et al.[115] investigated the surfactant-free emulsion polymerization of n-BA in the presence of a sulfobetaine monomer, 1-(dimethyl)-1-(3-methacryloxyethyl(-1-sulfopropyl ammonium betaine) (SPE). They studied the mode of polymerization (batch vs semi-continuous and unseeded vs seeded reactions) and found that the seeded semi-continuous emulsion polymerization was the best protocol for producing stable monodisperse latex with high 20 mol % SPE loadings. The S.C. was just 10 wt %. They

also investigated the effect of various salts (NaCl, $NaHCO_3$, Na_2CO_3, and NaH_2PO4) on the surfactant-free emulsion polymerization and revealed that the type and quantity of salt is important in determining the size and size distribution of the final latex particles.

Abele et al.[116] investigated on reactive cationic and zwitterionic dialkyl maleates surfactants with different hydrophobic chain lengths and different counter ions (I^-, Br^-, $HSO4^-$) for the cationic hydrophilic part. They compared reactive surfactants with the nonreactive analogues. Batch and seeded emulsion polymerization were used to prepare stable latex with less than 10% solids content. The colloidal stability of different latexes produced was compared, whereas the polymer films were evaluated in mechanical traction and water absorption measurements. In the case of reactive cationic surfactants, by both batch and seeded emulsion polymerization monodisperse latexes were obtained with particle size of 150 nm. In case of reactive zwitterionic surfactants, monodisperse latexes with particle size about 100-300 nm were achieved. Almost all the latex showed sensitivity towards freeze-thaw and electrolytes. The latexes synthesized with non-reactive surfactants were also colloidally stable; the films cast from these latexes were more fragile, but less sensitive to water than the films performed from the latex synthesized with the reactive analogues. Probable reason is that even using reactive surfactants, likely low incorporation onto polymer particles was achieved, and large amount of water-soluble species was synthesized, instead. However, the incorporation was not studied in this work.

Kamenska et al.[117] copolymerized vinyl acetate with different concentrations of 2-[3-dimethyl (methacryloyloxyethyl) ammonium propane sulfonate] (DMAPS) by surfactant-free emulsion polymerization at low S.C. All the latexes were coagulum free and presented narrow particle size distribution. Their findings revealed that the ionic cluster formation of zwitterionic units strongly influenced the swelling process, which in turn was affected by the ionic strength of the medium and temperature. The particles were further test on the drug delivery of metroprolol tartrate (MT).[118]

In another captivating study reported by Zhao and colleagues[119] the development of hierarchically porous membranes enhanced through the incorporation of amphiphilic copolymers is presented. These specialized copolymers consisted of two main components: zwitterionic poly [3-(methacryloylamino) propyl]-dimethyl (3-sulfopropyl) ammonium hydroxide (PSPP) and low surface energy poly (hexafluorobutyl methacrylate) (PHFBM) segments. The reaction was carried out in emulsion polymerization using SDS and KPS as conventional surfactant and thermal initiator, respectively. The integration of these copolymers into the membrane's design was skillfully executed to confer exceptional antifouling and self-cleaning properties. By meticulously fine-tuning the ratio between the hydrophilic PSPP segments and the low surface energy PHFBM segments on the membrane surface, they effectively suppressed membrane fouling.

Polzer et al.[120] synthesized core-shell particles by synthesizing divinylbenzene (DVB) cross-linked poly(styrene) core (PS-co-DVB), onto which linear zwitterionic poly (2-(methacryloyloxy)ethyl dimethyl-(3-sulfopropyl)ammonium hydroxide) (pMEDSAH) chains were chemically grafted by atom transfer radical polymerization (ATRP). The synthesis of the cross-linked PS-co-DVB particles (8% S.C.) was carried out by emulsion polymerization using SDS as conventional surfactant. Their study unveiled that the thickness of the zwitterionic layer increased upon heating, a phenomenon attributed to the upper critical solution temperature (UCST) behavior of the pMEDSAH chains. This behavior was further intensified when salt was introduced.

Vasantha et al.[121] conducted a research on functionalized non-spherical polymer particles (NSP) with tunable morphologies and iridescence. They used polystyrene/poly sulfobetaine (DMAPS) through surfactant -free emulsion polymerization at low solids content (< 10%). The addition of the sulfobetaine comonomer induced phase separation during polymerization, resulting in anisotropic NSP with regulated morphologies. These particles exhibited photonic bandgaps and vibrant structural colors due to their ordered architectures, enabling the development of stimuli-responsive photonic materials.

In an attempt to improve the antibiofouling capacity of ethylene-vinyl acetate copolymer (EVA) films by surface coating, Wang et al.[122] synthesized amphiphilic sulfobetaine copolymers by monomer-starved seeded semi-continuous emulsion polymerization, incorporating zwitterionic sulfobetaine (DMAPS) and 2,2,2-trifluoroethyl methacrylate (TFMA) monomers at varying ratios at less than 10% S.C. . During the emulsion polymerization process, conventional anionic surfactant SR-10 was used. The researchers observed that as the DMAPS/TFMA ratio increased, the particle diameter, polydispersity index, and water absorption of films decreased. Moreover, the films coated with the amphiphilic copolymer exhibited exceptional antifouling characteristics against proteins and microalgae.

Miyata et al.[123] synthesized p(styrene-*co*-methacrylic acid-*co*-2-methacryloyloxyethyl phosphoryl choline) (p(St-*co*-MAA-*co*-MPC)) particles by surfactant-free emulsion polymerization at low solids content. Afterwards, the surface of the particles was modified by maleimide moieties as photodimerizable groups. They investigated the photo-assembling behavior of these particles in aqueous media and assessed their biocompatibility. The introduction of photodimerizable groups led to inter-particle bond formation upon UV irradiation, resulting in assembled films with suppressed protein adsorption, cell adhesion, and platelet adhesion.

Yu et al.[124] synthesized two different ZM monomers, both of them presented the same ions, quaternary ammonium as the cation and carboxylate as the anion, however, one of the ZM monomer presented a vinyl functionality whereas the other an acrylic functionality. These ZMs were separately copolymerized with n-BA and MMA by emulsion polymerization using a polyvinyl alcohol aqueous solution as the dispersion medium. By changing the amount of ZM a series of zwitterionic polyacrylate latexes were synthesized and used as stiffening finish agents for textile (safety belt). When comparing both ZMs it was found that the one presenting the vinyl group presented higher initial tensile modulus, nevertheless, regardless the ZM the initial strength modulus increased with the amount of ZM.

Furthermore, the fabric treated with zwitterionic polyacrylate latex was able to maintain the same stiffness at higher temperatures.

Alkorta et al.[125] synthesized high solids content (40%) eco-friendly and industrially relevant coatings via surfactant-free semi-continuous emulsion copolymerization of butyl acrylate, acrylic acid and styrene using zwitterionic macro chain transfer agent (macro-CTA). The hydrophilic macro-CTA was first synthesized by reverse addition-fragmentation chain transfer-polymerization (RAFT) on aqueous solution. After purification process the macro-CTA, it was placed in the reactor together with the water and small amount (10%) of the total monomer mixture and the reaction was initiated by KPS. In this way, the hydrophilic polymer (macro-CTA) was chain extended with the acrylic monomers that led to the formation of amphiphilic block copolymers that resulted in the formation of micelles that grew during the monomer feeding along the reaction without producing new particles. The synthesized latex presented 100% conversion and about 142 nm particle size. However, the process was quite long and required 2 steps. First the synthesis (4h) followed by purification of the macro-CTA, and secondly the semi-continuous emulsion polymerization (8h). Additionally, they reported very low incorporation of the macro-CTA (4%). To the best of our knowledge apart from Alkorta et al. there are no works related with the synthesis and applications of high solids content waterborne dispersions using zwitterionic monomers as stabilizers, synthesized via emulsion polymerization, which will be the aim of this work.

Based on the presented state-of-the art, it is clear that zwitterionic monomer have been copolymerized in emulsion with more hydrophilic monomers. Nevertheless, most of the developed processes lack practical application significance because of the very low solids content and are not suitable for coating application. Even though, in some of these studies, the ZM employed has been used as a unique source of ions to stabilize colloidally the dispersions, the incorporation of the ZM onto particles has not been studied, to the best of the author's knowledge. The colloidal stability in emulsion system in which ZMs are used to provide colloidal stability is strongly related with the incorporation of ZM onto polymer

particles, because it is the only way to form amphiphilic species able to stabilize the particles, being the key issue enabling high solids content latexes. However, it is not straightforward, as the ZMs are hydrophilic and placed in aqueous phase of the emulsion, while the usual emulsion monomers are placed in the monomer droplets. There is another critical issue, strongly related with the incorporation of ZM onto polymer particles. The high ZM hydrophilicity increase the probability of aqueous phase polymerization and creation of water-soluble species, which will not contribute to colloidal stability. Oppositely, these species increased the ionic strength of the dispersions and increase the water sensitivity of the final films. These important issues have not been studied and reported in the available literature.

1.1. Motivation and objective of the thesis

The primary goal of this thesis is to use zwitterionic monomers in emulsion polymerization of (meth)acrylic monomer formulation for coating application to develop colloidally stable latexes with high solids content and film-forming properties, without the need for surfactants. The key focus is on achieving colloidal stability solely through the incorporation of chemically bonded zwitterionic moieties onto the polymer particles.

To accomplish this objective, a conventional coating formulation comprising n-BA/MMA in a 50/50 weight ratio was employed throughout the study. However, this task presents significant challenges. Zwitterionic monomers, due to their high water-solubility, tend to reside in the aqueous continuous phase, while the polymer particles are the main polymerization loci. Moreover, the hydrophilic nature of the zwitterionic moieties leads to an increased production of water-soluble oligomers, which has a dual negative impact. On one hand, their presence affects the colloidal stability by raising the ionic strength. On the other hand, when embedded within the polymer matrix, these oligomers can act as

plasticizers, compromising the mechanical properties of the resulting coating film. Therefore, it is crucial to achieve a high degree of zwitterionic moieties incorporation onto the polymer particles.

1.2. Outline of the thesis

The thesis is divided into seven chapters, beginning with a concise introduction and the underlying motivation for this research, presented in Chapter 1.

Chapter 2 focuses on the selection of an appropriate zwitterionic monomer from three commercially available options, each featuring different anionic group. The technique used to synthesize polymer latex was seeded semi-continues emulsion polymerization, where the seed was stabilized by conventional surfactant SDS. The chapter presents the initiator system's influence on the chemical incorporation of the selected zwitterionic monomer onto the MMA/n-BA polymer particles. Specifically, the initiators employed are carefully chosen to form either hydrophilic or hydrophobic radicals in both aqueous and organic phases. Moreover, the chapter explores the mechanical performance and water absorption properties of films prepared using different initiators, providing valuable insights into their influence on the resulting films.

In Chapter 3, the impact of 2-[(methacryloyloxy) ethyl] dimethyl-(3 sulfopropyl) ammonium hydroxide (DMAPS)] concentration in the formulation on the extent of incorporation onto the polymer particles and the film properties is studied. All synthesis were performed by seeded semi-continues emulsion polymerization in which the seed was stabilized with SDS. Additionally, the antifouling properties of the obtained films are studied using quartz crystal microbalance with dissipation (QCM-D) and multi parametric surface plasmon resonance (MP-SPR) techniques.

Chapter 4 is devoted to the development of completely surfactant-free high solids content dispersions where the incorporation of zwitterionic moieties (ZMs) within the (meth)acrylic polymer backbones serves as the sole source of colloidal stabilization. Furthermore, this chapter goes a step further by

presenting a proof-of-concept for the surfactant-free strategy using four different ZMs- 2-[(methacryloyloxy) ethyl] dimethyl-(3 sulfopropyl) ammonium hydroxide (DMAPS), 4-[[2-(methacryloyloxy) ethyl] dimethylammonio] butane-1-sulfonate (M3295), 3-[[2-(acryloyloxy) ethyl] dimethylammonio] propane-1-sulfonate (A3367) and 3-[(3-acrylamidopropyl) dimethylammonio] propane-1-sulfonate (A3361). These ZMs share a common cation (quaternary ammonium) and anion (sulfonate), with the primary difference lying in the functional group and chain length between the opposite charges. The chapter also includes additional study on anti-polyelectrolyte effect on the polymerization process and coating film properties.

Chapter 5 relies on the synthesis and characterization of thermo-responsive pressure sensitive adhesives (PSAs) stabilized with different ZMs, A3361 and DMAPS. The first part is focused on the synthesis and characterization of surfactant-free PSA by using petroleum-based conventional monomers n-BA and MMA, while the second part is based on the synthesis and characterization of thermo-responsive bio-based 2-octylacrylate (2-OA) and isoboryl methacrylate (IBOMA) PSAs stabilized with different ZMs DMAPS and A3361.

Chapter 6 of the thesis was conducted in collaboration with Synthomer Company (Portugal). The objective was to synthesize high solids content binders using a small quantity of ZM DMAPS and introduce them into enamel paint formulations for protective coatings. Various acrylic binders stabilized with ZM DMAPS were prepared and their performance was compared to reference binders stabilized using conventional surfactants and a surfmer supplied by Synthomer.

Finally, in Chapter 7, the most significant conclusions of this thesis are summarized.

At the conclusion of the manuscript, **Appendix I and II** provide detailed descriptions of the primary experimental procedures, latex synthesis, characterization techniques for polymer latex and films, as

well as methods for characterizing and applying paints. **Appendix III** contains a comprehensive list of acronyms and symbols.

1.3. References

1. Business wire. *Water Borne Coatings Global Market Report 2020*; Dublin, 2020.

2. *Sulfonated polystyrene ionomers prepared by emulsion copolymerization of styrene and sodium styrene sulfonate.* **Weiss, R. A., Turner, S. R. and Lundberg, R. D.** s.l. : Wiley Online Library, 1985, Journal of Polymer Science: Polymer Chemistry Edition, Vol. 23, pp. 525–533.

3. *Solvent replacement for green processing.* **Sherman, Julie, et al.** 1998, Environmental health perspectives, Vol. 106, pp. 253–271.

4. European Commission. Screening Study to Identify Reductions in VOC Emissions due to the Restrictions in the VOC Content of Products. **2002**, No. February, 3–130.

5. Directive 2004/42/CE of the european parliament and of the council. *Official Journal of the European Union*; 2004.

6. *Effect of acrylic binder type and calcium carbonate filler amount on the properties of paint-like blends.* **Alvarez, V. and Paulis, M.** s.l. : Elsevier, 2017, Progress in Organic Coatings, Vol. 112, pp. 210–218.

7. *Emulsion polymerization: from fundamental mechanisms to process developments.* **Asua, José M.** s.l. : Wiley Online Library, 2004, Journal of Polymer Science Part A: Polymer Chemistry, Vol. 42, pp. 1025–1041.

8. *Emulsion polymerization.* **Barandiaran, María J., Cal, José C. de la and Asua, José M.** s.l. : Wiley Online Library, 2007, Polymer reaction engineering, pp. 233–272.

9. *Emulsion polymerization: Kinetics of radical capture by the particles.* **Fitch, R. Mo and Shih, Lih-bin.** 2007. Interface Chemistry: Lectures of the 5th Northern European Symposium on Interface Chemistry Abo (Finnland) 1973. pp. 1–11.

10. *Mathematical modeling of multicomponent chain-growth polymerizations in batch, semibatch, and continuous reactors: a review.* **Dubé, Marc A., et al.** s.l. : ACS Publications, 1997, Industrial & engineering chemistry research, Vol. 36, pp. 966–1015.

11. *A general theory of the mechanism of emulsion polymerization1.* **Harkins, William D.** s.l. : ACS Publications, 1947, Journal of the American Chemical Society, Vol. 69, pp. 1428–1444.

12. *Particle nucleation in emulsion polymerization. I. A theory for homogeneous nucleation.* **Hansen, F. K. and Ugelstad, J.** s.l. : Wiley Online Library, 1978, Journal of Polymer Science: Polymer Chemistry Edition, Vol. 16, pp. 1953–1979.

13. *A concise review on surfactants and its significance.* **Dave, Nikunj and Joshi, Tejas.** 2017, Int. J. Appl. Chem, Vol. 13, pp. 663–672.

14. *Mixed surfactant systems: an overview.* **Holland, Paul M. and Rubingh, Donn N.** s.l. : ACS Publications, 1992.

15. *Industrial Applications of Surfactants, Royal Soc.* **Karsa, D. R.** 1990, Chem., Cambridge.

16. **Pletnev, Michael Y.** 1. Chemistry of surfactants. *Studies in interface science.* s.l. : Elsevier, 2001, Vol. 13, pp. 1–97.

17. **van Os, Nico M., Haak, Jan Remees and Rupert, Leonardus Antonius Maria.** *Physico-chemical properties of selected anionic, cationic and nonionic surfactants.* s.l. : Elsevier, 2012.

18. *Nonionic latices in aqueous media: Part 4: Preparation and characterisation of electrosterically stabilised particles.* **Ottewill, R. H. and Satgurunathan, R.** s.l. : Springer, 1995, Colloid and Polymer Science, Vol. 273, pp. 379–386.

19. *On the optimal surfmer addition profile in emulsion polymerisation.* **Aramendia, Esteban, Barandiaran, María J. and Asua, José M.** s.l. : Elsevier, 2003, Comptes Rendus Chimie, Vol. 6, pp. 1313–1317.

20. *In situ polymerization of surface-active agents on latex particles: III. The electrolyte stability of styrene/butadiene latexes.* **Greene, B. W. and Saunders, F. L.** s.l. : Elsevier, 1970, Journal of Colloid and Interface Science, Vol. 33, pp. 393–404.

21. *In situ polymerization of surface-active agents on latex particles I. Preparation and characterization of styrene/butadiene latexes.* **Greene, B. W., Sheetz, D. P. and Filer, T. D.** s.l. : Elsevier, 1970, Journal of Colloid and Interface Science, Vol. 32, pp. 90–95.

22. *A model for surfactant distribution in latex coatings.* **Gundabala, Venkata R., Zimmerman, William B. and Routh, Alexander F.** s.l. : ACS Publications, 2004, Langmuir, Vol. 20, pp. 8721–8727.

23. *Comparison of surfactant distributions in pressure-sensitive adhesive films dried from dispersion under lab-scale and industrial drying conditions.* **Baesch, S., et al.** s.l. : ACS Publications, 2016, ACS Applied Materials & Interfaces, Vol. 8, pp. 8118–8128.

24. *Simulation of vertical surfactant distributions in drying latex films.* **Gromer, A., et al.** s.l. : ACS Publications, 2017, Langmuir, Vol. 33, pp. 561–572.

25. *Adhesion of latex films; influence of surfactants.* **Charmeau, J. Y., Kientz, E. and Holl, Y.** s.l. : Elsevier, 1996, Progress in organic coatings, Vol. 27, pp. 87–93.

26. *Surface analysis and adhesion properties of coalesced latex films.* **Zhao, Cheng-Le, et al.** s.l. : Wiley Online Library, 1989, British Polymer Journal, Vol. 21, pp. 155–160.

27. **Keddie, Joseph and Routh, Alexander F.** *Fundamentals of latex film formation: processes and properties.* s.l. : Springer Science & Business Media, 2010

28. *Effect of surfactant systems on the water sensitivity of latex films.* **Butler, Lauren N., Fellows, Christopher M. and Gilbert, Robert G.** s.l. : Wiley Online Library, 2004, Journal of applied polymer science, Vol. 92, pp. 1813–1823.

29. *Distribution of surfactants near acrylic latex film surfaces: A comparison of conventional and reactive surfactants (surfmers).* **Aramendia, Esteban, et al.** s.l. : ACS Publications, 2003, Langmuir, Vol. 19, pp. 3212–3221.

30. *Surfactant kinetics and their importance in nucleation events in (mini) emulsion polymerization revealed by quartz crystal microbalance with dissipation monitoring.* **Ballard, Nicholas, et al.** s.l. : ACS Publications, 2014, Langmuir, Vol. 30, pp. 9053–9062.

31. *A comprehensive experimental study of surfactant-free emulsion polymerization of styrene.* **Tauer, K., et al.** s.l. : Springer, 1999, Colloid and Polymer Science, Vol. 277, pp. 607–626.

32. *Study of the mechanism of the emulsifier-free emulsion polymerization of the styrene/4-vinylpyridine system.* **Wang, Y.-M. and Pan, C. Y.** s.l. : Springer, 1999, Colloid and Polymer Science, Vol. 277, pp. 658–665.

33. *Kinetics and mechanism of emulsifier-free emulsion copolymerization: Styrene-methyl methacrylate-acrylic acid system.* **Yan, Cui'e, Cheng, Shiyuan and Feng, Linxian.** s.l. : Wiley Online Library, 1999, Journal of Polymer Science Part A: Polymer Chemistry.

34. *Kinetics of particle growth in emulsion polymerization systems with surface-active initiators.* **Kusters, Joseph M. H., et al.** s.l. : ACS Publications, 1992, Macromolecules, Vol. 25, pp. 7043–7050.

35. *Surfactants with transfer agent properties (transurfs) in styrene emulsion polymerization.* **Vidal, F., Guillot, J. and Guyot, A.** s.l. : Springer, 1995, Colloid and Polymer Science, Vol. 273, pp. 999–1007.

36. *Reactive surfactants in heterophase polymerization.* **Asua, J. M. and Schoonbrood, H. A. S.** s.l. : Wiley Online Library, 1998, Acta Polymerica, Vol. 49, pp. 671–686.

37. *Reactive surfactants in emulsion polymerization.* **Guyot, Al and Tauer, K.** s.l. : Springer, 2005, Polymer Synthesis, pp. 43–65.

38. *Water Whitening Reduction in Waterborne Pressure-Sensitive Adhesives Produced with Polymerizable Surfactants.* **Aguirreurreta, Ziortza, et al.** s.l. : Wiley Online Library, 2015, Macromolecular Materials and Engineering, Vol. 300, pp. 925–936.

39. *Emulsifier-free emulsion polymerization produces highly charged, monodisperse particles for near infrared photonic crystals.* **Reese, Chad E. and Asher, Sanford A.** s.l. : Elsevier, 2002, Journal of colloid and interface science, Vol. 248, pp. 41–46.

40. *Some colloidal considerations on the surface characteristics of various emulsifier-free polymer latices.* **Tamai, Hisashi, Fujii, Akiharu and Suzawa, Toshiro.** s.l. : Elsevier, 1987, Journal of colloid and interface science, Vol. 116, pp. 37–41.

41. *Monodispersed colloidal spheres: old materials with new applications.* **Xia, Younan, et al.** s.l. : Wiley Online Library, 2000, Advanced Materials, Vol. 12, pp. 693–713.

42. *A simple geometrical model for emulsifier free polymer colloid formation.* **Dionigi, Chiara, et al.** s.l. : Elsevier, 2004, Journal of colloid and interface science, Vol. 275, pp. 445–449.

43. *Mechanism of emulsion polymerization of styrene in soap-free systems.* **Goodall, A. R., Wilkinson, M. C. and Hearn, J.** s.l. : Wiley Online Library, 1977, Journal of polymer science: Polymer chemistry edition, Vol. 15, pp. 2193–2218.

44. *Kinetics of emulsifier-free emulsion polymerization of styrene.* **Song, Zhiqiang and Poehlein, Gary W.** s.l. : Wiley Online Library, 1990, Journal of Polymer Science Part A: Polymer Chemistry, Vol. 28, pp. 2359–2392.

45. *Kinetics of the surfactant-free emulsion polymerization of styrene:-The post nucleation stage.* **Hearn, J., et al.** s.l. : Wiley Online Library, 1985, Journal of Polymer Science: Polymer Chemistry Edition, Vol. 23, pp. 1869–1883.

46. *Synthesis of crosslinked poly (methyl methacrylate) beads in emulsifier-free emulsion polymerization.* **Park, Moon Soo.** s.l. : Polymer Society of Korea/한국고분자학회, 1994, Korea Polymer Journal, Vol. 2, pp. 54–60.

47. **Ottewill, Ronald Harry and Candau, Françoise.** *An Introduction to Polymer Colloids.* s.l. : Springer, 1990.

48. *Colloid chemical studies of polystyrene latices polymerized without any surfaceactive agents: I. Method for preparing monodisperse latices and their characterization.* **Kotera, Akira, Furusawa, Kunio and Takeda, Yoko.** s.l. : Springer, 1970, Kolloid-Zeitschrift und Zeitschrift für Polymere, Vol. 239, pp. 677–681.

49. **Kotera, Akira, Furusawa, Kunio and Takeda, Yoko.** s.l. : Springer, 1970, Kolloid-Zeitschrift und Zeitschrift für Polymere, Vol. 239, pp. 677–681.

50. *Molecular-scale observation of the surface of polystyrene particles by AFM.* **Yamamoto, Tetsuya, et al.** s.l. : Elsevier, 2005, Journal of colloid and interface science, Vol. 292, pp. 392–396.

51. *Study of particle nucleation, flocculation, and growth in the emulsifier-free polymerization of styrene in water by total intensity light scattering and photon correlation spectroscopy.* **Munro, D., et al.** s.l. : Elsevier, 1979, Journal of Colloid and Interface Science, Vol. 68, pp. 1–13.

52. *Surfactant-free emulsion polymerization of various methacrylates: towards monodisperse colloids for polymer opals.* **Egen, Marc and Zentel, Rudolf.** s.l. : Wiley Online Library, 2004, Macromolecular chemistry and physics, Vol. 205, pp. 1479–1488.

53. *Block copolymers prepared by emulsion polymerization with poly (ethylene oxide)-azo-initiators.* **Tauer, K.** s.l. : Wiley Online Library, 1995, Polymers for Advanced Technologies, Vol. 6, pp. 435–440.

54. *Crosslinkable dextrin-coated latex via surfactant-free emulsion polymerization.* **Aouay, Mohamed, et al.** s.l. : Elsevier, 2022, Colloids and Surfaces A: Physicochemical and Engineering Aspects, Vol. 632, p. 127776.

55. *Controlled soap-free emulsion polymerization stability using a novel cationic azo radical initiator with chloride or triflate counter anion.* **Yamazaki, Takashi, et al.** s.l. : Elsevier, 2021, Colloids and Surfaces A: Physicochemical and Engineering Aspects, Vol. 609, p. 125614.

56. *Extending the limits of emulsifier-free emulsion polymerization to achieve small uniform particles.* **Sajjadi, Shahriar.** s.l. : Royal Society of Chemistry, 2015, RSC advances, Vol. 5, pp. 58549–58560.

57. *Uniform polymer beads of micrometer size.* **Horak, D.** s.l. : Wiley Online Library, 1996, Acta polymerica, Vol. 47, pp. 20–28.

58. **Asua, José M.** *Polymeric dispersions: principles and applications.* s.l. : Springer Science & Business Media, 2012. Vol. 335.

59. *The effect of acrylic acid amount on the colloidal properties of polystyrene latex.* **Polpanich, Duangporn, Tangboriboonrat, Pramuan and Elaïssari, Abdelhamid.** s.l. : Springer, 2005, Colloid and Polymer Science, Vol. 284, pp. 183–191.

60. *Development of a laser shock adhesion test for the assessment of weak adhesive bonded CFRP structures.* **Ehrhart, Bastien, et al.** s.l. : Elsevier, 2014, International Journal of Adhesion and Adhesives, Vol. 52, pp. 57–65.

61. *Effect of ionic monomer concentration on latex and film properties for surfactant-free high solids content polymer dispersions.* **Bilgin, Sevilay, Tomovska, Radmila and Asua, José M.** s.l. : Elsevier, 2017, European Polymer Journal, Vol. 93, pp. 480–494.

62. *Towards improved performance of waterborne polymer dispersions through creation of dense ionic interparticle network within their films.* **Argaiz, Maialen, Aguirre, Miren and Tomovska, Radmila.** s.l. : Elsevier, 2023, Polymer, Vol. 265, p. 125571.

63. *Carboxyl-stabilized emulsion polymers.* **Ceska, G. W.** s.l. : Wiley Online Library, 1974, Journal of Applied Polymer Science, Vol. 18, pp. 2493–2499.

64. *Emulsifier-free emulsion copolymerization of styrene and butyl acrylate. I. Kinetic studies in the absence of surfactant.* **Guillaume, J. L., Pichot, C. and Guillot, J.** s.l. : Wiley Online Library, 1990, Journal of Polymer Science Part A: Polymer Chemistry, Vol. 28, pp. 119–136.

65. *Control of particle size and its distribution in soapfree emulsion copolymerization of MMA-EA-AA.* **Kang, K., et al.** s.l. : SCIENCE PRESS, BEIJING, 2004, ACTA POLYMERICA SINICA, pp. 580–584.

66. *Effect of carboxylic acid monomer type on particle nucleation and growth in emulsifier-free emulsion copolymerization of styrene-carboxylic acid monomer.* **Abdollahi, Mahdi.** s.l. : Nature Publishing Group, 2007, Polymer journal, Vol. 39, pp. 802–812.

67. *The preparation and characterisation of polymer latices formed in the absence of surface active agents.* **Goodwin, J. W., et al.** s.l. : Wiley Online Library, 1973, British polymer journal, Vol. 5, pp. 347–362.

68. *Synthesis of cationic core-shell latex particles.* **Dziomkina, Nina V., Hempenius, Mark A. and Vancso, G. Julius.** s.l. : Elsevier, 2006, European polymer journal, Vol. 42, pp. 81–91.

69. *Preparation of highly sulfonated polystyrene model colloids.* **Kim, J. H., et al.** s.l. : Wiley Online Library, 1989, Journal of Polymer Science Part A: Polymer Chemistry, Vol. 27, pp. 3187–3199.

70. *Emulsifier-free emulsion copolymerization of styrene and sodium styrene sulfonate.* **Kim, J. H., et al.** s.l. : Wiley Online Library, 1992, Journal of Polymer Science Part A: Polymer1 Chemistry, Vol. 30, pp. 171–183.

71. *Suspension, emulsion, and dispersion polymerization: A methodological survey.* **Arshady, R.** s.l. : Springer, 1992, Colloid and polymer science, Vol. 270, pp. 717–732.

72. *Surfactant-free high solids content polymer dispersions.* **Bilgin, Sevilay, Tomovska, Radmila and Asua, José M.** s.l. : Elsevier, 2017, Polymer, Vol. 117, pp. 64–75.

73. *Emulsifier-free emulsion polymerization with ionic comonomer.* **Juang, Mike Shi-Der and Krieger, Irvin M.** s.l. : Wiley Online Library, 1976, Journal of Polymer Science: Polymer Chemistry Edition, Vol. 14, pp. 2089–2107.

74. *Effects of surface charge density on emulsion kinetics and secondary particle formation in emulsifier-free seeded emulsion polymerization of methyl methacrylate.* **Cheong, I. W. and Kim, J. H.** s.l. : Springer, 1997, Colloid and Polymer Science, Vol. 275, pp. 736–743.

75. *Seeded semicontinuous emulsion copolymerization of methyl methacrylate, butyl acrylate, and phosphonated methacrylates: Kinetics and morphology.* **Gaboyard, Manuel, et al.** s.l. : Wiley Online Library, 2003, Journal of Polymer Science Part A: Polymer Chemistry, Vol. 41, pp. 2469–2480.

76. *Emulsifier-free emulsion copolymerization of styrene and butyl acrylate. II. Kinetic studies in the presence of ionogenic comonomers.* **Guillaume, J. L., Pichot, C. and Guillot, J.** s.l. : Wiley

Online Library, 1988, Journal of Polymer Science Part A: Polymer Chemistry, Vol. 26, pp. 1937–1959.

77. *Comparative study on the colloidal stability mechanisms of sulfonate latexes.* **Peula, J. M., et al.** s.l. : ACS Publications, 1997, Langmuir, Vol. 13, pp. 3938–3943.

78. *Colloid stability and electrokinetic characterization of polymer colloids prepared by different methods.* **Peula-Garcia, J. M., Hidalgo-Alvarez, R. and De Las Nieves, F. J.** s.l. : Elsevier, 1997, Colloids and Surfaces A: Physicochemical and Engineering Aspects, Vol. 127, pp. 19–24.

79. *Preparation of ion-containing elastomers by emulsion copolymerization of dienes with olefinic sulfonic acid salts.* **Siadat, B., Oster, B. and Lenz, R. W.** s.l. : Wiley Online Library, 1981, Journal of Applied Polymer Science, Vol. 26, pp. 1027–1037.

80. *Stabilization of polymer dispersions by using ionic monomers.* **Bilgin, Sevilay.** 2017.

81. *Fundamentals of chemical incorporation of ionic monomers onto polymer colloids: paving the way for surfactant-free waterborne dispersions.* **Bilgin, Sevilay, Tomovska, Radmila and Asua, José M.** s.l. : Royal Society of Chemistry, 2016, RSC advances, Vol. 6, pp. 63754–63760.

82. *Bioenabled surface-mediated growth of titania nanoparticles.* **Kharlampieva, Eugenia, et al.** s.l. : Wiley Online Library, 2008, Advanced Materials, Vol. 20, pp. 3274–3279.

83. *Ionic inter-particle complexation effect on the performance of waterborne coatings.* **Argaiz, Maialen, et al.** s.l. : MDPI, 2021, Polymers, Vol. 13, p. 3098.

84. *Strategies towards improved performance of waterborne coatings through multiplying the ionic interparticle interactions.* **Argaiz, Maialen, Aguirre, Miren and Tomovska, Radmila.** s.l. : Elsevier, 2023, Progress in Organic Coatings, Vol. 183, p. 107731.

85. *Surface hydration: Principles and applications toward low-fouling/nonfouling biomaterials.* **Chen, Shenfu, et al.** s.l. : Elsevier, 2010, Polymer, Vol. 51, pp. 5283–5293.

86. *New insight into "polyelectrolyte effect".* **Yang, Hu, Zheng, Qiang and Cheng, Rongshi.** s.l. : Elsevier, 2012, Colloids and Surfaces A: Physicochemical and Engineering Aspects, Vol. 407, pp. 1–8.

87. *Effect of the intramolecular charge separation distance on the solution properties of betaines and sulfobetaines.* **Weers, Jeffry G., et al.** s.l. : ACS Publications, 1991, Langmuir, Vol. 7, pp. 854–867.

88. *Amphoteric poly (amido amine) s with adjustable balance between transfection efficiency and cytotoxicity for gene delivery.* **Sun, Yanping, et al.** s.l. : Elsevier, 2019, Colloids and Surfaces B: Biointerfaces, Vol. 175, pp. 10–17.

89. *Stable and pH-responsive polyamidoamine based unimolecular micelles capped with a zwitterionic polymer shell for anticancer drug delivery.* **Wang, Yan, et al.** s.l. : Royal Society of Chemistry, 2016, RSC advances, Vol. 6, pp. 17728–17739.

90. *Antifouling zwitterionic pSBMA-MSN particles for biomedical applications.* **Beltrán-Osuna, Ángela A., et al.** s.l. : Wiley Online Library, 2019, Polymers for Advanced Technologies, Vol. 30, pp. 688–697.

91. *Adsorption behavior of heavy metal ions on a polymer-immobilized amphoteric biosorbent: Surface interaction assessment.* **Zheng, Chaofan, et al.** s.l. : Elsevier, 2021, Journal of Hazardous Materials, Vol. 403, p. 123801.

92. *Upper critical solution temperature behavior of pH-responsive amphoteric statistical copolymers in aqueous solutions.* **Sharker, Komol Kanta, et al.** s.l. : ACS Publications, 2021, ACS omega, Vol. 6, pp. 9153–9163.

93. *Zwitterionic copolymer additive architecture affects membrane performance: fouling resistance and surface rearrangement in saline solutions.* **Kaner, Papatya, et al.** s.l. : Royal Society of Chemistry, 2019, Journal of Materials Chemistry A, Vol. 7, pp. 4829–4846.

94. *Covalent grafting of antifouling phosphorylcholine-based copolymers with antimicrobial nitric oxide releasing polymers to enhance infection-resistant properties of medical device coatings.* **Liu, Qiaohong, et al.** s.l. : ACS Publications, 2017, Langmuir, Vol. 33, pp. 13105–13113.

95. *Biocompatibility of phosphorylcholine coated stents in normal porcine coronary arteries.* **Whelan, D. M., et al.** s.l. : BMJ Publishing Group Ltd and British Cardiovascular Society, 2000, Heart, Vol. 83, pp. 338–345.

96. *Phosphorylcholine-containing polymers for biomedical applications.* **Iwasaki, Yasuhiko and Ishihara, Kazuhiko.** s.l. : Springer, 2005, Analytical and bioanalytical chemistry, Vol. 381, pp. 534–546.

97. *Why do phospholipid polymers reduce protein adsorption?* **Ishihara, Kazuhiko, et al.** s.l. : Wiley Online Library, 1998, Journal of Biomedical Materials Research: An Official Journal of The Society for Biomaterials, The Japanese Society for Biomaterials, and the Australian Society for Biomaterials, Vol. 39, pp. 323–330.

98. *Phosphorylcholine impairs susceptibility to biofilm formation of hydrogel contact lenses.* **Selan, Laura, et al.** s.l. : Elsevier, 2009, American journal of ophthalmology, Vol. 147, pp. 134–139.

99. *The unique hydration state of poly (2-methacryloyloxyethyl phosphorylcholine).* **Ishihara, Kazuhiko, et al.** s.l. : Taylor & Francis, 2017, Journal of Biomaterials Science, Polymer Edition, Vol. 28, pp. 884–899.

100. *Preparation of 2-methacryloyloxyethyl phosphorylcholine copolymers with alkyl methacrylates and their blood compatibility.* **Ueda, Tomoko, et al.** s.l. : Nature Publishing Group, 1992, Polymer Journal, Vol. 24, pp. 1259–1269.

101. *Synthesis and solution properties of zwitterionic polymers.* **Lowe, Andrew B. and McCormick, Charles L.** s.l. : ACS Publications, 2002, Chemical reviews, Vol. 102, pp. 4177–4190.

102. *Hydrophobically modified sulfobetaine copolymers with tunable aqueous UCST through postpolymerization modification of poly (pentafluorophenyl acrylate).* **Woodfield, Peter A., et al.** s.l. : ACS Publications, 2014, Macromolecules, Vol. 47, pp. 750–762.

103. *The direct synthesis of sulfobetaine-containing amphiphilic block copolymers and their self-assembly behavior.* **Doncom, Kay E. B., Willcock, Helen and O'Reilly, Rachel K.** s.l. : Elsevier, 2017, European Polymer Journal, Vol. 87, pp. 497–507.

104. *Molecular simulation studies of protein interactions with zwitterionic phosphorylcholine self-assembled monolayers in the presence of water.* **He, Yi, et al.** s.l. : ACS Publications, 2008, Langmuir, Vol. 24, pp. 10358–10364.

105. *Dual thermo-and pH-responsive zwitterionic sulfobataine copolymers for oral delivery system.* **Chen, Ching-Yi and Wang, Hsiang-Ling.** s.l. : Wiley Online Library, 2014, Macromolecular rapid communications, Vol. 35, pp. 1534–1540.

106. *A new type of polyampholyte: Poly (4-vinyl pyridine betaine).* **Ladenheim, Harry and Morawetz, Herbert.** s.l. : Wiley Online Library, 1957, Journal of Polymer Science, Vol. 26, pp. 251–254.

107. *Development of zwitterionic polymer-based doxorubicin conjugates: tuning the surface charge to prolong the circulation and reduce toxicity.* **Wang, Zhen, et al.** s.l. : ACS Publications, 2014, Langmuir, Vol. 30, pp. 3764–3774.

108. *Dual-functional biomimetic materials: nonfouling poly (carboxybetaine) with active functional groups for protein immobilization.* **Zhang, Zheng, Chen, Shengfu and Jiang, Shaoyi.** s.l. : ACS Publications, 2006, Biomacromolecules, Vol. 7, pp. 3311–3315.

109. *Effect of the intramolecular charge separation distance on the solution properties of betaines and sulfobetaines.* **Weers, Jeffry G., et al.** s.l. : ACS Publications, 1991, Langmuir, Vol. 7, pp. 854–867.

110. *Functionalizable surface platform with reduced nonspecific protein adsorption from full blood plasma—Material selection and protein immobilization optimization.* **Vaisocherová, Hana, et al.** s.l. : Elsevier, 2009, Biosensors and Bioelectronics, Vol. 24, pp. 1924–1930.

111. *Sulfobetaine zwitterionomers based on n-butyl acrylate and 2-ethoxyethyl acrylate: Monomer synthesis and copolymerization behavior.* **Gauthier, Mario, Carrozzella, Tony and Penlidis, Alexander.** s.l. : Wiley Online Library, 2002, Journal of Polymer Science Part A: Polymer Chemistry, Vol. 40, pp. 511–523.

112. *Sulfobetaine zwitterionomers based on n-butyl acrylate and 2-ethoxyethyl acrylate: Physical properties.* **Gauthier, Mario, Carrozzella, Tony and Snell, Greg.** s.l. : Wiley Online Library, 2002, Journal of Polymer Science Part B: Polymer Physics, Vol. 40, pp. 2303–2312.

113. *Reconciling low-and high-salt solution behavior of sulfobetaine polyzwitterions.* **Mary, Pascaline, et al.** s.l. : ACS Publications, 2007, The Journal of Physical Chemistry B, Vol. 111, pp. 7767–7777

114. *Synthetic electrical analog of Proteins1.* **Alfrey Jr, Turner, et al.** s.l. : ACS Publications, 1950, Journal of the American Chemical Society, Vol. 72, pp. 1864–1864.

115. *Soap-free emulsion polymerization of n-butyl acrylate: Copolymerization with 1, 1-(dimethyl)-1-(3-methacryloxyethyl)-1-(sulfopropyl) ammonium betaine.* **Blom, Henk P., et al.** s.l. : Wiley Online Library, 1998, Journal of applied polymer science, Vol. 70, pp. 227–236.

116. *Cationic and zwitterionic polymerizable surfactants: quaternary ammonium dialkyl maleates. 1. Synthesis and characterization.* **Abele, S., et al.** s.l. : ACS Publications, 1999, Langmuir, Vol. 15, pp. 1033–1044.

117. *Emulsifier-Free Emulsion Copolymerization of Vinyl Acetate and 3-Dimethyl (methacryloyloxyethyl) ammonium Propanesulfonate and Swelling Behavior of their Copolymer Matrices.* **Kamenska, Elena, et al.** s.l. : Wiley Online Library, 2007, Macromolecular Reaction Engineering, Vol. 1, pp. 553–562.

118. *Synthesis and characterization of novel drug delivery nanoparticles based on polyzwitterionic copolymers.* **Kostova, Bistra, et al.** s.l. : Elsevier, 2013, European polymer journal, Vol. 49, pp. 637–645.

119. *Hierarchically engineered membrane surfaces with superior antifouling and self-cleaning properties.* **Zhao, Xueting, et al.** s.l. : Elsevier, 2013, Journal of membrane science, Vol. 441, pp. 93–101.

120. *Synthesis and analysis of zwitterionic spherical polyelectrolyte brushes in aqueous solution.* **Polzer, Frank, et al.** s.l. : ACS Publications, 2011, Macromolecules, Vol. 44, pp. 1654–1660.

121. *Highly monodisperse zwitterion functionalized non-spherical polymer particles with tunable iridescence.* **Vasantha, Vivek Arjunan, et al.** s.l. : Royal Society of Chemistry, 2019, RSC advances, Vol. 9, pp. 27199–27207.

122. *Improved antibiofouling properties of photobioreactor with amphiphilic sulfobetaine copolymer coatings.* **Wang, Yixuan, et al.** s.l. : Elsevier, 2020, Progress in Organic Coatings, Vol. 144, p. 105666.

123. *Photoresponsive behaviour of zwitterionic polymer particles with photodimerizable groups on their surfaces.* **Miyata, Takashi, et al.** s.l. : Royal Society of Chemistry, 2022, Journal of Materials Chemistry B, Vol. 10, pp. 2637–2648.

124. *Synthesis of zwitterionic polymer and its application in textile stiffening finish.* **Yu, Xia, et al.** s.l. : Wiley Online Library, 2022, Journal of Applied Polymer Science, Vol. 139, p. 51560.

125. *Characterisation of multifunctional colloids synthesided via aqueous emulsion polymerisation mediated by macromolecular chain transfer agent (macro-CTA).* **Alkorta Salegi, Janire.** 2019.

Chapter 2. Selection of Zwitterionic Monomer and Initiator for High Solids Content Surfactant-Free Waterborne Coatings

2.1. Introduction

As highlighted in the introduction chapter, the use of surfactants in water-based polymer dispersions has a significant impact on their colloidal properties and the microstructure of the polymer films. To address this issue and maintain stable emulsions without relying on surfactants, one promising approach might be the chemical incorporation of zwitterionic monomers onto the polymer particles. This strategy effectively would avoid the detrimental effects caused by the migration of hydrophilic species and preserves the desirable application properties. The use of zwitterionic monomers as in situ stabilizing species presents an enticing alternative to traditional surfactants.

Preliminary studies are essential to choose the best zwitterionic monomer for surfactant-free emulsion polymerization. This chapter delves into the process of choosing a suitable ZM specifically for the synthesis of MMA/n-BA high S.C. latex for coating applications. However, the use of zwitterionic monomers in emulsion polymerizations in literature is very rare to find[1-4] as they are primarily used in biological[5-7] and antifouling applications.[8-10]

Due to the complex synthesis process involved, comparison studies between zwitterionic monomers have been found to be scarce. In a study by van Andel et al.,[11] a comparison was made between different monomers used in antifouling coatings. The ZMs utilized in this study encompassed sulfobetaines, carboxybetaine, a phosphocholine, and an additional hydroxyl acrylamide monomer. The findings revealed that both the distance between opposite charges and the nature of the anionic groups

significantly influenced the antifouling performance of the coatings. Acrylamide and carboxybetaine ZM demonstrated the most favorable results in terms of antifouling properties. Birkimer et al.[12] conducted a study focused on comparing carboxybetaine and sulfobetaine zwitterionic monomers for stimuli-responsive ultrafiltration membranes. The research specifically investigated the effects of salt concentration and pH on the membrane performance. The results indicated that SB exhibited the best response across all pH levels studied. Conversely, CB were highly influenced by pH, suggesting that the protonation of the carboxylic acid side group played a significant role in the behavior and performance of the membranes. Zhao et al.[13] carried out a comparison of various ZMs for hydrogel applications. The study focused on assessing the swelling degree and mechanical properties and the results showed that CB ZM exhibited the highest swelling degree and superior mechanical properties, while SB ZM displayed a high crosslinking density. These variations in properties were attributed to differences in the intra-inter- molecular interactions among the zwitterionic units.

As previously discussed, achieving a high level of chemical incorporation of the selected zwitterionic monomer is essential to minimize the formation of water-soluble oligomers and as well as for improved properties. In this regard, the role of initiators is of paramount importance.

The entry of oligoradicals into polymer particles has been studied in the presence of monomers with limited or low water solubility, focusing on the effect of different types of initiators.[14-17] Additionally, there are reports available on studies that investigate the effect of initiator type on the chemical incorporation of water-soluble monomers into hydrophobic polymers.[18-23] Kim et al.[18] conducted a study to investigate the copolymerization of styrene and sodium styrene sulfonate using both thermal and redox initiators that were either water-soluble or oil-soluble. The results showed that the use of oil-soluble initiators led to significant coagulation. Although the utilization of potassium persulfate enhanced latex stability, a considerable amount of coagulum was still formed. The application of a redox initiator (potassium persulfate/sodium bisulfate) yielded the best outcomes, possibly due to the

generation of more sulfate end groups. However, the incorporation was not studied. Bilgin and coworkers[20] conducted another study to investigate the impact of the initiator system on the chemical incorporation of NaSS onto MMA/n-BA polymer particles at a high solids content. Initiators with various water solubility and decomposition mechanisms were used, and it was found that the redox initiator tert-butyl hydroperoxide /ascorbic acid (TBHP/As.Ac) resulted in the highest incorporation of NaSS. It happens due to creation of hydrophobic radicals in aqueous phase that decreases the time spent by growing oligoradicals in aqueous phase and decrease the possibility of termination there. Additionally, they examined the versatility of NaSS in stabilizing different monomer systems.

In another study, Shi Wang[24] and colleagues conducted an investigation into the nucleation and kinetics of emulsion polymerization of hydrophobic monomer n-butyl methacrylate (n-BMA) using KPS and a redox initiator consisting of hydrogen peroxide (HPO), As.Ac, and ferrous ion (Fe^{2+}). The study aimed to compare the effects of the two initiators on polymerization kinetics, degree of polymerization (DP), and molar mass $\overline{M_W}$. The findings revealed that the use of the redox initiator resulted in the formation of small, monodisperse particles with a high reaction rate and low $\overline{M_W}$.

To the best of the authors' knowledge, there is currently no existing research found on the incorporation of zwitterionic monomers in emulsion systems using various initiators.

This chapter is focus first on finding out the most suitable commercially available zwitterionic monomer ZM to synthesize surfactant-free MMA/n-BA polymer dispersions and second, to study the effect of the initiator systems on the incorporation of the selected ZM onto the polymer particles. To do so, commercially available three zwitterionic monomers presenting different anionic group were chosen, (methacryloxy) ethyl 2-(trimethylammonio) ethyl phosphate (M-2005), 3-[[2-(methacryloxy) ethyl] dimethylammonio] propionate (M-2359) and 2-(methacryloyloxy) ethyl] dimethyl-(3-sulfopropyl) ammonium hydroxide (DMAPS), presenting a phosphate, carboxylic and sulfonate, respectively. Then,

a series of surfactant-free batch emulsion polymerizations of MMA/n-BA by using the zwitterionic monomer as the unique stabilizing specie were carried out in the tumbler.

After selecting the most suitable ZM, the effect of the initiator system on the chemical incorporation of the previously selected ZM onto MMA/n-BA polymer particles was studied by using seeded semi-continuous emulsion polymerization at high solids content (50%) in which the seed was stabilized with a conventional surfactant. The initiators employed presented different water solubility and decomposition mechanisms. Potassium persulfate and azobisisobutyronitrile (AIBN) were used as thermal initiators, while tert-butyl hydroperoxide/ascorbic acid ,tert-butyl hydroperoxide/Bruggolite FF7 and hydrogen peroxide/ascorbic acid were used as redox initiators. The same seed was used in all the reactions in order to avoid the differences in particle size and consequently number of particles that may affect the oligo radical entry [25] and consequently the zwitterionic monomer incorporation onto the polymer particles.

2.2. Experimental section

2.2.1. Materials

The materials are given in Appendix I.

2.2.2. Polymerizations

2.2.2.1. Surfactant-free batch emulsion polymerizations in the tumbler

In order to make a screening that may help in selecting a suitable zwitterionic monomer and observe how other parameters (type of initiator, initiator concentration, and pH) affect the colloidal stability, a series of surfactant-free reactions were conducted in batch emulsion polymerization in the tumbler. This approach facilitates the concurrent execution of multiple reactions in distinct bottles at the same temperature but under different reaction conditions. The bottles are placed in a rotating

apparatus, to guarantee efficient mixing and consistency of the reactions. For that aim, commercially available three different zwitterionic monomers, M-2005, M-2359 and DMAPS were selected. All ZMs share the same cation, quaternary ammonium, but differ in their anionic group. M2359 presents a carboxylic group attached at the end, while M2005 has a phosphate anionic group located in the center, between the quaternary ammonium and the methacrylic moiety. On the other hand, DMAPS contains a sulfonate group attached at the end and in contrast to the other two ZMs presents an additional methylene group between the quaternary ammonium and the sulfonate. Their structures are illustrated in Scheme 2.1.

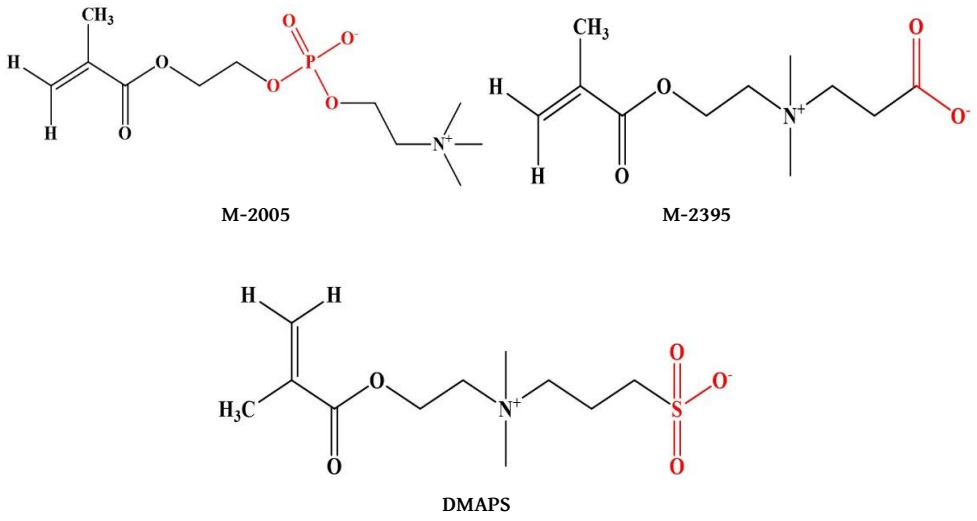

Scheme 2.1. Chemical structure of the different zwitterionic monomers used in this study. Anionic groups are marked in red colour.

In all surfactant-free batch emulsion polymerizations carried out in the tumbler, the main monomers (MMA/n-BA) (50/50) in S.C. of 10% were kept constant and the following parameters were varied: the type and amount of ZM, the amount and type of initiator, as well as the pH prior to polymerization.

Appendix I provides detailed information about the reactions that occur within the tumbler while Table I.1 outlines the specific conditions under which these reactions were studied.

2.2.2.2. Synthesis of the waterborne polymer latex

To synthesize waterborne latex stabilized by ZM DMAPS, a two-step seeded semi-batch emulsion polymerization approach was adopted. This involved using a standard acrylic formulation composed of a 50/50 ratio of n-BA and MMA. The initial phase consisted of synthesizing a seed using n-BA/MMA (50/50) at a solids content of 10%, using conventional surfactant sodium dodecyl sulfate (SDS). More detailed information about the synthesis procedure and formulations for the seed preparation can be found in Appendix I, Table I.2.

Afterward, the seed was grown using a semi-batch emulsion copolymerization method. The balance between the main monomers, n-BA and MMA, remained at an even 1:1 weight ratio.

In order to study the effect of initiator type on the colloidal stability and further film properties, five different initiators KPS, AIBN, HPO / As.Ac, TBHP/As.Ac, TBHP/FF7were used. KPS was used as a water-soluble thermal initiator that forms negatively charged hydrophilic radicals in the aqueous phase. AIBN was used as an oil soluble thermal initiator that forms radical pairs in the oil phase. Its partitioning in water is very small and its contribution to the overall conversion has been seen to be almost negligible.[28] On the other hand, HPO/As.Ac, TBHP/As.Ac and TBHP/FF7 were chosen as redox initiators. In the case of HPO/As.Ac, both components are water-soluble and yield neutral hydrophilic hydroxyl radicals. Concerning TBHP/As.Ac and TBHP/FF7, TBHP distributes between the organic and aqueous phase whereas As.Ac and FF7 are water soluble. Both redox pairs yield the same tert-butoxy neutral radicals in an aqueous phase, which are hydrophobic enough to directly enter into the organic phase. The radical formation in each initiator system is presented in Scheme 2.2.

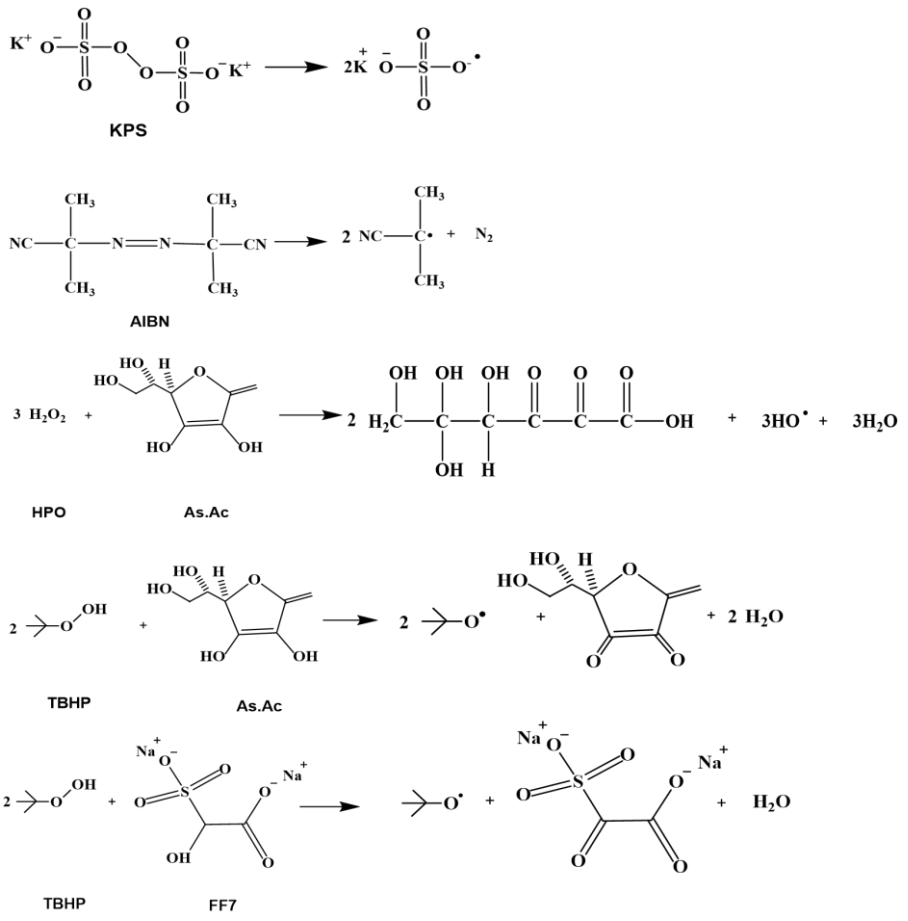

Scheme 2.2. Radical formation from the studied initiators.

Emulsion polymerization is carried out at temperatures ranging from 50 to 90 °C. Thermal initiators are used above their decomposition, however, redox pairs present a much higher radical generation rate and do not require so high temperatures. Therefore, taking this into account the reactions carried out with thermal and redox initiators were carried out at 70 °C and 50 °C, respectively.

On the other hand, since the components of a redox pair react quickly, it is usually introduced at least one of them into the reactor while the other one is fed along the reaction. However, determining the best feeding strategy for the redox system is a complex task. For instance, in the case of HPO/As.Ac, adding As.Ac to the HPO in the reactor was found to produce more free radicals than adding HPO to As.Ac[29,30] Since conducting a similar investigation was out of the scope of this work, the oxidant (TBHP or HPO) was added as a shot once the desired temperature was reached and the reductant (As.Ac or FF7) was fed during the reaction.

Appendix I outlines a comprehensive synthesis procedure for the seeded semi-continuous reaction and the corresponding recipes employed can be found in Table I.3.

2.2.3. Characterization

The characterization methods are given in Appendix II.

2.3. Results and discussion

2.3.1. Surfactant-free batch emulsion polymerizations in the tumbler

The characteristics of the surfactant-free batch emulsion polymerizations at 10% S.C., conducted in the tumbler in order to identify the most suitable zwitterionic monomer are given in Table 2.1. The smaller particle size, lack of coagulum and high monomer conversion were actually the criteria to determine the zwitterionic monomer, which is the most suitable for the present system.

Table 2.1. Characteristics of the surfactant-free latexes synthesized in batch emulsion polymerization in the tumbler (10% S.C.).

ZM	ZM (wbm %)	Initiator	Initiator (wbm %)	pH	Xt (%)	Dp (nm)	Coagulum (%)
M-2005	0.5-3 [a]	TBHP/As.Ac	0.5	8-9	-	-	-
	2	TBHP/As.Ac	1	2-3	8	-	-
	2	TBHP/FF7	1	2-3	32	-	Complete [c]
	0.5	KPS	1	6-7	96	417	6
	1	KPS	1	6-7	98	308	0
	2	KPS	1	6-7	100	230	0
	2	KPS	1	2-3	90	444	8
M-2359	0.5	TBHP/FF7	0.5	6-7	98	584	11
	2	TBHP/FF7	0.5	6-7	97	414	2
	2	TBHP/FF7	1	2-3	-	-	Complete
	2	TBHP/As.Ac	1	2-3	-	-	Complete
	2	KPS	1	2-3	-	-	Complete
DMAPS	0.5-1 [b]	TBHP/FF7	0.5	6-7	-	-	-
	2	TBHP/FF7	0.5	6-7	100	275	0
	3	TBHP/FF7	0.5	6-7	97	242	2
	2 [b]	TBHP/As.Ac	1	6-7	-	-	-
	2	KPS	1	6-7	100	489	0

[a] Monomers did not react, [b] phase separation of latex, [c] the coagulum was so big that was not possible to take it out from the bottle.

With respect to the phosphate containing monomer M-2005, it was found that when TBHP/As.Ac was used as redox initiator all the reactions failed independently of the amount of ZM, initiator or pH used. One should keep in mind that both components from the redox pair were included in the reactor since the beginning, which could accelerate the radical consumption. When TBHP/FF7 (1 wbm %) redox pair was used in the synthesis by using 2 wbm % M-2005 under acidic conditions, the reaction took place, however, the amount of coagulum was so big that it was not possible to remove it from the bottle in order to be quantified. Indeed, this result was expected working under acidic conditions the phosphate might be partially protonated, losing the ability to stabilize. The thermal initiator KPS seems to be the best candidate for the synthesis of surfactant-free latex stabilized with M-2005 since almost full conversion with negligible coagulum was obtained in all the reactions. When the reactions were carried

at neutral pH, the particle size decreased as the amount of M-2005 increased indicating clearly a higher incorporation of M-2005 in the polymer particles. However, when the reaction was performed under acidic conditions (even with the highest ZM concentration) the particle size increased significantly (444 nm), reaching sizes bigger than those obtained with the lowest ZM concentration under neutral pH (417 nm). Moreover, the conversion was also decreased, and some coagulum was observed, too. As explained before, the reason might be the partial protonation of the phosphate group under acidic conditions. Nevertheless, the good results obtained with KPS might be also related with the additional charges arising from the initiator because KPS,[31, 32] forms negatively charged radicals in contrast to the redox pairs studied.

Moving to the carboxylate containing ZM M-2359, when the reactions were carried out under neutral pH the reactions reached almost full conversion and with negligible amount of coagulum. When TBHP/FF7 was used as initiator, it was found that by increasing the ZM concentration the particle size decreased similar to what was observed for M-2005 with KPS, indicating a higher incorporation of M-2359, however, this time the particle sizes were bigger but also the amount of initiator used was lower.

When the reactions were performed under acidic conditions, independently of the initiator used the dispersions coagulated completely. Under the acidic conditions, the carboxylate group is mainly protonated losing the stabilization capacity; moreover, in contrast to M-2005 this time the charges arising from the KPS were not able to stabilize the system.

Following with ZM DMAPS, which has a sulfonate anionic group, all the reactions were carried out under neutral pH. Again, similar to what was observed for M-2359 (carboxylate group containing ZM), when the amount of ZM increased the particle size decreased when TBHP/FF7 was used as initiator, however, a minimum amount of ZM (>1%) was required. Nevertheless, the particle size was significantly lower (about 200 nm smaller) when DMAPS was employed with compared to M-2359. This time KPS did not

work so well because even using higher initiator concentration the particle size was close to the double than with redox pair.

From the aforementioned reactions, it is clear that due to the pH dependency of M-2359 and M-2005 the reactions should be carried under neutral pH. Considering full conversion, lowest particle size and absence of coagulum, the best results were obtained for M-2005 (2%) when 1% of KPS was used as initiator and for DMAPS (2%) when 0.5% TBHP/FF7 was used as redox pair initiator. Even the particle size obtained for M-2005 was slightly smaller it was decided to continue working with DMAPS because of different reasons. On one hand, because in order to properly study the effect of ZMs on the colloidal stability additional charges that may provide stability to the polymer particles as the case of negative charges arising from KPS were preferably avoided. On the other hand, because it is not pH dependent and it is the cheapest commercially available ZM, therefore, DMAPS was selected as the most suitable ZM and was further studied.

It is worth noting that the reactions were conducted in a tumbler, where the reaction conditions may be compromised and could affect the latex stability and because of this better result would be expected when moving to mechanically stirred reactors.

2.3.2. Seed synthesis

Following the best conditions obtained from the screening carried out in the tumbler, a surfactant-free seed with 10% S.C. stabilized with DMAPS using TBHP/FF7 as the redox initiator was performed in a mechanically stirred jacketed glass reactor. Nevertheless, the particle size was found too large to be used as a seed and therefore, a seed stabilized with conventional surfactant SDS was synthesized in order to get a smaller particle size that will be further used in all the seeded semi-continuous emulsion polymerization. Complete MMA/n-BA conversion was achieved, resulting in

particle size of 96 nm. Linear polymer chains with an average molar mass of 175 KDa were achieved, without any coagulum formation.

Table 2.2. Characteristics of the seed synthesized with SDS.

Stabilizer	Dp (nm)	Coagulum (%)	Gel (%)	$\overline{M_W}$ (kDa)	Đ
SDS	96	0	0	175	2.1

2.3.3. Seeded semi-continuous emulsion polymerization reactions

In an attempt to study the effect of the type of initiator on the colloidal stability of MMA/n-BA (50/50), high solids content (50%) latexes stabilized by DMAPS were polymerized by seeded semi-continuous mode employing the seed stabilized with SDS and different type of initiators. Stable latexes were produced with all the initiators except for AIBN and HPO/As.Ac. Their main characteristics are shown in Table 2.3.

Table 2.3. Characteristics of latexes stabilized with 2% DMAPS synthesized by seeded semi-continuous emulsion polymerization using different type of initiators.

Initiator	Xt (%)	Coagulum (%)	Dp (nm)	WSO* (g)	Gel (%)	$\overline{M_W}$ (kDa)	Incorporation (%)
AIBN	-	-	-	-	-	-	-
HPO/As.Ac	-	-	-	-	-	-	-
KPS–Feed	91	21	877	1.86	65	776	27
KPS-Shot	100	0	472	2.1	72	380	12
TBHP/As.Ac	87	14	630	1.6	0	145	34
TBHP/FF7	100	0	275	1.45	0	343	51

***WSO water-soluble oligomers**

The reaction performed with AIBN was unsuccessful, likely because AIBN forms radicals in polymer particles, which prevented them from reacting with DMAPS mainly located in the aqueous phase hindering the creation of in situ stabilizing species and as consequence provoking coagulation. Although

radicals can also be generated in the aqueous phase by the water-soluble fraction of AIBN, their contribution to the overall polymerization rate is almost negligible.[28]

In the case of HPO/As.Ac, the polymerization was neither successful. It can be due to the opposite reason than in case of AIBN, due to the highly hydrophilic nature of the hydroxyl radicals formed and the high concentration of DMAPS in aqueous phase. In such conditions, likely the average time of the growing radicals spent in the aqueous phase was too long, which increased the probability of termination in aqueous phase. Consequently, a high number of water-soluble species was likely produced that negatively affected the colloidal stability in the system.

When KPS was fed into the reactor, almost full conversion was achieved with a significant amount of coagulum (21%). As the initiator was fed, it is likely the concentration of radicals was too low to produce the sufficient amount of stabilizing units (oligomer chains in which DMAPS was incorporated), leading to coagulation of the growing particles in the system. The particle size in the latex was large (877 nm), which additionally was affected by the high concentration of water-soluble species in the system. On the contrary, when KPS was added as a shot, no coagulum was formed, which means the high number of radicals formed allowed the development of enough stabilizing species. However, the average particle size in this case was also high, which likely is a consequence of presence of water-soluble oligomers that increase the ionic strength in the system and decrease the colloidal stability inducing particle coagulation. The particle size was significantly lower when the KPS was added as a shot than when it was fed, which is an indication of a higher incorporation of DMAPS onto the polymer particles. However, the results on zwitterionic incorporation shown in Table 2.3 show opposite trend, and the incorporation in case of reaction with KPS shot the incorporation is very low (12%). In both reactions with KPS, high gel fraction was obtained 65% and 72%, KPS-Feed and KPS-Shot, respectively. The presence of free sulfate ions originating from KPS could be responsible for this effect, resulting in an increased ion concentration that renders the polymer chains insoluble in THF. Additionally, one should consider that

these reactions were performed at higher temperature than the redox couple initiator reactions, which could also affect the chain transfer to polymer reaction, contribute to higher gel fraction.[33]

In case of TBHP/As.Ac, redox couple initiator, lower conversion, relatively high coagulum amount and large average particle size (630 nm) was obtained. Conversely, the best results in terms of stability and particle sizes were obtained in case of TBHP/FF7 redox couple, which gave rise to full conversion, no coagulum and smallest average particle size (275 nm), that was related with the highest incorporation of DMAPS onto the polymer particles (51%), as seen in Table 2.3. The lower conversion achieved with TBHP/As.Ac cannot be attributed to the hydrophilicity of the radical since in both cases tert-butoxy radicals are produced therefore, it suggests that TBHP/As.Ac was consumed faster than TBHP/FF.[35] Moreover, the tert-butoxy radicals formed from TBHP/As.Ac and TBHP/FF7 are non-ionic and hydrophobic, which does not contribute to the hydrophilicity of the oligomers formed. This strategy as shown in Table 2.3 allows minimizing the water-soluble oligomers formation and increased incorporation of DMAPS onto polymer particles, which is a condition for colloidal stability.

Figure 2.1. Illustrates the evolution of the conversion of the volatile monomers (MMA and n-BA) in the seeded semi-continuous reactions using different type of initiators. A clear inhibition period for the reaction with KPS-Feed at the beginning was noticed, probably arising from the low radical concentration and lack of sufficient stabilizing unites, resulting finally in particle coagulation and large quantity of coagulum creation. Although MMA/n-BA conversion was 91%, taking into account the coagulum, it was considered that full monomer conversion was obtained. On the contrary, when KPS was added as a shot in the beginning of the reaction, the reaction was much faster due to the higher radical generation rate, inhibition period was disappeared, and full conversion without coagulum was achieved. When redox initiator TBHP/As.Ac was used an inhibition period of about 50 min was observed, similarly to KPS-Feed. Afterwards, the reaction was faster, however, lower conversion (87%) was achieved. Taking into account the large amount of coagulum (14%), it was considered that the

conversion was certainly higher. The reaction carried out with the TBHP/FF7 redox couple was faster than the reaction carried with TBHP/As.Ac and resulted in full conversion with no coagulum.

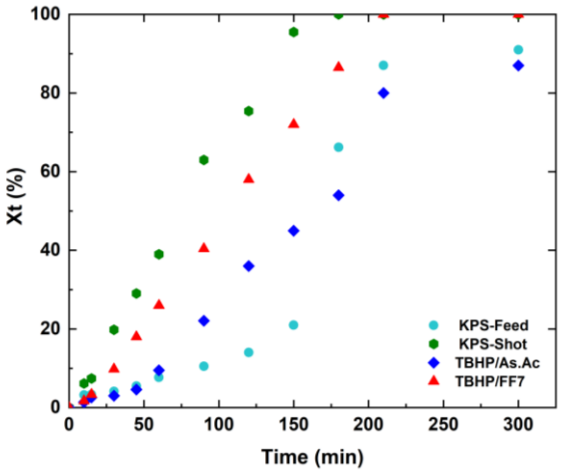

Figure 2.1. Time evolution of the conversion of the volatile (MMA/n-BA) monomers for the seeded semi-continuous reactions performed using different type of initiators.

Figure 2.2 shows the evolution of the particle size along the reaction for the polymerization reactions performed with different initiators. The experimental and theoretical particle sizes were determined and compared. The theoretical sizes were calculated by assuming a constant number of particles throughout the reactions. As expected, the particle size increased over time, however, only the reaction synthesized with TBHP/FF7 followed the theoretical particle size evolution, which once again shows the excellent colloidal stabilization in this system. In the case of KPS-Feed, the particle size remained constant during the initial reaction period but suddenly increased to 872 nm, indicating significant coagulation due to the lack of stabilizing species and formation of large amount of water-soluble species. When KPS was added as a shot, the average particle size of 473 nm was obtained by slow growing during the reaction. The particle size was smaller for TBHP/FF7, where the incorporation of DMAPS onto polymer particles was likely the most important factor, resulting in a final particle size of 275 nm. This

in fact left less quantity of DMAPS to create water-soluble species, which means that this dispersion would have the lower ionic strength, which is additional for better colloidal stability. In that case, TBHP produced hydrophobic radicals that are prone to enter into particles immediately after creation in water phase. However, when TBHP was used in combination with As.Ac, the particle size followed the expected particle size evolution until about 180 min when it started increasing significantly and doubled the particle size during the last 2 hours of the reaction, indicating coagulation, and a final average particle size of 672 nm was produced due to likely the lower DMAPS incorporation onto the polymer particles (Table 2.3) arising from the faster radical consumption.[35]

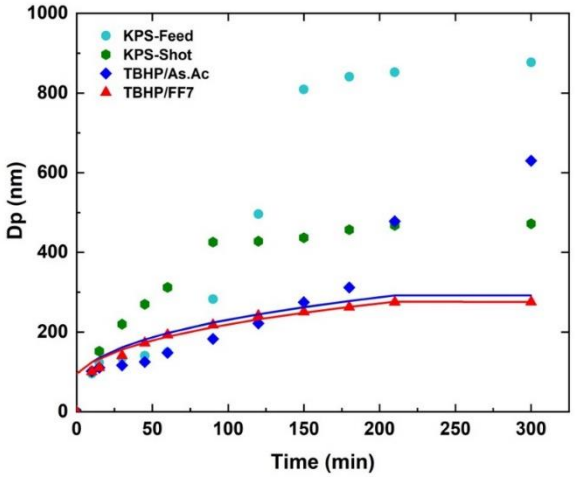

Figure 2.2. Time evolution of particle size for the seeded semi-continuous reactions performed by using different type of initiators. Experimental values are indicated by dots and theoretical once by continuous lines.

Figure 2.3 presents the evolution of the number of particles (Np, calculated from DLS measurements) for the seeded semi-continuous emulsion polymerizations carried out with different initiator and feeding strategies. It can be seen that, after the initial drop, Np remained relatively constant for all the reactions. The decrease was more pronounced for KPS-Shot system, probably due to the creation of high amount of WSO (Table 2.3) that were not contributing to the particle stability.

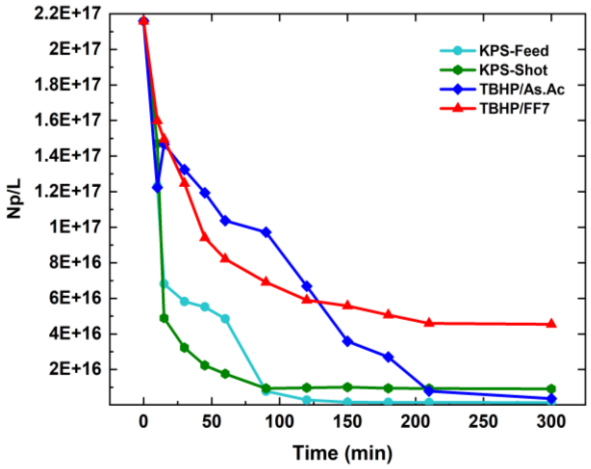

Figure 2.3. Time evolution of the number of particles (Np) in the seeded semi-continuous emulsion polymerization carried out with different type of initiators.

On the other hand, complete conversion of DMAPS was achieved in all the reactions as confirmed by ^{1}H NMR. In Appendix II, the provided ^{1}H NMR spectra (Figure II.I) showcase reaction mixtures with ZM DMAPS at various reaction times, utilizing the TBHP/FF7 initiator. The integration of vinyl hydrogen peaks was conducted to assess monomer conversion. These spectra distinctly indicate that after 5 hours of reaction, there is no observable unreacted ZM DMAPS in the system. This observation suggests a complete conversion, a trend consistent across different initiators.

The characteristics of the final latexes summarized in Table 2.3 show that the type of initiator and the feeding strategy affect the incorporation of DMAPS onto the polymer particles and consequently the colloidal stability. The results indicate that the differences on the particle sizes observed are due to the different amount of DMAPS incorporated onto the polymer particles that might be related to both, the locus of the radical generation and the hydrophobicity of the oligo radicals formed in the aqueous phase as represented in Scheme 2.3.

In order to achieve colloidal stability, it is necessary to incorporate the hydrophilic ZM DMAPS monomer in the hydrophobic MMA/n-BA chains so as to create stabilizing species that will be later attached onto the polymer particles. However, the incorporation of highly hydrophilic DMAPS monomer units in the MMA/n-BA hydrophobic chains is not straightforward, because DMAPS which is mainly located in the aqueous phase tends to create hydrophilic chains that if do not contain enough hydrophobic monomer (MMA/n-BA) units will terminate in the aqueous phase creating water-soluble oligomers. In contrast to the stabilizing species, these hydrophilic oligomers do not take place on the stabilization of the polymer particles; moreover, they increase the ionic strength and induce coagulation of particles. Therefore, the more hydrophobic the radical formed in the aqueous phase is, the easier the oligoradicals become surface active and attach onto the polymer particles increasing DMAPS incorporation onto the polymer particles and consequently reducing the amount of water-soluble oligomers. Once the surface-active oligoradicals are attached to the polymer particles, they will be mainly located on the surface of the particles to provide stability. Burring of these chains within the particles is less probable, because of the high hydrophilicity of the zwitterions present in the chains that remain turned towards the water phase.

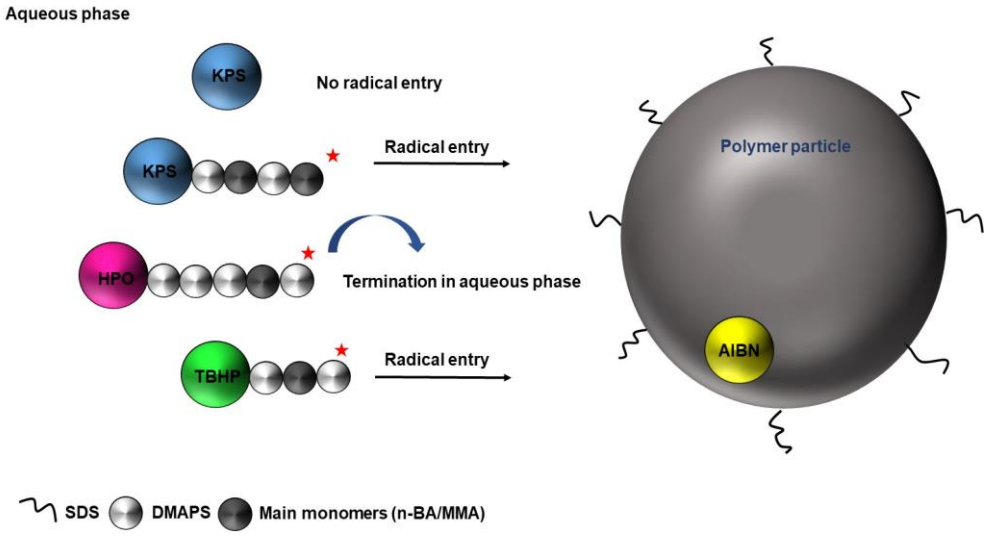

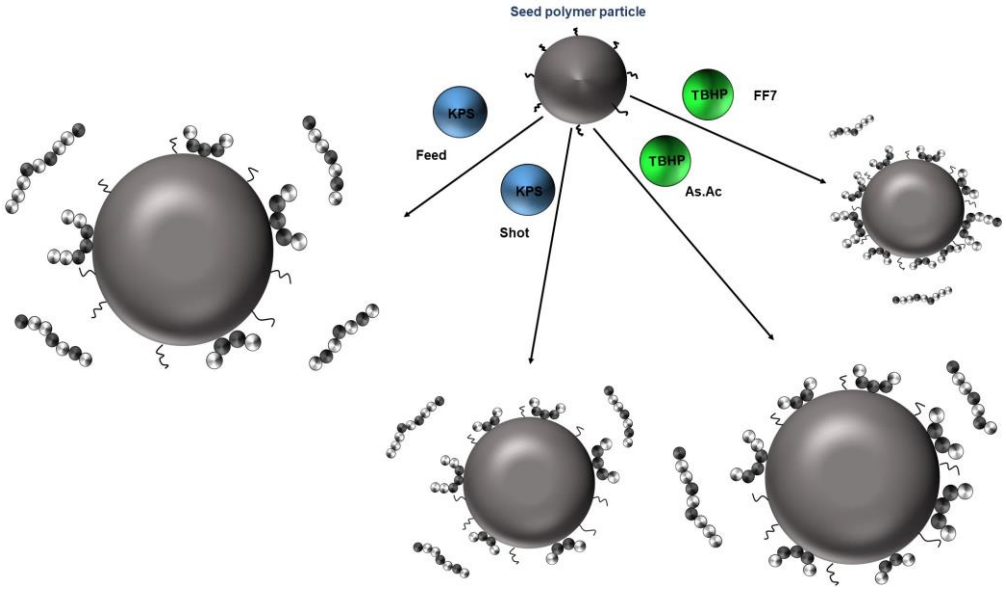

Scheme 2.3. Radical entry in emulsion polymerization of MMA/n-BA in the presence of ZM DMAPS using different type of initiators (top) and resulting latex (bottom).

Table 2.3 shows that sol molar masses were higher for KPS compared to the redox systems. This could be because the redox systems have a higher radical flux that promote bimolecular termination of growing chains, resulting in lower molar masses. The hydrophilic nature of sulfate ion radicals generated from KPS also affects radical entry. Additionally, different reaction temperatures can influence the radical generation rate, reaction rate constant, and particle number, thereby influencing the molecular mass.[24]

The type of initiator as well as the feeding strategy has also significant effects on the properties of the latexes and the films cast from these latexes. The salt and freeze-thaw stability are presented in Table 2.4 and 2.5, respectively. Due to the significant amount of water-soluble oligomers presented in the latexes, all the latexes were dialyzed and the measurements were performed on the original and dialyzed latexes.

It can be clearly appreciated from Table 2.4, that the latex synthesized with redox initiators TBHP/FF7 showed stability towards all the NaCl concentrations tested whereas, the rest presented change in particle size at any concentration. Moreover, KPS-Shot failed at the highest NaCl concentration (1M), probably due to the high amount of water-soluble species, since after dialysis, the latex was stable, indicating a clear effect of the water-soluble oligomers. Moreover, all the latexes presented better salt stability after dialysis. However, all latexes reported massive coagulation upon $CaCl_2$ addition. The high ion concentration affected the ionic strength and induced probably too many interactions between the particles, resulting into their coagulation.

Table 2.4. Salt stability of the latexes (original and dialysed) containing different initiators. The particle size is given in nm. (✓) means stable latex and no changes in particle size; (X) indicates massive coagulation.

Latex	Original				Dialysed			
	0.5M NaCl	0.75M NaCl	1M NaCl	1M $CaCl_2$	0.5M NaCl	0.75M NaCl	1M NaCl	1M $CaCl_2$
KPS-Feed (877 nm)	1080 nm	1116 nm	1026 nm	X	956 nm	1024 nm	1120 nm	X
KPS-Shot (478nm)	517 nm	650 nm	X	X	498 nm	510 nm	592 nm	X
TBHP/As. Ac (630nm)	990 nm	954 nm	1147 nm	X	✓	664 nm	672 nm	X
TBHP/FF7 (275nm)	✓	✓	✓	X	✓	✓	✓	X

Zwitterionic polymers are well known for their ability to exhibit anti-polyelectrolyte effect[36,37] where in contrast to ionic polymers tend to be collapsed in aqueous media and to dissolve upon salt addition. In this way, it is expected that polymer chains rich in DMAPS mainly located on the polymer surface might be collapsed, however, by the addition of salt these chains will be extended towards aqueous media making bigger the distance between particles and as a result reducing the probability of coagulation, enhancing the salt stability. However, likely the presence of the negative charges from KPS and SDS arising from the seed may hinders the full capacity of DMAPS to enhance the salt stability.

Concerning the freeze-thaw stability, the results are presented in Table 2.5. It can be seen that the latexes synthesized with both redox initiator systems failed in the test, however, the latexes synthesized with KPS showed good stability over freeze-thaw. The same results were obtained for the dialyzed latex, indicating water-soluble oligomers did not play an effect on the freeze-thaw stability. It seems as well that the incorporation of DMAPS onto the polymer particles does not affect the freeze-thaw stability, but it is difficult to conclude because of the presence of the negative charges arising from SDS and KPS that can also play a role. Probably the better freeze-thaw stability might be related with the presence of additional negative charges and the bigger particle sizes. Bigger particle sizes are usually more stable to

freezing. However, the latex synthesized with the redox pair TBHP/As.Ac exhibited significant particle size (630 nm) but still was not able to stand the test. Therefore, the main reason behind the better freeze-thaw stability might be related with the presence of negative charges arising from KPS that will enhance the hydration of the surface of the polymer particles avoiding their coagulation during the freeze-thaw test.

Table 2.5. Freeze-thaw stability of the latexes (before and after dialysis) synthesized with different initiators.

Latex	Original	Dialyzed
	Cycle 1	Cycle 1
KPS-Shot	✓	✓
KPS-Feed	✓	✓
TBHP/As.Ac	X	X
TBHPFF7	X	X

2.3.4. Polymer film performance

Polymer films were prepared from the latexes by casting the latex in the silicon molds and drying them at standard atmospheric conditions (23 ºC and 55% relative humidity). To determine if there was migration of the polymer chains that contained zwitterions, water contact angle (CA) measurements were conducted on the films cast from the original and dialyzed latexes, before and after rinsing them with water. The findings, presented in Figure 2.4, revealed that the films cast from the original and dialyzed latexes exhibited very similar CA values. Moreover, rinsing the films with water caused only minimal changes in the CA being more notorious in the case of the films with KPS probably due to the higher amounts of water-soluble species (Table 2.3), indicating that besides the important amount of water-soluble oligomers, there was no substantial migration of hydrophilic species to the film-air interface, the stabilizing units nor soluble oligomers.

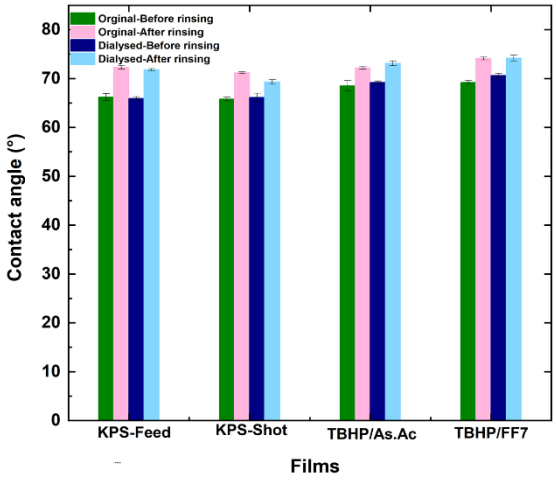

Figure 2.4. Water contact angles of the film-air interfaces of the films cast from the latexes (original and dialyzed) synthesized with different initiators, before and after rinsing with water.

Figure 2.5. Appearance of the polymer film cast from the latex containing DMAPS and synthesized with TBHP/FF7.

Homogeneous and transparent films were obtained in all the cases and example for the film cast from the latex synthesized with TBHP/FF7 is shown in Figure 2.5. The mechanical resistance of the polymer films cast from the latex synthesized with different initiators were evaluated by means of tensile

measurements. The stress-strain curves of the original films prepared at standard atmospheric conditions (23 °C and 55% relative humidity) and after annealing the films at 80°C for three days are displayed in Figures 2.6a and 2.6b, respectively. In addition, the mechanical properties are summarized in Table 2.6.

It is evident from Figure 2.6a that the film containing TBHP/FF7 initiator displayed superior mechanical properties compared to the rest of the films which taking into account the high gel contents of the latex synthesized with KPS (Table 2.3) was quite surprising. This confirms our hypothesis that the determined gel content actually represents fraction that is insoluble in THF because of high ions concentration. These results highlight the significant influence of DMAPS incorporation onto the polymer particles. The presence of ionic complexation between opposite charges as proposed Argaiz et al. could be the reason for enhanced mechanical properties.[38] On the contrary, in the cases where KPS was used, besides the high gel contents, the presence of significant amount of water-soluble species, comprised of short-length polymer chains rich in DMAPS, which are distributed between the polymer particles during film formation, can act as a plasticizer and influence the mechanical properties negatively. Among all, the film containing TBHP/As.Ac presented the lowest Young´s modulus and highest elongation at break. The same analyses were performed after annealing the films at 80°C for three days and it was found that in all the cases, except for TBHP/As.Ac that was not affected, the elongation at break increased after annealing likely due to the promoted polymer chains interdiffusion during the annealing process. The Young´s modulus for the films containing KPS especially KPS–Feed were not affected by the annealing process indicating that during annealing no significant changes happen, within the film or with other words, the polymer chains were likely already inter-diffused even in the original films. On the contrary, the modulus of the film containing TBHP/FF7 significantly dropped which might be related with the dissolution of the reinforcing network arising from the ionic-ionic interactions between the polymer chains rich in DMAPS mainly located on the polymer particle surface.[39]

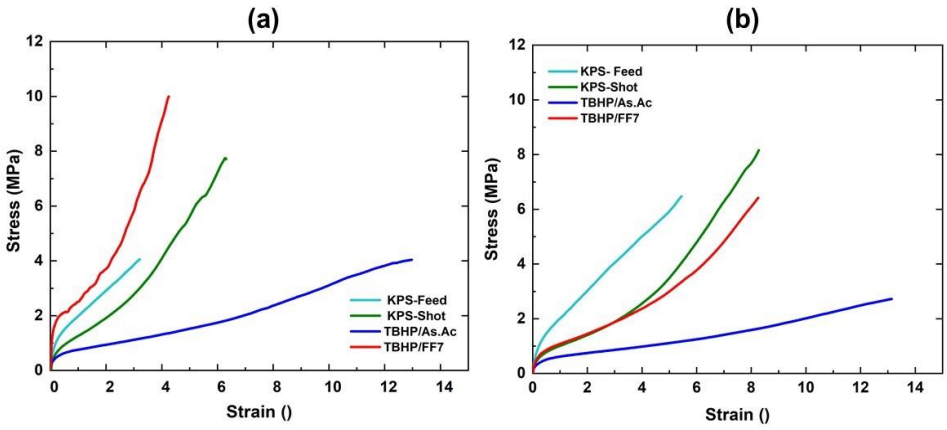

Figure 2.6. Stress-strain curves of the polymer films cast from the latexes synthesized with different initiators (a) prepared at standard atmospheric conditions (T = 23 °C and RH=55%), (b) annealed afterwards at 80 °C for three days.

Table 2.6. Mechanical properties of the films with different initiators, determined from stress-strain graphs.

	Film	Young's modulus (MPa)	Yield stress (MPa)	Ultimate tensile strength (MPa)	Elongation at break ( )
Non-Annealed	**KPS-Feed**	2.7±0.3	0.9±0.2	3.8±0.3	3.2±0.05
	KPS-Shot	2.1±0.3	0.5±0.1	7.8±2.1	6.6±0.3
	TBHP/As.Ac	1.9±0.2	0.4±0.2	4.0±0.2	12.8±0.95
	TBHP/FF7	3.2±7	1.8±0.6	9.2±0.6	4.3±0.8
Annealed	**KPS-Feed**	5.3±0.1	0.9±0.1	5.8±0.6	6.8±0.3
	KPS-Shot	0.4±0.2	0.5±0.1	7.5±1.2	7.6±0.7
	TBHP/As.Ac	0.2±0.2	0.5±0.2	2.6±0.4	13.1±1.3
	TBHP/FF7	0.3±0.7	0.4±0.5	6.8±0.3	8.3±0.8

The water uptake behavior of the polymer films is displayed in Figure 2.7, highlighting distinct patterns depending on the initiator employed. Notably, the film produced with KPS-Feed demonstrated reduced water absorption over a two-week period, while the KPS-Shot resulted in the film fracturing within three days of immersion. The high amount of water-soluble oligomers in the polymer prepared with KPS-Shot compromise the integrity of film. Surprisingly, the redox pair TBHP/FF7 displayed the highest

absorption rate, contradicting the expectation. The mechanical properties suggested that ionic bonding was stablished between polymer chains rich in DMAPS therefore, similar to what was observed by Argaiz et al.[38] with ionic complexation, lower water sensitivity was expected. This unexpected finding may be attributed to the presence of KPS and SDS arising from the seed that may introduce an imbalance between the ionic groups hindering the full capacity of DMAPS to avoid water penetration. Additionally, the presence of water-soluble species may have a negative impact on the film quality. The TBHP/As.Ac film was observed to be of poor quality and exhibited cracking after one week. KPS-feed present enhanced water resistance and the lowest water uptake. It might be because a large fraction of DMAPS, especially the one placed within the soluble oligomers, was removed within the coagulum, therefore, the film was more hydrophobic and less sensitive to water.

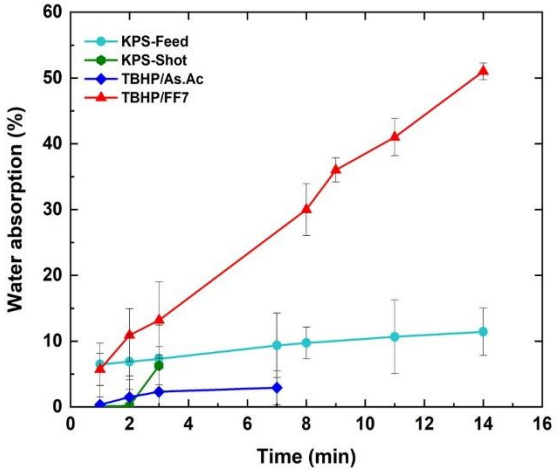

Figure 2.7. Water uptake of the films casted from the original latexes synthesized using different initiators.

2.4. Conclusions

From the surfactant-free batch emulsion polymerizations of MMA/n-BA carried out in the tumbler by using different commercially available zwitterionic monomers as the unique stabilizing species, DMAPS was selected as the most suitable zwitterionic monomer.

To investigate the chemical incorporation of DMAPS onto MMA/n-BA polymer particles, seeded semi-continuous emulsion polymerization was employed but unfortunately, since it was not possible to use a surfactant-free seed due to the big particle size obtained, a seed stabilized with conventional surfactant SDS was employed. The effect of the type of initiator on the incorporation of DMAPS onto the polymer particles was studied by using five different initiators. Specifically, KPS, a thermal initiator that dissolves in water and generates hydrophilic, negatively charged radicals in the aqueous phase. AIBN, an oil-soluble thermal initiator that mainly forms hydrophobic radicals in pairs in the organic phase, and three redox pair initiators, including HPO/As.Ac, a water-soluble system that forms neutral hydrophilic hydroxyl radicals and TBHP/As.Ac and TBHP/FF7, producing neutral hydrophobic radicals in the aqueous phase.

The ineffectiveness of the oil-soluble initiator AIBN was likely due to the generation of radicals in the organic phase reducing the creation of surface active species, which prevented them from interacting with DMAPS located in the aqueous phase and resulting in significant coagulation.

The synthesis carried out with HPO/As.Ac also failed but this time the reason might be the high hydrophilic character of the hydroxyl radicals that may spent long time growing in the aqueous phase, favoring the termination and yielding water-soluble species that did not contribute on the stabilization of the polymer particles.

Different feeding techniques were utilized for the thermal initiator KPS. The first method involved feeding the initiator where a latex with a higher particle size and considerable amount of coagulum was

obtained, likely due to the creation of lower amount of in situ stabilizing species. On the other hand, when KPS was added as a shot, the higher radical flux allowed formation of sufficient amount of stabilizing species, leading to the production of a latex with smaller particle size and coagulum-free.

The hydrophobicity of oligoradicals plays a significant role in the incorporation of DMAPS onto MMA/n-BA polymer particles, with tert-butoxy radicals showing the highest level of incorporation. Interestingly, when combined with FF7, tert-butoxy radicals showed the highest level of DMAPS incorporation, whereas when combined with As.Ac the incorporation was relatively low likely due to rapid radical consumption.

The choice of initiator had a significant impact on the properties of both the latexes and resulting polymer films. Latexes initiated with TBHP/FF7, which resulted in high DMAPS incorporation, demonstrated better salt stability. Conversely, the thermal initiator KPS exhibited good stability against freeze-thaw cycles probably due to the presence of sulfate functionalities.

In terms of polymer films, it was surprising to find that the redox initiator (TBHP/FF7) absorbed a higher amount of water compared to the thermal initiator KPS-Feed. It was expected that the presence of DMAPS onto polymer particles would decrease water absorption, but the additional charges from KPS and SDS arising from the seed may have interfered with the zwitterionic capacity, leading to negative effects on film performance. The mechanical properties were also affected by the choice of initiator, with TBHP/FF7 redox initiator showing the highest incorporation of DMAPS exhibiting the best behavior. It is believed that this improvement might be related with the creation of a reinforcing network arising from the ionic-ionic interactions between the polymer chains rich in DMAPS that may be mainly located on the surface of the particles. Nevertheless, after annealing the film, the mechanical properties dropped as a clear indication of the dissolution of the reinforcing network.

Based on the highest incorporation of DMAPS, the lack of additional charges and the favorable characteristics of the resulting latex, TBHP/FF7 was found to be the most promising initiator for the seeded semi-continuous emulsion copolymerization of MMA/n-BA stabilized with the zwitterionic monomer DMAPS.

2.5. References

1. *Cationic and zwitterionic polymerizable surfactants quaternary ammonium dialkyl maleates. Emulsion polymerization of styrene and butyl acrylate.* **Abele, S., et al.** s.l. : ACS Publications, 1999, Langmuir, Vol. 15, pp. 1045–1051.

2. *Cationic and zwitterionic polymerizable surfactants: quaternary ammonium dialkyl maleates. 1. Synthesis and characterization.* **Abele, S., et al.** s.l. : ACS Publications, 1999, Langmuir, Vol. 15, pp. 1033–1044.

3. *Soap-free emulsion polymerization of n-butyl acrylate: Copolymerization with 1, 1-(dimethyl)-1-(3-methacryloxyethyl)-1-(sulfopropyl) ammonium betaine.* **Blom, Henk P., et al.** s.l. : Wiley Online Library, 1998, Journal of applied polymer science, Vol. 70, pp. 227–236.

4. *Emulsifier-Free Emulsion Copolymerization of Vinyl Acetate and 3-Dimethyl (methacryloyloxyethyl) ammonium Propanesulfonate and Swelling Behavior of their Copolymer Matrices.* **Kamenska, Elena, et al.** s.l. : Wiley Online Library, 2007, Macromolecular Reaction Engineering, Vol. 1, pp. 553–562.

5. *Zwitterionic nanoparticles constructed with well-defined reduction-responsive shell and pH-sensitive core for "spatiotemporally pinpointed" drug delivery.* **Huang, Pingsheng, et al.** s.l. : ACS Publications, 2014, ACS Applied Materials & Interfaces, Vol. 6, pp. 14631–14643.

6. *Applications of zwitterionic polymers.* **Zheng, Liuchun, et al.** s.l. : Elsevier, 2017, Reactive and Functional Polymers, Vol. 118, pp. 51–61.

7. *Bioconjugation of protein-repellent zwitterionic polymer brushes grafted from silicon nitride.* **Nguyen, Ai T., et al.** s.l. : ACS Publications, 2012, Langmuir, Vol. 28, pp. 604–610.

8. *Romantic surfaces: a systematic overview of stable, biospecific, and antifouling zwitterionic surfaces.* **Baggerman, Jacob, Smulders, Maarten M. J. and Zuilhof, Han.** s.l. : ACS Publications, 2019, Langmuir, Vol. 35, pp. 1072–1084.

9. *Bio-inspired strategies for designing antifouling biomaterials.* **Damodaran, Vinod B. and Murthy, N. Sanjeeva.** s.l. : Springer, 2016, Biomaterials research, Vol. 20, pp. 1–11.

10. *Zwitterionic materials for antifouling membrane surface construction.* **He, Mingrui, et al.** s.l. : Elsevier, 2016, Acta biomaterialia, Vol. 40, pp. 142–152.

11. *Systematic comparison of zwitterionic and non-zwitterionic antifouling polymer brushes on a bead-based platform.* **van Andel, Esther, et al.** s.l. : ACS Publications, 2018, Langmuir, Vol. 35, pp. 1181–1191

12.*Ultrafiltration membranes with markedly different pH-and ion-responsivity by photografted zwitterionic polysulfobetain or polycarbobetain.* **Birkner, Marc and Ulbricht, Mathias.** s.l. : Elsevier, 2015, Journal of Membrane Science, Vol. 494, pp. 57–67.

13. *A comprehensive study and comparison of four types of zwitterionic hydrogels.* **Zhao, Weiqiang, et al.** s.l. : Springer, 2018, Journal of Materials Science, Vol. 53, pp. 13813–13825.

14. *Knowledge-based choice of the initiator type for monomer removal by postpolymerization.* **Ilundain, Pedro, et al.** s.l. : Wiley Online Library, 2002, Journal of Polymer Science Part A: Polymer Chemistry, Vol. 40, pp. 4245–4249.

15. *Styrene emulsion polymerization. The effects of initiator charge.* **Penboss, Ian A., Napper, Donald H. and Gilbert, Robert G.** s.l. : Royal Society of Chemistry, 1983, Journal of the Chemical Society, Faraday Transactions 1: Physical Chemistry in Condensed Phases, Vol. 79, pp. 1257–1271.

16. *Direct measurement of oligomers entry rate onto latex particles in an emulsion.* **Marestin, Catherine, et al.** 1998, Macromolecules, Vol. 31, pp. 1686–1689.

17. *Entry in emulsion polymerization: effects of initiator and particle surface charge.* **van Berkel, Kim Y., Russell, Gregory T. and Gilbert, Robert G.** s.l. : ACS Publications, 2003, Macromolecules, Vol. 36, pp. 3921–3931.

18. *Emulsifier-free emulsion copolymerization of styrene and sodium styrene sulfonate.* **Kim, J. H., et al.** s.l. : Wiley Online Library, 1992, Journal of Polymer Science Part A: Polymer Chemistry, Vol. 30, pp. 171–183.

19. *Comparing emulsion polymerization of methacrylate-monomers with different hydrophilicity.* **Ali, A.M. Imroz, Tauer, Klaus and Sedlak, Milos.** s.l. : Elsevier, 2005, Polymer, Vol. 46, pp. 1017–1023.

20. *Surfactant-free high solids content polymer dispersions.* **Bilgin, Sevilay, Tomovska, Radmila and Asua, José M.** s.l. : Elsevier, 2017, Polymer, Vol. 117, pp. 64–75.

21. *Sulfonated polystyrene ionomers prepared by emulsion copolymerization of styrene and sodium styrene sulfonate.* **Weiss, R. A., Turner, S. R. and Lundberg, R. D.** s.l. : Wiley Online Library, 1985, Journal of Polymer Science: Polymer Chemistry Edition, Vol. 23, pp. 525–533.

22. *Preparation of ion-containing elastomers by emulsion copolymerization of dienes with olefinic sulfonic acid salts.* **Siadat, B., Oster, B. and Lenz, R. W.** s.l. : Wiley Online Library, 1981, Journal of Applied Polymer Science, Vol. 26, pp. 1027–1037.

23. *Emulsion copolymerization of butyl acrylate with cationic monomer using interfacial redox initiator system.* **Luo, Yingwu and Schork, F. Joseph.** s.l. : Wiley Online Library, 2001, Journal of Polymer Science Part A: Polymer Chemistry, Vol. 39, pp. 2696–2709.

24. *Isothermal emulsion polymerization of n-butyl methacrylate with KPS and redox initiators: Kinetic study at different surfactant/initiator concentrations and reaction temperature.* **Wang, Shi, et al.** s.l. : Wiley Online Library, 2016, Journal of Applied Polymer Science, Vol. 133.

25. *Measurement of transfer constant for butyl acrylate free-radical polymerization.* **Maeder, Serge and Gilbert, Robert G.** s.l. : ACS Publications, 1998, Macromolecules, Vol. 31, pp. 4410–4418.

26.Handbook of Chemistry and Physics, 57th ed., CRC Press, Cleveland 1976

27. *pKa data compiled by R. Williams.* **Williams, R., Jencks, W. P. and Westheimer, F. H.** 2004, University of Wisconsin-Madison, https://www. chem. wisc. edu/areas/reich/pkatable/pKa_{c}{o}{m}pilation-1-Williams. pdf (Accessed 20 Feb. 2019). Google Scholar There is no corresponding record for this reference.

28. *(Mini) emulsion polymerization kinetics using oil-soluble initiators.* **Autran, Céline, de La Cal, José C. and Asua, Jose M.** s.l. : ACS Publications, 2007, Macromolecules, Vol. 40, pp. 6233–6238.

29. *Ascorbic acid oxidation by hydrogen peroxide.* **Deutsch, John C.** s.l. : Elsevier, 1998, Analytical biochemistry, Vol. 255, pp. 1–7.

30. *Interaction of surfactant and initiator types in emulsion polymerisations: A comparison of ammonium persulfate and hydrogen peroxide.* **Boutti, Salima, et al.** s.l. : Wiley Online Library, 2005, Macromolecular Chemistry and Physics, Vol. 206, pp. 1355–1372.

31. *Mechanism of emulsion polymerization of styrene in soap-free systems.* **Goodall, A. R., Wilkinson, M. C. and Hearn, J.** s.l. : Wiley Online Library, 1977, Journal of polymer science: Polymer chemistry edition, Vol. 15, pp. 2193–2218.

32. *Colloid chemical studies of polystyrene latices polymerized without any surface-active agents: II. Coagulation into secondary minimum.* **Kotera, Akira, Furusawa, Kunio and Kudō, K.** s.l. : Springer, 1970, Kolloid-Zeitschrift und Zeitschrift für Polymere, Vol. 240, pp. 837–842.

33. *Adhesion enhancement in waterborne acrylic latex binders synthesized with phosphate methacrylate monomers.* **Gonzalez, Inigo, et al.** s.l. : Elsevier, 2008, Progress in organic coatings, Vol. 61, pp. 38–44.

34. *Fundamentals of chemical incorporation of ionic monomers onto polymer colloids: paving the way for surfactant-free waterborne dispersions.* **Bilgin, Sevilay, Tomovska, Radmila and Asua, José M.** s.l. : Royal Society of Chemistry, 2016, RSC advances, Vol. 6, pp. 63754–63760.

35. *Redox initiator systems for emulsion polymerization of acrylates.* **Kohut-Svelko, Nicolas, et al.** s.l. : Wiley Online Library, 2009, Journal of Polymer Science Part A: Polymer Chemistry, Vol. 47, pp. 2917–2927.

36. *Zwitterionic polymers with antipolyelectrolyte behavior in solution.* **Zhang, L. M.** 1998, Polym. Bull, pp. 82–87.

37. *New polyampholytes: The polysulfobetaines.* **Hart, R. and Timmerman, D.** s.l. : Wiley Online Library, 1958, Journal of Polymer Science, Vol. 28, pp. 638–640.

38. *Ionic inter-particle complexation effect on the performance of waterborne coatings.* **Argaiz, Maialen, et al.** s.l. : MDPI, 2021, Polymers, Vol. 13, p. 3098.

39. *UCST wetting transitions of polyzwitterionic brushes driven by self-association.* **Azzaroni, Omar, Brown, Andrew A. and Huck, Wilhelm T. S.** s.l. : Wiley Online Library, 2006, Angewandte Chemie International Edition, Vol. 45, pp. 1770–1774.

Chapter 3. The Influence of DMAPS Concentration on Latex and Film Properties

3.1. Introduction

In Chapter 2 of the thesis, a comprehensive assessment was conducted on commercially available zwitterionic monomers with diverse anionic groups. Through this evaluation, a suitable candidate, ZM DMAPS, was carefully chosen. The subsequent investigation involved the incorporation of DMAPS onto hydrophobic MMA/n-BA polymer particles using various initiators. Remarkably, the combination of TBHP/FF7 exhibited the highest level of DMAPS incorporation.

The synthesized latex relies on ZP DMAPS as a surfactant replacement. Consequently, it is envisaged that the variation in DMAPS concentration will exert a profound influence over the polymerization kinetics and the ensuing characteristics of both the latexes and films. Several studies have investigated the impact of using ionic comonomers as stabilizing units in surfactant-free emulsion polymerization on the particle size and particle size distribution.

Kim et al.[1] and shouldice et al.[2] focused on the emulsifier-free emulsion copolymerization of styrene and sodium styrene sulfonate (NaSS), and found that adding NaSS led to smaller latex particle sizes. They suggested that at higher NaSS concentrations, NaSS polymerized significantly in the aqueous

*A part of the content of this chapter has been published in:

Zwitterionic monomers as stabilizers for high solids content polymer colloids for high-performance coatings applications. **Murali, Sumi, Agirre, Amaia and Tomovska, Radmila.** s.l. : Elsevier, 2022, Progress in Organic Coatings, Vol. 173, p. 107196.

phase, acting as a site for further polymerization due to presence of high amount of water-soluble oligomers. Blom et al.[3] reported analogous findings concerning DMAPS with n-BA, showing that the latex exhibited monodisperse particle size distribution with DMAPS concentrations up to 5%. Nevertheless, it is worth mentioning that their reactions were conducted at lower solids content (<10%) and the amount of incorporation of DMAPS was not investigated. Additionally, Kostova et al.[4,5] synthesized polymer nanoparticles using a polyzwitterionic copolymer consisting of vinyl acetate (VA) and DMAPS through surfactant-free emulsion copolymerization. Their study revealed that the quantity of DMAPS had a significant impact on various characteristics of the nanoparticles, including particle size, time for latex formation, coagulum formation and drug encapsulation efficiency.

In a different study conducted by Wang and their team, amphiphilic sulfobetaine copolymers were synthesized. These copolymers were formed by combining different ratios of sulfobetaine (DMAPS) and 2,2,2-trifluoroethyl methacrylate (TFMA). The primary aim was to enhance the antibiofouling properties of ethylene-vinyl acetate copolymer film through a surface coating approach. In this investigation, the impact of adjusting the DMAPS/TFMA ratio on both the resulting latexes and their coating properties was examined. The findings indicated that an elevated DMAPS/TFMA ratio led to noteworthy alterations. Specifically, the particle diameter, polydispersity index, and water uptake of the latexes and coatings exhibited a decrease. However, it is important to note that the study did not delve into the exploration of incorporation. The film showcased remarkable attributes in terms of anti-biofouling effects. Notably, a significant reduction of 92% in attached protein and 50% in microalgae was achieved when compared to the reference ethylene vinyl acetate film.[6] These collective findings strongly suggest that sulfobetaine monomers exhibit similar behavior to ionic monomers and thus, varying the amount of sulfobetaine monomers in the formulation can significantly impact the final latex and film properties. However, the amount of DMAPS incorporated on to polymer particles was not investigated in any of the previously mentioned works.

This chapter focuses on the synthesis of n-BA/MMA waterborne polymer dispersions under similar conditions to industrial processes, synthesizing high solids content (50%) latexes by seeded semi-continuous emulsion polymerization. The study involves the addition of a small amount of DMAPS zwitterionic monomer at varying concentrations. This research is the first to investigate the impact of different DMAPS content (ranging from 0.5% to 5% by weight based on monomer) on reaction kinetics, DMAPS incorporation onto polymer particles, and the properties of latexes and films. Additionally, a comprehensive comparison is made between all latex and film properties obtained using DMAPS and those obtained from the reference latex, which utilized SDS conventional surfactant.

3.2. Experimental section

3.2.1. Materials

The materials are presented in Appendix I.

3.2.2. Polymerizations

The seed used in this work was prepared at 10% S.C. n-BA/MMA (50:50) using conventional surfactant SDS by batch emulsion polymerization. The seed with a particle size of 96 nm did not present any gel. A detailed description of the seed synthesis process and the properties of the resulting latex can be found in Appendix 1 and in Chapter 2.

For the seeded semi-continuous reactions of all DMAPS latexes, the experimental setup and the detailed procedure along with formulations can be found in Appendix I.

3.2.3. Characterization

The characterization methods are given in Appendix II.

3.3. Results and discussion

3.3.1. Latex properties

By utilizing SDS stabilized seed, varying quantities (0.5–5wbm %) of DMAPS zwitterionic monomer were polymerized with n-BA/MMA in a seeded semi-continuous mode, resulting in the production of colloidally stable latexes. To provide a basis for comparison, a reference latex consisting of MMA/n-BA stabilized solely by 2 wbm% SDS was also synthesized. Table 3.1 provides a summary of the properties of the synthesized latexes. The conversion of DMAPS was monitored using ^{1}H NMR. Figure II.1 in the Appendix II displays representative ^{1}H NMR spectra of reaction mixtures containing 2% DMAPS at different reaction times during the seeded semi-continuous emulsion polymerization. The pronounced peak at 5.7 ppm, corresponding to the vinyl group of DMAPS, was utilized to track the conversion. As the reaction progressed, the intensity of the peak decreased, indicating the polymerization of DMAPS. For all reactions employing different amounts of DMAPS, the final conversion was found to be ≥97%.

Table 3.1. Characteristics of latexes containing different amount of DMAPS.

DMAPS (%)	0.5	1	2	3	5	Reference
Xt (%)	82	100	100	100	86	100
Dp (nm)	347	280	275	265	236	243
Coagulum (%)	30	1.7	1	5.5	14.6	0.9
WSO (g)*	1.24	0.95	1.25	1.81	4.4	-
z-potential (mV)	-39	-52	-45	-39	-35	-38
DMAPS incorporation (%)	31.4	67.9	50.6	51.6	44.4	-
DMAPS incorporation (g)	0.16	0.67	1.01	1.54	2.2	-
Gel Content (%)	0	0	0	10	31	0
$\overline{M_W}$ (kDa)	369	414	343	331	451	706
Dispersity (Đ)	2.9	2.7	2.5	2.8	3	2.7
Tg (°C)	15	12	13	13	11	9

*** WSO water-soluble oligomers fraction**

Figure 3.1 illustrates the progression of MMA/n-BA monomer conversion in the reactions carried out with varying concentrations of DMAPS and reference.

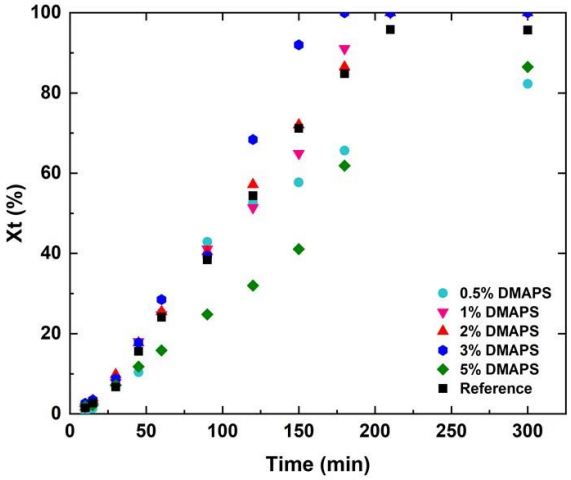

Figure 3.1. Time evolution of total monomer conversion (*Xt*) for seeded semi-continuous reactions by using different DMAPS concentrations and reference.

Almost complete conversion was achieved for all DMAPS concentrations, except for 0.5% and 5% (as shown in Figure 3.1 and Table 3.1). Based on the results presented in Figure 3.1, it can be clearly observed that the reactions carried out in the presence of DMAPS proceeded at a slower rate compared to the reference reaction that employed the conventional surfactant SDS. However, this observed difference in reaction rate decreased with increasing DMAPS concentration and even surpassed the reference reaction rate when 3% DMAPS was utilized. These findings provide evidence of successful incorporation of DMAPS onto the hydrophobic MMA/n-BA polymer particles. However, when DMAPS concentration was increased to 5%, a significant decrease in reaction rate was observed, similar to that observed for 0.5% DMAPS reaction. This suggests that in the case of 0.5%, likely there was no sufficient creation of stabilizing chains, whereas in case of 5 % DMAPS as shown in Table 3.1 the presence of soluble oligomers was observed, leading to an increase in the ionic strength within the dispersion. Consequently, coagulation was promoted, resulting in 30% and 14% coagulum for 0.5% and 5% DMAPS, respectively.

The growing polymer particles experienced coagulation due to an insufficient amount of stabilizing chains present in the case of 0.5% DMAPS. In contrast, the coagulum amount was notably lower for the 5% DMAPS concentration, likely due to a higher incorporation of DMAPS onto the polymer particles. Therefore, coagulation was promoted by the high ionic strength in this case. The dispersions stabilized with 1%, 2%, and 3% DMAPS, as well as the reference, exhibited lower levels of coagulum. To determine the composition of the coagulum, FTIR analysis was conducted. Figure 3.2 presents the representative spectra of the coagulum from 5% DMAPS reaction, indicating a significant presence of DMAPS and both monomers (MMA/n-BA) in the coagulum.

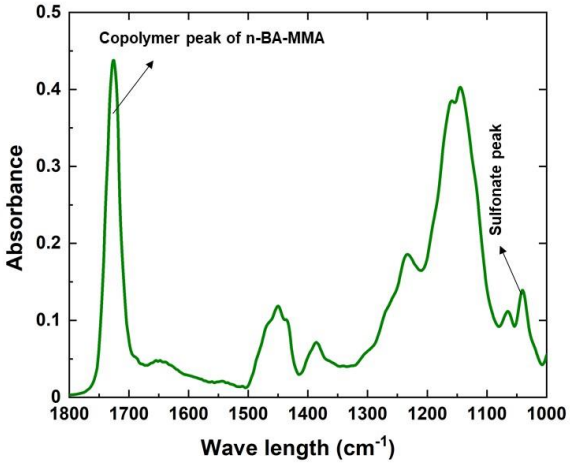

Figure 3.2. FTIR spectra of the coagulum obtained in 5% DMAPS reaction (characteristic peak of C=O in MMA/n-BA copolymer at 1737 cm $^{-1}$, characteristic peak of DMAPS sulfonate group at 1030 cm $^{-1}$).

Following the elimination of coagulum, the latex samples achieved stability and exhibited zeta potentials ranging from -38 to -52 mV. The presence of negative z-potential values was as expected, aligning with the findings reported by various authors.[7-10] The occurrence of a negative zeta potential in DMAPS latex, indicating an anionic surface charge, is not consistent with the inherent electro-

neutrality of DMAPS units . This observation can be attributed to the specific chemical properties of the DMAPS. In the structure of the DMAPS, the quaternary ammonium (cation) is positioned closer to the reactive group, while the negative charge is located at the end of the molecule. During the reaction with the main monomers, the chain portion containing the DMAPS moieties, being hydrophilic in nature, tends to locate itself on the surface of the particles, contributing to the colloidal stability. As a result, the negative charge originating from the sulfonate group extends towards the aqueous phase, while the quaternary ammonium is retained within the particles, in close proximity to the reactive groups that incorporate the DMAPS molecules into the MMA/n-BA chains. This distribution leads to an anionic nature for the polymer particles, with the cations being hindered. Similar observations have been reported in studies comparing the stabilizing effects of anionic and cationic surfactants on polystyrene particles, where the cationic surfactant exhibited a much lower absolute value of zeta potential, despite achieving the same coverage, when compared to the anionic surfactant.[11]

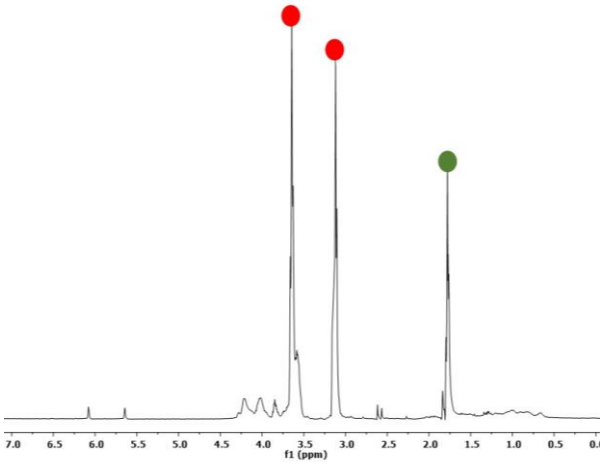

Figure 3.3. ^{1}H NMR spectra of dried serum of water-soluble species, where red colour marks the peak characteristic for DMAPS and green colour marks peaks characteristic for MMA.

The presence of water–soluble species was demonstrated by ^{1}H NMR analysis of the water phase, after centrifugation of the latex, separation and drying of the aqueous phase. The spectra are shown in Figure 3.3 and demonstrates the presence of oligomers that contain DMAPS and MMA, as one may expect, since MMA has much higher water solubility than n-BA and is more available for copolymerization with DMAPS. Such water-soluble growing oligoradicals are too hydrophilic to enter onto particles and rather terminate in aqueous phase. The amount of water-soluble species (Table 3.1) was calculated based on total solids content of the latex and as expected, it increased with the amount of DMAPS. The only exception was the polymer with the lowest DMAPS content, which presented higher fraction of water-soluble species. This may be a consequence of the less colloidally stable system and larger particle size, thus, the DMAPS incorporation onto polymer particles was likely low, but the formation of water-soluble oligomers was favored. Due to the presence of water-soluble species, it was decided to dialyze the latex and compare the properties of polymer films produced from dialyzed and non-dialyzed latex (original). Even though dialysis process lack practical importance and is costly and environmentally unfriendly, it was employed here in order to observe the clear effect of the zwitterionic monomer incorporation on the polymer properties.

Regarding the incorporation of DMAPS onto the polymer particles, one would expect that the level of incorporation would increase with the concentration of DMAPS, as previously observed in the case of NaSS stabilized MMA/n-BA latexes.[12] However, the results obtained for DMAPS exhibited an opposite trend, which can be attributed to the formation of coagulum that influenced the calculated fractions. It is possible that a significant portion of DMAPS was incorporated within the coagulum, particularly for the 0.5% and 5% DMAPS concentrations. Nonetheless, the total amount of DMAPS incorporated onto the polymer particles (after removing the coagulum) was found to be proportional to the initial DMAPS concentration, as indicated in Table 3.1. Detailed procedure of incorporation study DMAPS and FTIR

spectra's of latex together with the calibration curve are shown in Appendix II, Figure II.2 and Figure II.3, respectively.

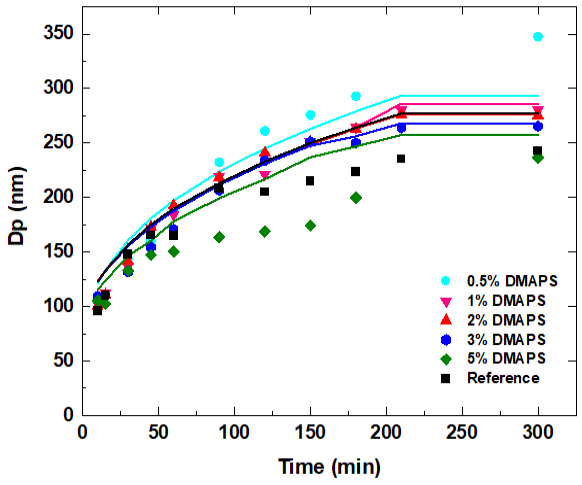

Figure. 3.4. Time evolution of particle size (*Dp*) of the latex synthesized by seeded semi-continuous mode with different DMAPS concentrations and reference latex (experimental indicated by dots and theoretical indicated by continuous lines).

Figure 3.4 illustrates the evolution of average particle size (both theoretical and experimental) for the latexes synthesized with different concentrations of DMAPS, as well as the reference latex. As expected for seeded semi-continuous polymerization reactions, the particle size progressively increases with monomer conversion. The comparison reveals that particles containing DMAPS are larger than those stabilized with SDS, suggesting that certain DMAPS-based latexes displayed reduced stability and encountered particle coalescence. This phenomenon becomes evident through the observed deviation from theoretical to experimental results, particularly noticeable in the cases involving 0.5% and 5% DMAPS concentrations. The average particle sizes, presented in Table 3.1 (ranging from 230 nm to 340 nm), clearly demonstrate that an increase in DMAPS concentration leads to a decrease in particle size. This can be attributed to a higher quantity of DMAPS being incorporated onto the polymer particles;

resulting in particle sizes approaching those of conventionally stabilized particles when 5% DMAPS was employed (approximately 240 nm).

The particle size distribution, as determined by capillary hydrodynamic fractionation (CHDF), is shown in Figure 3.5, with the exception of the latexes containing 0.5% and 5% DMAPS, the rest of the latexes exhibit relatively narrow and unimodal particle size distributions. However, in the case of 0.5% DMAPS, a shoulder at larger particle sizes is observed, indicating the presence of a small fraction of larger particles resulting from coagulation. Similarly, the latex with 5% DMAPS displays a fraction of large particles, which this time might be related to the high ionic strength caused by the abundance of soluble oligomers, leading to latex destabilization. Moreover, an additional population of small particles is observed, probably related to secondary nucleation. This suggests that at the highest DMAPS concentration of 5 %, probably there was sufficient quantity of in situ stabilizing chains to stabilize colloidally the new particles created in aqueous phase by homogeneous nucleation.

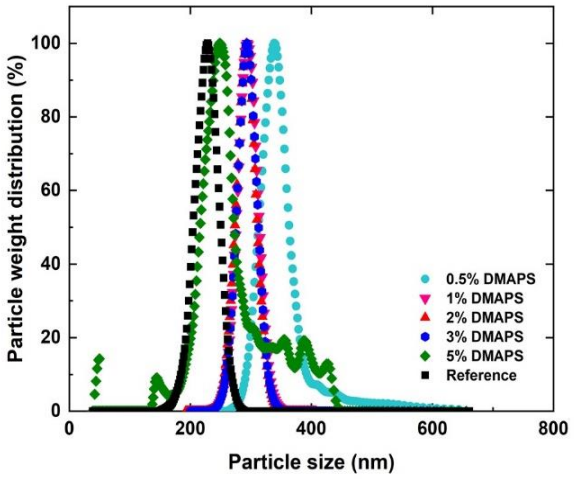

Figure. 3.5. Particle size distribution (by CHDF) of the latexes synthesized using different DMAPS concentrations and reference.

The stability of the latexes during storage was excellent, as no sedimentation or changes in particle size (measured by DLS) were observed over a period of 3 years.

Polymer microstructure was determined by means of gel content (THF insoluble polymer fraction) and the polymer average molar masses both shown in Table 3.1, along with the molar mass distributions shown in Figure 3.6. Except for the highest DMAPS concentrations of 3% and 5%, the gel content was found to be zero. Furthermore, the reference polymer does not present any gel. In acrylic systems, the gel is formed by intermolecular chain transfer to polymer followed by termination by combination.[13] However, it has been seen that the presence of MMA affects negatively the formation of gel,[14] due to the absence of abstractable hydrogens in the MMA chains, lower reactivity of the MMA terminated chains for hydrogen abstraction, and their predominant termination by disproportionation.[14] Along with the fact that a higher gel fraction was observed at high DMAPS contents indicates that the gel content is related to the presence of ionic groups originating from DMAPS. Likely, the ionic groups induce ionic interactions between the polymer chains reducing their solubility in THF and resulting on a physical gel. To confirm this, DMF (containing 0.05M LiBr) was used as an alternative solvent and complete polymer solubilization was indeed achieved. This demonstrates the absence of a chemical gel in the system.

From the average molar masses of the polymers analyzed by size exclusion chromatography (SEC) in DMF (Table 3.1). It was observed that, except for the latexes with 0.5% and 5% DMAPS, the average molar mass decreased with increasing DMAPS content. In Figure 3.6 it can also be clearly appreciated how except for the polymer with 5 % DMAPS, the MMD shifted to lower values with respect to the reference. Particle size obviously affected the MMD, the smaller particle size, the higher the concentration of radicals, promoting bimolecular termination and the formation of shorter chains, however; in this case, it is difficult to explain the shifts because of different quantity of coagulum obtained. Namely, if the coagulum is consider as polymer that loss colloidal stability, for as high coagulum fractions as 14 % and

30 % for 0.5 % and 5 % reactions, respectively, it is clear that the molar mass distribution for these latexes cannot be considered as representative of the whole polymer.

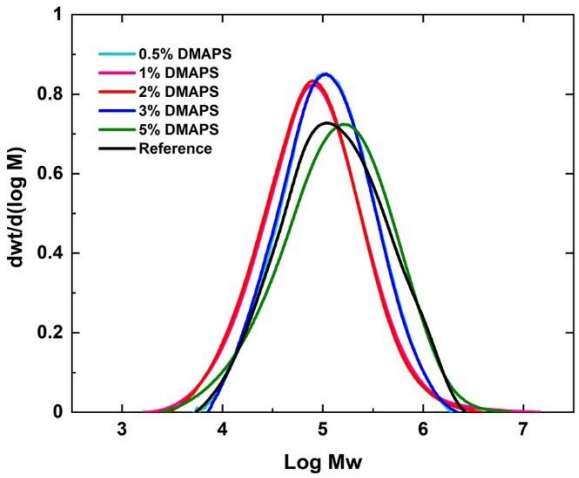

Figure 3.6. Molar mass distributions of polymers with different amounts of DMAPS and reference polymer.

Colloidal stability of ionically stabilized polymer particles in a latex is usually described by the balance between two opposite forces, electrostatic repulsive and attractive Van der Waals forces. When two colloids approach each other, their electrical double layer (EDL) interacts, maximizing the repulsion, however, this repulsive force tends to be zero outside the EDL. Simultaneously their attractive forces also increased. By the addition of salts into the medium the EDL is compressed (Figure 3.7) by the interactions of the ions from the salt with these of EDL. In such conditions, the attractive particle forces became dominating and usually results in particles coagulation. Therefore, more colloidally stable latexes will have this point of coagulation postponed towards the higher salt's concentration.

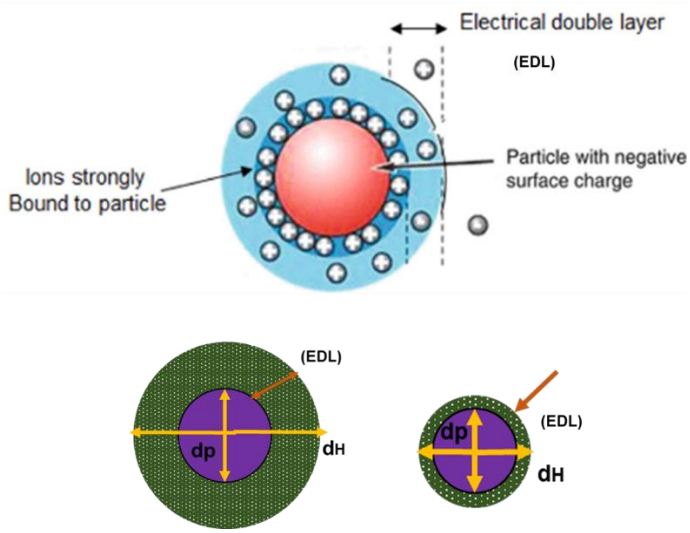

Figure 3.7. Schematic representation of the EDL at low ionic concentration (left) and at high ionic concentration (right) for a particle stabilized with anionic surfactant.

In this way, the salt stability of the different latexes was studied by measuring the particle size prior and after addition of aqueous solutions of different salts and concentrations. Since DMAPS was not fully incorporated onto the polymer particles, the latexes synthesized with different amounts of DMAPS were dialyzed in order to remove the water-soluble species and to study how their presence could affect the salt stability. In addition, since all the latexes were synthesized by using SDS stabilized seed, some of the surfactant could also be removed during dialysis. From Table 3.2, it is evident that under the addition of low concentrations of NaCl colloidal stability for all the latexes were maintained except for those containing 0.5% and 1% DMAPS due to their lower incorporation of DMAPS units onto the polymer particles (Table 3.1). Nevertheless, when higher concentrations of NaCl (1M) were introduced, there was a notable increase in the particle size of the latexes. Conversely, for the dialyzed counterparts, an enhancement in salt stability was observed as indicated by a less pronounced particle size increase. This suggests that as expected the presence of water-soluble species have a negative effect on the colloidal

stability due to an increase of the ionic strength of the medium. Concerning $CaCl_2$ addition, all the latexes coagulated except for 3% and 5% DMAPS containing latexes, where in the first case an increase in the particle size was observed whereas in the last case, there was no particle size change. Moreover, for the latex synthesized with 5% DMAPS the particle size was not altered by the addition of NaCl and $CaCl_2$ at any concentration and the same behaviour was observed for the original and dialyzed. For the reference latex, these results were not surprising since as explained before; by the addition of salts, the EDL is compressed and usually results in latex coagulation. Taking into account that Ca^{2+} is a divalent cation, whereas, Na^{+} is a monovalent cation, under the same salt concentration, the $CaCl_2$ will compress more easily the EDL making the particles closer and yielding coagulation. The excellent colloidal stability of the latex with 5% DMAPS is likely due to the higher amount of DMAPS incorporated onto polymer particles (Table 3.1) that after salt addition were extended due to the anti-polyelectrolyte effect.[15]

Table 3.2. Salt stability of the latexes containing different amounts of DMAPS and reference latex. The particle size is given in nm and shown in parenthesis. (✓) means stable latex and no changes in particle size; (X) indicates massive coagulation.

	Original				**Dialyzed**			
	NaCl			**$CaCl_2$**	**NaCl**			**$CaCl_2$**
DMAPS (%)	**0.5M**	**0.75M**	**1M**	**1M**	**0.5M**	**0.75M**	**1M**	**1M**
0.5% (dp=347)	X	X	X	X	X	X	X	X
1% (dp=280)	✓	X	X	X	✓	464	X	X
2% (dp=275 nm)	✓	401	647	X	✓	323	329	X
3% (dp=265 nm)	✓	391	464	453	✓	312	544	521
5% (dp=236 nm)	✓	✓	✓	✓	✓	✓	✓	✓
Reference (dp=243)	✓	✓	✓	X	-	-	-	-

The enhanced salt stability of 5% DMAPS latex results might be related to the anti-polyelectrolyte effect of zwitterionic polymers. The anti-polyelectrolyte behaviour, means that when the zwitterionic polymer chains are dispersed in water, in contrast to ordinary polyelectrolytes they are in collapsed state (Figure 3.8 left) due to inter- and intra- chain ionic interactions. However, by the addition of salts

into the medium, the single chains of polyzwitterions are expanded due to the break-up of the ionic attraction between the zwitterions, introduced by the added ions (Figure 3.8 right). In the polymer latex, due to high hydrophilicity of DMAPS, likely the polymer chains rich in DMAPS are located on the surface of the polymer particles (they provide colloidal stability to MMA/n-BA particles). Due to the inter- and intra- molecular attractions initially these chains are shrunk, however, after salt addition these chains got extended conformation due to interaction of salt ions with the zwitterions (Figure 3.9). In such a way the distance between the particles is kept larger, preventing the coagulation of the latex. This phenomenon seems to be more pronounced in case of 5% DMAPS latex, because of higher DMAPS incorporation onto the polymer particles.

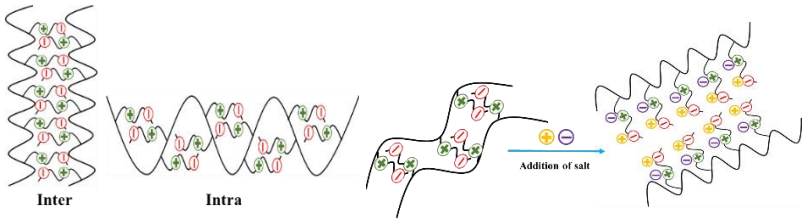

Figure 3.8. Different interaction modes between polymeric zwitterions (left) and anti-polyelectrolyte effect after salt addition (right).

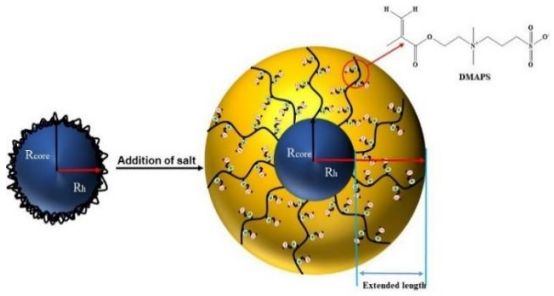

Figure 3.9. Expected chain extension after salt addition of the polymer chains rich in DMAPS located on the surface of the polymer particles.

3.3.2. Polymer film performance

In an attempt to determine if the in situ created DMAPS containing colloidal stabilizing species migrated to the surface of the film during film formation, water contact angles (Table 3.3) of the films were measured before and after rinsing the films with water. The CA of the films prepared from dialyzed latexes are presented as well in Table 3.3. Both, original and dialyzed DMAPS films displayed very similar behavior, as CAs before and after rinsing with water changed slightly, suggesting that there was no significant migration of stabilizing species to the film-air interface, except probably the SDS from the seed. Furthermore, the CAs of the films prepared from original latexes confirm that the water-soluble species did not migrate neither. On the contrary, the CA of the reference film increased significantly upon rinsing with water (from 40° to 80°), showing that SDS indeed migrated significantly towards the film-air interface. Much higher hydrophilicity of reference (40°) than that of DMAPS films (about 70°) might be the result of different effects. On one hand, due to the accumulation of hydrophilic SDS on film surface making the reference more hydrophilic. On the other hand, the drop of hydrophilicity of the films containing DMAPS might arise from the interactions between zwitterionic moieties. Azzaroni et al.[16] reported similar contact angles for DMAPS brushes grafted on silicone surfaces and they attributed these high contact angles to a super collapsed state arising from the high number of inter- and intra-chain polymer interactions, however, by increasing the temperature above the upper critical solubility temperature (UCST), these interactions were disrupted and the surface turned to be very hydrophilic (C.A.~10°). Similarly, Argaiz et al.[17] found that the observed increase of the contact angle was due to the neutralization effect as a result of the interaction between the ions. In addition, the higher hydrophobicity of films containing DMAPS could be also likely due to the orientation of zwitterionic groups away from the air-film surface, driven by the minimization of surface energy in the dried state.[18]

Table 3.3. Contact angle (CA) of drop of water on the films with different amounts of DMAPS and reference film before and after rinsing.

DMAPS (%)	Original		Dialyzed	
	CA (°) before rinsing	CA (°) after rinsing	CA (°) before rinsing	CA (°) after rinsing
Reference	40±0.1	81±0.2	-	-
0.5	69.9 ±0.4	71.3±0.3	72.9±0.4	73.5 ±1.3
1	69.5 ±0.7	70.7±0.5	71.9±0.3	74.3±1.0
2	69.2±0.4	74.1±0.3	70.6±0.4	74.2±0.6
3	67.9±0.2	71.6±0.9	70.2±1.0	72.5±1.0
5	73.9±0.4	76.8±0.3	78.3±0.2	79.6±0.7

The surface morphology of the films containing 2% DMAPS (before and after dialysis) and 5% DMAPS as well as the reference film was analysed by AFM imaging. The phase images of the film surface are shown in Figure 3.10. Presence of white aggregates arising from the SDS migration towards the film-air interface during film formation can be clearly appreciated in the reference film (Figure 3.10a). They introduced the strong hydrophilicity observed at the surface of the reference film (Table 3.3). The presence of whitish structures in the DMAPS films (Figure 3.10b and 3.10d) are attributed to the small quantity of SDS coming from the seed. This quantity is the least on the surface of dialyzed 2% DMAPS film (Figure 3.10c), because most of the SDS was removed when 2% DMAPS was dialyzed. On the other hand, the amount of 5% DMAPS film was much lower than 2% DMAPS film, because large coagulum amount was removed from this latex prior to film formation.

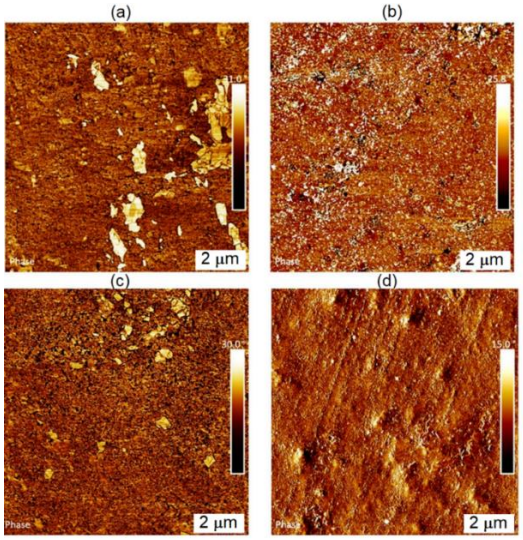

Figure 3.10. AFM phase images of film-air interfaces of (a) reference; (b) 2% DMAPS; (c) 2% DMAPS dialysed; (d) 5% DMAPS.

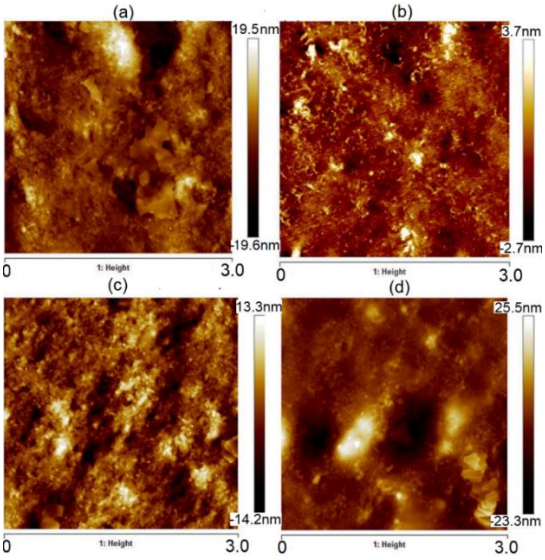

Figure 3.11. AFM height images of film-air interfaces of (a) reference (b) 2% DMAPS (c) 2% DMAPS dialysed (d) 5% DMAPS.

On the other hand, it is well known that the roughness of the film also has important impact to the antifouling properties[19] therefore, the height AFM images of the films surface were also analysed (Figure 3.11). The rough surface is considered favourable to improve the fouling behaviour, however, it has been reported that the roughness of the surface coated with zwitterionic polymer brushes is reduced when the film is immersed in water.[20-22] The smoother surface created would reduce the antifouling arising from the roughness. In Figure 3.11, the height scale bar presented in each of the images determines the maximum peak to valley height over the sample. The absolute values between the highest and lowest points along to the colour difference of the film surface were used to compare the roughness of the different films. According to these criteria, the reference film (Figure 3.11a) is quite rough; probably the irregular surface was created by the distributed SDS aggregates with different sizes over the film surface. On the other hand, the both 2% DMAPS films original and dialyzed (Figures 3.11b and 3.11c) are the smoothest one, whereas the most irregular and rough surface is that of 5% DMAPS film (Figure 3.11d). The roughness trend does not correspond to the tendency in the contact angles observed in Table 3.3. Nevertheless, the DMAPS films being less hydrophilic by chemical nature and ionic complexation process are secondary affected by the roughness that might further increase the contact angle.

The mechanical resistance of the polymer films was evaluated by means of tensile measurements. The stress-strain curves of the original films prepared at standard atmospheric conditions are displayed in Figure 3.12a, whereas the modulus and other characteristics determined from these graphs are shown in Table 3.4.

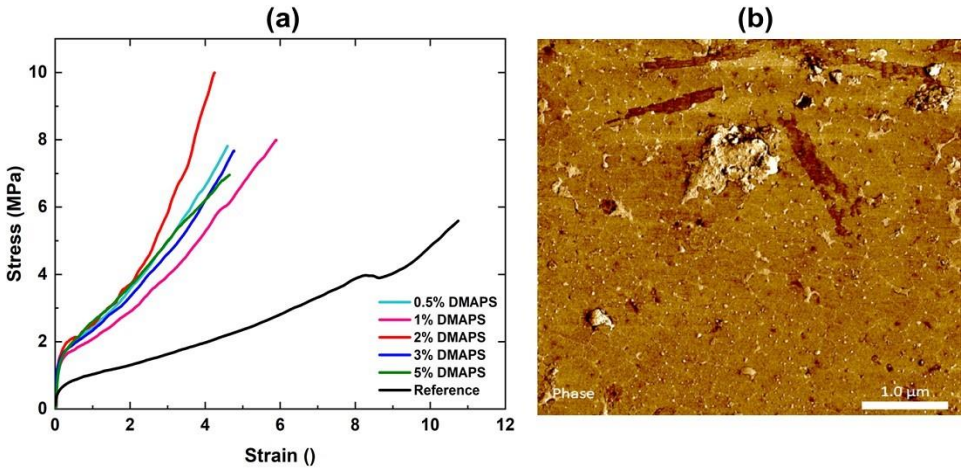

Figure 3.12. (a) Stress-strain curves of the polymer films with different DMAPS quantities and the reference film, prepared at standard atmospheric conditions (T=25 ºC and 55% relative humidity) from original latexes; (b) AFM phase image of the cross-section of polymer film with 2% DMAPS.

Table 3.4. Mechanical properties of the films with different DMAPS concentrations and reference film, determined from stress-strain graphs of films (prepared from original latexes at standard atmospheric conditions, T=25 °C and RH=55%).

DMAPS (%)	Young's modulus (MPa)	Yield stress (MPa)	Ultimate tensile strength (MPa)	Elongation at break (%)
Reference	1.8±1.2	0.4±0.4	5.8±0.3	1134.9±0.7
0.5	1.1±5	1.2±0.8	6.6±0.2	458.6±0.2
1	4.6±2	1.4±0.4	7.8±0.2	701.2±0.1
2	3.2±7	1.8±0.6	9.2±0.6	428.6±0.8
3	3.7±2	1.6±0.3	7.2±1	454.6±0.1
5	10.9±0.3	1.5±0.5	6.2±1	445.9±0.1

The presence of DMAPS in the films improved the mechanical properties significantly with respect to those of reference film. According to Table 3.4, the Young's modulus was increased up to almost one order of magnitude, whereas the yield stress was four fold enhanced, but with a small drop of the elongation at break. These results indicate that the polymers with small amount of DMAPS were stiffer and still extensible. Taking into account that the chains that contain DMAPS provided colloidal stability

to the particles, they might be placed in majority on the particle surface. During film formation, these chains probably formed stiff network within the film that induce a mechanical percolation and the observed enhancement. To confirm this hypothesis, the morphology of the film cross-sections was studied by AFM. Figure 3.12b shows a representative AFM phase image of the cross-section film with 2% DMAPS, in which the presence of the honeycomb ionic network in bright colour within the darker polymer matrix is clearly appreciated. As well, large brighter structures might be observed in Figure 3.12b, attributed to the presence of aggregates made of water-soluble species in the film. This network is created around each polymer particles, which deformed, but did not lose the identity, indicating lack of chain interdiffusion. Similar behaviour was observed previously in case of use of NaSS anionic monomer for stabilization of polymer colloids[23], but the observed increase of Young's modulus due to the stiff network within the film was significantly lower than in the present case of DMAPS. The stronger effect of DMAPS presence on mechanical properties encountered in Figure 3.12a and Table 3.4 is attributed to the multiple ionic interactions established between the particles containing zwitterions on the surface.

In an attempt to increase the rate of interdiffusion of the polymer chains and eventually improve further the mechanical properties, the films were annealed at 80 °C for three days. The tensile curves of annealed films are presented in Figure 3.13a, the mechanical properties in Table 3.5, whereas the AFM phase image of the 2% DMAPS film cross-section in Figure 3.13b. Oppositely than expected, the mechanical properties of the films dropped after annealing, according to tensile curves in Figure 3.13a. Table 3.5 shows that Young's modulus, of the films were almost one order of magnitude lower than in the original films before annealing, whereas the other properties were a bit enhanced (for example the elongation at break), indicating that the films are less stiff but more extendable. In the case of reference film, annealing does not introduce any important changes in the tensile behavior. AFM image of the

cross-section of the representative film containing 2 % DMAPS (Figure 3.13b) presents continuous structure without any indication of particle presence.

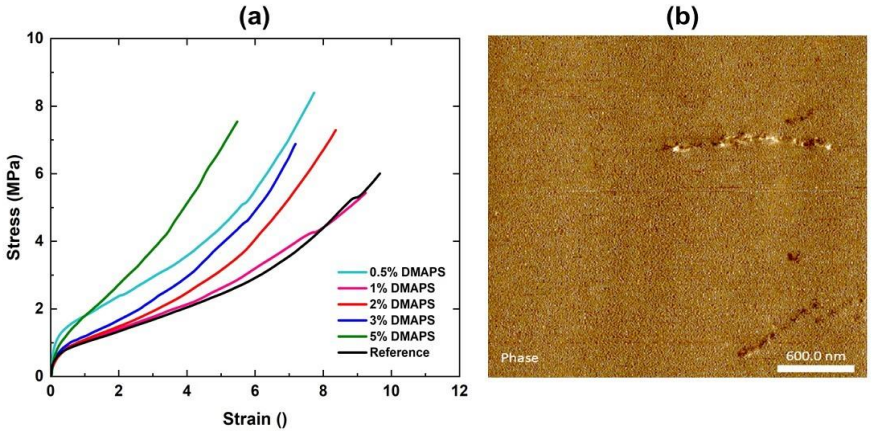

Figure 3.13. (a) Stress-strain curves of the polymer films with different DMAPS quantities and the reference film, prepared at standard atmospheric conditions (T=25 ºC and 55% relative humidity) from original latexes and annealed afterwards at 80 ºC for 3 days; (b) AFM phase image of the cross-section of polymer film with 2% DMAPS.

Table 3.5. Mechanical properties of the films with different DMAPS quantities determined from stress-strain graphs of films, prepared from original standard atmospheric conditions and afterwards annealed at 80 ºC for 3 days. Reference film was not annealed.

DMAPS (%)	Young's modulus (MPa)	Yield stress (MPa)	Ultimate tensile strength (MPa)	Elongation at break (%)
Reference	1.5±0.6	0.3±0.2	5.4±0.1	889±1.2
0.5	0.1±0.6	0.9±0.3	7.9±0.8	780.4±12
1	0.38±0.2	0.6±0.7	5.2±1.3	986.8±6
2	0.34±0.7	0.5±0.5	6.8±0.3	831.3±0.8
3	0.62±0.4	0.6±0.3	6.5±0.7	722.2±2.3
5	0.51±0.6	0.7±0.4	6.9±3	532.1±4

As the annealing temperature is higher than Tg of the MMA/n-BA/ DMAPS films (9–15 °C) and as well is higher than Tg of DMAPS homopolymer (Tg = 28°C), the annealing process induced high chain mobility. The reinforcing network made of DMAPS rich chains (observed in Figure 3.12b) was diluted, promoting

interdiffusion of MMA/n-BA chains and formation of the perfectly continuous film, shown in Figure 3.13b. The dissolution of the reinforcing network is probable the main cause of the observed drop of the Young's moduli. The films analyzed so far contain the water-soluble oligomers rich in DMAPS molecules that likely acts as a plasticizer, decreasing the mechanical performance. To investigate this effect, the latexes containing 1 % and 2 % DMAPS were compared with their dialyzed counterparts. From these dialyzed latexes, the DMAPS films were prepared at standard atmospheric conditions (25 °C and 55 % RH) and their mechanical properties were studied. The tensile curves shown in Figure 3.14a certainly reveal incredible increase of Young's modulus, moreover proportional to the incorporated amount of DMAPS (Table 3.1). Table 3.6 discloses that the Young's moduli were two order of magnitude higher, even though the films lost flexibility, which is characteristic for reinforced materials. The loss of flexibility may be related with the lack of the oligomeric species, removed during dialysis. As these oligomers are densely charged with both positive and negative charges, likely they form a kind of ionic complexed aggregates, distributed within the films prior to dialysis, conveying flexibility. AFM image of the cross-section of the dialyzed films, shown in Figure 3.14b, presents similar structure as the original, non-annealed films (Figure 3.12b). Nevertheless, in Figure 3.14b improved organization of the particles may be noticed. The lack of oligomeric species, which are placed in the aqueous continuous phase of the latexes, and distributed within the film during drying, obviously disturb the organization of the particles (Figure 3.12b). Oppositely, from the dialyzed latexes the particles packed much better, allowing regular creation of multiple ionic interactions that reinforced significantly the films.

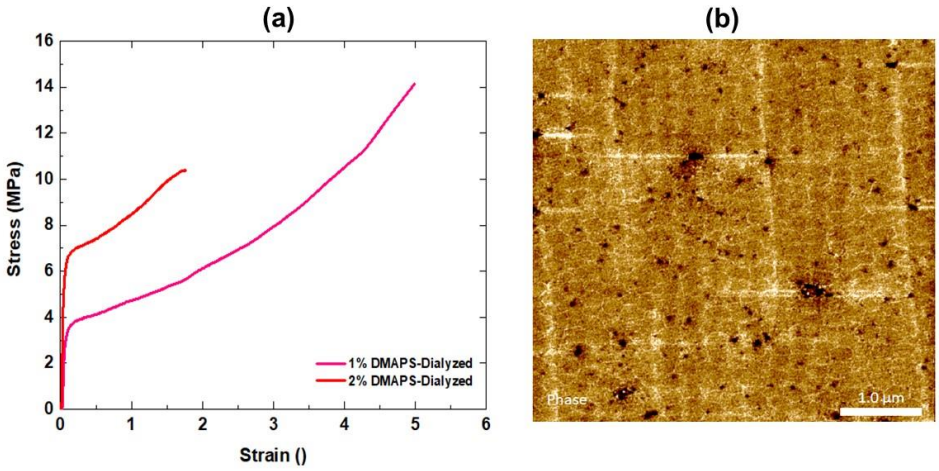

Figure 3.14. (a) Stress-strain curves of the polymer films with 1% and 2% DMAPS contents, prepared at standard atmospheric conditions (T=25 ºC and RH=55%) from dialyzed latexes prior to film formation; (b) AFM phase image of the cross-section of polymer film with dialyzed 2% DMAPS (T=25 ºC and RH=55%).

Table 3.6. Mechanical properties of the films with 1 and 2% DMAPS determined from stress-strain graphs of films, prepared from dialyzed latexes at standard atmospheric conditions (25 °C and 55 % RH).

DMAPS (%)	Young's modulus (MPa)	Yield stress (MPa)	Ultimate tensile strength (MPa)	Elongation at break (%)
1	37.4	3.8	14.1	619.1
2	14.4	6.6	10.4	296.4

The water sensitivity of polymer films is a crucial property for their use in protective coatings. Since the studied systems are waterborne, they typically exhibit high water sensitivity. However, based on the results obtained thus far, which indicate the establishment of ionic bonding and a decrease in the hydrophilicity of the film surface as determined by contact angle measurements (Table 3.3), it was expected that the DMAPS films would show reduced water sensitivity than reference film stabilized with SDS. To evaluate the water absorption of the films with different DMAPS concentrations, the films were immersed in water for an extended period of two weeks, and the water uptake was measured. The

results of water uptake for films obtained from original and dialyzed latexes are presented in Figure 3.15(a) and (b), respectively.

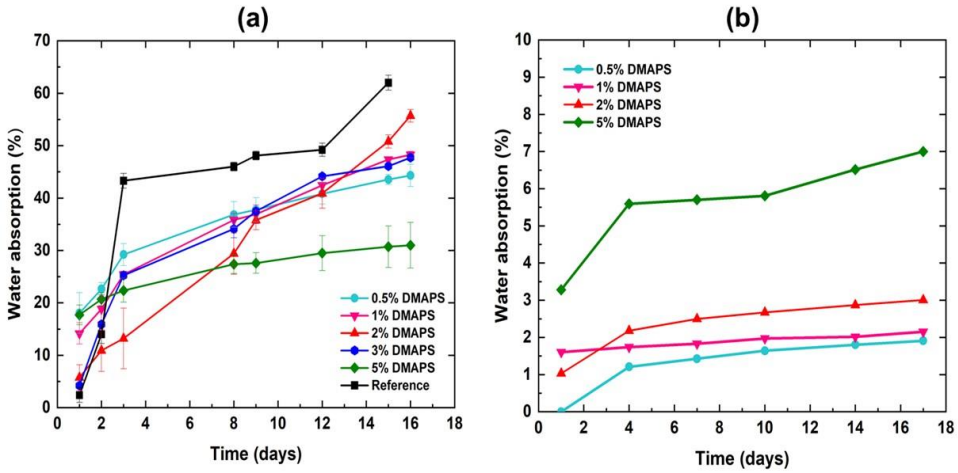

Figure. 3.15. Water uptake of the polymer films with different DMAPS amounts and the reference film prepared from: (a) original and (b) dialyzed latexes.

For the original latexes (Figure 3.15a), it was observed that the films containing DMAPS absorbed less water than the reference film. Even though there was not any clear trend established with respect to the DMAPS incorporated quantity, the film with highest DMAPS content absorbed importantly less water quantity than the reference and the other DMAPS film. The lower water sensitivity is probably related with the strong ionic-ionic interactions between the polymer chains rich in DMAPS, similarly as observed by Argaiz et al. by the ionic complexation established within the polymer film made of oppositely charged polymer particles.[23] Nevertheless, DMAPS containing films still present important water sensitivity, which is likely result on two effects. On one hand, the small quantity of conventional surfactant (SDS) coming from the seed synthesis probably created hydrophilic pockets within the film. On the other hand, the latexes synthesized with DMAPS present an important quantity of water-soluble oligomers that are distributed within the film. To check if the effect of water-soluble oligomers over the

water sensitivity is important, the water uptake measurements were performed with films prepared from dialyzed latexes. As Figure 3.14b reveals, certainly the dialyzed films absorbed significantly less water quantity, which demonstrates that even though the water-soluble species might be ionically complexed, still they affect negatively the water absorption ability of the films.

The barrier properties of a film usually determined by the permeability is the result of three consecutive steps. First of all, the film absorbs the vapour, which then diffuses through the film from which it is finally desorbed. The presence of the network made of polymer chains rich in zwitterionic units within the polymer matrix, which moreover are interconnected by ionic bonds, could provide very good barrier to the polymer films against humidity diffusion. To check this, the moisture permeability of the polymer films was studied and the results are presented in Table 3.7. The reference film exhibited significant permeability to moisture, attributed to the high concentration of SDS that migrates during film formation, leading to a more hydrophilic film surface and the formation of hydrophilic regions within the film. When SDS was replaced by DMAPS, the moisture permeability of the original film at atmospheric conditions decreased by more than one order of magnitude compared to the reference film. This excellent barrier performance can be attributed to the presence of ionic complexation, forming a network within the film matrix composed of chains rich in DMAPS, which are likely rigid and charged, as observed in Figure 3.12b. The network creates physical barriers to humidity penetration throughout the film. To further investigate this, the annealed film, in which the ionic network was dissolved due to improved inter-diffusion of the polymer chains at an increased temperature (Figure. 3.13b), was subjected to humidity permeation analysis. Surprisingly, when this reinforcing network was destroyed by annealing of the film (Figure 3.13b), the water barrier properties were not significantly changed since during heating of the film above its Tg, the polymer chains got increased mobility, the ionic complexation likely was further promoted by the improved contact between the zwitterions. Therefore, the enhanced humidity barrier might be related rather with the ionic complexation within

the whole film that decreased the hydrophilicity than with the ionic complex reinforcing network. Taking this into account, the higher DMAPS concentration lower should be the moisture permeation. Contrary to expectations, the quantity of DMAPS had a minimal impact on the resistance to water vapor blocking.

Table 3.7. Moisture permeability of reference polymer film, and films containing 2% DMAPS (original and dialyzed) and 5% DMAPS prepared at atmospheric conditions) and 2% DMAPS original but annealed.

Film	Moisture permeability ($g \cdot mm/m^2 \cdot day$)
Reference	75.1±8
2% DMAPS	6.7±2.5
2% DMAPS annealed	3.1±1.2
2% DMAPS dialyzed	5.3±1.3
5% DMAPS	12.6±2.7

3.3.2.1. Study of antifouling of DMAPS containing films

Zwitterionic polymers possess an inherent antifouling property and even it has been quite deeply studied, there are not clear rules to predict their antifouling efficiency and the mechanism remain still unrevealed.[24] Commonly, the antifouling mechanism is explained by a water barrier layer formation on the surface of the film that reduces significantly the adsorption of the foulant (protein) due to steric repulsions.

Bovine serum albumin (BSA) was the selected protein to evaluate the capability of the films for protein adsorption. Under aqueous conditions, the zwitterionic moieties arising from DMAPS are expected to be oriented to the aqueous phase giving negative surface charge as suggested by the zeta potential measurements (Table 3.1). In the same way, under the phosphate buffer solution (PBS) employed during the experiment (pH=7.4) the protein (BSA) with an isoelectric point (IEP) of approximately 4.8[25,26] might be strongly negatively charged favouring the repellency between the protein and substrate. The same

interactions are expecting to happen in the case of reference latex, which is negatively charged due to SDS rich surface.

Even though in literature [27-29] the excellent anti-fouling characteristics of zwitterionic polymer coatings are explained by the electrostatically induced hydration layer by the high density ions, the water contact angles present in Table 3.3 indicates that DMAPS films are less hydrophilic than the reference and probably less prone to form hydrating layers. In order to determine the antifouling properties of the polymer films, BSA adsorption on the four polymer films including reference was evaluated by QCM-D studies. Both the change in frequency (Δf) and dissipation (ΔD) were monitored over time (Figures 3.16a and 3.16b, respectively). It can be observed in Figure 3.16a that all the films, including the reference show relatively low protein adsorption. Nevertheless, the reference film presents the largest Δf, fivefold that of DMAPS containing films. Between the DMAPS containing films, that with 5% DMAPS adsorbed the least protein quantity, less than both original and dialyzed 2% DMAPS films. In addition, there was not significant difference between 2% DMAPS original and dialyzed, which was quite surprising, due to the lower concentration of DMAPS in the dialyzed 2% DMAPS. Likely, the DMAPS concentration on the surface of the film was not affected by the dialysis process, which is related to the lack of migration of DMAPS containing water-soluble oligomers towards film-air surface during film formation.

The change in the dissipation, shown in Figure 3.16b, is the largest for 5% DMAPS film, whereas the reference shows the lowest dissipation, indicating that the protein is more rigidly and permanently attached to the reference surface, whereas the BSA on the 5% DMAPS film surface is weakly and reversibly adsorbed.

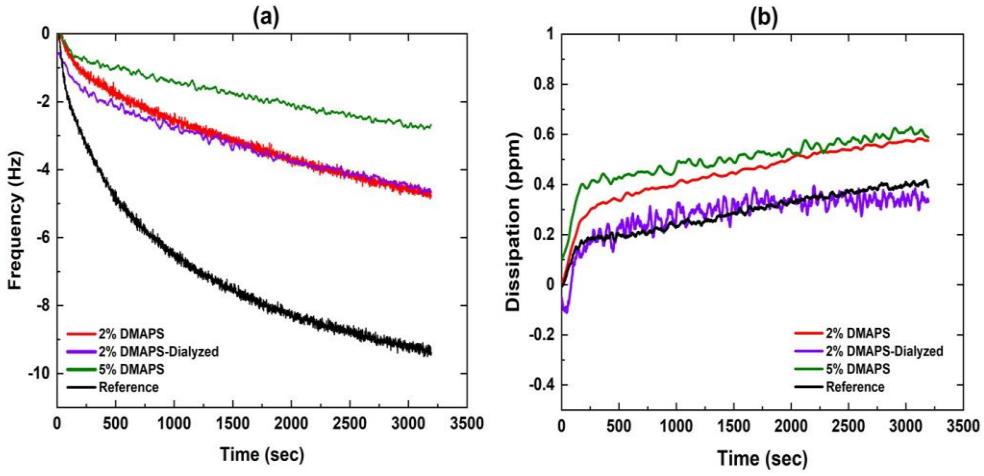

Figure 3.16. Representative QCM-D frequency (a) and dissipation (b) profile with time of polymer films exposed to BSA in PBS solution.

Nevertheless, it should be taken into account that QCM-D determines both the adsorbed BSA and its associated water ("wet mass"). Therefore, in order to shed a bit of light on the matter, the films were analysed by MP- SPR and the results are shown in Figure 3.17. In contrast to QCM-D that determines the frequency change due to adsorbed amount of material, MP-SPR is an optical technique that measures the change in the refractive index. Therefore, the detected values are exclusively due to protein adsorption, and do not cover the water absorbed by the film (it determines the "dry mass"). Figure 3.17 also shows that the reference film present the highest BSA adsorption, whereas the 5% DMAPS film the lowest one. Taking into account that the antifouling character arises from the presence of DMAPS, these results are in agreement with the expected ones since higher is DMAPS concentration in the film, lower is the BSA adsorption.

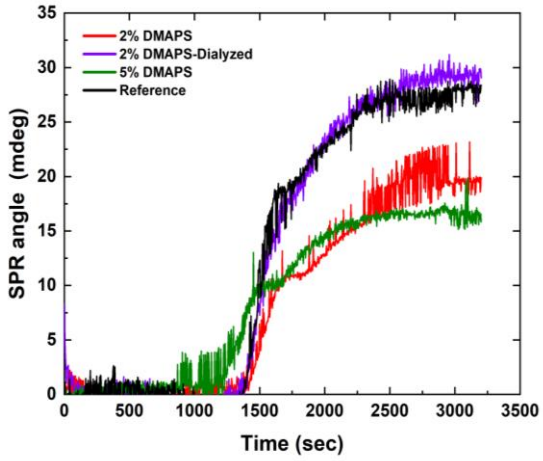

Figure 3.17. Adsorption of BSA 1000ppm on sensors deposited with different latex in MP-SPR.

However, in contrast to the QCM-D and as expected, MP-SPR results mark a clear difference between the BSA adsorption on the 2% DMAPS original film and the dialyzed one. The BSA adsorption on the 2% DMAPS dialyzed film is very similar to that of the reference, probably due to the reduction of DMAPS amount in the film after dialysis with respect to the original 2% DMAPS. While dialyzing the latex, all the water-soluble oligomers presenting smaller molecular sizes than the pore size of the membrane are removed from the latex and subsequently from the film. In this way, the DMAPS that was not incorporated onto the polymer particles (50%) would be removed, resulting in a film with lower amount of DMAPS.

To understand the results better, the approximate surface masses for both, QCM-D and MP-SPR results were calculated (Table 3.8). For the approximation of the adsorbed mass determined by QCM-D, Sauerbrey equation was used (eq.1).

$$\Delta m = -C \cdot \Delta f / n \qquad \text{(eq.1)}$$

In this equation, C is a constant (17.7 ng $cm^{-2}s^{-1}$ for this equipment) and n is the resonance overtone number (n=5 was used here). Where appropriate, a 2nd order data noise smoothing was applied for better visualization of the data. This equation is a linear relationship between the resonance frequency (eq. 2) changes of an oscillating quartz crystal and its surface mass changes and it is defined as follows:

$$\Delta m = 17.7 \cdot \Delta f \qquad \text{(eq.2)}$$

Where, Δf is the resonance frequency change (Hz), Δm is the surface mass of the adsorbed layer (ng/cm^2) and, 17.7 ng/cm^2 Hz is a constant comprising sensor specific characteristic parameters.

On the other hand, for the MP-SPR results, a linear relationship between peak minimum angle change in the MP-SPR and its surface mass changes was used to approximately calculate the BSA adsorbed on the surface of the film, presented by eq. 3.

$$\Delta m = 0.8333 \cdot \Delta \theta \qquad \text{(eq.3)}$$

Where, $\Delta \theta$ is the peak minimum angle change (mdeg), Δm is the surface mass of the added layer (ng/cm^2). 0.8333 ng/cm^2 mdeg is a constant, which approximately correlates the change in angle to the change in surface mass for a measurement wavelength of 670 nm.

The resulting surface masses in ng/cm^2 together with the amount of associated water calculated from the difference between the measured BSA adsorption by QCM-D and MP-SPR are presented in Table 3.8.

Table 3.8. Amount of BSA adsorbed on the different films calculated by Eq. (2, 3) for QCM-D results and Eq. (4) for MP-SPR results, and the amount of associative water.

BSA adsorbed	mQCM-D [ng/cm^2]	mMP-SPR [ng/cm^2]	Associated water (QCM-D) [ng/cm^2]
2% DMAPS-Original	80	16	64
2% DMAPS -dialyzed	80	24	56
5% DMAPS	44	14	30
Reference	168	23	145

Table 3.8 shows that the surface masses determined by MP-SPR were significantly (3-7 times) lower than the same measured by QCM-D, clearly demonstrating that the QCM-D results encompass both the BSA and the water adsorption. On the other hand, it is clear that the reference film adsorbed 3-fold higher water quantity than the DMAPS containing films, for which the associated water quantity dropped with increasing DMAPS content. Interestingly, 2% dialyzed DMAPS contains less DMAPS than original 2% DMAPS and presents less amount of associative water. The difference might be because of the SDS removal during the dialysis, which make the difference in their hydrophilicity. The quantity of BSA adsorbed follows similar trend, thus 5% DMAPS film seems to be less prone to fouling. These results are in concordance with the tendency in hydrophilicity shown in Table 3.3, according to which 5% DMAPS is the least hydrophilic, supported also by the lowest associated water quantity in Table 3.8.

Considering that in the literature the antifouling capacity of the polymer film surface is related with the capability of the film to associate water and form a thicker hydrophilic layer that prevents protein adsorption on the film, along to the strength of the water molecules bonding, these results indicate that there is another phenomenon happening that affects the antifouling behaviour.

5% DMAPS film is the least hydrophilic according to the CA measurements and associative water on this film is the lowest, demonstrating that the water film created on the surface of this film will be the thinnest in comparison to the other DMAPS containing films and the reference one, in accordance to the associated water quantity (Table 3.8). On the other hand, as AFM images shown (Figure 3.7) this film is the roughest one, which capture the water molecules more stable once bounded strongly on the surface. Since the protein is also strongly hydrophilic, having the thinner water layer surrounding the film, less protein would have access to the film. Due to strongly, electrostatically bound water, stabilized moreover by the rougher surface rich in DMAPS units, there will be less free adsorption sites for the protein adsorption. On the contrary, there is a thicker associative water layer created on the reference film that can be an efficient medium to bring more proteins to the film. The water molecules are weakly

bound on the surface and might easily be replaced by the BSA molecules. Another effect rarely investigated in the literature is a coverage of the film surface with the DMAPS units. Taking into consideration that in 5% DMAPS film there is a double DMAPS quantity (incorporation is 2.2 g per 100 g of polymer) than in 2% DMAPS film (1 g per 100 g polymer), it is clear that for higher DMAPS quantity in the films, higher is the coverage of the surface, which results in less original MMA/n-BA film to interact with the protein. This is probably an additional parameter that affects the fouling behaviour and explains the observed differences in the BSA adsorption.

On the other hand, the QCM-D results show that the 5% DMAPS film presented the highest dissipation indicating a more viscoelastic attachment between the protein and the film surface whereas, the reference presented the lowest dissipation as an indicative of a more rigid attachment between the BSA and the surface of the film. The change in dissipation can be related with the associative water, and usually for higher associative water quantity, higher is the dissipation. However, the associative water amounts presented in Table 3.8 showed the opposite trend, being the reference with the highest amount of associative water and the 5% DMAPS with the lowest. Furthermore, the trend observed in the amount of associative water was in agreement with the water uptake results presented in Figure 3.15 where it was found that the water absorption decreased as DMAPS concentration in the film increased. Similar results were found by Bengani et al.[18] where they found that the swelling for the copolymers containing low amount of DMAPS was negligible due to the low interconnectivity between DMAPS domains. Even more, when the water uptake was repeated for the 2% DMAPS after dialysis the water uptake decreased even more as so did the amount of associative water (Table 3.8). Therefore, it seems that the higher dissipation observed by the QCM-D on the films with increased DMAPS content clearly can be related to a weaker adsorption. A possible consequence could be that regeneration (removal of BSA adsorbed) of DMAPS 5% film could be easier than with the reference sample. A schematic representation of the effect

of DMAPS concentration on the BSA adsorption on the films with different DMAPS coverage is given in Figure 3.18.

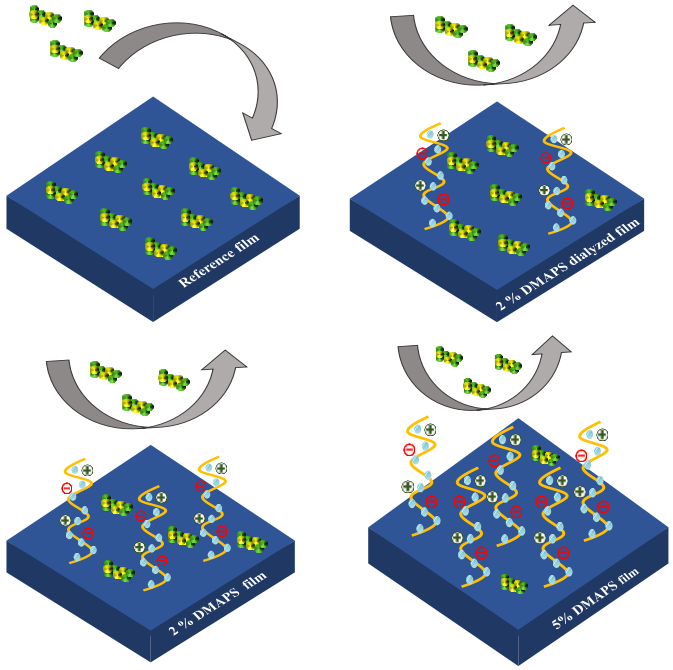

Figure 3.18. Schematic representation of the effect of DMAPS concentration on the antifouling of BSA.

3.4. Conclusions

High solids content collodial polymer dispersions composed of MMA/n-BA polymers stabilized with a small amount of the zwitterionic monomer DMAPS (0.5–5 %) were successfully synthesized through seeded semi-continuous emulsion polymerization.

Comparing the characteristics of DMAPS containing polymers with a reference polymer film stabilized with conventional SDS surfactant, it was evident that the concentration of DMAPS significantly

influenced the colloidal stability. At low DMAPS concentration (0.5 wbm%), there were insufficient stabilizing units created in situ, resulting in a high fraction of coagulum and large particle size. Conversely, at high DMAPS concentration (5 wbm%), although the produced latex exhibited a decent particle size (237 nm), a large amount of coagulum was obtained, likely due to the high concentration of water-soluble oligomers, increasing the ionic strength in the dispersion. In the optimal DMAPS concentration range (1–3 %), colloidal stability was achieved, with low coagulum quantity and particle size around 270 nm. The incorporation of DMAPS onto particles was studied as a crucial requirement for colloidal stability, with higher initial DMAPS concentrations resulting in a higher quantity of incorporated DMAPS.

Water contact angles before and after rinsing the DMAPS containing polymer films with water demonstrated no migration of DMAPS containing polymer chains towards the film-air interface, including the water-soluble species. The DMAPS containing films displayed mechanical reinforcement compared to conventionally stabilized films, with a higher Young's modulus of elasticity attributed to a stiff network made of polymer chains rich in DMAPS units, as determined by AFM imaging. This network provided strong and multiple ionic bonding, likely contributing to high flexibility even with increased stiffness. Consequently, the DMAPS containing films showed decreased water absorption and significantly enhanced humidity barrier performance, with humidity penetration one order of magnitude lower than in the reference film.

After annealing the films at a temperature higher than Tg, the network was dissolved, redistributing the DMAPS-containing chains within the matrix, likely due to improved interdiffusion of the polymer chains. As a result, the stiffness of the films decreased, while the barrier properties were further improved. The higher humidity penetration in the non-annealed film was attributed to the presence of some free anions within the ionic network, forming a conductive pathway for humidity. After dissolution of the network by annealing, these pathways were disrupted, further improving the water

barrier performance. Moreover, the removal of water-soluble species positively affected the properties of the polymer films

The resulted DMAPS containing films demonstrated reduced hydrophilicity, rougher textures, and significantly lower fouling tendencies. Particularly surprising was the film with 5% DMAPS, which exhibited the least fouling behavior despite its association with a smaller amount of water. This exceptional performance was attributed to a combination of electrostatic interactions and the rough surface, which enhanced the strong binding of the limited water present.

The remarkable properties exhibited by the zwitterionic monomer DMAPS in the MMA/n-BA polymer coating films open up new possibilities and alternatives for colloidal stabilization beyond conventional surfactants. Moreover, this study expands the potential applications of waterborne polymers, particularly in the development of high-performance barrier coatings that are highly resistant to fouling.

3.5. References

1. *Surfactant-free emulsion copolymerization of styrene and sodium styrene sulfonate.* **Kim, J. H., et al.** s.l. : Wiley Online Library, 1992, Journal of Polymer Science Part A: Polymer Chemistry, Vol. 30, pp. 171–183.

2. *Practical aspects of the surfactant-free emulsion polymerization of styrene.* **Shouldice, Grant T. D., Vandezande, Gerald A. and Rudin, Alfred.** s.l. : Elsevier, 1994, European polymer journal, Vol. 30, pp. 179–183.

3. *Soap-free emulsion polymerization of n-butyl acrylate: Copolymerization with 1, 1-(dimethyl)-1-(3-methacryloxyethyl)-1-(sulfopropyl) ammonium betaine.* **Blom, Henk P., et al.** s.l. : Wiley Online Library, 1998, Journal of applied polymer science, Vol. 70, pp. 227–236.

4. *Polyzwitterionic copolymer nanoparticles loaded in situ with metoprolol tartrate: synthesis, morphology and drug release properties.* **Kostova, Bistra, et al.** s.l. : Springer, 2013, Journal of Polymer Research, Vol. 20, pp. 1–8.

5. *Surfactant-Free Emulsion Copolymerization of Vinyl Acetate and 3-Dimethyl (methacryloyloxyethyl) ammonium Propanesulfonate and Swelling Behavior of their Copolymer Matrices.* **Kamenska, Elena, et al.** s.l. : Wiley Online Library, 2007, Macromolecular Reaction Engineering, Vol. 1, pp. 553–562.

6. *Improved antibiofouling properties of photobioreactor with amphiphilic sulfobetaine copolymer coatings.* **Wang, Yixuan, et al.** s.l. : Elsevier, 2020, Progress in Organic Coatings, Vol. 144, p. 105666.

7. *Surface engineering of styrene/PEGylated-fluoroalkyl styrene block copolymer thin films.* ***Martinelli, Elisa, et al.*** *s.l. : Wiley Online Library, 2009, Journal of Polymer Science Part A: Polymer Chemistry, Vol. 47, pp. 267–284.*

8. *Formation of protein charge ladders by acylation of amino groups on proteins.* ***Colton, Ian J., et al.*** *s.l. : ACS Publications, 1997, Journal of the American Chemical Society, Vol. 119, pp. 12701–12709.*

9. *Highly monodisperse zwitterion functionalized non-spherical polymer particles with tunable iridescence.* ***Vasantha, Vivek Arjunan, et al.*** *s.l. : Royal Society of Chemistry, 2019, RSC advances, Vol. 9, pp. 27199–27207.*

10. *Reconciling low-and high-salt solution behavior of sulfobetaine polyzwitterions.* **Mary, Pascaline, et al.** s.l. : ACS Publications, 2007, The Journal of Physical Chemistry B, Vol. 111, pp. 7767–7777.

11. *Effect of the ionic surfactant concentration on the stabilization/destabilization of polystyrene colloidal particles.* **Jódar-Reyes, Ana B., Martín-Rodríguez, Antonio and Ortega-Vinuesa, Juan L.** s.l. : Elsevier, 2006, Journal of colloid and interface science, Vol. 298, pp. 248–257.

12. *Fundamentals of chemical incorporation of ionic monomers onto polymer colloids: paving the way for surfactant-free waterborne dispersions.* **Bilgin, Sevilay, Tomovska, Radmila and Asua, José M.** s.l. : Royal Society of Chemistry, 2016, RSC advances, Vol. 6, pp. 63754–63760.

13. *Seeded semin-BAtch emulsion polymerization of n-butyl acrylate. Kinetics and structural properties.* **Plessis, Ch, et al.** s.l. : ACS Publications, 2000, Macromolecules, Vol. 33, pp. 5041–5047.

14. *Adhesion enhancement in waterborne acrylic latex binders synthesized with phosphate methacrylate monomers.* **Gonzalez, Inigo, et al.** s.l. : Elsevier, 2008, Progress in organic coatings, Vol. 61, pp. 38–44.

15. *New insight into "polyelectrolyte effect".* **Yang, Hu, Zheng, Qiang and Cheng, Rongshi.** s.l. : Elsevier, 2012, Colloids and Surfaces A: Physicochemical and Engineering Aspects, Vol. 407, pp. 1–8.

16. *UCST wetting transitions of polyzwitterionic brushes driven by self-association.* **Azzaroni, Omar, Brown, Andrew A. and Huck, Wilhelm T. S.** s.l. : Wiley Online Library, 2006, Angewandte Chemie International Edition, Vol. 45, pp. 1770–1774.

17. *Ionic inter-particle complexation effect on the performance of waterborne coatings.* **Argaiz, Maialen, et al.** s.l. : MDPI, 2021, Polymers, Vol. 13, p. 3098.

18. *Self-assembling zwitterionic copolymers as membrane selective layers with excellent fouling resistance: effect of zwitterion chemistry.* **Bengani-Lutz, Prity, et al.** s.l. : ACS Publications, 2017, ACS Applied Materials & Interfaces, Vol. 9, pp. 20859–20872.

19. *A review of surface roughness in antifouling coatings illustrating the importance of cutoff length.* **Howell, Dickon and Behrends, Brigitte.** s.l. : Taylor & Francis, 2006, Biofouling, Vol. 22, pp. 401–410.

20. *Surface charge control for zwitterionic polymer brushes: Tailoring surface properties to antifouling applications.* **Guo, Shanshan, et al.** s.l. : Elsevier, 2015, Journal of colloid and interface science, Vol. 452, pp. 43–53.

21. *Surface properties and reduced biofouling of graft-copolymers that possess oppositely charged groups.* **Herzberg, Moshe, et al.** s.l. : ACS Publications, 2011, Biomacromolecules, Vol. 12, pp. 1169–1177.

22. *Influence of silicone surface roughness and hydrophobicity on adhesion and colonization of Staphylococcus epidermidis.* **Tang, Haiying, et al.** s.l. : Wiley Online Library, 2009, Journal of Biomedical Materials Research Part A: An Official Journal of The Society for Biomaterials, The Japanese Society for Biomaterials, and The Australian Society for Biomaterials and the Korean Society for Biomaterials, Vol. 88, pp. 454–463.

23. *Towards improved performance of waterborne polymer dispersions through creation of dense ionic interparticle network within their films.* **Argaiz, Maialen, Aguirre, Miren and Tomovska, Radmila.** s.l. : Elsevier, 2023, Polymer, Vol. 265, p. 125571.

24. *Molecular design of zwitterionic polymer interfaces: searching for the difference.* **Laschewsky, André and Rosenhahn, Axel.** s.l. : ACS Publications, 2018, Langmuir, Vol. 35, pp. 1056–1071.

25. *Reversible Protein adsorption on mixed PEO/PAA Polymer brushes: Role of Ionic strength and PEO content.* **Bratek-Skicki, Anna, et al.** s.l. : ACS Publications, 2018, Langmuir, Vol. 34, pp. 3037–3048.

26. *Molecular packing of lysozyme, fibrinogen, and bovine serum albumin on hydrophilic and hydrophobic surfaces studied by infrared- visible sum frequency generation and fluorescence microscopy.* **Kim, Joonyeong and Somorjai, Gabor A.** s.l. : ACS Publications, 2003, Journal of the American Chemical Society, Vol. 125, pp. 3150–3158.

27. *Preparation and characterization of novel zwitterionic poly (arylene ether sulfone) ultrafiltration membrane with good thermostability and excellent antifouling properties.* **Rong, Guolong, et al.** s.l. : Elsevier, 2018, Applied Surface Science, Vol. 427, pp. 1065–1075.

28. *Cleaning of oil fouling with water enabled by zwitterionic polyelectrolyte coatings: overcoming the imperative challenge of oil–water separation membranes.* **He, Ke, et al.** s.l. : ACS Publications, 2015, ACS nano, Vol. 9, pp. 9188–9198.

29. *Highly durable antifogging coatings resistant to long-term airborne pollution and intensive UV irradiation.* **Yu, Xiaodong, et al.** s.l. : Elsevier, 2020, Materials & Design, Vol. 194, p. 108956.

Chapter 4. Surfactant-Free Emulsion Polymerization using Different Sulfobetaine-Zwitterionic Monomers

4.1. Introduction

The previous chapters demonstrated the viability of using a small amount of zwitterionic monomer, DMAPS, to stabilize high solids content (50%) (meth)acrylic polymer dispersions. The stabilizing species were created in situ through incorporation of DMAPS onto MMA/n-BA particles. Moreover, incorporating DMAPS into the (meth) acrylic chains led to significant enhancements in mechanical resistance and humidity barrier properties of the resulting polymer films. However, full potential of DMAPS was not achieved, due to the presence of ions from the SDS-stabilized seed particles, leading to ionic imbalance. As a consequence, the water sensitivity of the polymer films was compromised. Although the incorporation of DMAPS remained modest, the presence of water-soluble oligomers posed potential implications for the stability of the dispersions.

The primary objective of this study is to synthesize completely surfactant-free polymer dispersions with high solids content using different sulfobetaine based zwitterionic monomers, eliminating the reliance on conventional surfactants during seed particle synthesis.

*A part of the content of this chapter has been published in:

Chemical structure of zwitterionic monomers as a tool to produce colloidally stable (meth) acrylic polymer colloids. **Murali, Sumi, et al.** s.l. : Elsevier, 2023, Polymer, p. 126421.

Furthermore, this study explores different sulfobetaine zwitterionic monomers to evaluate how the chemical structure would affect the incorporation and subsequently their potential to stabilize the polymer colloids, and subsequently to broaden the versatility of this surfactant-free strategy.

This study involved the use of four sulfobetaine zwitterionic monomers (ZMs), including 2-[(methacryloyloxy) ethyl] dimethyl-(3 sulfopropyl) ammonium hydroxide (DMAPS), 4-[[2-(methacryloyloxy) ethyl] dimethylammonio] butane-1-sulfonate (M3295), 3-[[2-(acryloyloxy) ethyl] dimethylammonio] propane-1-sulfonate (A3367), and 3-[(3-acrylamidopropyl) dimethylammonio] propane-1-sulfonate (A3361). These ZMs share a common cation (quaternary ammonium) and anion (sulfonate), but they differ in their polymerizing functional groups and the distances between charges in their structures.

Compared to methacrylic DMAPS, M3295 has an extra methylene group between the charges, enhancing its hydrophobic nature. In contrast, A3367 shares the same structure as DMAPS, except for the presence of an acrylic polymerizing group. Lastly, A3361 combines an additional methylene between the charges with acrylamide polymerizing moieties, thereby contributing to its heightened hydrophobicity. These differences in functional groups and charge distances can significantly influence the copolymerization of ZMs with (meth)acrylic monomers, as well as their incorporation into polymer particles and the final properties of the resulting polymer. Scheme 4.1 displays the chemical structures of the zwitterionic monomers used in this study.

In the latter section of this chapter, an increased incorporation of acrylamide ZM A3361 prompted a more extensive investigation into its anti-polyelectrolyte properties. This investigation was carried out under lower pH conditions to ascertain the potential impact of this characteristic on the overall attributes of latex and films. To achieve this, a minor quantity of HCl was introduced into the pre-emulsion. Moreover, a polymer latex more reminiscent of industrial conditions (50% S.C.) was also synthesized by employing ZM A3361.

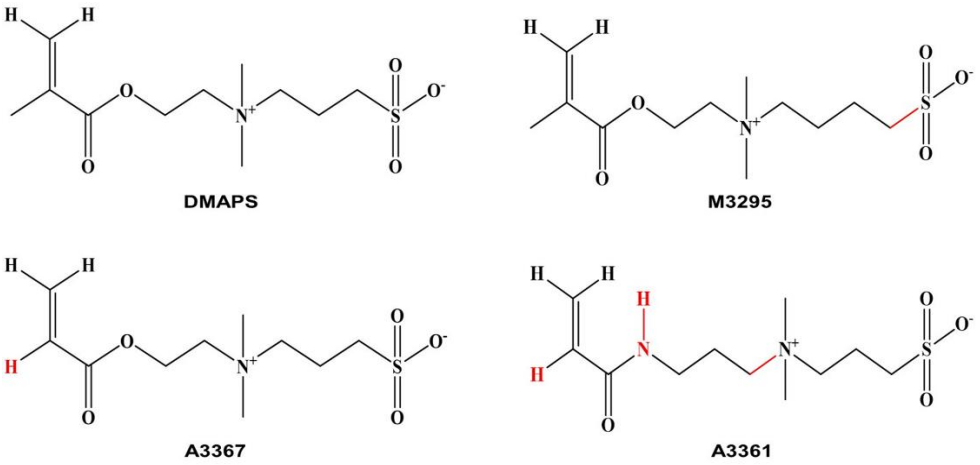

Scheme 4.1. Chemical structure of the different zwitterionic monomers used. Difference in their structure is marked by red colour.

4.2. Experimental section

4.2.1. Materials

The materials are given in Appendix I.

4.2.2 Polymerizations

4.2.2.1. Homopolymerization of zwitterionic monomers

The details of homopolymerization of the zwitterionic monomers used in this study can be found in Appendix I.

4.2.2.2. Synthesis of the seed

The experimental set up used to synthesize the latex is described in Appendix I. Surfactant-free seeds were successfully synthesized using different ZMs through a semi-continuous emulsion

polymerization process and a representative recipe using 2 wbm % DMAPS is outlined in Table 4.1. To reduce the formation of water-soluble species and enhance ZM incorporation onto polymer particles, a more hydrophobic monomer, BMA, was utilized for the seed synthesis. The process began by filling the reactor with an aqueous solution containing ZMs and BMA. Upon reaching the target temperature of 50 °C, separate feedings of the aqueous solutions of reductant FF7 and oxidant TBHP were gradually introduced into the reactor over a 90-minute period. The reaction then continued in batch mode at the same temperature for 2.5 hours. In order to investigate the anti-polyelectrolyte effect of ZM DMAPS, an additional seed was synthesized using an aqueous solution containing 0.02 M NaCl in a similar manner. Additionally, a seed with SDS was synthesized, and the detailed description of the polymerization procedure is provided in Appendix I.

Table 4.1. Representative recipe for the surfactant-free seed stabilized using 2 wbm % DMAPS (10 % S.C.). The feeding rate of initiator TBHP/FF7 were 1 g/min.

Ingredients	Initial charge (g)	Feed 1(g)	Feed 2 (g)
BMA	80.03	---	---
ZMs [a]	1.62	---	---
TBHP [b]	---	0.81	---
FF7 [b]	---	---	1.14
Water/0.02 M NaCl	540.8	90.06	90.12

[a] 2% wbm, [b] 1% wbm

4.2.2.3. Synthesis of surfactant-free latexes using different ZMs

For the seeded semi-continuous reactions, the experimental set up described in Appendix I was employed. To investigate the influence of the anti-polyelectrolyte behavior of ZM with acrylamide functionality (A3361), an additional reaction was conducted at a lower pH of (3-4) by adding a small amount of 0.01 M HCl. With ZM A3361, a higher solids content latex with a more industrial-like composition (50% S.C.) was produced as well. For comparison, a reference latex was synthesized using

2% SDS with solids content of 50%. Detailed descriptions of all experimental procedures and formulations can be found in Appendix I.

4.2.3. Characterization

The characterization methods are given in Appendix II.

4.3. Results and discussion

4.3.1. Synthesis of surfactant-free seed

To avoid the use of conventional surfactants during seed synthesis, zwitterionic monomers were used. To develop the seed synthesis procedure, DMAPS was selected due to its availability and lower cost. Both batch and semi-continuous emulsion polymerization methods were studied, and targeted S.C. of the seed was 10%. Redox pair TBHP/FF7 was utilized to produce highly hydrophobic tert-butoxy radicals in the aqueous phase, which reduce residence time of oligoradicals in the aqueous phase, minimizing termination and water-soluble oligomer formation.

In the initial trials, n-BA/MMA monomers (1:1 weight ratio) were polymerized in batch, by varying amount of DMAPS in a range of 1-3 wbm% to the main monomers. However, the resulting particle size exceeded 300 nm independently on DMAPS quantity employed, rendering them unsuitable as seed particles. Even though, it was expected that increasing the DMAPS amount would decrease the particle size due to higher incorporation, likely DMAPS's high hydrophilicity led to the formation of higher quantity of water-soluble species, increasing the ionic strength of the system and resulting in the formation of larger particle size seed latexes. These outcomes suggest that the reactivity ratios between DMAPS and n-BA and MMA monomers are not very favorable for copolymerization, leading to delayed incorporation and a lack of stabilization units during the initial reaction period, when particles are nucleated. If indeed the reactivity ratios are an issue, employing a semi-continuous process by feeding

the MMA/n-BA monomers in pre-emulsion containing DMAPS, might lead to improved incorporation and creation of stabilizing species, thus, smaller particle sizes.

During the semi-continuous mode, a pre-emulsion of n-BA/MMA (1:1) with DMAPS was prepared. The quantity of DMAPS added to the pre-emulsion was adjusted, spanning from 25% to 75% of the total required amount (2 wbm %). The remaining DMAPS was introduced in the reactor at reaction start. Redox pair TBHP/FF7 initiator was employed, with FF7 being added to the pre-emulsion and TBHP added separately as shot to the reactor. Nevertheless, the outcomes indicated that the particle size did increase >400 nm, and remained too large to serve as a suitable seed. Even the monomer concentration was low in the reactor that eliminated the effect of reactivity ratios on the incorporation of DMAPS, likely the low concentration of DMAPS in the reactor resulted in not sufficient creation of colloidal stabilizing species. Consequently, the newly nucleated particles coagulated, giving rise to increased average particle sizes.

In further trials, n-BA/MMA were replaced with much more hydrophobic butyl methacrylate (BMA), following the positive experience of Sevialy et al.[1] when NaSS hydrophilic monomer was introduced onto MMA/n-BA particles. By using BMA, the growing oligoradicals would spend less time in the aqueous phase, decreasing the probability of their termination in aqueous phase and creation of water-soluble oligomers. The BMA seed was prepared by varying amounts of DMAPS, ranging from 25% to 75%, similarly as explained previously. The average particle size of the BMA seed from these attempts are shown in Table 4.2.

Table 4.2. Particle size of surfactant-free seeds synthesized with BMA and DMAPS ZM.

Seed	DMAPS in reactor (%)	Dp (nm)
1	25	309
2	50	292
3	75	255
4	100	233

From Table 4.2., as the amount of DMAPS increased in the reactor, the particle size of the seeds decreased, likely due to increased quantity of stabilizing species created at higher DMAPS quantity. The smallest particle size (233 nm) was achieved when all DMAPS was added in the reactor since the reaction start. The smallest average particle size in case of BMA with respect to MMA/n-BA mixture (>400 nm) indicates that the quantity of water-soluble species should be lower when more main hydrophobic monomer was employed for the synthesis. Furthermore, this strategy was employed for synthesis of a range of seeds using different ZM monomers. The average particle sizes of the seed particles stabilized ZMs were in the similar range as DMAPS stabilized seed, as shown in Table 4.3.

Table 4.3. Particle size of seeds synthesized with different ZMs.

Seed	Dp (nm)
DMAPS	233
M3295	258
A3367	234
A3361	261

Even though the lowest average seed particle size obtained of 233 nm is high, as it is completely surfactant-free, it was thought that if we used higher seed quantity than usual, we will be able to prepare surfactant-free latex with high solids content.

4.3.2. Latex properties

Using surfactant-free seeds, 30% S.C. MMA/n-BA polymer latexes were synthesized by seeded semi-continuous mode using different ZMs. For the synthesis of each of the latex, their corresponding seed synthesized with the same ZM, was used. All reactions were conducted at their natural pH, approximately 7.

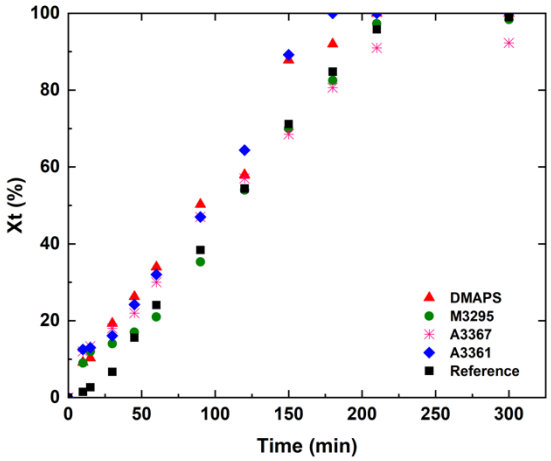

Figure 4.1. Time evolution of total monomer conversion *(Xt)* for seeded semi-continuous reactions by using different ZMs and reference.

Figure 4.1 depicts the time evolution of total monomer conversion for the reactions performed with different ZMs. The reaction rates are quite similar for the reference and the ZM-stabilized reactions. The small differences observed are likely result on the different ZM chemistry that affects the copolymerization with the main monomers. Nearly complete conversion of MMA/n-BA was achieved in all latexes, except for the A3367 ZM with acrylic functionality, where the monomer conversion was about 92%. Conversely, in the case of A3361 ZM with acrylamide functionality, full conversion was achieved slightly faster compared to the other ZMs. The extent of colloidal stabilization provided by the ZMs is likely closely linked to their incorporation onto the polymer particles. These results suggest that A3361 exhibited higher incorporation, while A3367 displayed the lowest incorporation among the ZMs studied.

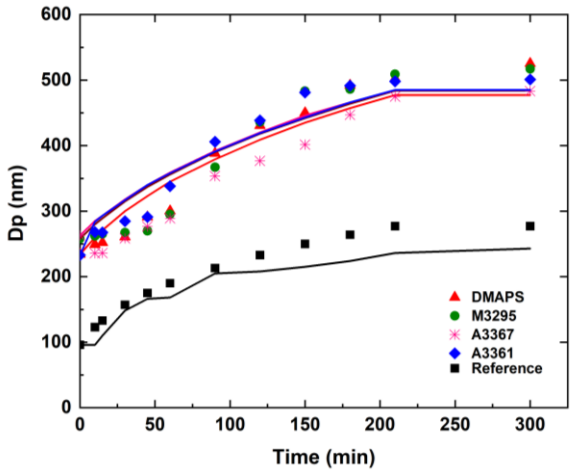

Figure 4.2. Time evolution of particle size (*Dp*) of latexes synthesized by seeded semi-continuous mode with different ZMs and reference latex **(**experimental indicated by dots and theoretical indicated by continuous lines).

Figure 4.2 illustrates the time evolution of the average particle size of the latexes synthesized using various ZMs and the reference latex. The experimental and theoretical particle sizes were determined and compared. The theoretical sizes were calculated by assuming a constant number of particles throughout the reactions. In the initial stage of the reactions, the experimental average particle size of all dispersions was smaller than the theoretical, indicating the formation of new particles by secondary nucleation. This trend was kept continuous for the reference latex. However, for the ZM containing latexes, the experimental size overcame the theoretically calculated, meaning that some particles coagulated. The larger particle size of these latexes than that of reference can be attributed to the larger average particle size of the ZM seeds (ranging from 233-261 nm) in comparison to the reference seed (96 nm).

Table 4.4. Characteristics of latexes containing different ZMs and the reference latex.

Latex	DMAPS	M3295	A3367	A3361	Reference
S.C. (wt%)	28	28	26	30	50
Xt(%)	100	98.4	92.3	100	100
Coagulum (%)	2	1	6.5	0	0
Dp (nm)	525	517	483	501	241
Dp_{theo}(nm)	478	482	475	477	277
Z-potential (mv)	-35.2	-42.1	-39.3	-35	-38
ZM Incorp. (%)	42	61	28	74	---
Gel content	16	18	23	19	0
$\overline{M_w}$ (kDa)	203	302	273	345	706
Tg (°C)	12	11	15	13	12

Table 4.4 provides a summary of the properties of the synthesized latexes. The conversion of ZMs in the polymer latexes was monitored using ^{1}H NMR and complete conversion was achieved for all ZMs. In all latexes, except for the acrylic ZM A3367 containing latex, the MMA/n-BA monomers were fully converted. The MMA/n-BA conversion in A3367 latex was Xt=92 %. This lower conversion can be attributed to the formation of a significant amount of coagulum during the synthesis (6.5%, Table 4.4), which likely included a portion of the monomers. Negligible coagulum formation was observed in the other latexes.

The zeta potential values of the latexes were all above 30 mV, indicating stable latexes in all cases. The incorporation of the ZMs was assessed through FTIR analysis of films prepared with the full-added quantity of ZM and films made from dialyzed latex to remove water-soluble species and the results regarding the incorporation of different ZMs onto polymer particles are presented in Table 4.4.

From Table 4.4, it is evident that the acrylamide containing ZM A3361 exhibited the highest incorporation rate (74%), followed by M3295 with a significant incorporation rate (61%), and DMAPS with a moderate incorporation rate (42%). On the other hand, the acrylic ZM A3367 showed the lowest incorporation (28%). These results align with the discussions on the total conversion of MMA/n-BA

monomers shown in Figure 4.1. The incorporation process is likely influenced by the chemical structure of the ZMs.

Two characteristics of ZM monomers likely affect these results. On one hand, it is the relative hydrophilicity of each ZM and on the other hand, their ability to copolymerize with the main monomers (mostly with MMA, considering its higher water solubility than n-BA). The increased hydrophobicity of A3361, attributed to the presence of acrylamide and an additional methylene group in its structure, is likely responsible for reducing the time spent by growing oligomers in the aqueous phase containing A3361. This accelerates the entry of such oligoradicals onto the polymer particles, providing colloidal stability, decreasing the formation of water-soluble species and increasing the incorporation. Similarly, M3295, with an additional methylene group, is expected to be more hydrophobic than DMAPS, leading to higher incorporation compared to DMAPS. The lower incorporation observed for A3367 suggests that the copolymerization of A3367 with MMA/n-BA is hindered by unfavourable reactivity ratios, even in the case of a semi-continuous reaction. The time evolution of the instantaneous monomer conversion for these reactions, presented in Figure 4.3, shows that there is indeed a monomer accumulation in the initial period of the reactions. This means that under the conditions studied, the reactivity ratios still have important effect on the copolymerization of each ZM with the MMA/n-BA to create stabilizing species. It has been reported that when ZMs are copolymerized with n-BA, they present increased reactivity than n-BA, presenting important compositional drift.[2,3] Nonetheless, there is random and alternative copolymerization between ZM and methacrylates and methacrylamides.[4-6] Following this, ZM in our systems would react quite readily with the MMA present in majority in the aqueous phase creating the stabilizing units. Nevertheless, the results indicate that in case of methacrylic ZM (DMAPS, M3295) and acrylamide ZM (A3361) this copolymerization is promoted over that of acrylic ZM (A3367), which finally resulted in lack of sufficient colloidal stability and creation of coagulum in the last. These results are in line with well-known reactivity in copolymerization of these type of monomers.

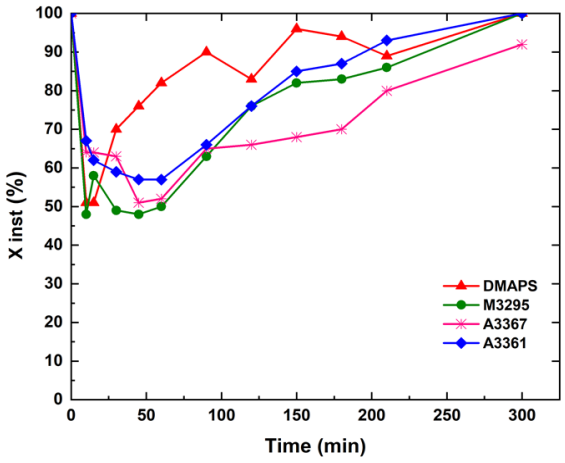

Figure 4.3. Time evolution of instantaneous monomer conversion (X_{inst}) of MMA/n-BA monomers in seeded semi-continuous emulsion polymerization, using different ZMs.

Attempts were made to determine the quantity of water-soluble polymer species within the ZM latexes based on reported procedures for surfactant-free latexes stabilized by NaSS.[1] However, the results obtained were inconsistent and irreproducible, and therefore, they are not reported here. It is likely that the soluble polymer chains strongly interact with each other and with other chains containing ZM units through ionic bonding, making their separation from the polymer dispersions challenging. Nevertheless, considering the full conversion of ZM and knowing the amount incorporated onto particles, it is possible to deduce the fraction of ZM involved in the formation of water-soluble polymeric species. Therefore, higher is the incorporation of ZM onto polymer particles; lower is their amount in the water phase in form of soluble oligomers. The exception is acrylic ZM A3367, in which there is additional fraction of ZM into coagulum.

The polymer microstructure was analysed by measuring the gel content (insoluble fraction of the polymer in THF solvent) and the molar mass of the soluble fraction. The reference polymer did not exhibit any gel content, likely because MMA units do not present any abstractable hydrogens in the

structure able to create branches, and, that their radicals terminate by disproportionation. The ZMs containing polymers present a gel fraction ranged from 15% to 23%, which probably refers to the insolubility of the polymer chains in THF induced by the presence of ionic species in the chains. Regarding the molar mass of the soluble fraction, the polymers synthesized in the presence of ZMs exhibited molar masses ranging from 203 to 345 kDa, which were significantly lower than that of the reference polymer (706 kDa). This could be attributed to the incorporation of higher molar mass polymers containing ionic moieties into the insoluble gel fraction, resulting in lower molar masses of the soluble fractions. The glass transition temperature (T_g) of the copolymers synthesized with different ZMs was quite similar, ranging from 11 to 15 °C, and comparable to that of the reference polymer due to the nearly identical composition of the copolymers, predominantly composed of MMA/n-BA.

Table 4.5. Freeze-thaw stability of surfactant-free latexes stabilized with different ZMs and reference latex. (✓) means no coagulation (X) indicates massive coagulation.

Latex	Cycle 1	Cycle 2	Cycle 3	Cycle 4	Cycle 5	Cycle 6
DMAPS	X	---	---	---	---	---
M3295	X	---	---	---	---	---
A3367	✓	✓	✓	✓	✓	✓
A3361	✓	✓	✓	✓	✓	✓
Reference	X	---	---	---	---	---

The freeze-thaw stability of the latexes was investigated to assess their performance under extreme weather conditions. Table 4.5 shows that the latexes containing DMAPS and M3295, as well as the reference latex, did not pass the freeze-thaw test. However, the A3361 (containing an acrylamide group) and A3367 (acrylic) latexes remained stable even after 6 freeze-thaw cycles. The superior freeze-thaw stability of A3361 can be attributed to its higher incorporation onto polymer particles, which allows the latex to retain a higher quantity of water bound ionically around the particles that remains unfrozen during the freezing cycle. Nevertheless, the low incorporation of A3367 indicates presence of other source of stability during freeze-thaw cycles. Previous reports have shown that the polymer T_g affects the latexes' freeze-thaw stability[7,8] and that harder particles tend to exhibit enhanced stability.

Considering that the ZM units are primarily located on the surface of the polymer particles, their T_g may play a significant role in freeze-thaw. Both homopolymers based on acrylic ZM (A3367) and acrylamide ZM (A3361) have considerably higher Tg values (83 and 143 °C, respectively) compared to others (28 and 63 °C). This indicates that polymer chains rich in these ZMs form a rigid shell around the MMA/n-BA particles, imparting exceptional stability during multiple freeze-thaw cycles.

Table 4.6. Salt stability of the latexes containing different ZMs and reference latex. The particle size is given in nm and shown in parenthesis. (✓) means stable latex and no changes in particle size; (X) indicates massive coagulation.

Latex	NaCl			$CaCl_2$
	0.5M	**0.75M**	**1M**	**1M**
DMAPS (525nm)	✓	✓ (670nm)	X	X
M3295(517nm)	✓	✓	✓	X
A3367 (483nm)	✓	✓	✓	✓(962nm)
A3361 (501 nm)	✓	✓	✓	✓
Reference (243 nm)	✓	✓	✓	X

To assess the colloidal stability of the latexes at increasing ionic strength, NaCl at different concentrations up to 1M and 1M $CaCl_2$ were added to the latexes. The salt tolerance is presented in Table 4.6, along with the original particle size of the latexes and that after the salt addition. With NaCl, all latexes, including the reference latex, exhibited good salt stability at all salt concentrations. Exception is the DMAPS latex, which destabilized at lower NaCl concentration and coagulated at 1M NaCl. In the case of $CaCl_2$, only the A3361 latex demonstrated remarkable stability. These results can be attributed to the higher incorporation of A3361 onto MMA/n-BA particles. Zwitterionic polymers are known to exhibit anti-polyelectrolyte effect.[9,10] Accordingly, polymer chains collapse in aqueous solutions due to inter- and intra-chain electrostatic interactions, however, the ions present in the added salt interrupt these interactions and induce chains expansion that can improve the colloidal stability of the particles in the latexes. As seen in chapter 3, the present water-soluble oligomers that likely are rich in ZM units, introduce additional interactions with the added salt units, contributing to increase even further the

ionic strength in the dispersions and subsequent colloidal destabilization. Consequently, the salt stability is a result on the balance of ZM units present on the particles and in the water phase. Higher is the incorporation of ZM onto polymer particles, as it is the case for A3361 latex, lower is the fraction of soluble oligomer and consequently this latex presents superior colloidal stability.

To delve further into the anti-polyelectrolyte properties of zwitterionic stabilized latex, an additional DMAPS seed latex was synthesized in the presence of salt (0.02M NaCl) and compared with DMAPS seed without salt. The corresponding particle size was measured using two techniques: Dynamic Light Scattering (DLS) to determine the hydrodynamic diameter and Transmission Electron Microscopy (TEM) to observe the dry state. Table 4.7 clearly shows that the DLS measurements indicate an increase in particle size with the addition of salt, attributed to chain extension arising from the anti-polyelectrolyte effect. When measured by TEM, the particle size appears similar for both cases. These results are consistent with findings reported by Polzer et al.[11] where they observed an increase in the thickness of the grafted DMAPS brush onto the PS cross-linked particles at high NaCl concentrations. Similarly, in this study the salt-free latex exhibited a well-defined core-shell structure (Figure 4.4a), characterized by distinct core and shell regions. The relatively smaller and well-defined shell area indicated strong ionic bonding. However, upon introducing salt (Figure 4.4b), a significant transformation occurred. The once clear border between the core and shell became obscured, leading to the near loss of the particle's identity. This change can be attributed to the extension of DMAPS polymer chains on the particle surface, even though they are in a collapsed state some chains were capable of stretching further away from the core, resulting in a corrugation of the shell. These results confirmed the presence of anti-polyelectrolyte effect in the ZM stabilized latexes, which probably is the main reason for the improved salt stability of the latexes.

Table 4.7. Particle size of surfactant free latex in the presence and absence of salt.

Latex	Dp DLS (nm)	Dp TEM (nm)
DMAPS in the absence of salt	234	242
DMAPS in the presence of salt	320	258

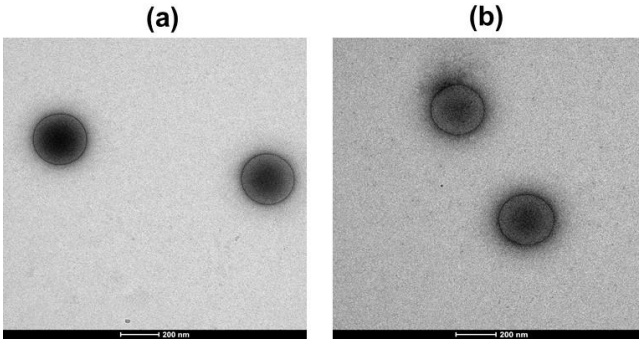

Figure 4.4. TEM images of surfactant-free latex in the absence of salt (a) and in the presence of salt (b).

4.3.3. Polymer film performance

The polymer films were prepared by casting the dispersions into silicon molds and allowing water evaporation under standard atmospheric conditions (T=23 ºC and relative humidity of 55%). Since the ZMs are incorporated onto the polymer particles, it was not expected for the stabilizing units to migrate during film formation. However, water-soluble oligomers rich in ZM units could potentially diffuse through the film towards the film's surfaces and affect their properties. To investigate this, water contact angles were measured on the film-air surface before and after rinsing the surface with water. Table 4.8 shows that the films containing different ZMs exhibited very similar CAs before and after rinsing, indicating minimal migration of species containing ZM (both stabilizing and soluble oligomeric units). In contrast, CA of the reference latex film increased significantly after rinsing its surface with water, indicating substantial migration of SDS to the film-air interface, which was subsequently

removed during the rinsing process. It is worth noting that the ZM containing films exhibited lower hydrophilicity compared to the SDS containing reference film (prior to rinsing with water). This could be attributed to the orientation of the zwitterionic groups away from the surface exposed to air, to minimize surface energy in the dried state,[12] along to the intra- and inter-molecular ionic interactions that result in a more hydrophobic surface.[13]

Table 4.8. Water contact angles (CAs) on the films with different ZMs and reference film, before and after rinsing the films with water.

Latex	CA(°) (before rinsing)	CA(°) (after rinsing)
DMAPS	70±2	73±2
M3295	67±3	69±2
A3367	70±3	71±2
A3361	56±3	64±2
Reference	40±0	81±0

Tensile measurements were performed to assess the mechanical strength of the polymer films. The stress-strain curves of the original films, prepared under standard atmospheric conditions, are presented in Figure 4.5 and the modulus and other relevant characteristics derived from these curves can be found in Table 4.9.

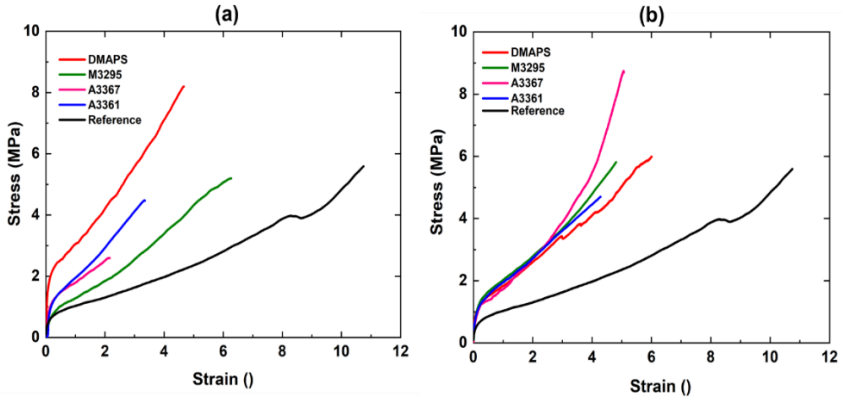

Figure 4.5. Stress-strain curves of the polymer films cast from the latex synthesized with different ZMs and reference (a) prepared at standard atmospheric conditions (T = 23 °C and RH=55%), (b) annealed afterwards at 80 °C for three days.

The incorporation of ZM in the polymer films results in improved mechanical resistance, characterized by higher Young's modulus and lower elongation at break compared to the reference film. Among the surfactant-free films, the highest Young's modulus is observed in the films containing DMAPS (36 MPa), followed by A3361 (26 MPa), A3367 (16 MPa), and M3295 (7 MPa). This trend in the mechanical properties certainly is not what one may expect, taking into consideration the highest incorporation of A3361 with the highest T_g. To investigate the effect of chain reordering on the mechanical properties, the films were annealed at 80 °C as shown in Figure 4.5b. Interestingly, the significant differences in mechanical properties between the original films containing different ZMs, as observed in Figure 4.5a, diminished after annealing. As a result, all the films exhibit similar mechanical properties in Figure 4.5b, albeit enhanced compared to the reference film.

Table 4.9. Mechanical properties of the films with different ZMs and reference, determined from stress-strain graphs.

	Film	Young's modulus (MPa)	Yield stress (MPa)	Ultimate tensile strength (MPa)	Elongation at break ( )
Original	**DMAPS**	36.3±5	2.2±0.2	8±0.2	4.68±0.8
	M3295	7±2.4	0.9±0.2	4.9±0.3	6.5±0.2
	A3367	16±3	1.3±0.1	2.4±0.2	2.5±0.5
	A3361	26±6	1.5±0.1	3.6±0.3	4.5±0.3
	Reference	1.8±1	0.4±42	5.8±0.3	11.3±0.7
Annealed	**DMAPS**	19.5±5	1.4±0.1	6.8±1.3	5.8±0.5
	M3295	15.2±4	1.7±0.1	6.5±0.2	6.2±0.2
	A3367	5.5±0.6	1.2±0.1	8±0.7	5.8±0.6
	A3361	15.5±3	1.5±0.0	4.6±0.2	4.5±0.5
	Reference	---	---	---	---

The reinforcing effect observed in polymer films containing DMAPS has been previously reported (Chapter 3) and attributed to the formation of a rigid ionic complexed network within the films. This network arises from strong inter- and intra-molecular ionic interactions established between the polymer chains enriched with DMAPS, which are actually the colloidal stabilizing units distributed around the particles in the latex. During drying and film formation, these units create the mentioned

honeycomb-like network within the film that acts as a reinforcing structure in the film. As observed previously, annealing of the films promotes chain interdiffusion, leading to the dissolution of this network and a subsequent drop in the mechanical properties.

To examine whether a similar phenomenon occurs in these surfactant-free films, an AFM study was conducted on both the as prepared films containing different ZMs and the annealed films. In the following section, each ZM containing film will be studied individually to understand its morphology, its relationship with the mechanical properties, and the impact of annealing on this relationship.

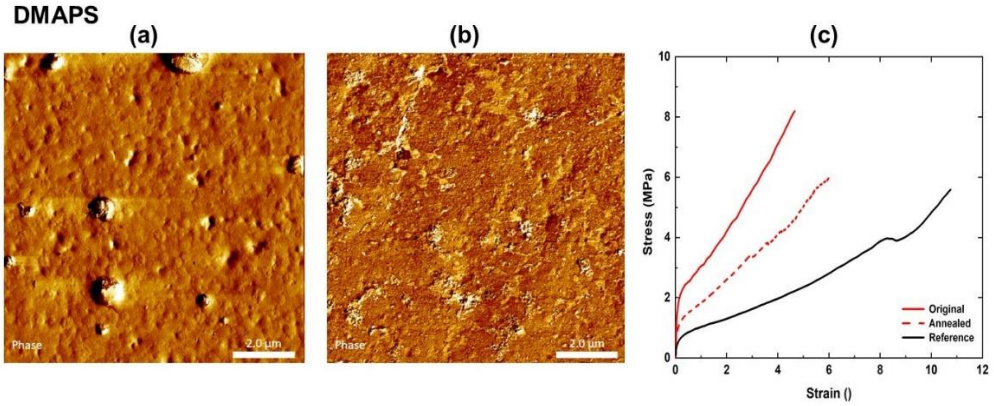

Figure 4.6. AFM phase images of film cross-section of DMAPS containing film as prepared (a); annealed at 80 ºC (b); and comparison of the stress-strain curves before and after annealing and the reference film (c).

The AFM image of the DMAPS film cross-section, as shown in Figure 4.6a, reveals the presence of distinct particle borders and lack of interdiffusion of polymer chains between the individual particles, caused by the formation of a rigid ionic complexation around each polymer particle. However, upon annealing at 80 °C, as depicted in Figure 4.6b, the particle borders are no longer apparent, indicating the formation of a continuous film facilitated by increased chain interdiffusion due to the elevated temperature. The T_g of the DMAPS homopolymer is approximately 28 °C. Hence, the MMA/n-BA chains enriched with DMAPS readily diffused across the particle borders during annealing at 80 ºC. A comparison of the stress-

strain behavior of the DMAPS film before and after annealing (Figure 4.5c) demonstrates a decrease in Young's modulus (from 36 MPa to 19 MPa) and an increase in chain flexibility after annealing (elongation at break increased from 4.6 to 5.8). These changes can be attributed to variations in the film morphology resulting from the annealing process. Namely, dissolution of the ionic complexed network results in drop of Young's modulus, whereas promoted contact between all chains containing ZM resulted in improved flexibility.

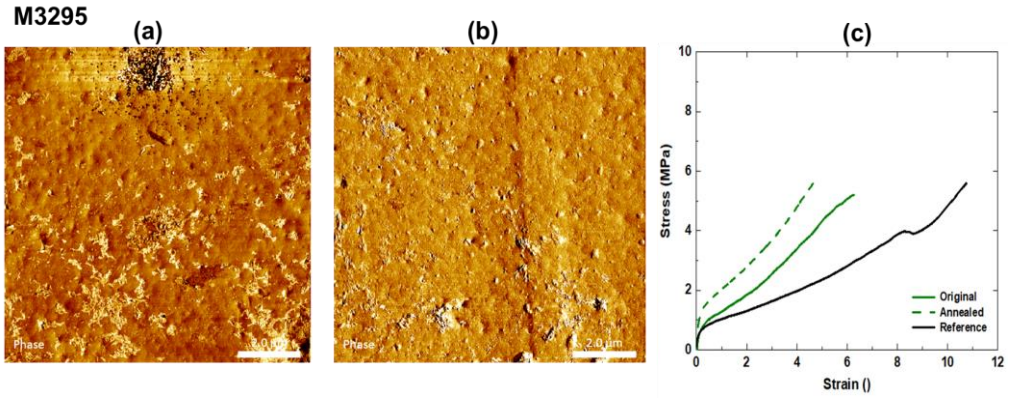

Figure 4.7. AFM phase images of film cross-section of M3295 containing film as prepared **(**a); annealed at 80ºC (b); and comparison of the stress-strain curves before and after annealing and the reference film (c).

The morphology investigation and mechanical properties of the M3295-containing polymer are illustrated in Figure 4.7. Before annealing, Figure 4.7a reveals the presence of well-defined particle borders, indicating limited diffusion of polymer chains within the film. Surprisingly, even after annealing at 80 ºC, Figure 4.7b shows that the particles remained visible in the film, suggesting incomplete interdiffusion of the polymer chains during the annealing process. The annealing conditions at 80 ºC were insufficient to promote full interdiffusion of the polymer chains. However, it is noteworthy that the mechanical properties of the film improved after annealing. The Young's modulus increased from 7 MPa to 15 MPa, without a significant decrease in elongation at break, as depicted in Figure 4.7c Thus, the material became stiffer while still maintaining its flexibility.

The M3295 zwitterionic homopolymer, with a T_g of approximately 63 °C, exhibited a higher incorporation onto the polymer particles than DMAPS. Surprisingly, despite these advantageous factors, the original film containing M3295 demonstrated inferior mechanical properties compared to the film containing DMAPS (Figure 4.6c). This observation emphasizes that the mechanical properties of the films are not solely determined by the incorporation of ZM units onto particles and the T_g. Other factors, such as, the creation of ionic bonds between the polymer chains, likely occur not only between the incorporated ZM units but also between the soluble oligomers rich in ZM units that remain in the polymer films after film formation. These ionic clusters, instead of acting as plasticizers, may act as reinforcing agents, as their presence will affect the thickness of the layer surrounding each particle, significantly influencing the stiffness and flexibility of the film. The extent of these rearrangements may vary for different ZMs, resulting in different observed properties, affected by the chemical structure of each ZM, their incorporation and ZM quantity present in the film. Further evidence for the incorporation of soluble oligomers in the network comes from the water contact angle measurements, which did not change after rinsing the polymer films with water. Moreover, the remarkable resistance of this network in the case of M3295, which was further improved when the film was annealed at a temperature higher than the T_g of the ZM polymer, supports this hypothesis.

Considering that, the same weight percentage of ZMs was added to the dispersions, DMAPS, with a lower molecular weight, has a higher molar concentration compared to M3295. Table 4.10 shows the molar concentration of all the used ZMs, and the respective number of molecules added to the dispersions. As shown, the number of DMAPS molecules is significantly higher than that of M3295, leading to a higher ion concentration and potentially the establishment of a denser ionic network. A recent study has demonstrated that the formation of a denser ionic network, resulting from a higher ion concentration between colloidal anionic and cationic MMA/n-BA polymer particles, significantly reinforces the resulting film.[13] This reasoning may explain the observed superior properties for DMAPS compared to

other ZM systems. Furthermore, the structural configuration of ZMs is of significant importance. In the case of M3295, the presence of an additional CH_2 group between both ions results in a reduction of the cationic quaternary ammonium's electro positivity. Therefore, M3295 exhibits a decreased capacity to bind anions, which in turn leads to a less dense ionic network and a reduced enhancement of mechanical properties.[14]

Table 4.10. Molar concentration of all ZMs used and their respective number of molecules added to the seeded semi-continues emulsion polymerization.

Latex	Mol (%)	No of molecules
DMAPS	0.85	$5.10^{*}\ 10^{21}$
M3295	0.80	$4.8^{*}10^{21}$
A3367	0.89	$5.4\ ^{*}10^{21}$
A3361	0.85	$5.12^{*}\ 10^{21}$

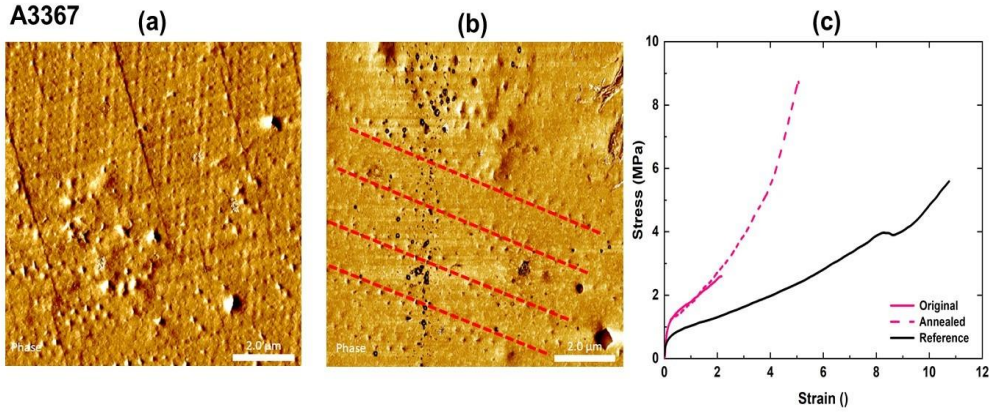

Figure 4.8. AFM phase images of film cross-section of A3367 containing film as prepared **(**a); annealed at 80 ºC (b); and comparison of the stress-strain curves before and after annealing and the reference film (c).

AFM images in Figures 4.8a and 4.8b depict cross-sections of the films containing A3367 ZM, before and after annealing, respectively. Similarly, as in the previous systems, the presence of a stiff network created by the polymer chains rich in A3367 forms a barrier that prevents interdiffusion of the chains

across particles' borders during film formation, as shown by the visible borders in both original and annealed films. Since the T_g of A3367 homopolymer is higher than in the previous cases (83 °C), heating below the T_g did not induce the particles fusion. After annealing, the films exhibit increased flexibility, elongation at break (from 2.5 to 6), and incredible improvement of the tensile strength (from 2.4 MPa to 8 MPa) indicating improved ductility. Figures 4.8a and 4.8b show that both original and annealed films display small superficial holes very ordered in zig-zag structures. The ordering was improved after annealing of the film, in which multiple parallel zig-zag structures might be observed in Figure 4.8b (marked with red dashed lines). As the ionic network and individual particles are still present in the film after the annealing, one may conclude that the reordering induced by heating only improved particles packing and establishing of more ionic interactions between the particles, refining film flexibility without significant effect on the modulus. The different behavior of the A3367 film compared to other ZM films may be attributed to the coagulum creation, in which we assume that the water-soluble oligomers were introduced, thus their presence did not disturb the particle packaging as in the other ZM films. On the contrary, despite higher fractions of molecules of A3367 were added to the system (Table 4.10) compared to DMAPS, a portion of it was incorporated into the coagulum, resulting in fewer ionic interactions. As a result, system with A3367 has lower mechanical performance than that of DMAPS (Figure 4.6c).

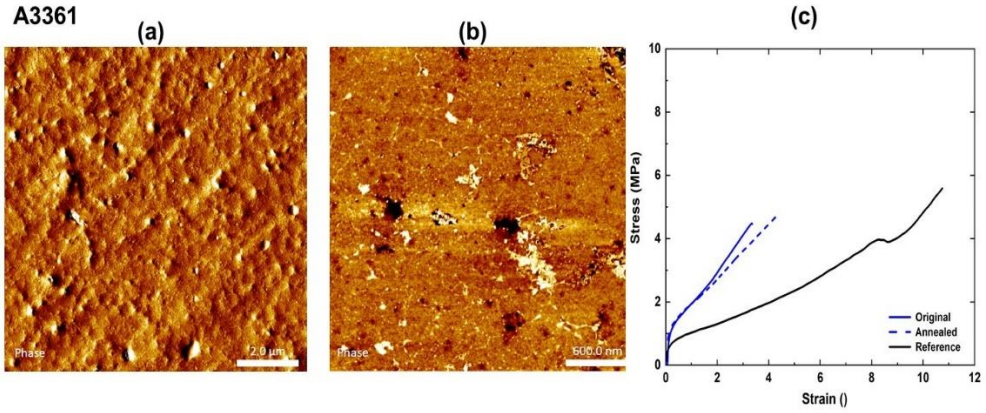

Figure 4.9. AFM phase images of film cross-section of A3361 containing film as prepared **(**a); annealed at 80 ºC (b);and comparison of the stress-strain curves before and after annealing and the reference film (c).

The films containing A3361 exhibit a similar behavior to that of A3367 film. In the original film (Figure 4.9a), deformed particle structures with a rigid network between them are observed, and this morphology remains unchanged even after annealing (Figure 4.9b). The A3361 homopolymer has the highest T_g among the studied ZMs (143 °C) and a highest incorporation rate of 74%. However, despite both A3361 films and DMAPS films containing the same number of molecules, the A3361 films demonstrate inferior mechanical properties, as depicted in Figure 4.6c. To explain this unusual and unexpected behavior, the chemistry of the both ZMs was elaborated. It was found that in DMAPS, the presence of an electro-attractive oxygen within the carboxylate group significantly enhances the electropositivity of the cationic ammonium site (CH_3-N^+), resulting in stronger interactions between ions both within and between the molecules. On the other hand, A3361 has a less electropositive cationic ammonium site due to a combination of a less electro-attractive amido carrying function and an additional methylene group (-CH_2-) positioned between the ammonium (NH^+) and the amido carrying function. Consequently, A3361 has a reduced ability to bind anions, leading to a sparser ionic network and diminished improvement of the mechanical properties.[14] Furthermore, following annealing, the modulus of the films remains largely unchanged, but there is a slight increase in elongation at the point

of break. This can be attributed to the improved arrangement and packing of particles within the film structure.

To investigate whether annealing of the films at temperatures above the T_g of the ZMs would dissolve the ionic network, the A3361 film was annealed at 150 °C for 1 day. Figure 4.10b demonstrates that the reinforcing rigid network was indeed destroyed after annealing. Unfortunately, the mechanical properties could not be measured as the film was partially stuck to the substrate, making it impossible to prepare dog-bone-shaped samples for the tensile analysis.

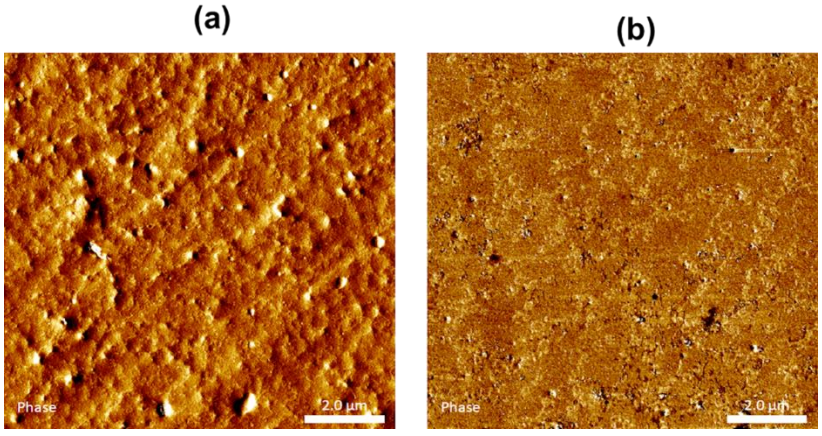

Figure 4.10. AFM phase images of film cross-section of A3361 film as prepared (a), annealed at 150 °C (b).

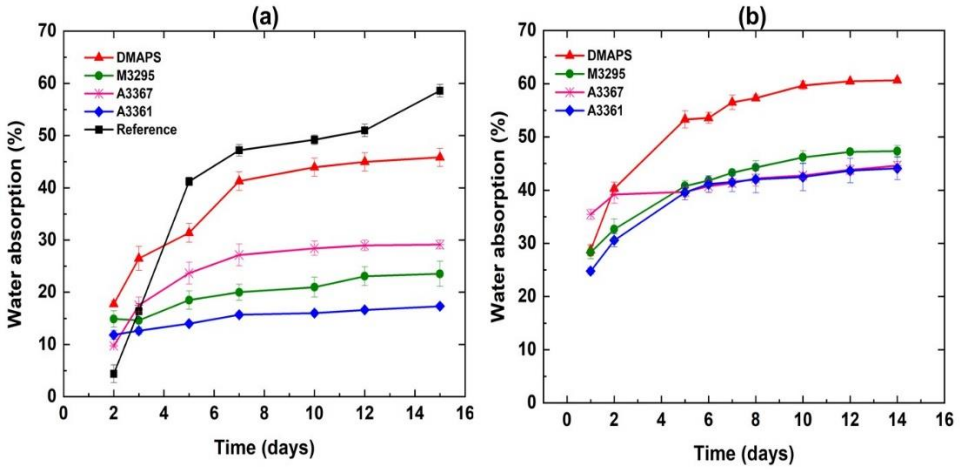

Figure. 4.11. Water uptake of the polymer films with different ZMs and the reference film prepared from: (a) original latexes; and (b) annealed latex (reference was not annealed).

Figure 4.11a and 4.11b present the water sensitivity of films containing various ZMs and a reference film, both in their non-annealed and annealed states, as determined by water uptake measurements. Figure 4.11a demonstrates that films with ZMs exhibited lower water absorption compared to the reference film after two weeks of immersion. Among the films with different ZMs, the trend in water absorption was DMAPS > A3367 > M3295 > A3361, with A3361 absorbing as little as 17% water compared to the reference film's uptake of 60%. The water resistance of these films can be attributed to the interplay between two effects: the presence of an ionic network acting as a barrier to water diffusion and the quantity of non-bounded water-soluble oligomers within the film, which confer highly hydrophilic properties upon contact with water. DMAPS, having a lower resistance to water, contains a higher quantity of these oligomers, as only 42% was incorporated onto particles. A3367 exhibited the lowest incorporation onto particles (28%), but a portion of the water-soluble oligomers was included in the coagulum. M3295 and A3361, on the other hand, displayed higher incorporation, resulting in the

formation of a dense ionic network and a lower quantity of water-soluble oligomers, thereby enhancing the water resistance of the MMA/n-BA polymer films prone to water absorption.

After annealing (Figure 4.11b), the water uptake of all ZM-containing films increased significantly. The increase in water uptake of the DMAPS film can be attributed to the observed dissolution of the ionic complexed network during annealing. However, in the other films, the ionic network remained intact after annealing, as evidenced by the AFM images in Figures 4.6-4.9. Although the annealing at 80 °C may not have provided sufficient energy to completely dissolve the ionic network, the heating likely induced chain reordering, potentially disrupting the ionic interactions [15,16] and rendering the polymer films more hydrophilic. It is worth mentioning that these films were immersed in water for long period of time and show water absorption that likely affects the state of the ionic polymer chains, different than while mechanical properties were measured, when the films were completely dried.

The presence of a network of polymer chains rich in zwitterionic units interconnected by ionic bonds within the polymer matrix can serve as an effective barrier against moisture diffusion as seen in chapter 3. To verify this, the water vapour transmission rate (WVTR) of the films containing different ZMs, and the reference film was investigated, and the results are presented in Table 4.11.

Table 4.11. WVTR of reference polymer film, and films containing 2 % ZMs.

Film	WVTR (g·mm/m²·day)
DMAPS	6±0.6
M3295	27.2±1.5
A3367	19.05±2.1
A3361	57.9±5.6
Reference	75.1±1.8

Table 4.11 provides insights into the WVTR of the films, with the reference film exhibiting high humidity diffusion of approximately 75 g·mm/m²·day. The presence of SDS molecules within the film may create pathways for humidity diffusion and provokes a high interaction between the sample and the permeant.

In contrast, films containing ZMs displayed strong barrier characteristics, likely due to the presence of a rigid ionic complexed network that acts as a physical obstacle against water penetration. The film with DMAPS demonstrated the best performance, with a WVTR as low as 6 g·mm/m²·day. This result is unexpected considering the high water absorption observed in the DMAPS film. It is worth noting that during the water absorption tests, the films were fully immersed in water, which increased the mobility of the flexible and softer polymer chains containing DMAPS (stabilizing units and oligomers). This increased mobility facilitated the easy diffusion of water molecules through the films, leading to higher water absorption. This effect may be attributed to the hydro-plasticizing effect of water in polymer films.[17] However, when evaluating barrier properties in terms of WVTR, the diffusing water vapor would not have the same ability to move the softer polymer chains as when the film is immersed in water. These polymer chains instead act as barriers to the moisture vapor passing through the film.

The A3367 containing film also exhibited low WVTR of approximately 19.05 g·mm/m²·day, followed by the M3295 film and then the A3361 film. The observed variation in WVTR can be attributed to the relative difference in hydrophilicity of each ZM, which likely influences the moisture permeability of the MMA/n-BA film. Assuming there is no migration of water-soluble species during water contact angle measurements on the film surfaces before and after rinsing with water (Table 4.8), the water contact angle values can measure the film's hydrophilicity. Table 4.8 indicates a decreasing hydrophilicity trend in films containing ZMs, following the order A3361 > M3295 > A3367 > DMAPS, which correlates with the observed trend in WVTR. However, the last two ZMs exhibit similar hydrophilicity, while DMAPS provides a significantly better barrier against humidity permeation, suggesting the presence of additional factors influencing permeation. Since the DMAPS containing network is much softer (Tg of DMAPS homopolymer is approximately 28 °C) and prevents interdiffusion of polymer chains during film formation, the network is softer than that of A3367 (Tg of the homopolymer is approximately 83 °C). This implies that the MMA/n-BA particles surrounded by DMAPS-rich polymer units are more

deformable, allowing for the formation of higher-quality films compared to those containing A3367. The polymer chains rich in the much harder A3367 units maintain a spherical particle morphology, resulting in films with certain defects. The AFM image of the cross-section of the DMAPS film (Figure 4.6a) reveals a nearly continuous film, while the A3367 film (Figure 4.8a) exhibits self-ordered polymer chains that, due to their rigidity, form small pores acting as defects that allow some humidity permeation. Nevertheless, the barrier properties of the A3367 films are still superior to those of the reference film.

4.4. Study of anti-polyelectrolyte effect of ZM on colloidal stability and film properties in case of A3361

To study the anti-polyelectrolyte effect on the colloidal stabilization potential of A3361, 30% S.C., surfactant-free polymer latex was prepared at acidic pH of 3-4 and compared with A3361 latex synthesized at neutral pH. A3361 ZM was selected for this study, because of the highest incorporation onto MMA/n-BA particles achieved. At neutral pH, it was expected that the polymer chains rich in A3361 would be collapsed due to numerous inter- and intra-molecular ionic interaction between the zwitterion units. By addition of ions to decrease the pH, it was expected that they interacts with the zwitterions, disrupting their bonding. Subsequently, the polymer chains rich in zwitterions would be extended that might improve their capacity to provide colloidal stability because of the creation of extended double layer and hydrodynamic diameter of the particles. Reference latex was synthesized using SDS conventional surfactant for comparison with both A3361 stabilized latexes.

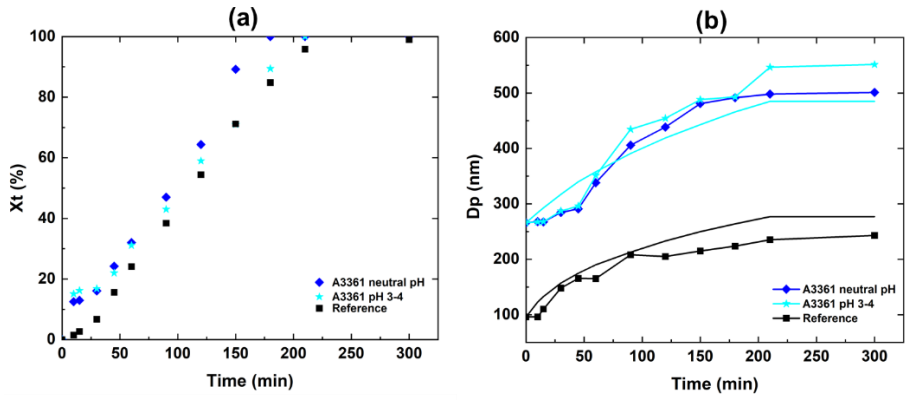

Figure 4.12. Time evolution of (a) total MMA/n-BA conversion (X_t); and (b) average particle size (d_p) at different pH-s. Reference system is shown for comparison. In (b), the points represent experimental d_p values, whereas the full lines represent theoretical particle size.

Figure 4.12a shows the time evolution of total MMA/n-BA monomer conversion for the 30% S.C. reactions carried out with ZM A3361 and for the reference latex. Initially, the reactions with A3361 are faster than the reference reaction, permitting much earlier full conversion of MMA/n-BA, which is surprising when consider much higher average diameter of the A3361 stabilized seed particles (Figure 4.12b, at time zero). The presence of amide group in the structure of A3361 may contribute to improved stability of the system. Oppositely than expected, A3361 reaction at neutral pH is faster than at acidic pH in the last period of reaction. The increased ionic strength due to pH adjustment might affect slightly the system stability, as well as, some amide hydrolysis can happen under acid conditions,[14] resulting in the formation of acrylic acid (AA) and amine molecules, according to Scheme 4.2. While the acrylic acid may react with the monomers, the amine will remain free in the aqueous phase, decreasing the fraction of stabilizing species in the system and increasing water-soluble components in the dispersions. Moreover, under acidic conditions the AA is protonated and hence will not contribute to the polymer particle stability. Therefore, the stability of the latex is reduced. All of these issues screened the anti-polyelectrolyte effect on the colloidal stability. However, considering similarity of the processes, one

may assume that anti-polyelectrolyte effect counteracts the above-mentioned occurrences that otherwise would destabilize the system more importantly.

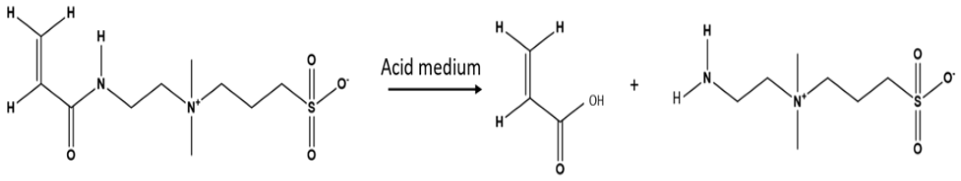

Scheme 4.2. Hydrolysis reaction of A3361 under acidic conditions.

Figure 4.12b presents the evolution of average particle size in the latexes synthesized with A3361 and in the reference latex. Both surfactant-free latexes present higher particle sizes than the reference latex stabilized with SDS, likely related with larger particle size of the seed (261 nm) employed for the synthesis of A3361 latexes than that of the reference seed (96 nm). As expected, the particle size increased along the reaction with the monomer feeding and polymerization. Theoretical particle sizes are also shown in Figure 4.12b, calculated by assuming a constant number of particles throughout the reactions. At the beginning of reaction, for A3361 neutral and acidic pH, the experimental particle sizes are consistently smaller than the theoretical size, indicating formation of new particles probably by homogeneous nucleation. The lack of surfactant in these systems resulted in fast coagulation of these small and instable particles, as a consequence of which both the experimental and theoretical sizes become similar latter in the reaction. The coagulation of smaller instable particles created initially is obvious from the higher particle size diameter for A3361 reactions than theoretically determined in latter reaction stages. In the presence of additional ions added to decrease the pH of the reaction medium, the intra and inter-molecular ionic interactions between the opposite charges are disrupted, turning the chains from collapsed state into an extended one. Such extended conformation of stabilizing chains containing A3361, increases the hydrodynamic particle diameter determined by DLS.

Table 4.12. Characteristics of A3361 polymer latexes and reference.

Latex	A3361 neutral pH	A3361 pH 3-4	Reference
MMA/n-BA conversion (Xt,%)	100	100	100
Coagulum (%)	0	0	0
D_p (nm)	501	551	241
D_{ptheo} (nm)	477	477	277
ZM incorporation (wt%)	74	65	---
Gel content	19	13	0
$\overline{M_w}$ (kDa)	345	248	706
T_g (°C)	13	12	12

Table 4.12 summarizes the latex and polymer properties. It is clear from Table 4.12 that MMA/n-BA monomers were fully converted into polymer, with no coagulum formation in any of the reactions. At neutral pH higher fraction of A3361 was incorporated onto polymer particles than at acidic pH (74% versus 65%), which can be due to the hydrolyzed fraction of ZM at acidic conditions. The zwitterionic molecule created by A3361 hydrolysis (Scheme 4.2) as un-reactive molecule, remains in aqueous phase. Moreover, in presence of additional ions, A3361 is more water-soluble, thus, the created oligoradicals in aqueous phase by A3361 reaction with solubilized MMA and n-BA are more hydrophilic in such condition. This increases the time that oligoradicals spend in aqueous phase and increase the possibility of aqueous phase termination, creating more water-soluble species and less incorporation of ZM onto polymer particles. A3361 containing latexes present small fraction of THF insoluble polymer (gel content) that likely represent the fraction of polymer chains containing ionic moieties. The reference polymer presents only linear chains soluble in THF, because MMA within the chains is less susceptible to chain transfer to polymer and termination by combination. The polymer chains obtained at lower pH present lower molar mass, likely due to a denser hairy layer made of the extended ZM chains that made less effective the radicals entry from aqueous phase into particles, keeping the average radical concentration per particle lower.[18] The T_g was not affected by either of the parameters studied, likely because all the polymers are mostly made of MMA/n-BA (about 98%). Even though, it was difficult to

observe directly the anti-polyelectrolyte effect on the reaction, the latex characteristics and polymer microstructure are affected without any doubts.

Therefore, the anti-polyelectrolyte effect on the salt and freeze-thaw stabilities of the latexes was studied. The salt and freeze-thaw stabilities of the latexes are important characteristics from applicative point of view related with different conditions of latex storage and transportation. The salt stability was studied by addition of NaCl or $CaCl_2$ salts in different concentration to the latexes, and the average particle size was followed as an indication of the colloidal stability. The results are shown in Table 4.13. However, no differences could be observed for the A3361 latexes, indicating that the zwitterion units in both conformations provide excellent stability in the presence of both types of salts. Namely, by addition of salts to the latexes, the anti-polyelectrolyte effect was induced even in the case of the latex produced at neutral pH, causing extension of the zwitterionic units and improved stabilization. The added ions instead to contribute to increase ionic strength they preferentially interact with the zwitterions. In lack of similar effect, the reference latex coagulated after addition of 1M NaCl or 1M $CaCl_2$. Similar outcome was obtained for the case of freeze-thaw stability; both A3361 latexes were stable for at least six cycles of freeze and thaw. We attributed this effect on the hydration capability of both conformation of A3361 containing chains. While the ionic complexed, collapsed chains have entrapped water molecules within the ionic network around the particle, one would expect that the highly hydrophilic extended chains establish strong interactions with the water molecules. Both effects ensure water layer around the particles that was not frozen during the freeze cycle, thus ensured colloidally stable particles during thaw cycle. Again, the reference latex coagulated after the first freeze-thaw cycle.

Table 4.13. Salt and freeze-thaw stability of the A3361 latexes and reference latex. The particle size is given in nm and shown in parenthesis. (✓) means stable latex and no changes in particle size; (X) indicates massive coagulation.

Latex	NaCl			$CaCl_2$	Freeze-thaw stability (Cycles)					
	0.5M	0.75M	1M	1M	1	2	3	4	5	6
A3361 pH 7 (501 nm)	✓	✓	✓	✓	✓	✓	✓	✓	✓	✓
A3361 pH 3-4 (551nm)	✓	✓	✓	✓	✓	✓	✓	✓	✓	✓
A3361 50% S.C. (367 nm)	✓	✓	✓	✓	X	--	--	--	--	--

4.4.1. Polymer film performance

The polymer films were prepared by casting the latex in silicon moulds and water evaporation under standard atmospheric conditions (25 ºC, 55% relative hummidity). To check if a migration of stabilizing units or soluble oligomeric species occur during the film formation process, water contact angles was measured on the films' surface before and after rinsing it with water. The results are shown in Table 4.14, making evident that the films containing A3361 present comparable contact angles before and after water rinsing. It demostrates that there was no migration of the stabilizing chains nor the soluble oligomers. It is appealing to notice that the A3361 film produced from neutral pH latex present more hydrophilic surface than the film from acidic pH latex.

Table 4.14. Contact angles (CAs) of a drop of water on the films with different ZMs and reference before and after rinsing.

Latex	CA(°) (before rinsing)	CA(°) (after rinsing)
A3361 (pH=7)	56±3	64±2
A3361 (pH=3-4)	66±2	70±2
Reference	40±0	81±0

At low pH 3-4, the zwitterionic units adopt extended conformations due to the disruption of the inter- and intra ionic interactions by interactions with the added salt ions to control pH. The extended conformation may provide additional ionic bonding sites, thereby resulting in polymer chain entanglements and denser ionic network, which consequently make the film less hydrophilic. This effect has been already observed in case of ionic inter particle complexed films.[19,20] A schematic representation of anti-polyelectrolyte behavior of polymer chains is given in Figure 4.13. In case of the reference latex, one may observe the importance of the conventional surfactant migration on the film-air interface during the film formation, because the contact angle was more doubled after rinsing with water.

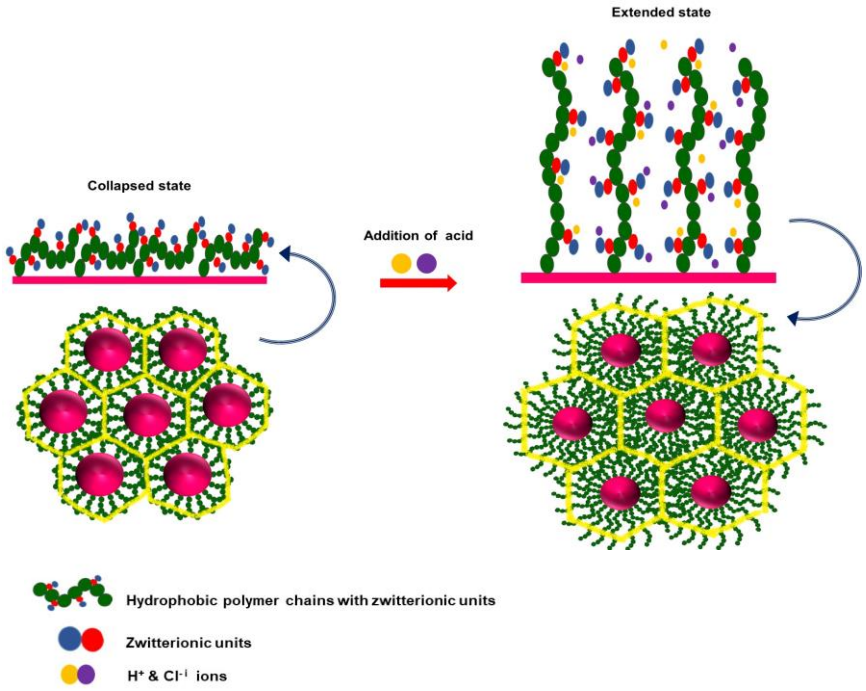

Figure 4.13. Schematic illustrations of extraordinary ion-responsible behavior of ZM rich polymer chains, exhibiting the anti-polyelectrolyte effect. Addition of counter ions extended the polymer chains around the polymer particles resulted in thick hairy layer and rigid network, which improved the film properties.

The mechanical properties of the polymer films were evaluated by means of tensile measurements. The stress-strain curves of the A3361 films and reference film are displayed in Figure 4.14, whereas the modulus and other characteristics determined from these graphs are shown in Table 4.15.

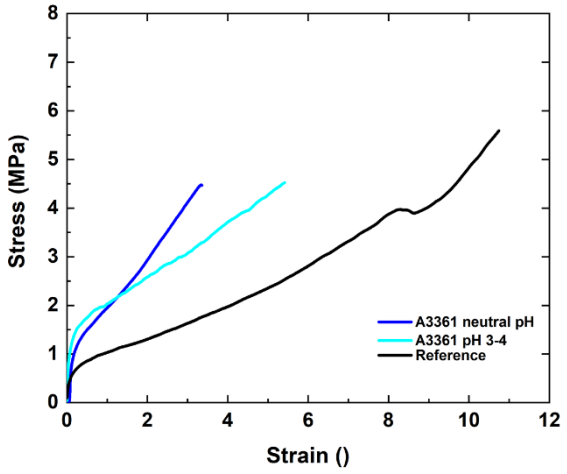

Figure 4.14. Stress-strain curves of the A3361 polymer films and reference film as received and prepared at standard atmospheric conditions (T = 25 °C).

Table 4.15. Mechanical properties of the A3361 films and reference film, determined from stress-strain graphs.

Film	Young's modulus (MPa)	Yield stress (MPa)	Ultimate tensile strength (MPa)	Elongation at break ( )
A3361	26±6.1	1.5±0.1	3.6±0.3	4.5±0.3
A3361 pH3-4	33.5±4.4	2±0.1	4.1±0.4	5.4±1.3
Reference	1.8±1.2	0.4±4.2	5.8±0.3	11.3±0.7

The both films containing A3361 demonstrated superior Young's modulus values, ranging from 26 to 34 MPa, than the reference film with a Young's modulus of 2 MPa. Simultaneously, A3361 films present lower elongation at break, indicating presence of reinforcing effect with respect to the reference film. Similar evidence was already observed in Chapter 3 for DMAPS ZM monomer used for MMA/n-BA particle stabilization during emulsion polymerization, even though this effect was not so high. The

reinforcement was achieved by creation of an ionic complexed network, made of MMA/n-BA chains rich in ZM units. As these chains provide colloidal stability to the latex particles, they are distributed at the surface of the particles and during the film formation when particle packing happens due to water evaporation, these chains interconnect and form the network. In the present work, the reinforcing is even higher, likely due to much higher Tg of the A3361 polymer chains (143 °C). The second observed effect from Figure 4.14 is that, when the film was produced from acidic pH latex, the mechanical properties were further improved with respect to the film from neutral pH latex, from about 26 to 34 MPa. This huge enhancement of the film stiffness is likely a consequence on the extended conformation of the chains, which during drying create entanglements and improved ionic complexation between the neighboring particles. These entanglements seem to reinforce the particle interactions within the film and make thicker the ionic network, that likely improved the elongation at break, as already observed in case of ionic interparticle complexation within waterborne polymer film.[16]

To check this hypothesis, AFM study of the cross-section of the A3361 containing films was performed. In Figure 4.15 AFM phase images of both films obtained at different pH are shown. Surprisingly, the film obtained at neutral pH (Figure 4.15a) does not show the typical network observed previously for DMAPS stabilized polymer particles, but rather light brown areas (stiffer material) distributed within the dark brown matrix (softer material). Probable reason for this behavior is that within the latex produced at neutral pH, there are strong inter and intramolecular ionic complexation, that made too stiff these chains to distribute around the particles and form the network. On the other hand, Figure 4.14b clearly shows a network formed by ionic complexation of zwitterion-rich chains around the individual MMA/n-BA particles in the film produced from acidic pH latex. The extended chains with interrupted ionic interactions due to anti-polyelectrolyte effect, likely presented much higher flexibility. Consequently, the ionic complexes were distributed around each particle and interconnected between each other, resulting in the corresponding ionic network as it can be observed in Figure 4.15b, as observed previously for DMAPS. Additionally, as mentioned having the chains rich in zwitterions extended and

entangled between various particles, the ionic complexation probability is also increased. This is likely the reason for the further improved mechanical properties observed within the films obtained from latex at acidic conditions.

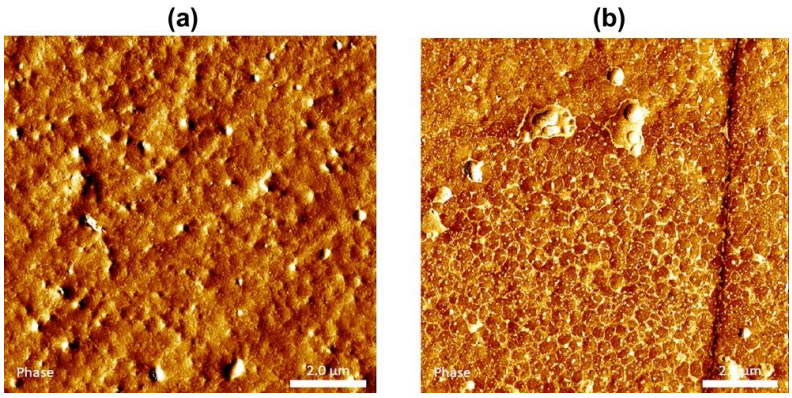

Figure 4.15. AFM phase images of film cross-section of A3361 as received and prepared at standard atmospheric conditions (T = 25 °C) (a), synthesized at neutral pH (b) synthesized at acidic pH.

Surface AFM analysis was also performed on the films to gain a better understanding of the film morphology (Figures 4.16a and 4.16b). The results revealed that in the case of neutral pH latex, distinct distribution of polymer particles were present in the surface of the all films. The brown color in images represents the softer segments and bright yellow represents the harder segments rich in A3361 units. For neural pH film, Figure 4.16a demonstrates a highly organized arrangement of polymer particles connected between each other. These connections have been observed previously by Argaiz et al.[21] in polymer films made of blends of anionic and cation particles, attributed to the ionic complexation. On the other hand, AFM image of A3361 film surface obtained under lower pH, depicted in Figure 4.16b, is remarkably different. Likely, the presence of additional ions in this system, affects the distribution of particles. The particles still can be observed, even though they are not so well ordered as in Figure 4.16a, likely due to denser ionic network and thicker stiff area between the particles present in this case.

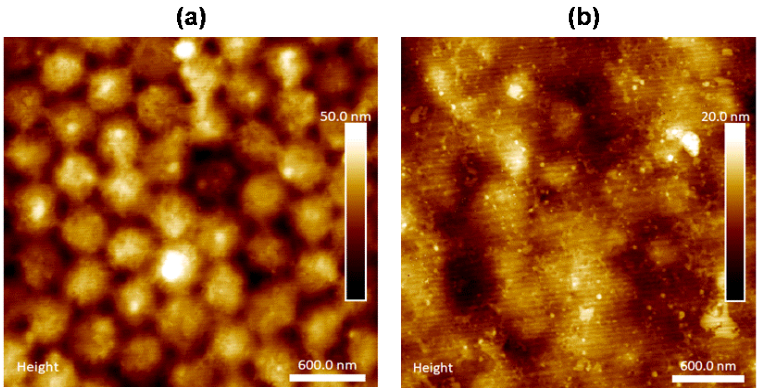

Figure 4.16. AFM height images of film surface of A3361 film as prepared (a) A3361 at neutral pH (b) A3361 at pH 3-4.

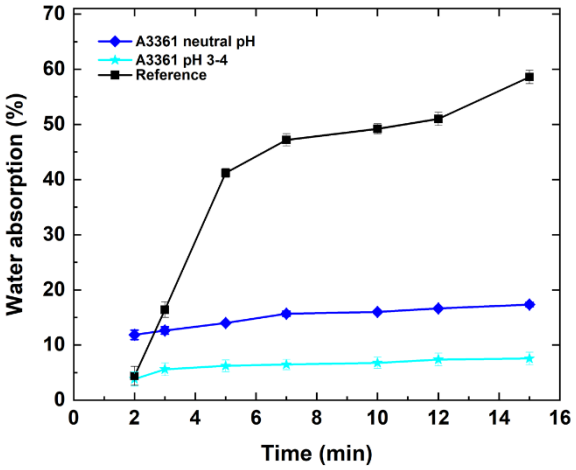

Figure 4.17. Water uptake of A3361 polymer films and reference film as received and prepared at standard atmospheric conditions (T = 25 °C).

Figures 4.17 depicts the water uptake of different A3361 films and the reference film. The figure clearly illustrates that the reference film exhibits high sensitivity to water due to the presence of hydrophilic aggregates created by the SDS surfactant.[22] Notably, there is a substantial difference in water uptake between the reference film and the A3361 films, attributed to the lack of aggregates due to strong ionic

complexes formation within the both films. Complexed ions creates double effects, they are not hydrophilic as free ions and they create a network of stiff polymer chains (MMA/n-BA rich in zwitterions) within the matrix, which presents a barrier to water diffusion through the film. Moreover, it is evident that the A3361 film obtained from acidic pH latex exhibits further decreased of the water absorption, the effect that can clearly be attributed to the dense ionic network created from the entangled polymer chains rich in zwitterions (as observed in the AFM image in Figure 4.15b).

To further demonstrate the barrier effect of the ionic network, moisture permeability of the films with A3361 and the reference film was investigated, and the results are presented in Table 4.16. As expected, the reference film displayed high humidity diffusion, which can be attributed to the presence of SDS within the film that create a hydrophilic path for humidity diffusion. The moisture permeability clearly decreased for about 27% within the film containing A3361 produced from neutral pH latex. Nevertheless, the permeability drops for about 65% within the A3361 film prepared from acidic pH latex. These results once again demonstrate that the ionic network served as a robust barrier, effectively impeding the penetration of moisture through the polymer film and that the extended conformation of the stabilizing polymer chains rich in zwitterions ensures thicker and less permeable network than the collapsed conformation of the same.

Table 4.16. Moisture permeability of reference polymer film, and films containing 2 % A3361.

Film	Moisture permeability (g·mm/m²·day)
A3361 pH 7	57.9±5.6
A3361 pH 3-4	27.2±2.8
Reference	75.1±1.8

4.5. Synthesis of 50% S.C. A3361 polymer latex

To rise the practical application possibility of ZM latexes and to have industrially relevant products, the S.C. should be increased to about 50%. Encouraged by the high incorporation of A3361 and enhanced properties and performance of the films obtained consequently, it was thought that ZM A3361 can serve to increase the solids contents of polymer latex to 50%.

Table 4.17. Characteristics of 50% S.C. A3361 polymer latex.

Latex	A3361 50% S.C.
MMA/n-BA conversion (Xt %)	100
Coagulum (%)	0
D_p (nm)	367
D_{ptheor} (nm)	477
ZM incorporation (wt %)	52
Gel content (%)	19
$\overline{M_w}$ (kDa)	345
T_g (°C)	13

Indeed, the ability of A3361 to be incorporated onto MMA/n-BA particles in higher fraction ensures sufficient colloidal stability to extend further the S.C. The characteristics of this latex are shown in Table 4.17. Full (meth)acrylic monomers conversion was achieved, giving rise to colloidally stable latex without any coagulum, with 367 nm average particle size diameter. The smaller average particle size here than in case of 30% solids content latex (500 nm, Table 4.4) implies that there is a secondary nucleation happening during this process when the reaction was performed at higher S.C. The secondary nucleation process can be caused if there is high monomer concentration in the reactor and subsequently in the aqueous phase and is not typical for the processes in which the monomers were introduced in the reactor in semi-continuous way. This was further investigated by determining the instantaneous monomer conversion in the reactor during the process (Figure 4.18). Indeed, a monomer accumulation can be noticed in Figure 4.18, induced likely by faster monomer feeding rate than the monomer consumption by polymerization. In such conditions, the propagating oligoradicals in aqueous

phase got higher possibility of propagation and precipitation forming new particles, than radical entry into particles. The newly created hydrophobic species in aqueous phase become stabilized by the chains that contain zwitterions, nucleating new particles. Supplementary demonstration was obtained by analysing the particle size distribution of this latex by CHDF. As shown in the inset of Figure 4.18 the particle size distribution is bimodal, made of small fraction of particles with average size of 250 nm and larger fraction with average size of about 400 nm. The former fraction was created latter in the process by the homogeneous nucleation explained.

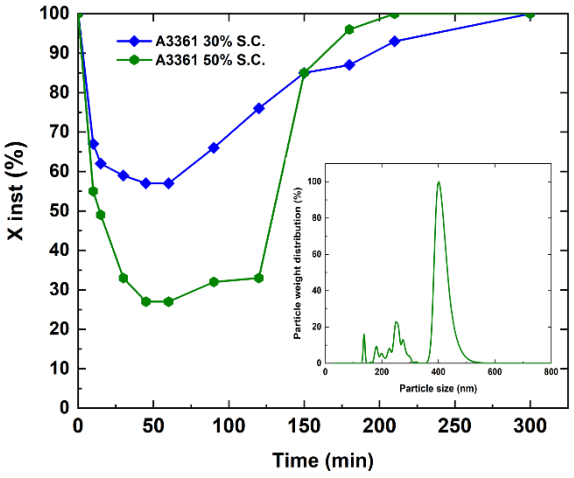

Figure 4.18. Instantaneous monomer conversion (*Xi*) for A3361 latex with 30% and 50% S.C. under neutral pH conditions. The inset provides the particle size distribution measured by CHDF for A3361 with 50% S.C.

The incorporation of A3361 was determined to be 52%, which is lower compared to the 30% solids content reaction under the same pH (neutral), for which 74 % A3361 incorporation was achieved. This decrease in incorporation can likely be attributed to the phenomenon of higher monomer accumulation in the reactor during the 50% solids content reaction. As explained previously, under these conditions aqueous phase reactions are promoted, which also increased the possibility of aqueous phase termination that hinders the incorporation of A3361 onto the particles. For comparison, in Figure 4.18

the instantaneous monomer conversion of both reaction are presented in which 30% S.C. showing lesser monomer accumulation and higher incorporation of the ZM.

Films' mechanical properties and water absorption were assessed for both A3361 50% S.C. and compared to the 30% S.C. counterpart, with the corresponding graph provided in Figure 4.19a and b respectively. Notably, it is evident that A3361 at 50% S.C. exhibits enhanced mechanical properties compared to the 30% S.C. formulation. One might anticipate the opposite outcome due to the lower incorporation of A3361 in the 50% S.C. formulation. However, this reduced incorporation results in a higher presence of water-soluble species within the film. Ionic interactions are also formed between soluble oligomers enriched in ZM units that persist within the polymer films and these ionic clusters, rather than serving as plasticizers, may function as reinforcing agents. Their presence is expected to influence the thickness of the layers encompassing each particle, thereby exerting a substantial influence on the film's stiffness. Simultaneously, these water-soluble species can have a detrimental impact on the water resistance of the films. Consequently, for A3361 at 50% S.C., due to the higher concentration of water-soluble species compared to the 30% S.C. A3361, it exhibits slightly increased water absorption.

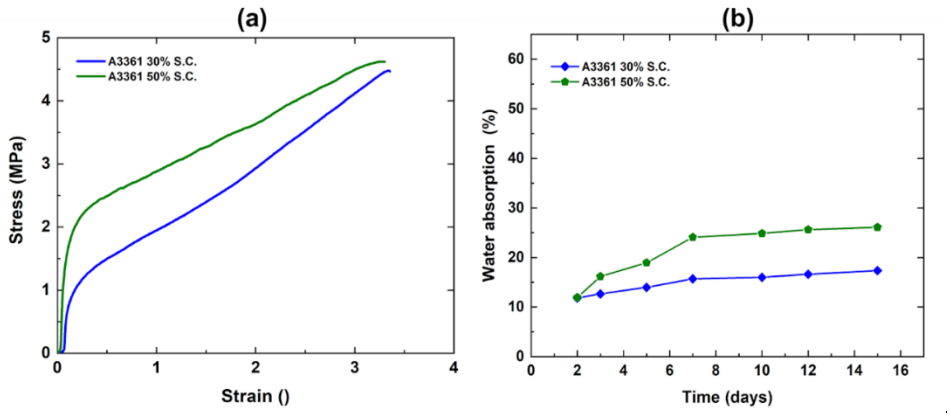

Figure 4.19. Comparison graphs of A3361 30% S.C and 50% S.C. (a) Stress-strain curves prepared at standard atmospheric conditions (T = 25 °C) (b) Water uptake of the A3361 polymer films prepared at standard atmospheric conditions (T = 25 °C).

4.6. Conclusions

In this chapter, the influence of different zwitterionic monomers (ZMs) as the sole source of stabilizing agent on the colloidal stability of MMA/n-BA polymer particles in high solids content (30-50%) latexes was investigated. Four sulfobetaine ZMs were explored: DMAPS and M3295 with methacrylic functionality, A3367 with acrylic functionality, and A3361 with acrylamide functionality. The goal was to synthesize completely surfactant-free latexes and understand how the chemical structure variations of these ZMs influenced their incorporation onto the latex particles, which plays a crucial role in both colloidal stability and overall polymer performance.

The findings revealed that the relative hydrophilicity of the ZM and their copolymerization reactivity ratios with MMA affects the incorporation of ZM onto MMA/n-BA polymer particles. For instance, compared to the ZM DMAPS with a 42% incorporation rate, the presence of an extra methylene group in ZM M3295 rendered it slightly less hydrophilic and increased the incorporation rate to 61%. On the other hand, ZM A3361, containing an acrylamide functionality, exhibited a remarkable impact on

incorporation, achieving an impressive rate of 74%. In contrast, the acrylic ZM A3367 showed the lowest incorporation of 28%, likely due to unfavorable reactivity ratios with the MMA and n-BA monomers, leading to a relatively large coagulum formation. Higher incorporation of ZMs onto the particles resulted in improved salt and freeze-thaw stability.

Polymer films, prepared from these ZM-containing latexes by water evaporation under standard atmospheric conditions. During this process, there was not any migration observed of the ZM containing polymer chains. The films containing ZMs exhibited substantial mechanical reinforcement compared to conventionally stabilized films, which can be attributed to the formation of a rigid network comprising polymer chains rich in ZM units united ionically, as confirmed by AFM imaging. This network structure with multiple ionic bonds contributes to reduced water absorption and significantly improved humidity barrier performance of the ZM films. Notably, exposure to high temperatures led to reorganization of the ionic connections within the films, resulting in altered behavior.

Moreover, the study delved into the introduction of additional ion sources to study the effect of anti-polyelectrolyte properties of ZM A3361 on the reaction and film properties. The presence of extra ions during polymer synthesis induced extended conformation of the stabilizing chains rich in zwitterions, distributed on the particle surface to provide colloidal stability. Consequently, it led to the development of a denser ionic network surrounding the polymer particles within the polymer film, as observed in AFM studies. The mechanical properties, water sensitivity and moisture barrier of the film were improved due to the presence of this denser ionic complexed network, placing the anti-polyelectrolyte behavior of zwitterion rich polymer chains as an additional tool to further improve latex and film characteristics and performance.

Furthermore, this research highlighted the adaptability of ZM A3361 due to ability to be incorporated in high fraction to MMA/n-BA particles, in producing high solids content latex under conditions

reminiscent of industrial settings, achieving concentrations of up to 50%, while keeping the enhanced characteristic of the latex and films containing A3361.

4.7. References

1. *Fundamentals of chemical incorporation of ionic monomers onto polymer colloids: paving the way for surfactant-free waterborne dispersions.* **Bilgin, Sevilay, Tomovska, Radmila and Asua, José M.** s.l. : Royal Society of Chemistry, 2016, RSC advances, Vol. 6, pp. 63754–63760.

2. *Statistical n-butyl acrylate-sulphonatopropylbetaine copolymers: 1. Synthesis and molecular characterization.* **Ehrmann, Marc and Galin, Jean-Claude.** s.l. : Elsevier, 1992, Polymer, Vol. 33, pp. 859–865.

3. *In situ synthesis of amply antimicrobial silver nanoparticle (AgNP) by polyzwitterionic copolymers bearing hydroxyl groups.* **Dong, Peng, et al.** s.l. : Elsevier, 2020, Reactive and Functional Polymers, Vol. 153, p. 104609.

4. *Zwitterion-containing polymer additives for fouling resistant ultrafiltration membranes.* **Kaner, Papatya, et al.** s.l. : Elsevier, 2017, Journal of Membrane Science, Vol. 533, pp. 141–159.

5. *Macromolecular microstructure, reactivity ratio and viscometric studies of water-soluble cationic and/or zwitterionic copolymers.* **Liaw, Der-Jang, et al.** s.l. : Elsevier, 2000, Polymer, Vol. 41, pp. 6123–6131.

6. *Surfactant-free high solids content polymer dispersions.* **Bilgin, Sevilay, Tomovska, Radmila and Asua, José M.** s.l. : Elsevier, 2017, Polymer, Vol. 117, pp. 64–75.

7. **Zong, Zhengang, Li, Yi-Zhong and Ruiz, Jose.** Latex binders, aqueous coatings and paints having freeze-thaw stability and methods for using same. *Latex binders, aqueous coatings and paints having freeze-thaw stability and methods for using same.* s.l. : Google Patents, November 2013. US Patent 8,580,883.

8. **Palmer Jr, Charles Francis, Haney, I.I. Lester Arnold and Wicker Jr, Calvin M.** Additives to improve open-time and freeze-thaw characteristics of water-based paints and coatings. *Additives to improve open-time and freeze-thaw characteristics of water-based paints and coatings.* s.l. : Google Patents, April 2016. US Patent 9,309,376.

9. *Zwitterionic polymers with antipolyelectrolyte behavior in solution.* **Zhang, L. M.** 1998, Polym. Bull, pp. 82–87.

10. *New polyampholytes: The polysulfobetaines.* **Hart, R. and Timmerman, D.** s.l. : Wiley Online Library, 1958, Journal of Polymer Science, Vol. 28, pp. 638–640.

11. *Synthesis and analysis of zwitterionic spherical polyelectrolyte brushes in aqueous solution.* **Polzer, Frank, et al.** s.l. : ACS Publications, 2011, Macromolecules, Vol. 44, pp. 1654–1660.

12. *Self-assembling zwitterionic copolymers as membrane selective layers with excellent fouling resistance: effect of zwitterion chemistry.* **Bengani-Lutz, Prity, et al.** s.l. : ACS Publications, 2017, ACS Applied Materials & Interfaces, Vol. 9, pp. 20859–20872.

13. *Ionic inter-particle complexation effect on the performance of waterborne coatings.* **Argaiz, Maialen, et al.** s.l. : MDPI, 2021, Polymers, Vol. 13, p. 3098.

14. *Reconciling low-and high-salt solution behavior of sulfobetaine polyzwitterions.* **Mary, Pascaline, et al.** s.l. : ACS Publications, 2007, The Journal of Physical Chemistry B, Vol. 111, pp. 7767–7777.

15. *Order-disorder transition of ionic clusters in ionomers.* **Tadano, Kenji, et al.** s.l. : ACS Publications, 1989, Macromolecules, Vol. 22, pp. 226–233.

16. *Dynamic mechanical relaxations of ethylene ionomers.* **Tachino, Hitoshi, et al.** s.l. : ACS Publications, 1993, Macromolecules, Vol. 26, pp. 752–757.

17. *Hydroplasticization of latex films with varying methacrylic acid content.* **Voogt, Benjamin, et al.** s.l. : Elsevier, 2019, Polymer, Vol. 166, pp. 206–214.1

18. *Preparation of high solids content waterborne acrylic coatings using polymerizable surfactants to improve water sensitivity.* **Aguirreurreta, Ziortza, de la Cal, José C. and Leiza, Jose R.** s.l. : Elsevier, 2017, Progress in Organic Coatings, Vol. 112, pp. 200–209.

19. *Emulsifier-free (meth) acrylic colloids stabilized by cationic monomer containing two charged moieties.* **Argaiz, Maialen, Aguirre, Miren and Tomovska, Radmila.** s.l. : Elsevier, 2022, Colloid and Interface Science Communications, Vol. 50, p. 100659.

20. *Towards improved performance of waterborne polymer dispersions through creation of dense ionic interparticle network within their films.* **Argaiz, Maialen, Aguirre, Miren and Tomovska, Radmila.** s.l. : Elsevier, 2023, Polymer, Vol. 265, p. 125571.

21. *Strategies towards improved performance of waterborne coatings through multiplying the ionic interparticle interactions.* **Argaiz, Maialen, Aguirre, Miren and Tomovska, Radmila.** s.l. : Elsevier, 2023, Progress in Organic Coatings, Vol. 183, p. 107731.

22. *Effect of ionic monomer concentration on latex and film properties for surfactant-free high solids content polymer dispersions.* **Bilgin, Sevilay, Tomovska, Radmila and Asua, José M.** s.l. : Elsevier, 2017, European Polymer Journal, Vol. 93, pp. 480–494.

Chapter 5. Thermo-Responsive Waterborne Pressure Sensitive Adhesives Stabilized with Zwitterionic Monomers

5.1. Introduction

Surfactant-free latexes with high solids content have been successfully synthesized through the incorporation of small amounts of diverse zwitterionic monomers used to create stabilizing specie. Simultaneously, zwitterionic monomers have imparted significantly enhanced properties to the latexes and films. Notably, AFM studies have revealed that the stabilizing chains rich in ZM units, placed on the particle surface in the latexes, formed a hexagonal network within the MMA/n-BA film matrix, providing reinforcement and mechanical stability. However, when the films were exposed to increased temperature (above Tg of the ZM homopolymers), the reinforcing network was partially dissolved and consequently the mechanical properties dropped, especially for zwitterionic polymers with lower Tg. These intriguing findings opened up a new potential application in development of thermo-responsive pressure-sensitive adhesives (PSAs) for removable labels. In such applications, applying heat to the label would cause the adhesive to cohesively fail and to be easily removed from the substrate as a result of the dissolution of the reinforcing network.

As it is well known, PSAs are viscoelastic materials that can firmly adhere to a wide range of surfaces by the application of a light pressure for a short contact time.[1,2] PSAs must be permanently tacky at room temperature and should have perfect balanced viscous and elastic properties, therefore, the final material has to present a low glass transition temperature (typically lower than -15 °C).[3-5]

An important family of polymers for PSA applications belongs to acrylic copolymers, which are mainly composed by a low Tg acrylate (e.g. n-butyl acrylate or 2-ethylhexyl acrylate), which provides softness and tackiness, and a low percentage of a hard monomer (e.g. methyl methacrylate) in order to improve cohesiveness of the system.

The primary objective of this chapter is to explore if thermo-responsiveness could be introduced in a conventional petroleum-based acrylic PSA, by replacing the conventional surfactant with zwitterionic monomers. To carry out this investigation, a waterborne surfactant-free PSA was synthesized utilizing a seeded semi-continuous emulsion polymerization approach. The petroleum-based acrylic PSA was created by using n-BA/MMA in a 90/10 ratio and employing ZM A3361 as a precursor to form the stabilizing species. ZM A3361 was selected because the superior incorporation onto n-BA /MMA polymer particles, that enables the synthesis of 50% S.C. and because of the highest Tg (143 °C) of its homopolymer, expecting higher cohesion.

The seed utilized in this process was the BMA surfactant-free seed; synthesize using solely A3361, as previously shown in Chapter 4. To enable a thorough comparative analysis, a reference PSA was also synthesized using the same procedure and monomers, but by replacing ZM A3361 with the conventional surfactant SDS.

Due to the good results obtained and in order to go one-step further, petroleum-based monomers were replaced with bio-based alternatives, drawing inspiration from Badia et al.'s research.[6,7] Specifically, commercially available 2-octylacrylate (2-OA) derived from castor oil, which boasts a bio-content of 71% and exhibits a Tg of -44°C, was used as the soft monomer. Additionally, isobornyl methacrylate (IBOMA) from pine resin, with a bio-content of 73% and a Tg of 150°C, was employed as the hard monomer. The chemical structures of these monomers are illustrated in Scheme 5.1. In this phase of the study, two different ZMs were studied (DMAPS and A3361) and for the sake of comparison, a bio-based PSA was synthesized in the presence of conventional surfactant Dowfax 2A1.

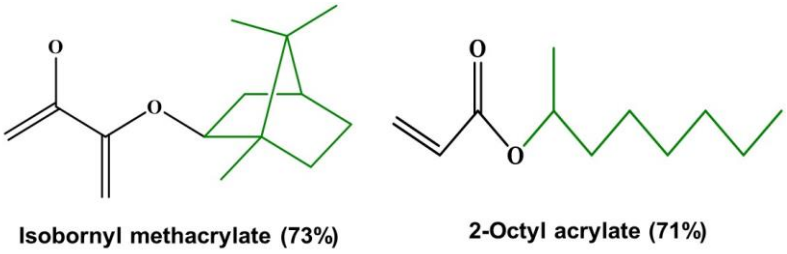

Scheme 5.1. Chemical structure of the bio-based monomers used in this work and their bio-content value. The green part belongs to the structure coming from the nature.

5.2. Experimental section

5.2.1. Materials

All the materials used throughout this chapter are given in Appendix I.

5.2.2. Polymerizations

The surfactant-free BMA seed was utilized for synthesis the petroleum-based n-BA/MMA PSA. The detailed procedure for seed synthesis has been provided in Chapter 4. To conduct the seeded semi-continuous reactions, we utilized the experimental setup and procedure described in Appendix I. For comparison purposes, a reference latex was also synthesized by replacing the A3361 with SDS using a seed containing SDS.

The bio-based seed was synthesized using the same reaction setup outlined in Appendix I, and the recipe is detailed in Table 5.1. To prepare the seed, a mixture of water, IBOMA/MMA (95:5), and Dowfax 2A1 were initially introduced into the reactor. The reaction mixture was then stirred at 180 rpm, while purged with nitrogen. When the temperature reached 70 °C, the thermal initiator KPS, previously dissolved in water, was added in a single dose. The system underwent a batch-wise reaction for 4 hours,

resulting in a latex with a solids content of 20%. Following this, the obtained seed was utilized in the production of bio-based waterborne PSAs, employing ZM A3361 or DMAPS.

Table 5.1. Recipe of bio-based seed (20 wt% S.C.).

Ingredients	Amount (g)
IBOMA	152
MMA	8
Dowfax 2A1 [a]	5.3
KPS [b]	0.8
H_2O	640

[a] 2% wbm, [b] 1.5% wbm

For the bio-based PSAs, the solids content was set at 50%, and the reactions were carried out using seeded semi-continuous emulsion polymerization. The same procedure as that used for the petroleum-based PSA was followed, but by replacing the petroleum-based monomers by the bio-based monomers, 2-OA and IBOMA. The recipe involving DMAPS is provided in Table 5.2 with a soft-to-hard co-monomer ratio of (2-OA: IBOMA: MMA) as (84:10:6). For comparison purposes, a reference latex was synthesized by replacing the ZM with Dowfax 2A1.

Table 5.2. The representative recipe for seeded semi-continuous reactions (50% S.C.) of bio-based PSA by 2% DMAPS. The feeding rate of the reaction was 0.76g/min.

Ingredients	Initial charge (g)	Feed (g)
Seed	40.03	
2-OA		81.64
IBOMA		9.94
MMA	---	5.8
DMAPS [a]	---	1.95
TBHP [b]	1.3	---
FF7 [b]	---	1.05
EHTG		0.1
H_2O	---	82.8

[a] 2% wbm [b] 1% wbm [b] 0.1% wbm

5.2.3. Characterization

The characterization methods are given in Appendix II.

5.3. Results and discussion

5.3.1. Surfactant-free PSA synthesized from petroleum-based monomers

Drawing upon the knowledge from the previous chapters, which focused on the coating application of ZM stabilized latexes, it was found that the mechanical properties of the materials were enhanced due to the reinforcing ionic network formed between the polymer chains rich in ZM units. However, it was noted that these properties exhibited changes with temperature, attributed to the partial or complete dissolution of the reinforcing network. Building on this insight, the idea arose that if a responsive network of this nature was incorporated into PSA films, the adhesion properties of a PSA containing ZM could also be tuned with temperature. To test this concept, a surfactant-free waterborne PSA based on n-BA/MMA (90/10) was synthesized, employing A3361 as an exclusive source of stabilizing species, following the same synthesis strategy shown in the previous chapters.

The main characteristics of both waterborne PSAs are presented in Table 5.3. Full MMA/n-BA conversion was achieved in both cases, without any coagulum formation. The particle sizes in the two latexes were different, in the PSA synthesized in the presence of A3361 (pet-PSA-A3361) displayed significantly larger particle size (612 nm) than the reference (pet-PSA-SDS, 198 nm). This was related to the large particle size seed employed (263 nm for the A3361 seed vs 96 nm reference seed) and the fact that larger particles grown faster volumetrically than smaller, due to larger number of radical per particle. Both polymers displayed similar gel content and as is expected in acrylic systems, the gel is formed by intermolecular chain transfer to polymer followed by termination by combination.[8] The average molar mass of the PSAs was determined, and as can be appreciated from Table 5.3 the pet-PSA-

SDS exhibited a smaller molar mass. Taking into account the bigger particle size and as a consequence the lower number of particles presented in pet-PSA-A3361, one would expect the opposite. Due to the lower number of particles, the average number of radicals per particle would be higher and consequently, termination would be promoted resulting in lower molar masses. Nevertheless, it seems that here the effect comes from the fact that due the hydrophilic character of ZM A3361, polymerization and termination in the aqueous phase is promoted, decreasing the number of radicals that can go into the particles and consequently higher molar masses were obtained. As anticipated, 76% incorporation of A3361 was found to be significant, as already observed in Chapter 4. The glass transition temperatures of the polymers were also determined and found similar for both (-39 and -40 °C).

Table 5.3. Characteristics of the petroleum-based reference (pet-PSA-SDS) and surfactant-free (pet-PSA-A3361) PSAs.

PSA	pet-PSA-SDS	pet-PSA-A3361
S.C. (%)	50	50
MMA/n-BA conversion (Xt,%)	100	100
Coagulum (%)	0	0
Dp (nm)	198	612
Gel content (%)	34	38
$\overline{M_W}$ **(kDa)**	64	109
Đ	2.9	2.8
Incorporation (%)	---	76
Tg (°C)	-40	-39

Tack, peel strength, and shear strength represent the three fundamental adhesive properties that govern the performance of PSAs. Tack pertains to the instantaneous adhesion happening when the adhesive is pressed against a substrate surface. Peel strength quantifies the force necessary to detach a standardized PSA strip from a specified test surface (substrate) at a predetermined test angle (e.g., 90° or 180°) and standardized conditions. Shear adhesive failure temperature (SAFT) on the other hand, is the temperature at which the adhesive fails and it characterizes the internal and cohesive potency of the adhesive. Typically, it is gauged as the temperature failure for a standard PSA strip to disengage from a test panel following the application of a load.

Among various measurement techniques, the probe tack test stands out as advantageous when compared to conventional adhesive assessments (peel, shear, and loop tack). This method offers insights into deformation mechanisms during the detachment process over time. In this procedure, a standard material's disc or hemisphere (e.g., a stainless-steel ball probe, as used in this study) comes into contact with the adhesive surface and it is then detached slowly under controlled conditions. Initially, the adhesive layer undergoes uniform deformation, followed by the initiation of voids formation at the probe-adhesive interface (cavitation process). These voids grow until stress reaches its peak. This peak is subsequently followed by either a sharp stress reduction or its stabilization at a consistent level. If the stress sharply decreases, the adhesive layer quickly separates from the probe, resulting in low adhesion energy (W_{adh}). Conversely, stress stabilization (plateau formation in the stress-strain curve) signifies the creation of a fibrillar structure, where the preexisting voids are transformed into fibril walls (fibrillation process). In this scenario, adhesion energy can be notably high, particularly for highly deformable materials. As a result, the collected data, initially in the form of a force-displacement curve, can be transformed into a stress-strain curve. This curve essentially plots the force normalized by the initial contact area against the increase in film thickness normalized by its initial thickness.

Regarding the adhesion properties (Table 5.4), both PSAs, pet-PSA-SDS and pet-PSA-A3361, exhibited similar 180° peel strength and loop tack values. This similarity may be attributed to both PSA formulations sharing a similar composition and have similar Tg values. Moreover, these two PSAs exhibit relative low tackiness and can be classified as easily removable adhesive materials. Nevertheless, it should be noticed that this formulation is not optimized, and it was used just as a platform for evaluation of the effect of A3361 presence. Figure 5.1 illustrates probe tack measurements for the PSAs. The graph clearly shows that pet-PSA-SDS displays a stress-strain curve typical of brittle failure, signifying the formation of cavities at the probe-adhesive interface and their lateral expansion with minimal deformation. For pet-PSA-A3361, a slight plateau in the curve is observed at a lower stress level.

This curve indicates adhesive debonding, signifying that cavitation takes place, where cavities deform vertically until eventual detachment from the probe. This change in curve clearly indicates difference in the work of adhesion (W_{adh}) measured from the area under the stress-strain curves for both PSAs and as indicated in Table 5.4, pet-PSA-A3361 exhibits a significantly higher W_{adh} compared to pet-PSA-SDS. Concerning the behavior of the pet-PSA-SDS, the stress peak is followed by a rapid decrease, indicating the swift detachment of the adhesive layer from the probe. This results in a low work of adhesion (W_{adh}), which likely is result of lack of sufficient mechanical strength and stiffness. Conversely, when looking at Figure 5.1, for pet-PSA-A3361, a modest stabilization of stress (forming a plateau) becomes evident. Even the effect is very small; this particular trend signifies the emergence of a fibrillating structure, wherein the fibrils form the confines of pre-existing cavities through a fibrillation process. This is probably due to improved mechanical properties due to the presence of the ionic network within this film containing A3361. Due to the same chemical compositions of both adhesives, except the small quantity of A3361 replacing SDS (2%), likely the large difference in work of adhesion (19 versus 64 J/m^2) is the result of the increased interaction of the chains (ionic bonding) between the chains containing A3361.

Table 5.4. Adhesion properties of the petroleum-based waterborne PSAs.

PSA	Peel strength (N/25mm)	Loop Tack (N/25mm)	W_{adh} (J/m^2)	SAFT (°C)	SAFT Annealed* (°C)
pet-PSA-SDS	3.3±0.1	1.5±0.4	19±4	70±4	67±1
pet-PSA-A3361	3.6±0.1	1.5±0.3	64±2	83±4	74±1

***Performed with the films previously annealed at 80 °C overnight**

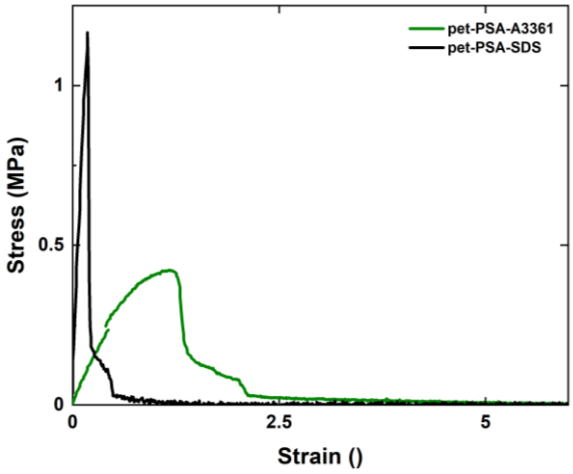

Figure 5.1. Stress-strain curves obtained from the probe tack experiments for petroleum-based waterborne PSAs.

The same reason can be attributed to higher SAFT of pet-PSA-3361 than that of pet-PSA-SDS. We supposed that probably reinforcing ionic network was created in the MMA/n-BA matrix of the pet-PSA-A3361, similar to what was observed in the case of the coating film synthesized with A3361 in Chapter 4. In order to confirm if the reinforcing network affects the SAFT performance, the SAFT measurement was conducted for both films after annealing them at 80 °C overnight. As shown in Table 5.4, the SAFT of pet-PSA-SDS remained nearly unchanged after annealing, while the PSA synthesized with A3361 displayed a decreased SAFT for almost 10 °C, which could only be explained by the reordering or partial dissolution of the reinforcing network.

In order to have a better insight in this issue, the cross-section of the pet-PSA-A3361 was analyzed by AFM. The cross-section, phase AFM images are presented in Figure 5.2, in which the presence of two different phases is clearly appreciated. The dark brown phase is assigned to MMA/n-BA areas, created by the polymer particles, whereas the light brown colored phase is likely made of copolymer chains rich in A3361 units, filling the interstitial spaces between the particles. The structure presented in Figure 5.2a shows incredibly ordered features that most probably are result on the intra- and inter-ionic

interactions between the zwitterions. There is no clear appearance of the hexagonal network structures, as it was observed in the AFM images presented in Chapter 4, probably due to the importantly lower Tg values of the adhesive formulation (Tg= -39°C) that facilitates the inter-diffusion of the MMA/n-BA chains. However, upon annealing (Figure 5.2b) noticeable morphological changes were observed, first of all complete loss of the ordering and a presence of white aggregates (probably arising from the polymer chains rich in A3361) became predominant. We hypothesize that these aggregates are exclusively made of chains rich in A3361, which phase separated during heating from the MMA/n-BA matrix. These observations explains well to the SAFT results. Before annealing of the pet-PSA-A3361, the ordered structure, in which the A3361 rich chains are distributed homogeneously within the MMA/n-BA matrix moreover reinforced with in ionic interactions, performed better than the SDS stabilized counterpart PSA. Nevertheless, these ionic interactions seem to be broken by increasing the temperature during annealing, and at the same time, the inter-diffusion and phase separation were promoted, resulting in the formation of aggregates of polymer chains rich in A3361. Consequently, a drop of adhesion properties (SAFT) happened in A3361 stabilized films after annealing. Regardless to the conditions, the failure mode observed was adhesive, since no residue of the adhesive was observed on the substrate, even though after the heating there is a drop in the mechanical strength of the film, therefore cohesion failure was expected. This means that there is change even in adhesive force happening during annealing. Considering all these results, it can be concluded that the surfactant-free PSA synthesized in the presence of A3361 (pet-PSA-A3361) exhibits thermo-responsive behavior.

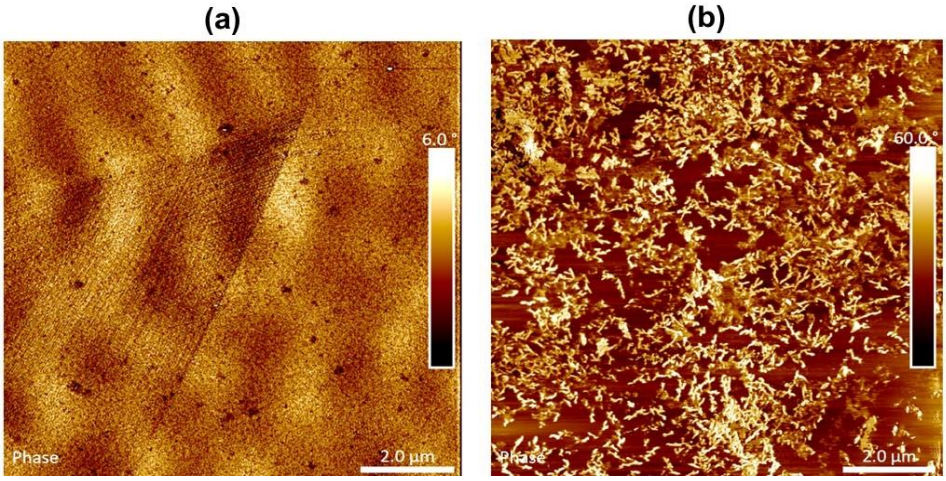

Figure 5.2. AFM phase image of the cross-section of polymer film cast from surfactant-free pet-PSA-A3361, (a) prepared at standard atmospheric conditions (T = 23 °C and 55% RH) and (b) annealed afterwards at 80 °C for three days.

5.3.2. Thermo-responsive PSAs synthesized from bio-based monomers (2-OA & IBOMA) using different ZMs (DMAPS & A3361)

5.3.2.1. Synthesis of the bio-based seed

In an attempt to go one-step further, the conventional petroleum-based monomers were substituted with bio-based alternatives to synthesize surfactant-free waterborne thermo-responsive PSAs. The first attempt was to synthesize a surfactant-free bio-based seed (20% S.C.). This time DMAPS was selected as the ZM and IBOMA as the bio-based monomer. DMAPS was selected to work with it due to its higher availability, lower price, but also due to much lower hompolymer's Tg, that would make more easily observable the thermal responsiveness. However, the reaction did not work, probably because of very high hydrophobicity of IBOMA (2.45×10^{-5} mol/L or $5.45 \cdot 10^{-4}$ g·100 g_{H2O}^{-1}).[9] As this reaction was initiated with KPS, the hydrophilic radicals reacted with the water soluble DMAPS but

these oligoradicals were not able to react with the IBOMA units due to its very low concentration in water, avoiding the formation of stabilizing species. In a second trial, DMAPS was replaced by conventional surfactant Dowfax 2A1, this time the reaction proceeded better, although high coagulum amount was created (15%). The reason behind this coagulation could be twofold, on one hand, due to the high hydrophobicity of p-IBOMA higher amount of surfactant molecules is necessary to stabilize them[9] and on the other hand, the low water solubility of IBOMA (2.45×10^{-5} mol/L or $5.45 \cdot 10^{-4}$ g·100 g_{H2O}^{-1}) which might limit the monomer transport from monomer droplets to polymer particles.[9] Previous research by Schork et al.[10-12] highlighted the potential benefits of incorporating a more hydrophilic comonomer to enhance the emulsion polymerization of hydrophobic monomers. Llorente et al.[13] faced a similar challenge with the stability of p-IBOMA dispersion, but successfully addressed it by introducing a more hydrophilic monomer, MMA. Thus, following this idea, a third trial was conducted, where 5 wt% of the IBOMA content was replaced by MMA and Dowfax 2A1 was used as surfactant. As presented in Table 5.5, this time the amount of coagulum was negligible and the particle size was low enough to be used as a seed. It is worth mentioning that DMAPS was also used instead of Dowfax 2A1 for the seed synthesis, employing either KPS or TBHP/FF7 initiators, without success, the system coagulated even in presence of MMA. Therefore, even though the seed was not surfactant-free, it was employed for the synthesis of thermo-responsive bio-based PSAs using different ZMs.

Table 5.5. Properties of the different bio-based seeds (S.C. 20 %).

Seed	Composition (IBOMA/MMA)	Surf./ZM	S.C. (%)	Coagulum (%)	Dp (nm)
S-IBOMA-DMAPS	100/0	DMAPS	-	-	-
S-IBOMA-DOW	100/0	Dowfax 2A1	17	15	132
S-IBOMA/MMA-DOW	95/5	Dowfax 2A1	18	2	121

5.3.2.2. Synthesis of the thermo-responsive PSAs using bio-based monomers and different ZMs

50% S.C. waterborne PSAs containing 2-OA and IBOMA bio-based monomers were synthesized by seeded semi-continuous emulsion polymerization in presence of two ZM (DMAPS or A3361) and afterwards, their adhesion properties were evaluated. In all the cases, the employed seed was the conventionally stabilized, bio-based seed (S-IBOMA/MMA-DOW) (Table 5.5.).

Since the idea was to maximize the bio-based content in the waterborne PSA, initially, it was tried to synthesize a pure bio-based PSA, comprising 95 wt% of the soft monomer 2-OA (Tg -44 °C) and 5 wt% of the hard monomer IBOMA (Tg 150 °C), with DMAPS. Nevertheless, probably due to the low water solubility of these bio-based monomers, (for IBOMA, 2.45 x 10^{-5} mol/L, for 2-OA it is 5.15 x 10^{-3} mol/L),[9] there was no sufficient creation of copolymers with DMAPS which is exclusively placed in aqueous phase, thus, it was not possible to create enough stabilizing species and the latex coagulated. The same strategy as in the seed synthesis was followed in the next trial, therefore, a more hydrophilic monomer (MMA) was included in the formulation, to increase the monomer concentration in water and assist in the formation of stabilizing species. Furthermore, inspired by the work of Badia et al.,[6,7] the formulation was modified to attain an optimal balance between polymer structure and adhesion properties. To do so, the monomer ratio was changed to 2-OA/IBOMA/MMA (84/10/6) since they found that by increasing the amount of IBOMA the fibrils were stiff enough and flexible as to detach under a greater strain. Additionally 0.1 wt% of CTA 2-ethylhexyl thioglycolate (2EHTG) was included in the formulation in order to adjust crosslinking density of the polymer, and help controlling the sol molar mass providing good initial adhesion. Small CTA concentration is enough to significantly reduce the chain transfer to polymer and hence gel formation, resulting in a decrease of the kinetic chain length.

This time a decent latex, named bio-PSA-DMAPS, was obtained, even though, as it is shown in Table 5.6, relatively high coagulum amount was obtained (11%). Taking it into account, it was considered that full conversion was reached, even though lower conversion was determined. The average particle size of about 350 nm was obtained. The same reaction was repeated using ZM A3361 (bio-PSA-A3361) using the same seed, with expectation that the higher incorporation of A3361 would induce increasing colloidal stability and decrease the quantity of coagulum. As can be observed in Table 5.6, indeed the particle size and coagulum amount significantly decreased. For the sake of comparison, a reference PSA (bio-PSA-Dowfax) was synthesized by replacing the ZM with conventional surfactant Dowfax 2A1. This particular latex exhibited the smallest particle size and was free of coagulum. Regarding the gel content, gel formation was evident in all cases and exhibited similar values. Both bio-PSA-DMAPS and bio-PSA-A3361 presented similar molar masses and significantly higher than the reference PSA (bio-PSA-Dowfax). Once again, due to the lowest particle size of bio-PSA-Dowfax one would expect higher molar masses, however, the same effect was observed for the petroleum based PSAs (Table 5.3) that was attributed to the high hydrophilic character of the ZMs that promoted the polymerization and termination in the aqueous phase. The glass transition temperatures (Tg) of the films were determined and fell within the range of -29 to -26°C.

Table 5.6. Characteristics of the bio-based waterborne PSAs synthesized using different ZMs.

PSA	bio-PSA-Dowfax	bio-PSA-DMAPS	bio-PSA-A3361
S.C. (%)	50	43	45
Xt (%)	100	90	95
Coagulum (%)	0	11	5
DP (nm)	215	348	258
Gel content (%)	12	15	19
$\overline{M_W}$ **(kDa)**	68	110	115
Đ	3.1	3.1	3.0
Tg (°C)	-29	-26	-30

The adhesive properties of bio-based PSA stabilized with both ZMs and with Dowfax 2A1 are summarized in Table 5.7, whereas the probe tack curves are depicted in Figure 5.3. The peel strength, loop tack, and work of adhesion were found to be quite similar for the PSAs synthesized with ZMs, and they were slightly higher than those of bio-PSA-Dowfax. Taking into consideration the same chemical composition, the difference is likely result on multiple inter and intra-ionic interactions that improved the cohesive properties of the PSAs. In Figure 5.3, it is evident that the three PSAs, including the bio-PSA-Dowfax, displayed a plateau formation, indicating formation of fibrils during detachment. These graphs illustrate certain balance of viscoelastic properties leading to adhesive failure. Among these PSAs, bio-PSA-DMAPS exhibited a significantly longer plateau phase when compared to bio-PSA-A3361 with a modest stabilization of the plateau. Moreover, bio-PSA-A3361 showed high stress value followed by a small decrease, where the adhesive layer is debonded fastly from the probe. Meanwhile, for both bio-PSA-Dowfax and bio-PSA-DMAPS, same stress is obtained but the stabilization of the plateau was less pronounced for bio-PS A3361 compared to the bio-PSA-DMAPS.

The distinctions observed between the two PSAs containing ZM can be attributed to variations in the glass transition temperature (Tg) of the zwitterionic homopolymers. Specifically, the lower Tg of DMAPS units (28°C) imparts greater flexibility to the polymer, thereby giving rise to more extended plateaus in comparison to A3361. In contrast, A3361, with its substantially higher Tg (143°C), with heightened polymer incorporation, resulting in a denser network and a higher elastic modulus loss flexibility and the plateau is less pronounced.[14,15] When comparing our study to Badia's,[6] which used a fairly similar formulation, we both observed adhesive de-bonding, also showing similar adhesion and SAFT outcomes. Furthermore, both studies exhibited comparable extended plateaus, however, in our case, it is important to note that the stress required for detachment from the probe was significantly low indicating good adhesive properties.

The probe tack test was performed also at increased temperature of 60 °C (which is above the Tg of p-DMAPS) for the bio-PSA-Dowfax and bio-PSA-DMAPS to check if there is any thermally responsive behavior. For DMAPS, it was observed in Chapters 3 and 4, that when the film was annealed at 80 °C, the reinforcing network was dissoluted and the mechanical properties dropped. Table 5.7 shows that as anticipated, there is a significant decrease in the work of adhesion for the DMAPS PSA at 60 °C with respect to that at room temperature. Surprisingly, a similar behavior was noted for the reference PSA, too. It was thought that the migration of the surfactant Dowfax 2A1 to the film surface during the film annealing, affected negatively the adhesive properties.

Table 5.7. Adhesion properties of the bio-based waterborne PSA.

PSA	Peel strength (N/25mm)	Loop Tack (N/25mm)	W_{Adh} (J/m^2) T_{room}	W_{Adh} (J/m^2) 60 °C	SAFT (°C)	SAFT Annealed (°C) *
bio-PSA-Dowfax	2.9±0.4	1.2±0.3	86±26	26±6	100±3	76±4
bio-PSA-DMAPS	3.4±0.2	1.4±0.4	93±16	24±5	87±6	63±4
bio-PSA-A3361	3.6±0.2	1.7±0.5	91±14	-	91±4	61±8

***Performed with the films previously annealed at 80 °C overnight**

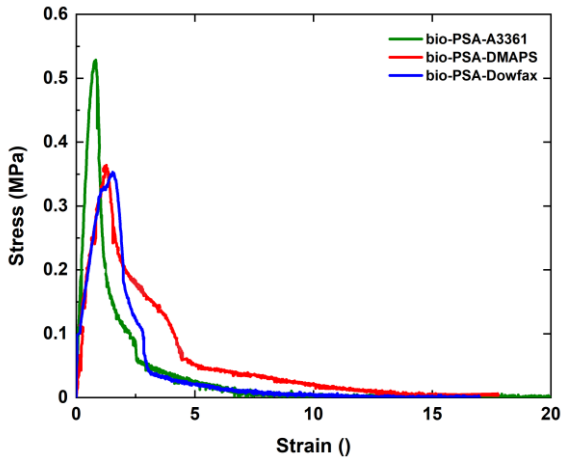

Figure 5.3. Stress-strain curves obtained from the probe tack experiments for bio-based waterborne PSAs.

Regarding the SAFT, quite unexpectedly the incorporation of ZMs did not improve it with respect to the reference PSA stabilized conventionally, (Table 5.7). The bio-PSA-Dowfax exhibited the best SAFT, followed by the PSA synthesized with A3361, and lastly, the DMAPS containing PSA. The performance of ZM PSAs can be attributed to various factors. As explained in prior chapters, the unavoidable presence of water-soluble species can act as plasticizers, potentially causing destabilization of polymer particles and subsequent deterioration in mechanical properties. Conversely, the surfactant Dowfax 2A1 present in the PSAs from the seed, probably establish ionic interactions with the zwitterionic units, potentially resulting in an imbalance of ions and much weaker reinforcement than in case of completely emulsifier-free formulations. These interactions could hinder the realization of the full capacity of ZMs to improve the PSAs performance. Moreover, the existence of coagulum within ZM PSAs, which ideally should consist of substantial proportions of both IBOMA and ZM, contributes to the reduction in their properties. The presence of the hard monomer IBOMA in the coagulum can significantly influence binding strength between adhesive layer and adherent, therefore loss of IBOMA in coagulum markedly affects the SAFT values.

After annealing the films overnight at 80 °C, the SAFT considerably decreased for the PSAs containing ZMs, indicating the restructuration of polymer film and probably diminish the inter-intra molecular ionic interactions affecting likely the both the adhesive and cohesive strength of the PSAs. Surprisingly, a similar behavior was observed for the bio-PSA-Dowfax after annealing, but in this case, it might be linked to the migration of the surfactant, as previously explained in the probe tack experiments conducted at 60 °C.

In order to confirm if the drop observed in the SAFT experiments for the ZM containing PSA was due to the morphological changes in the films before and after annealing, AFM studies were conducted. The corresponding AFM images of the cross-section of both, DMAPS and A3361 containing films are provided in Figure 5.4 and 5.5, respectively.

As can be appreciated from Figure 5.4a DMAPS containing film (bio-PSA-DMAPS) present a continuous and homogeneous film in which the two areas of lighter and darker colors are not well distinguished, likely due to rather even lower Tg of the DMAPS rich chains than these of A3361 (AFM image presented in Figure 5.2). There is a presence of white spots that might be related with the surfactant Dowfax 2A1 from the seed. Upon annealing (Figure 5.4b) the morphology of the film changed, the film is more homogeneous and there is an appearance of small holes. These small black holes were also observed on the film cast from surfactant-free coating when ZM A3367 was used (Chapter 4) and were attributed to the disruptions of ionic interactions between the ZM units followed by phase-separation. As annealing takes place, the aggregation of DMAPS harder segments were created within the soft matrix that includes 2-OA. Therefore, it seems that the ionic interactions between the polymer chains rich in DMAPS are uniformly distributed along the film increasing the cohesion, however, upon the annealing process, the mobility of these chains is promoted and they aggregate between them along the film reducing the cohesion of the film and subsequently diminished the adhesion properties. These observations strongly indicate that the film's adhesion behavior was indeed altered after subjecting it to higher temperatures.

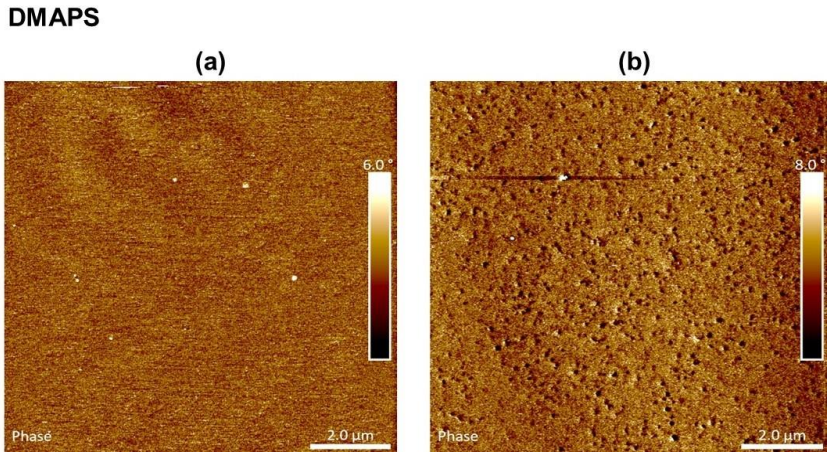

Figure 5.4. AFM phase image of the cross-section of bio-PSA-DMAPS films (a) prepared at standard atmospheric conditions (23 °C, 55% RH), (b) annealed afterwards at 80 °C for three days.

Concerning bio-PSA-A3361, similar to the DMAPS containing film, the images before annealing (Figure 5.5a) exhibit a continuous film but with the presence of numerous white structures. Due to the high concentration of white species, their origin should be different. Therefore, besides the presence of surfactant Dowfax 2A1, polymer chains containing ZM A3361 might be also present; in addition, the presence of polymer chains rich in IBOMA cannot be neither discarded. Significantly, both A3361 units and Dowfax 2A1 exhibit localized presence, demonstrating a distinct interaction between Dowfax 2A1 and A3361. Their consistent proximity suggests a significant interactions and this observation underscores the role of Dowfax in partially screening interionic interactions.

After annealing (Figure 5.5.b) the film showed a clear phase separation where besides the white species (this time more homogeneously distributed along the film) a darker phase (soft phase probably rich in 2-OA) and a lighter phase (harder phase where besides 2-OA might be enriched in IBOMA and A3361).This observed phase separation indicates the interruption of ionic bonds which might be the responsible of the observed drop in SAFT.

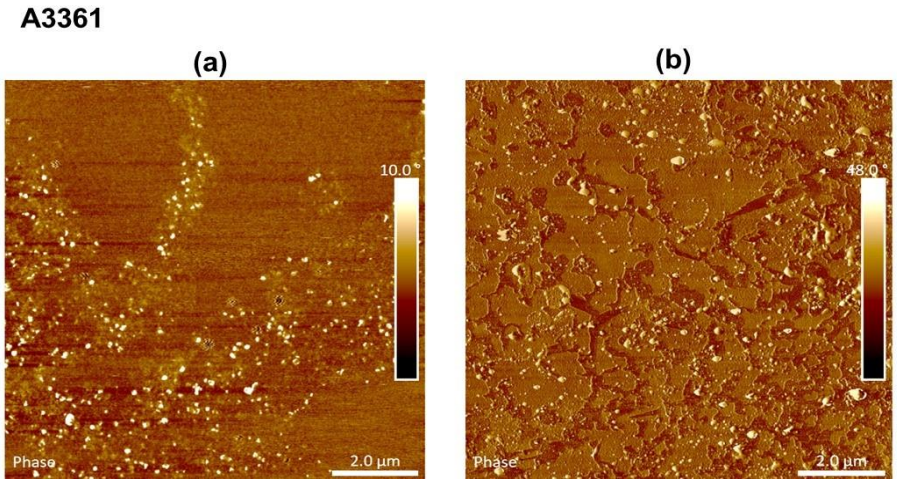

Figure 5.5. AFM phase image of the cross-section of bio-PSA-A3361 film (a) prepared at standard atmospheric conditions (23 °C and 55% RH), (b) annealed afterwards at 80 °C for three days.

It is clear from the AFM images that by increasing the temperature, the morphology of the PSA films containing different ZMs is changed and as a consequence, the adhesion properties can be also tuned, therefore, the synthesized bio-based waterborne PSAs present thermo-responsiveness, however, similar behavior was observed for the reference bio-based PSA stabilized with conventional surfactant Dowfax 2A1. The coagulum found in the ZM-synthesized PSAs might have impeded their optimal performance. Furthermore, the existence of Dowfax 2A1 originating from the initial mixture could have introduced an additional factor that might have influenced the results.

To accurately assess the impact of ZMs on the adhesion properties, it is imperative to avoid the influence of the surfactant, by synthesizing a surfactant-free seed. However, it has been seen that due to the high hydrophobic character of IBOMA, this is still quite challenging and a thorough study (monomer composition, initiator type, feeding strategies etc.) will be required. On the other hand, the final waterborne bio-based PSA containing ZM must be free of coagulum and this objective could potentially be met by decreasing the solids content (S.C.), although this task is expected to be difficult due to the varying behaviors of bio-based monomers. As a result, the optimization of the formulation through additional studies becomes a necessary step. These refinements will facilitate a more accurate investigation of the effects of ZMs on the adhesion properties of waterborne bio-based PSAs.

5.4. Conclusions

In this study, thermo-responsive PSAs stabilized with ZMs were succefully synthesized. The first approach involved developing a surfactant-free PSA using ZM A3361 as the sole stabilizing agent in conjunction with petroleum-based conventional acrylic monomers (n-BA and MMA). The resulting surfactant-free PSA (pet-PSA-A3361) exhibited comparable peel strength and loop tack to the reference PSA (pet-PSA-SDS), which utilized conventional surfactant SDS instead of ZM A3361. However, the surfactant-free PSA demonstrated significantly higher work of adhesion and SAFT, likely attributed to

the ionic interactions between the polymer chains rich on A3361 chains in the polymer particles (stabilizing units). Notably, upon annealing the films at 80 °C overnight, the SAFT of the surfactant-free PSA decreased by approximately 10 °C. AFM investigations validated the existence of uniform and continuous films prior to annealing. However, upon annealing, A3361 units aggregated into distinct entities. These outcomes imply the promising utility of this surfactant-free PSA in removable labels, where the use of heat for removal is viable.

In an alternative approach, the objective was to develop a thermo-responsive bio-based PSAs stabilized with different zwitterionic monomers - DMAPS and A3361 - using 2-OA and IBOMA as the bio-based monomers. Due to the high hydrophobicity of IBOMA, a conventional surfactant (Dowfax 2A1) was necessary during the seed synthesis, while the subsequent synthesis of bio-based PSAs was carried out with ZMs. Interestingly, the bio-based PSAs (bio-PSA-DMAPS and bio-PSA-A3361) exhibited higher adhesion properties, including peel strength, loop tack, and work of adhesion, when compared to the reference bio-based PSA (bio-PSA-Dow) due to the presence of multiple ionic interactions. However, upon subjecting the bio-PSA-DMAPS to the probe tack experiment at 60 °C, a significant decrease in the work of adhesion was observed, likely due to the aggregation of the DMAPS containing polymer chains as revealed by AFM studies. Interestingly, a similar effect was also observed in the reference bio-based PSA, possibly attributed to surfactant migration to the film's surface.

In contrast to the surfactant-free petroleum-based PSAs, the bio-based PSAs stabilized with different ZMs displayed lower SAFT compared to the bio-based reference. This discrepancy may be related to the formation of water-soluble species and additional influence of Dowfax 2A1 on ionic interactions. Moreover, the presence of coagulum content in the bio-based PSAs can also greatly influence the adhesive properties. This coagulum primarily consists of the hard monomer (IBOMA) and a substantial amount of ZM, leading to reduced cohesion within the bio-based PSAs. Additionally, after annealing the films at 80 °C overnight, a notable decrease in SAFT was observed in the bio-based PSAs stabilized with

different ZMs, due to the re-ordering of ZM containing polymer chains as seen in AFM studies. Surprisingly, the bio-based reference PSA exhibited a similar behavior, which might be attributed to surfactant migration to the film's surface.

In a general assessment, ZM bio-based PSAs displayed marginal enhancements in adhesive properties compared to PSAs stabilized with conventional surfactants. However, it is essential to acknowledge that the complete adhesive potential of ZM bio-based PSAs remained untapped due to presence of surfactant in the seed and formation of coagulum. Therefore, to assess the thermo-responsive capabilities of the bio-based PSAs, additional research is necessary. Specifically, synthesizing coagulum and surfactant-free bio-based PSAs would be vital for a more comprehensive investigation. The successful utilization of ZM has highlighted its potential in thermo-responsive applications. However, the endeavor to synthesize coagulum-free PSAs presents its own set of challenges. Within this context, an intriguing innovative approach can be the possibility of further reducing solids content through the introduction of a novel optimized formula. Addressing these aspects will provide deeper insights into the thermo-responsive behavior of the bio-based PSAs and open avenues for exploring their potential applications in various areas. This further research plays a crucial role in advancing the development of environmentally friendly and temperature-sensitive adhesives, which is essential to meet the increasing demand for sustainable and innovative adhesive solutions.

5.5. References

1. **Benedek, Istvan.** *Pressure-sensitive adhesives and applications.* s.l. : CRC press, 2004.

2. *Handbook of pressure sensitive adhesive technology.* **Satas, Donatas.** s.l. : Springer US, 1989, (No Title).

3. *Adhesives and sealants.* **Pocius, A. V.** s.l. : Elsevier, 2012.

4. *Improving adhesion of acrylic waterborne PSAs to low surface energy materials: Introduction of stearyl acrylate.* **Agirre, Amaia, et al.** s.l. : Wiley Online Library, 2010, Journal of Polymer Science Part A: Polymer Chemistry, Vol. 48, pp. 5030–5039.

5. *Pressure-sensitive adhesives: an introductory course.* **Creton, Costantino.** s.l. : Springer, 2003, MRS bulletin, Vol. 28, pp. 434–439.

6. *High biobased content latexes for development of sustainable pressure sensitive adhesives.* **Badía, Adrián, et al.** s.l. : ACS Publications, 2018, Industrial & Engineering Chemistry Research, Vol. 57, pp. 14509–14516.

7. *UV-tunable biobased pressure-sensitive adhesives containing piperonyl methacrylate.* **Badía, Adrián, et al.** s.l. : ACS Publications, 2019, ACS Sustainable Chemistry & Engineering, Vol. 7, pp. 19122–19130.

8. *Seeded semibatch emulsion polymerization of n-butyl acrylate. Kinetics and structural properties.* **Plessis, Ch, et al.** s.l. : ACS Publications, 2000, Macromolecules, Vol. 33, pp. 5041–5047.

9. *High biobased content waterborne latexes stabilized with casein.* **Allasia, Mariana, et al.** s.l. : Elsevier, 2022, Progress in Organic Coatings, Vol. 168, p. 106870.

10. *Monomer Transport in Emulsion Polymerization II: Copolymerization.* **Schork, F. Joseph.** s.l. : Wiley Online Library, 2021, Macromolecular Reaction Engineering, Vol. 15, p. 2100022.

11. *Monomer Transport in Emulsion Polymerization III Terpolymerization and Starved-Feed Polymerization.* **Schork, F. Joseph.** s.l. : Wiley Online Library, 2022, Macromolecular Reaction Engineering, Vol. 16, p. 2200010.

12. *Monomer transport in emulsion polymerization.* **Schork, F. Joseph.** s.l. : Wiley Online Library, 2022, The Canadian Journal of Chemical Engineering, Vol. 100, pp. 645–653.

13. *Challenges to incorporate high contents of bio-based isobornyl methacrylate (IBOMA) into waterborne coatings.* **Llorente, Oihane, et al.** s.l. : Elsevier, 2022, Progress in Organic Coatings, Vol. 172, p. 107137.

14. *Ionic inter-particle complexation effect on the performance of waterborne coatings.* **Argaiz, Maialen, et al.** s.l. : MDPI, 2021, Polymers, Vol. 13, p. 3098.

15. *Towards improved performance of waterborne polymer dispersions through creation of dense ionic interparticle network within their films.* **Argaiz, Maialen, Aguirre, Miren and Tomovska, Radmila.** s.l. : Elsevier, 2023, Polymer, Vol. 265, p. 125571.

Chapter 6. Assessing Surfactant-Free Zwitterionic Waterborne Binders for Paint Applications

6.1. Introduction

By employing small quantities of various zwitterionic monomers with sulfonate anionic groups, we successfully synthesized surfactant-free waterborne dispersions. The addition of these zwitterionic moieties resulted in remarkable improvements to the latex properties. Notably, the interparticle ionic interactions introduced through this incorporation brought forth a plethora of benefits, elevating the mechanical strength, water resistance, barrier properties, and resistance to fouling of the produced films.

In the preceding chapters, it was conclusively demonstrated that the presence of water-soluble species in the latex has a detrimental impact on the overall properties. Furthermore, it was established that the removal of these species through dialysis resulted in enhanced film properties. However, it is important to acknowledge that the dialyzing process presents practical challenges from an industrial perspective. Notably, it is time-consuming and expensive, mainly due to the significant water consumption and the high cost of the specific membranes used. Nonetheless, despite these challenges, it remains imperative to assess the performance of this innovative latex in a suitable paint formulation. Understanding how this novel latex behaves in real-world applications will be crucial for its successful integration into various industrial processes.

In this chapter, we present the findings of a three-month internship conducted at Synthomer (Sintra, Portugal). The primary focus of the internship was to synthesize high solids content binders using a small quantity of ZM DMAPS as a substitute for traditional surfactants. These newly developed binders

were then integrated into enamel paint formulations for protective coatings. The main objective was to evaluate the performance of these latexes as binders in paints and investigate the influence of DMAPS on the final properties of the coatings. Several acrylic binders stabilized with ZM DMAPS were compared with reference binders stabilized with conventional surfactants, as well as a surfmer provided by Synthomer.

6.2. Experimental section

6.2.1. Materials

The materials are given in Appendix I.

6.2.2. Polymerizations

Table 6.1 displays the various binders utilized throughout this study, along with their respective acronyms. For the purpose of comparison, three reference binders were synthesized: two of them were stabilized with a conventional surfactant (Synth A1 and Synth A2), while the last one (Synth_Surf) was stabilized with a surfmer containing a double bond in its structure capable of chemically incorporating into the polymer particles during polymerization, thereby preventing migration.[1] Additionally, Table 6.1 also includes the latex A4_50:50_S.F., which is a completely surfactant-free latex synthesized in the POLYMAT lab by polymerizing MMA/n-BA in a 50/50 weight ratio with 30% solids content.

Table 6.1. Summary of all the synthesized latexes.

Latex Code	Monomer ratios
Synth A1	n-BA:MMA (58:42)
Synth A2	n-BA:MMA (58:42)
Synth_Surf	n-BA:MMA (58:42)
A4_50:50_S.F[a]	n-BA:MMA (50:50)
A5_50:50	n-BA:MMA (50:50)
A6_50:50_6L [b]	n-BA:MMA (50:50)
A7_50:50_Sty	n-BA:Styrene (50:50)
A8_58:42	n-BA:MMA (58:42)
A9_50:50_AA	n-BA:MMA:AA (49.5:49.5:1)
A10_50:50_HEMA	n-BA:MMA:HEMA (49.5:49.5:1)

[a]completely surfactant-free latex, 30% S.C.,
[b]reaction in steel reactor

The remaining latexes were all synthesized using seed particles stabilized by the conventional surfactant SDS. Latexes A5_50:50 and A6_50:50_6L share the same composition of MMA/n-BA with 50% solids content. The primary distinction lies in the scale-up process of latex A6_50:50_6L, which was increased from 2.5 L to 6 L to investigate the process's scalability and its impact on characteristics. In the case of latex A7_50:50_Sty, the MMA in the formulation was replaced by styrene to examine how the incorporation of a more hydrophobic monomer would affect the particle size, or more specifically, the incorporation of DMAPS onto particles.

To ensure a fair comparison with the reference latex, latex A8_58:42 altered the ratio of MMA/n-BA, as indicated in the acronym, using a MMA/n-BA 58/42 weight ratio. For the last two latexes, A9_50:50_AA and A10_50:50_HEMA, a small quantity of functional monomers (1%) AA and HEMA, respectively, was added to the common MMA/n-BA formulation of 50/50. This addition aimed to explore how further functionalization of the particles would influence DMAPS incorporation and interactions between the components in the paint formulations. It is important to note that while the incorporation of DMAPS onto particles was not directly studied, it was estimated from the average particle size of the latexes, based on previous research demonstrating a direct relationship between them.

The target solids content of 50% was achieved by using 2wt % of DMAPS in all cases. To promote the incorporation of hydrophilic DMAPS units, the redox initiator TBHP/FF6 was chosen, generating hydrophobic radicals in the aqueous phase. This facilitated their rapid entry onto polymer particles and minimized the likelihood of aqueous phase polymerization. However, this approach resulted in very low conversions, primarily due to the low efficiency of the reductant FF6.[2] Unfortunately, reductant FF7 was not available in the company, leading to the decision to use sodium persulfate (NaPS) thermal initiator for all the reactions.

6.2.2.1. Reaction set up

A jacketed 2.5 L glass reactor was employed, which included a stainless steel pitched blade impeller, a reflux condenser, a nitrogen inlet, a temperature probe, a sampling tube, and one feeding inlet. The pre-emulsion was carefully fed into the reactor by manually controlling the pump. Prior to and throughout the reaction, the reactor was purged with nitrogen to ensure an inert atmosphere.

6.2.2.2. Seed synthesis

Table 6.2 provides a comprehensive recipe outlining the step-by-step procedure for synthesizing the seed stabilized with the conventional surfactant SDS. Initially, water, SDS, and the MMA/n-BA mixture were combined in the reactor and stirred at a rate of 150 rpm under a nitrogen (N_2) atmosphere. Once the temperature reached the desired level of 80 °C, an aqueous solution of initiator NaPS was added swiftly. The system underwent batch-wise reaction for a duration of 4 hours. After completion of the reaction, the mixture was cooled to below 40 °C, and biocides CIT/MIT 1.5% and BIT 20-D were introduced and stirred for 10 minutes. The solids content (S.C.) of the resulting seed was 10%. This seed had an average particle size of 60 nm and was subsequently utilized in all the seeded semi-continuous emulsion polymerization reactions. To achieve a latex solely stabilized by the ZM DMAPS, a surfactant-free seed was synthesized following the procedure given in Chapter 4.

Table 6.2. Recipe for the seed synthesized with conventional surfactant SDS (10 % S.C.).

Ingredients	Wt (%)	Amount (g)
n-BA	4.97	114.20
MMA	4.97	114.20
SDS[a]	0.2	4.57
NaPS [b]	0.1	2.28
CIT/MIT 1.5%[b]	0.1	2.28
BIT 20-D[b]	0.1	2.28
Water	88.4	2060.17

[a]2 wt% ,[b] 1 wt% based on monomers

A representative recipe for seeded semi-continuous emulsion polymerization reactions, conducted in the presence of 2% DMAPS, is provided in Table 6.3. The target solids content for all the latexes was set at 50%. To begin the process, an appropriate amount of the seed was placed in a 2.5 L reactor and purged with nitrogen (N_2) under stirring at 150 rpm until the end of the reaction. Once the reactor reached the desired temperature of 80 °C, an aqueous solution of the initiator NaPS was introduced rapidly, followed by the feeding of the pre-emulsion consisting of MMA/n-BA mixture in a 1:1 weight ratio and DMAPS for 3.5 hours. After this, the system was allowed to undergo a batch-wise reaction for 1.5 hours. Upon completion of the reaction, the latex was cooled down to room temperature, and biocides were added and thoroughly stirred. Subsequently, the pH of all binders was measured and adjusted to above 6 using a 10% NaOH solution.

On the other hand, for the completely surfactant-free latex with a solids content of 30%, a previously synthesized surfactant-free seed was utilized. The procedure followed was similar to the one explained above, with the exception of the addition of biocides. In this case, the TBHP/FF7 (1%) redox pair was used as the initiator instead of the thermal initiator NaPS. TBHP was added as a shot, while FF7 was included in the pre-emulsion, and the reaction temperature was set to 50°C. The detailed recipe can be found in Table 6.4.

Table 6.3. Recipe of seeded semi-continuous reaction (2% DMAPS and 1% NaPS) (50% S.C.).

Ingredients	Wt (%)	Amount (g)
Seed	19.6	445.85
n-BA/MMA	23.5/23.5	539.68/539.68
DMAPS	0.9	21.6
NaPS	0.47	10.79
CIT/MIT 1.5%	0.1	2.27
BIT 20 D	0.1	2.27
NaOH*	---	20-30
Water	31.9	734

*** The amount of NaOH was varied in different reactions**

Table 6.4. Recipe of completely surfactant-free seeded semi-continuous reaction (2% DMAPS and 1% TBHP/FF7) (30% S.C.).

Ingredients	Wt (%)	Amount (g)
Seed	20	320
n-BA / MMA	28.8	231/231
DMAPS	0.57	9.2
TBHP	0.38	6.2
FF7	0.28	4.6
Water	53.6	858

6.2.3. Preparation of paints

The waterborne paints were prepared using an enamel paint formulation with a pigment-volume concentration (PVC) of 21%. Enamel paint is known for its durable coatings that dry to an opaque, lustrous finish, with the binder being the key component. The paint preparation involves several steps, with the first one being the preparation of the millbase, which consists of carefully mixing different components. The recipe for the millbase, along with the specific function of each constituent, can be found in Table 6.5.

To prepare the millbase, water, dispersant, biocide, antifoaming agent, pH modifier, and co-solvent were accurately weighed and added to a 3 L cylindrical vessel. The mixture was stirred using a high-speed dispersant at 500 rpm for 20 minutes. Next, titanium dioxide (pigment) was slowly added, and the

stirring rate was increased to 2000 rpm. The entire dispersion was mixed for another 30 minutes to ensure a homogeneous system. To determine the fineness of the pigment particles, the final quality check of the millbase was conducted using a Hegman gauge, and it should meet the requirement of being below 40 µm.

Table 6.5. Formulation of millbase.

Ingredients	Functions	Amount (g)	Wt (%)
Water	...	158.70	15.87
Additol VXW 6200	Dispersing agent	6.50	0.65
Preventol D12	Biocide	2.00	0.20
Agitan E-256	Defoamer	0.30	0.03
1,2–Propylene glycol	Co-solvent	20.00	2.00
Tiona RCL 535	Pigment	210.0	21.00
NaOH 10%	pH modifier	6.00	0.60

After preparing the millbase, the subsequent stage is the letdown process. This step involves combining the millbase with the binder (latex) and other specified ingredients, as outlined in Table 6.6. To achieve the desired viscosity, measurements were taken and adjusted to 85-90 KU by adding an appropriate amount of thickener. Different quantities of thickener were used for each case.

To ensure comparability between the different paints, it was essential for all of them to have a similar solids content (S.C.). Consequently, adjustments were made to the amount of water and binder used in both stages for latex Synth_Surf, A4_50:50_S.F, and A7_50:50_Sty, as they have different solids content compared to the rest of the latexes.

Table 6.6. Letdown stage.

Ingredients	Functions	Amount (g)
Millbase	---	403.5
Binder*	---	524.4
Texanol	Coalescing agent	15
Water*	---	45.6
Aquaflow NMS 450**	Thickener	---

***The amount of binder and water was varied with respect to S.C. of binders**
**** Amount of thickener depends on the viscosity of the paints**

6.2.4. Characterization

The characterization methods are given in Appendix II.

6.3. Results and discussion

6.3.1. Latex (binder) properties

Table 6.7 presents the key properties of the synthesized latexes. It is important to highlight that, with the exception of the completely surfactant-free latex (A4_50:50_S.F), all other DMAPS-containing latexes will have a small amount of SDS, which originates from the seed.

Table 6.7. Characteristics of synthesized latex (binders).

Latex code	S.C. (%)	Dp (nm)	pH	Viscosity * (maP.S)	MFFT (°C)	RTM (min/°C)
Synth A1						
Synth A2	50	109		1604 (s2/20)	0	
Synth_Surf	45	205	8.5	94.5 (s1/20)	0	30/41
A4_50:50_S.F	30	560	6	7 (s1/20)	13	8/30
A5_50:50	50	413	9.5	21 (s1/20)	11	30/30
A6_50:50_6L	50	422	8.5	25 (s1/20)	12	30/33
A7_50:50_Sty	46	234	7.6	25 (s1/20)	17	30/27
A8_58:42	49.7	423	7.5	26 (s1/20)	0	30/30
A9_50:50_AA	49.6	407	7.6	21 (s1/20)	11	30/31
A10_50:50_HEMA	49.6	460	6.3	21 (s1/20)	11	30/42

***(s-1, 2, 3 indicates code of spindle used)**

The latexes synthesized using DMAPS demonstrated notably larger particle sizes compared to the reference latexes. The particle sizes ranged between 400-500 nm, except for the latex synthesized with styrene, which yielded a particle size of 234 nm. The initiator employed in the synthesis of all these latexes, with the exception of the surfactant-free latex A4_50:50_S.F was NaPS. NaPS is a water-soluble thermal initiator known for providing hydrophilic radicals. In the case of MMA/n-BA systems, these radicals predominantly react with DMAPS and MMA present in the aqueous media, resulting in the formation of highly hydrophilic oligoradicals. These hydrophilic oligoradicals have a tendency to remain in the aqueous phase rather than being incorporated into the polymer particles. Consequently, they terminate in the aqueous phase and form water-soluble oligomers, leading to a reduced incorporation of DMAPS onto the particles. As a result of this lower incorporation of DMAPS and the increased presence of water-soluble species, which elevate the ionic strength in the dispersion, the colloidal stability of the latexes appears to be affected, ultimately resulting in the observation of larger particle sizes.

On the other hand, the A7_50:50_Sty latex exhibited a significantly smaller average particle size (234 nm), which could be attributed to the higher hydrophobicity of styrene compared to MMA. The incorporation of a small amount of styrene units into the DMAPS-containing oligoradicals in the aqueous phase promoted easier entry of these oligoradicals onto the polymer particles, leading to an increased incorporation of DMAPS on the particles. As a result, the fraction of water-soluble oligomers formed in the aqueous phase decreased, contributing to enhanced colloidal stability and, consequently, smaller particle size.

In the case of the surfactant-free latex (A4_50:50_S.F), TBHP/FF7 redox initiator was utilized, and although the incorporation of DMAPS (42%) was relatively high, the large particle size of 590 nm might be attributed to the size of the seed particles used (234 nm). Interestingly, the inclusion of HEMA and AA functional monomers did not lead to any significant improvement in DMAPS incorporation, as

evidenced by the similar particle sizes of these latexes to the other DMAPS-containing ones. While previous studies[3] have shown that increasing the water solubility of main monomers or introducing hydrophilic functional monomers can enhance the incorporation of certain substances onto polymer particles, this effect was not observed in this case.

Throughout the latex synthesis process, the pH was generally maintained between 2.5 and 3. However, when a buffer was added, the pH was increased to above six for most latexes, except for the completely surfactant-free latex. In the case of the surfactant-free latex, no buffer was used, and its pH remained around 6. The latexes synthesized with DMAPS exhibited notably lower viscosities compared to the reference latexes. This decrease in viscosity should not present any issues as long as the viscosity response of the latex is appropriate for formulation, as will be discussed later.

The minimum film forming temperatures (MFFT) of the latexes stabilized with DMAPS were generally in the range of 11-17 °C, except for latex A8_58:42, which had the same monomer composition as those provided by Synthomer and presented a lower MFFT (0 °C) due to the higher concentration of the soft monomer (n-BA).

Regarding the thermal and mechanical stability of the binders, all of them remained stable under high shear rate, except for the surfactant-free latex (A4_50:50_S.F.), which coagulated after 8 minutes of stirring. This instability is likely attributed to the large particle size and the presence of water-soluble oligomers, making it less stable under such conditions. Despite the low colloidal stability under high, shear rates, latex A4_50:50_S.F. was still utilized for paint formulation, albeit with potential challenges in the process.

6.3.1.1. Water blanching of films prepared from the binders

Water blanching tests were conducted on films prepared from the latexes and dried under controlled conditions at 23 °C and 50% relative humidity for 1 day. After 24 hours of immersion in water,

the results are displayed in Figure 6.1. Visual inspection revealed that the films made from Synth A1, A4_50:50_S.F and A8_58:42 exhibited poor water resistance and detached from the glass plate. In the case of Synth A1, this may be attributed to the formation of hydrophilic pockets arising from surfactant aggregation, which could increase water sensitivity. Surprisingly, Synth_A2, despite having the exact same composition and synthesis method as Synth A1, displayed much better water resistance.

The lower water sensitivity of DMAPS films can be attributed to the presence of water-soluble species distributed within the films in the case of binders A4_50:50_S.F and A8_58:42. Additionally, the presence of sulfate ions from the initiator may introduce an imbalance of ionic groups, limiting the full potential of DMAPS. Moreover, weaker repulsive interactions between particles could facilitate the plasticization effect of water, leading to more whitening of DMAPS latex films.

In contrast, the reference binder synthesized with the surfmer (Synth_Surf) demonstrated good resistance to water absorption, likely due to the absence of water-soluble oligomers. It is important to note that the experiments were conducted over a 24-hour period, and for a comprehensive understanding of DMAPS capabilities, longer experiments should be conducted. Previous experience with DMAPS-containing films has shown that initially, they absorb a larger quantity of water compared to SDS-containing films. However, over time, the water adsorption of DMAPS films reaches saturation and remains below that of SDS-containing films. Detailed observations of water blanching at specific time intervals of immersion are provided in Table 6.8.

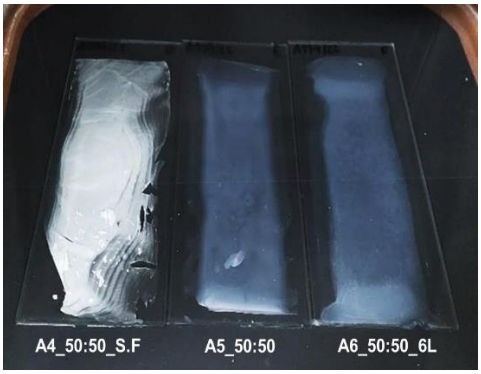

Figure 6.1. Blanching of latex films after 24 hours.

Table 6.8. Results from water blanching test of the latex films.

Latex code	5 (min)	10 (min)	15 (min)	30 (min)	1(hr)	4 (hr)	24 (hr)
Synth A1	0	0-1	1	1	1-2	3-4	4-5
Synth A2	0	0-1	0-1	0-1	1	2-3	3
Synth_Surf	3	3-4	3-4	4	4	2	2
A4_50:50_S.F	0-1	1-2	1-2	2	2	2-3	4-5
A5_50:50	1	1	1	1	1	1	1-2
A6_50:50_6L	1-2	1-2	1-2	1-2	1-2	1-2	2
A7_50:50_Sty	0-1	0-1	0-1	0-1	1	1	1
A8_58:42	2	2-3	2-3	3	3-4	4-5	5
A9_50:50_AA	1-2	2	2	2	2	2-3	3
A10_50:50_HEMA	1	1	1-2	1-2	1-2	2	2-3

(Evaluation, 0-Good resistance; 5-Poor resistance)

6.3.2. Properties of liquid paints

The properties of the liquid paints are summarized in Table 6.9. As part of the quality control process, the solids content and specific gravity (S.G) were measured for the paints. All paints fell within the expected values, indicating that the paint preparation step was well executed. To achieve the desired stormer viscosities in the range of 85-95 Ku, an associative thickener was used. Thickeners play a crucial role in paints and other coating materials, as they help attaining specific rheological properties. With

their surface activity, they can influence various paint properties, such as improving appearance, gloss, and flow.

The theoretical amount of thickener in the formulation was 4wt%. However, the actual amount of thickener required by the paints could be more or less than the theoretical amount, depending on the thickening response of the binder. Figure 6.2 illustrates the thickening response of each binder used in this study, highlighting how the composition of the binder significantly affects this response. The thickening response refers to the binder's ability to react to the addition of a thickening agent and is likely influenced by the binders' capacity to interact with the thickener. It is important to consider that the addition of thickeners increases the cost of the paints. Therefore, by using a lower amount of thickener that still achieves the desired viscosity alteration, the overall cost of the paint can be minimized.

Table 6.9. Characteristics of the paints.

Latex code	S.C. (%)	S.G (g/cm^3)	Viscosity			pH
			Stromer (KU)	ICI (Poise)	Brookfield * (mPa.s)	
Synth A1	47.9	1.231	89.3	2.2	1460 (3)	8.2
Synth A2	48.4	1.232	93.7	2.1	1850 (3)	8.5
Synth_Surf	47.4	1.227	86.1	1.1	2395 (3)	8.6
A4_50:50_S.F	45.3	1.191	57	2.3	249 (1)	7.7
A5_50:50	47.6	1.229	82.9	0.9	2200 (3)	8.9
A6_50:50_6L	46	1.236	75.3	0.9	1310 (3)	8.6
A7_50:50_Sty	48.2	1.219	97.2	1.1	5010 (4)	8.7
A8_58:42	46.7	1.218	73.6	0.9	828 (2)	8.5
A9_50:50_AA	45.7	1.213	70.3	1.2	712 (2)	9.1
A10_50:50_HEMA	45.8	1.210	67.1	1.3	550 (2)	8.0

***(s-1, 2, 3 indicates code of spindle used)**

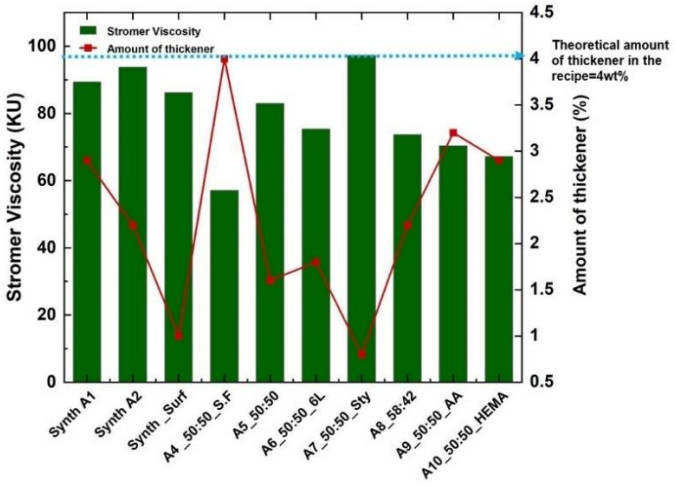

Figure 6.2. Thickening response of the binders upon addition of thickener.

The associative thickener plays a crucial role in enhancing the viscosity of liquid paints by establishing bridges between the polymer particles through adsorption. This adsorption process depends on both the characteristics of the thickener and the surface properties of the particles. In the context of DMAPS paints, with the exception of paint A7_50:50_Sty, all others failed to achieve the required viscosity range (85-90KU).

The exceptional thickening response observed for paint A7_50:50_Sty can be attributed to two key factors. Firstly, the expected higher incorporation of DMAPS onto polymer particles, especially after obtaining a relatively small average particle size (as indicated in Table 6.7), results in an increased concentration of sulfonate groups on the particle surfaces. This facilitates efficient bridging with the thickener, enhancing viscosity. Secondly, the small particle size of the binder and its larger surface area, along with higher functionalization with sulfonate groups, fosters increased particle-particle interactions, making it easier to establish bridges between them.[4] For the other DMAPS paints with larger particle sizes, the addition of thickener beyond a certain amount did not lead to significant increases in viscosity, and they were used as is. This lack of response could be attributed to the lower

incorporation of DMAPS, resulting in fewer sulfonate groups available on the particle surfaces, in addition to the larger particle size.

The completely surfactant-free paint A4_50:50_S.F. exhibited the worst thickening response, likely due to its larger particle size and potentially higher content of water-soluble polymers. These water-soluble polymers might interact with the thickener, leaving fewer available sites for relating the particles. Similar explanations apply to the AA and HEMA-containing latexes, which also required relatively high amounts of thickener, despite the initial expectation that the presence of functionalities might positively influence particle-thickener interactions. In contrast, the reference paints showed a good thickening response, likely owing to their smaller particle size and increased availability of the thickener for interaction with the particles. Moreover, the compatibility of the thickener with the binder can also influence viscosity, and the careful selection of a suitable alternative thickening agent may enhance the thickening response of the DMAPS binders.

6.3.2.1. Storage stability at 50 °C

The alterations in paint appearances after being stored at 50 °C for 28 days were carefully examined. During storage, all paints, except Synth A1 and A2, exhibited phase separation. However, after mixing the paints again, they returned to their initial appearances. The comprehensive measurements conducted following latex storage are presented in Table 6.10. It can be concluded that all the paints remained stable after 1 month of storage at 50 °C since there were no significant differences in viscosity and pH compared to the initial values. Although a slight augmentation in viscosity was observed, it did not affect the overall stability of the paints.

Table 6.10. The difference of the characteristic of the paints before and after storing during 28 days at 50 °C. (The characteristics of the paints before storage are shown in brackets).

Latex code	Synersis (%)	Viscosity			pH
		Stromer (KU)	ICI (Poise)	Brookfield * (mPa.s)	
Synth A1	0	94.8 (89.3)	2.1(2.2)	1725(3)(1460)	8.2 (8.2)
Synth A2	0	100(93.7)	2.0(2.1)	2210 (3)(1850)	8.5 (8.5)
Synth_Surf	46	88.8(86.1)	1.1(1.1)	2565 (3)(2395)	8.6(8.6)
A4_50:50_S.F	46	55.6(57)	2.1(2.3)	144 (1)(249)	7.5 (7.7)
A5_50:50	21	88.4(82.9)	1.1(0.9)	1955(3)(2200)	8.2 (8.9)
A6_50:50_6L	21	87.7(75.3)	0.9(0.9)	1280(3)(1310)	7.8 (8.6)
A7_50:50_Sty	14	97.1(97.2)	1.7 (1.1)	4650(4)(5010)	7.5(8.7)
A8_58:42	28	81.5 (73.6)	1.2(0.9)	2270(2)(828)	7.7(8.5)
A9_50:50_AA	28	83.8 (70.3)	1.0 (1.2)	2135 (2)(712)	8.0 (9.0)
A10_50:50_HEMA	36	72.1 (67.1)	1.1(1.3)	1325(2)(550)	7.6 (8.0)

***(s-1, 2, 3 indicates code of spindle used)**

Product application was assessed by measuring the coating brushability, which determines the ease of spreading the paint on a surface. Table 6.11 presents the brushability and application results of all paints tested on wooden substrates, and in all cases, the application turned out to be favorable. No cracking or bubbles were observed in any of the paint films, indicating good paint film preparation.

Leveling, which indicates the ability of the paint to form a smooth surface by eliminating ripples, pockmarks, and brush marks after application, was generally good for all paints, except for A7_50:50_Sty. The lower level of leveling observed in A7_50:50_Sty may be attributed to its highly viscous nature (97 KU), which hindered its surface flow during application.

One notable finding was the build observed for paint A4_50:50_S.F, likely resulting from its lower viscosity and potential incompatibility with other paint components. Despite these isolated issues, overall, the paints demonstrated satisfactory application properties, making them suitable for coating wooden substrates.

Table 6.11. Product application of paints.

Latex code	Brushability	Cracking	Micro foams	Air bubbles	Levelling	Build
Synth A1	0	0	0	0	0	0
Synth A2	0	0	0	0	0	0
Synth_Surf	0	0	0	0	0	1
A4_50:50_S.F	0	0	0	0	0	2-3
A5_50:50	0	0	0	0	1	0-1
A6_50:50_6L	0	0	0	0	0	0-1
A7_50:50_Sty	0	0	0	0	3	0
A8_58:42	0	0	0	0	0	1
A9_50:50_AA	0	0	0	0	0	0
A10_50:50_HEMA	0	0	0	0	0-1	0

(Evaluation, 0-Good, 5-Poor)

6.3.3. Properties of the paint films

6.3.3.1. Hardness

The investigation into the evolution of coating hardness over time yielded intriguing results, as shown in Figure 6.3 As expected, the paint films displayed an increase in hardness during the drying process, and this hardness was notably influenced by the composition of the binders. An interesting trend was observed concerning the impact of the n-BA monomer content in the binder on the copolymer's hardness. Generally, the higher the n-BA content, the softer the copolymer, consequently leading to lower hardness.

In most cases, with the exception of A8_58:42, the paints synthesized with DMAPS demonstrated higher hardness compared to the reference paints. Several factors may contribute to this phenomenon. Firstly, the higher glass transition temperature (Tg) of the polymers made from MMA/n-BA with a 50/50 weight ratio may play a role. Additionally, previous findings have revealed the presence of a reinforcing network formed by DMAPS-rich polymer chains that undergo ionic interactions. These chains are distributed around the particles, providing colloidal stability in the dispersions and creating a rigid ionic

network within the films. Among the DMAPS-containing paints, the best performance was observed for A7_50:50_Sty. In this case, it is likely that the presence of numerous aromatic functionalities from styrene within the polymer chains contributed to increased rigidity compared to the MMA hard monomer.

Furthermore, the presence of AA and HEMA also had a favorable effect on the hardness of the final polymers. It is possible that these functionalities facilitated the establishment of hydrogen bonding between the MMA/n-BA chains, which, in conjunction with the DMAPS-rich network, resulted in even harder materials[5-7] compared to MMA/n-BA materials without these functional polymers.

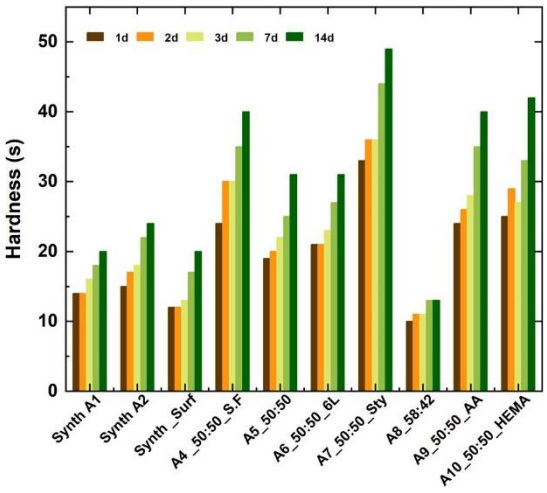

Figure 6.3. Evolution of pendulum hardness with time.

6.3.3.2. UV exposure

After subjecting the paint films to 5 days of UV irradiation, measurements of the L*a*b* parameters were conducted. The differences in the parameter (Δb) and color change (ΔE) of all the paints before and after UV exposure are presented in Table 6.12

Across all paints, slight color changes (ΔE) were observed, but they were imperceptible to the naked eye. This indicates that the paints exhibited excellent resistance to UV light, maintaining their original color appearance even after exposure. However, there was an exception with the DMAPS paint A7_50:50_Sty, which showed a slightly yellowish appearance. This can be attributed to the aromatic ring present in polystyrene, which exhibits higher UV light absorption compared to the MMA/n-BA systems. As a result, a suite of photochemical oxidation pathways is activated, leading to the observed color change in this particular paint.[8] Overall, the results demonstrate that the majority of the paints possess robust UV resistance, making them suitable for applications in environments exposed to sunlight.

Table 6.12. L*a*b* parameters after exposure to UV after 5 days.

Latex code	Δb (a.u.)	ΔE (a.u.)
Synth A1	0.13	0.26
Synth A2	0.14	0.48
Synth_Surf	0.10	0.15
A4_50:50_S.F	0.27	0.28
A5_50:50	0.17	0.28
A6_50:50_6L	0.27	0.31
A7_50:50_Sty	3.63	3.75
A8_58:42	0.22	0.24
A9_50:50_AA	0.21	0.40
A10_50:50_HEMA	0.23	0.58

6.3.3.3. Block resistance

The evaluation of blocking resistance involved measuring the force required to detach surfaces covered with the same paints that were stacked together. If the force needed to unstack both coating films exceeded 300 g/cm^2, it was considered as poor block resistance. This assessment was conducted at two different temperatures: room temperature (23 °C) and elevated temperature (50 °C). The results obtained are presented in Figure 6.4.

Upon analysis, it was evident that all the paints displayed very poor blocking properties at the higher temperature of 50 °C. However, when the blocking resistance was tested at room temperature, the paints synthesized with DMAPS demonstrated good blocking resistance. A noteworthy exception was observed with paint A8_58:42, which contained a higher concentration of n-BA similar to the reference paints, leading to poor blocking performance due to the softer nature of the polymer.

The positive blocking performance of the DMAPS-synthesized paints can be attributed to their significantly higher hardness, as indicated in Figure 6.3. This hardness was a consequence of the formation of a reinforcing rigid ionic network facilitated by polymer chains enriched with DMAPS units, along with the higher Tg resulting from the n-BA/MMA 50/50 composition. Previous research has shown that at elevated temperatures, this ionic network becomes diluted, causing a softening effect on the polymers, leading to the observed poor blocking properties. The findings reveal that DMAPS paints offer a desirable balance of mechanical properties, characterized by high hardness and good blocking resistance.

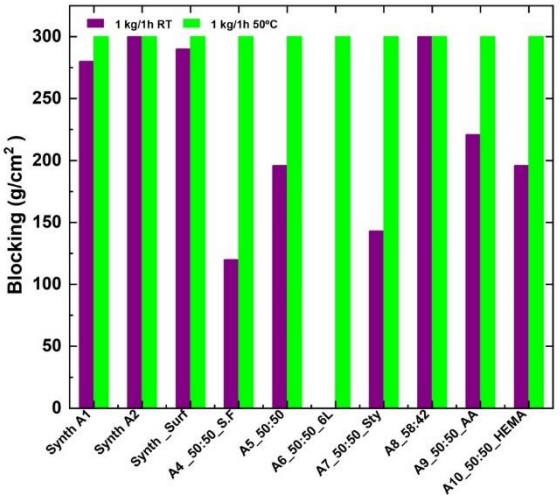

Figure 6.4. Blocking resistance of the paint films.

6.3.3.4. Gloss and contrast ratio

The gloss of the paint films was carefully assessed at 60° (Figure 6.5), and the corresponding results are summarized in Table 6.13. Films achieving gloss values higher than 60 gloss units were considered to be highly glossy. Given the low PVC (21%) utilized in the formulation of enamel paints, it was expected that the coatings would exhibit a glossy appearance. As anticipated, all the films demonstrated high gloss, except for A9_50:50_AA and A10_50:50_HEMA. The slightly lower gloss observed in A9_50:50_AA and A10_50:50_HEMA could be attributed to the presence of functional monomers (AA and HEMA, respectively) in their formulations. These functional monomers may have influenced the surface roughness of the films, resulting in a minor reduction in gloss compared to other paints.[9]

Furthermore, the opacity of the paints was evaluated by determining the contrast ratio of the coated films. Remarkably, high opacity values (above 90%) were achieved in all cases, except for the completely surfactant-free paint and the paints containing AA and HEMA. These observations provide valuable insights into the optical characteristics of the paints, and they align well with the intended application of creating highly glossy and opaque coatings.

Table 6.13. Gloss (60°) and contrast ratio of all paints.

Latex code	Gloss (60°)	Contrast ratio
Synth A1	67.2	92.47
Synth A2	70.5	93.01
Synth_Surf	77.2	96.72
A4_50:50_S.F	61.8	89.2
A5_50:50	66.2	94.42
A6_50:50_6L	59.9	94.66
A7_50:50_Sty	62.6	92.68
A8_58:42	70.7	94.97
A9_50:50_AA	43.1	89.66
A10_50:50_HEMA	47.4	89.87

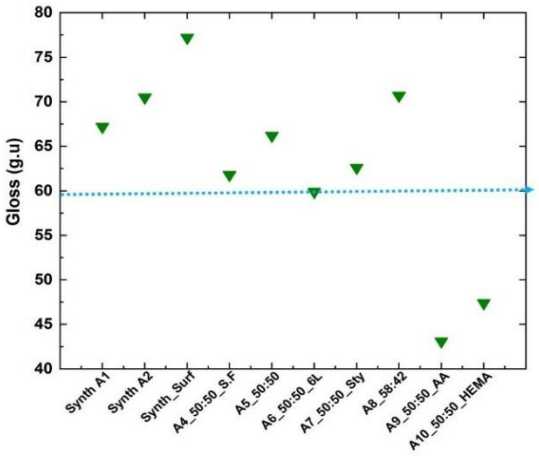

Figure 6.5. Gloss values of the paints measured at 60° angle.

6.3.3.5. CIE L*a*b* parameters

The colorimetric values (L* a*b*) of the paints were determined and are given in Table 6.14. As expected, the measured L*value is lower than 100%, which means the paint is slightly yellower than perfect white and shifted to a blue-yellow dimension.

Table 6.14. CIE L*a*b* parameters of paints.

Latex code	Colour points		
	L*	a*	b*
Synth A1	97.20	-0.98	1.08
Synth A2	97.19	-0.96	1.03
Synth_Surf	97.87	-0.93	1.07
A4_50:50_S.F	96.77	-1.04	0.66
A5_50:50	97.62	-0.94	1.05
A6_50:50_6L	97.72	-0.97	0.98
A7_50:50_Sty	97.47	-1.03	1.17
A8_58:42	97.37	-0.99	0.82
A9_50:50_AA	96.48	-1.09	0.81
A10_50:50_HEMA	96.73	-1.09	0.81

6.3.3.6. Color-rubout

The results of the rubout, in terms of color difference between the areas subject to spreading and the remaining film, are given in Table 6.15. All coatings except Synth_Surf showed a big color difference in the visual inspection test. These detected color differences are indicative of the destabilization of pigments used in the formulation (Figure 6.6).

Table 6.15. Rubout test of paints.

Latex code	Colour DB.BE	Colour DB.NO	Colour SF.NH
Synth A1	2	2	2
Synth A2	1-2	2	2
Synth_Surf	0-1	1-2	1
A4_50:50_S.F	2+	2+	2+
A5_50:50	2	1	1
A6_50:50_6L	2	1	2
A7_50:50_Sty	2	1-2	2
A8_58:42	2+	1-2	2
A9_50:50_AA	2+	2+	2+
A10_50:50_HEMA	2+	2+	2+

Evaluation (0-Good, 5-Poor)

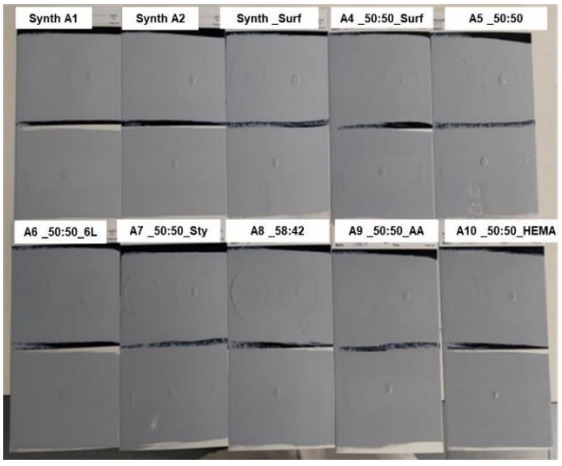

Figure 6.6. Colour difference in paints in rubout (colour SF.NH).

6.3.3.7. Snail trail

Snail trails refer to shiny vertical run-marks that become visible on dry paint films when water (rain) washes away the water-soluble paint components. The visual inspection results of the paint films are presented in Table 6.16. It was observed that all paints exhibited snail trails to some extent. However, in comparison to the reference paints, the DMAPS paints generally performed slightly better, with the exception of A4_50:50_S.F.

The migration of surfactants and water-soluble species exuded from the paint films is the primary cause of these trails. The presence of DMAPS in the paints seemed to mitigate this issue to some degree, resulting in improved performance compared to the reference paints in most cases, except for A4_50:50_S.F. Interestingly, for paints A4_50:50_S.F, A9_50:50_AA, and A10_50:50_HEMA, colored water was observed, which can be attributed to pigment incompatibility. This incompatibility was also evident in the rubout test, highlighting the potential challenges associated with pigment dispersion and stability in these particular paints.

Table 6.16. Snail trail of paints (drying time 4h at RT + 16h at 5 ºC).

Latex code	
Synth A1	2-3
Synth A2	3
Synth_Surf	3
A4_50:50_S.F*	4
A5_ 50:50	1-2
A6_50:50_6L	2
A7_50:50_Sty	2-3
A8_58:42	1-2
A9_50:50_AA*	1-2
A10_50:50_HEMA*	2

Evaluation (0-Good, 5-Poor) * Water with color

6.3.3.8. Stain resistance

The stain resistance of the paints was assessed using various household and writing products. Visual inspections of all the films were conducted, and the outcomes are presented in Figure 6.7. Overall, the paints performed similarly in all scenarios, but A7_50:50_Sty demonstrated the best stain resistance. This superior performance could be attributed to its hydrophobic surface and higher incorporation of DMAPS units, resulting in a lower fraction of water-soluble oligomers. As a result, there was no migration of soluble species to the surface after cleaning, facilitating easy stain removal. Moreover, it was observed that all paints exhibited improved stain resistance after washing with cleaning products, as indicated in Table 6.17. However, in some instances involving DMAPS paints, blistering was noticed, which might need further investigation and optimization. For the writing products, the stain removal was measured, and the results are summarized in Table 6.17. The water-based yellow highlighter was successfully removed from all paint films. In contrast, the stain of the permanent black marker could not be removed by any of the coatings. The stain removal of the ballpoint pen and blue water-based marker fell in between, displaying varying degrees of effectiveness.

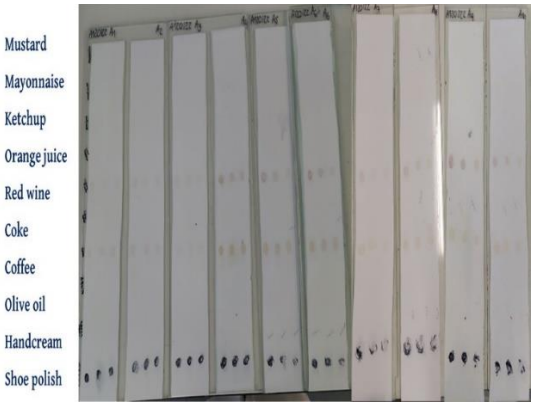

Figure 6.7. Stain resistance of paints (stain subjected to wiping with paper (left), washing with water (middle) and with cleaning product (right).

Table 6.17. Stain resistance of paints to home products after cleaning with water ,soap, writing products 400 cycles of scrub resistance.

Latex code	Synth A1	Synth A2	Synth _Surf	A4_ 50:50 _S.F	A5_ 50:50	A6_ 50:50 _6L	A7_ 50:50 _Sty	A8_ 58:42	A9_ 50:50 _AA	A10_ 50:50_ HEMA
Mayonnaise	0	0	0	0	0	0	0	0*	0-1	0-1
Mustard	0	0	0	0-1	0	0	0	0	0-1	0-1
Ketchup	0	0	0	0	0	0	0	0	0-1	0-1
Orange juice	0	0	0	0	0	0	0	0*	0	0
Coffee	5	5	5	5	5	5	4-5	5*	5	5
Red wine	3-4	4	3	5	4	4	2-3	4	4-5	4
Coke	0	0	0	1	0-1*	0-1*	0	0*	1*	0-1*
Olive oil	0	0	0	0-1	0	0	0	0	0	0
Hand cream	0	0	0	1	1*	1*	1	2*	1*	1*
Shoe polish	4-5	4-5	4-5	5	4	4	4	4	4-5	4-5
highlighter	0	0	0	0	0	0	0	0	0	0
Black marker	2	2	2	2	2	2	2	2	2	2
Water marker	1	0-1	0	1-2	1	1-2	1-2	2	1	1-2
Ballpoint pen	1	0-1	1	1	1	1	1	1-2	0-1	1-2

(For home products, Evaluation 0-Good removal of stain, 5-Poor stain removal * blistering in the surface)

6.3.3.9. Cyclic water absorption and weight loss

The water absorption of the paint films was meticulously measured, and the results are illustrated in Figure 6.8. Interestingly, all the films exhibited similar water absorption after one week of immersion. The presence of surfactants in the reference paints could have created hydrophilic pockets within the film, while the significant quantity of water-soluble oligomers distributed within the DMAPS paint films might have contributed to their water sensitivity.

Notably, for A4_50:50_S.F, an immediate increase in water absorption was observed after 24 hours of immersion. This rapid increase could be attributed to the formation of water-soluble species, and the potential incompatibility of the binder with the other paint components might have also played a role. Typically, one would expect an exponential increase in water absorption with time. However, in this case, fluctuations in the rate of water absorption were observed, likely due to the leakage of water-soluble paint components from the films.

The weight loss of the films during water immersion was also measured (Figure 6.9). This weight loss is indicative of the diffusion of water-soluble species from the film into the water. As expected, the film that absorbed the most water exhibited the highest weight loss. Over time, the weight loss decreased with each cycle of immersion. After the final cycle of 7 days of immersion, the reference paints showed the highest weight loss compared to the DMAPS paints. This is because all surfactants gradually diffused toward the water phase in the reference paints. However, in the case of DMAPS, the surfactant from the seed and the water-soluble species were almost entirely removed during the first day of immersion, and the remaining DMAPS units were stabilized as they were chemically incorporated into the polymer particles.

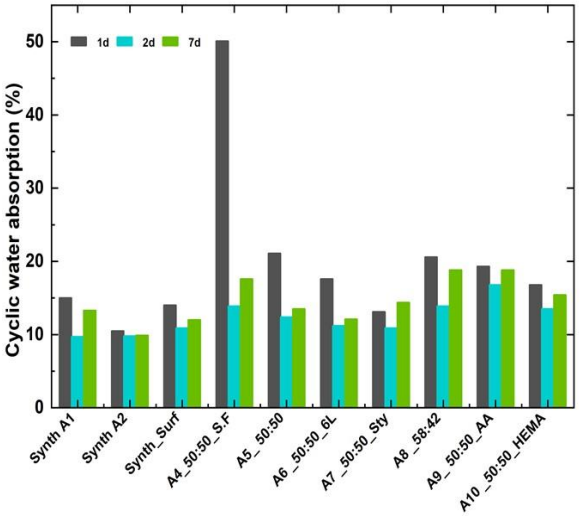

Figure 6.8. Cyclic water absorption of the paints.

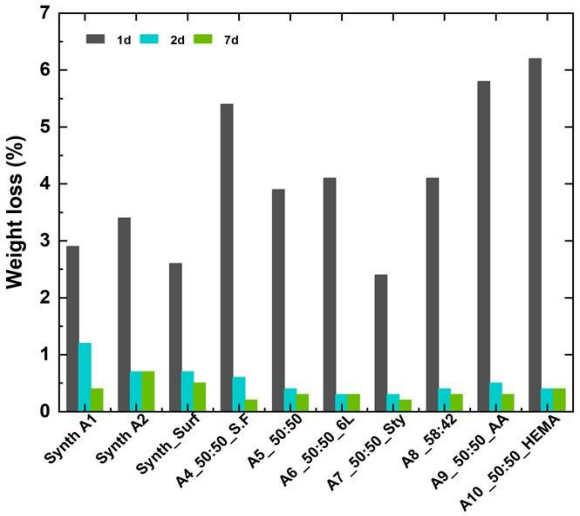

Figure 6.9. Weight loss of the paints.

6.3.3.10. Water vapor permeability

The water vapor permeability of coatings was measured, and the results are given in Table 6.18. All paints showed a medium transmission rate after two weeks. Among them, A7_50:50_Sty, containing styrene monomer, exhibited the least permeability to water vapor. The presence of SDS from the seed in all DMAPS paints might induce ionic imbalance with the zwitterions from DMAPS, potentially leading to moisture conductive paths. As a result, moderate water vapor transmission was observed in all DMAPS-containing paints.

Table 6.18. Water vapour transmission rate of paints (g/ (m^2.d).

Latex code	7days	14 days
Synth A1	99.45	112.97
Synth A2	99.17	93.91
Synth_Surf	92.20	89.49
A4_50:50_S.F	119.80	114.47
A5_50:50	90.63	88.64
A6_50:50_6L	97.04	92.13
A7_50:50_Sty	68.29	65.16
A8_58:42	115.68	109.77
A9_50:50_AA	107.71	103.51
A10_50:50_HEMA	112.55	108.35

6.3.3.11. QUV ageing/accelerated weather test

After subjecting the paints to accelerated weathering using QUV ageing, a thorough inspection was conducted after 28 days. Table 6.19 provides a summary of the Lab parameters (Δb and ΔE) along with the gloss measurements taken after 4 weeks of exposure to UV light. A comparison with the gloss measured before exposure (Table 6.13) reveals a significant reduction in gloss for the reference paints (Synth A1, A2) and some of the DMAPS paints (A4_50:50_S.F and A7_50:50_Sty).

Regarding the color changes determined by the Lab parameters, no significant alterations were observed for the reference paints and most DMAPS paints, with the exception of the paint containing

styrene. The variation in color for the styrene-containing paint is likely a result of its higher UV absorption compared to the other materials. However, it is important to note that all the DMAPS paints exhibited the formation of craters due to paint degradation. This degradation process occurred during the accelerated weathering test and resulted in the formation of these surface defects.

Table 6.19. Gloss and Lab parameters of coatings after 4 weeks of exposure to accelerated weathering conditions.

Latex code	Gloss 60°	Δb (a.u.)	ΔE (a.u.)
Synth A1	19.7	-0.34	0.98
Synth A2	26	0.00	1
Synth_Surf	66.6	-0.31	0.41
A4_50:50_S.F	17.2	-0.33	0.55
A5_50:50	60.3	-0.44	0.48
A6_50:50_6L	64.8	-0.42	0.49
A7_50:50_Sty	18.5	1.22	1.2
A8_58:42	64.5	-0.32	0.42
A9_50:50_AA	36.5	-0.32	0.54
A10_50:50_HEMA	33.3	-0.40	0.46

6.4. Conclusions

In conclusion, this study compared latexes with different polymer compositions stabilized with a small amount of zwitterionic monomer DMAPS to reference binders provided by Synthomer, stabilized with conventional surfactants or surfmer. The latexes were synthesized using seeded semi-continuous emulsion polymerization, and the resulting paints were evaluated for various performance properties in enamel paint formulations.

Viscosity is a crucial factor in determining paint application properties. While a thickener was used to adjust viscosity, the DMAPS-containing paint formulations did not achieve the required viscosity, indicating potential incompatibility with the thickening agent used. Overall, all paints showed satisfactory storage stability for one month, with some phase separation that could be easily rectified by agitation before use. DMAPS paints demonstrated good gloss properties comparable to reference

paints, except for those containing functional monomers HEMA and AA, which showed reduced gloss due to increased surface roughness. The films exhibited good whitening index and contrast ratio for all paints, but rubout performance was poor except for the surfmer-stabilized paint.

The presence of DMAPS positively affected the hardness and blocking resistance of the films, likely due to the creation of an ionic network within the film and possible ionic interactions within it. DMAPS paints displayed excellent stability towards UV exposure, except for the styrene-containing paint, which was more sensitive to UV irradiation due to the presence of aromatic rings in its structure.

In terms of stain resistance, DMAPS paints performed well, especially the styrene-containing paint, which exhibited the best stain removal. However, stain removal for writing products was comparable across all paints. Water absorption and permeability of the films were similar for DMAPS and reference paints, indicating that the presence of water-soluble oligomers affected water resistance similarly to conventional surfactants. The accelerated weathering test showed that most paints performed similarly, with the exception of the styrene-containing paint, which showed increased sensitivity to UV irradiation due to its aromatic structure. In summary, DMAPS-stabilized paints demonstrated comparable properties to conventional paints and even outperformed them slightly in snail trail performance. The influence of DMAPS incorporation on paint properties was evident, with the composition of major monomers significantly affecting paint performance.

For future studies, it would be interesting to explore latexes with higher DMAPS (or other zwitterionic monomers) incorporation and compare their performance against standard paints. These findings contribute to the understanding of zwitterionic monomers' potential as stabilizers in paint formulations and their impact on paint properties.

6.5. References

1. *Reactive surfactants in heterophase polymerization.* **Asua, J. M. and Schoonbrood, H. A. S.** s.l. : Wiley Online Library, 1998, Acta Polymerica, Vol. 49, pp. 671–686.

2. *Redox initiator systems for emulsion polymerization of acrylates.* **Kohut-Svelko, Nicolas, et al.** s.l. : Wiley Online Library, 2009, Journal of Polymer Science Part A: Polymer Chemistry, Vol. 47, pp. 2917–2927.

3. *Fundamentals of chemical incorporation of ionic monomers onto polymer colloids: paving the way for surfactant-free waterborne dispersions.* **Bilgin, Sevilay, Tomovska, Radmila and Asua, José M.** s.l. : Royal Society of Chemistry, 2016, RSC advances, Vol. 6, pp. 63754–63760.

4. *Control of particle size distribution for the synthesis of small particle size high solids content latexes.* **de FA Mariz, Inês, de la Cal, José C. and Leiza, Jose R.** s.l. : Elsevier, 2010, Polymer, Vol. 51, pp. 4044–4052.

5. *Hydrogen-bond driven formation of microstructured pressure sensitive adhesives (PSAs) with enhanced shear resistance.* **Jimenez, N., Ballard, N. and Asua, J. M.** s.l. : Elsevier, 2021, Polymer, Vol. 233, p. 124210.

6. *Hydrogen bond-directed formation of stiff polymer films using naturally occurring polyphenols.* **Jiménez, Nerea, Ballard, Nicholas and Asua, José M.** s.l. : ACS Publications, 2019, Macromolecules, Vol. 52, pp. 9724–9734.

7. *Fundamental Insights into Free-Radical Polymerization in the Presence of Catechols and Catechol-Functionalized Monomers.* **Jimenez, Nerea, et al.** s.l. : ACS Publications, 2021, Macromolecules, Vol. 55, pp. 49–64.

8. *Studies on the photooxidation mechanism of polymers. I. Photolysis and photooxidation of polystyrene.* **Rabek, Jan F. and Rånby, Bengt.** s.l. : Wiley Online Library, 1974, Journal of Polymer Science: Polymer Chemistry Edition, Vol. 12, pp. 273–294.

9. *Effects of hydroxyethyl methacrylate comonomer in styrene/acrylate latex on coating structure and printability.* **Kwon, Soojin, et al.** s.l. : Elsevier, 2020, Progress in Organic Coatings, Vol. 147, p. 105862.

10. ISO 7724-1:1984 *Paints and Varnishes-Colorimetry-Part 1:Principles.*

11. ISO 7724-2:1984 *Paints and Varnishes-Colorimetry-Part 2:Colour measurement.*

12. ISO 7724-3:1984 *Paints and Varnishes-Colorimetry-Part 3: Calculation of colour differences.*

13. ISO 2813:201 *Paints and Varnishes-Determination of gloss value at 20°,60° and 85°.*

14. ISO 6504:3:2019 *Paints and varnishes- Determination of hiding power-Part3: Determination of hiding power of paints for masonry, concrete and interior use.*

15. ASTM D 7190 -2010 -R2015: *Standard Practice to Evaluate Leaching of Water-Soluble Materials from Latex Paint Films.*

16. ISO 1522:2006 *Paints and varnishes -Pendulum damping test.*

17. ASTMD1849 -95-1987: S*tandard Test Method for Package Stability of Paint.*

18. ISO 4622:1992 P*aints and varnishes. Pressure test for stackability.*

19. ISO 62:2008 *Plastics-Determination of water absorption.*

20. ISO 783:2018 *Paints and Varnishes –Determination of water –vapour transmission properties-Cup method.*

21. ISO 16474-1:2013 *Paints and varnishes-Methods of exposure to laboratory light sources-Part 1: General guidance.*

Chapter 7. Conclusions

The objective of this PhD thesis is to synthesize surfactant-free latexes that are colloidally stable, high in solids content, and capable of forming films. The key feature here is that the colloidal stability is achieved solely through the chemical incorporation of zwitterionic ionic moieties onto the polymer particles.

To achieve this aim, the study utilized major monomers, specifically MMA/n-BA (50/50 by weight), in the coating formulation. Furthermore, a range of zwitterionic monomers enriched with anionic sulfonate groups was carefully selected. These choices were guided by their well-documented stability across various pH levels, offering a suitable replacement for conventional surfactants. The technique employed for polymer latex synthesis involved seeded semi-continuous emulsion polymerization. Executing this concept was not a straight forward due to the unique properties of the monomers involved. MMA and n-BA, which have limited solubility in water, are mainly situated within the polymer particles and monomer droplets. On the other hand, ZMs are highly water-soluble and primarily reside in water phase. To ensure the stability of the polymer dispersions throughout the synthesis and storage processes, while also preventing any detrimental effects stemming from the movement of hydrophilic oligomers, it became necessary to chemically incorporate ZMs onto the polymer particles and thereby minimize the fraction of ZMs remaining in the aqueous phase as water-soluble polymer.

Owing to the distinctive attributes inherent in zwitterionic monomers, there is an anticipated improvement in the overall qualities of the polymer latex. Furthermore, the presence of both positive

and negative charges in zwitterionic polymers is predicted to facilitate the occurrence of ionic complexation during the film formation process. This, in turn, is expected to bolster the overall properties of the films, effectively mitigating the undesirable impacts often associated with the use of surfactants.

The use of zwitterionic monomers in emulsion polymerization is not commonly encountered. Chapter 1 of the thesis offers a comprehensive overview of the synthesis of polymer latex using surfactant-free emulsion polymerization, employing initiators, reactive surfactants and functional monomers. This literature review demonstrates improvements in the qualities of waterborne dispersions. However, it is important to note that the inclusion of hydrophilic elements also amplifies the materials' susceptibility to water, which presents a key challenge. In this context, the distinctive attributes of zwitterionic monomers hold promise as potential solutions to overcome this challenge.

In Chapter 2, a range of zwitterionic monomer options with distinct anionic groups was examined, and experimental reactions were carried out to identify the most fitting zwitterionic monomer. Owing to the presence of an anionic sulfonate group that is stable in all pH window, ZM DMAPS emerged as the chosen candidate for further studies. The polymer latexes were synthesized using seeded semi-continuous emulsion polymerization, where the seed was stabilized using conventional surfactant SDS. To examine the impact of initiator type on the incorporation of DMAPS onto the polymer particles, five different initiators were employed. Specifically, KPS, a water-soluble thermal initiator, generates hydrophilic and negatively charged radicals in the aqueous phase. AIBN, an oil-soluble thermal initiator, primarily forms hydrophobic radicals in the organic phase. Additionally, three redox pair initiators were employed: HPO/As.Ac, a water-soluble system yielding neutral and hydrophilic hydroxyl radicals; and TBHP/As.Ac and TBHP/FF7, both generating neutral and hydrophobic radicals in the aqueous phase.

The level of hydrophobicity displayed by oligoradicals plays a crucial role in how DMAPS is incorporated into MMA/n-BA polymer particles. When hydrophilic radicals are involved, the incorporation of ZM

DMAPS units within the polymer chains is reduced, resulting in the formation of water-soluble oligomers. In contrast, hydrophobic tert-butoxy radicals, display the highest degree of incorporation, especially when combined with FF7. This effect can be attributed to the slower rate of radical consumption associated with this particular pairing. Initiator choice significantly influenced latex properties and resulting films. TBHP/FF7- latexes, with high DMAPS incorporation, showed improved salt stability, while KPS-initiated ones exhibited resilience against freeze-thaw cycles due to additional sulfate groups arising from KPS and seed. Surprisingly, TBHP/FF7-initiated films absorbed more water than KPS-initiated ones, possibly due to interference from extra charges from seed on film performance. TBHP/FF7-initiated films with highest DMAPS showed superior mechanical behavior, potentially due to ionic interactions reinforcing polymer chains. However, annealing reduced mechanical properties, indicating network dissolution. Considering optimal DMAPS incorporation, absence of extra charges, and favorable latex characteristics, TBHP/FF7 proved the most promising initiator for seeded semi-continuous emulsion copolymerization of MMA/n-BA stabilized with DMAPS.

In Chapter 3, effect of ZM DMAPS concentration was studied by synthesizing high solids content colloidal polymer dispersions consisting of MMA/n-BA polymers stabilized with a small amounts of the zwitterionic monomer DMAPS (0.5–5%) and for comparison SDS stabilized reference latex was synthesized too. The seed used for the reactions were stabilized with SDS. From these studies, DMAPS concentrations significantly influenced colloidal stability. Low DMAPS concentration led to inadequate stabilizing units and increased coagulation. High DMAPS concentration resulted in large coagulum due to excessive water-soluble oligomers. Optimal DMAPS concentration (1–3%) achieved colloidal stability, low coagulum, and particle size around 270 nm. Incorporating DMAPS onto particles was critical for stability, with higher DMAPS concentrations enhancing incorporation. High DMAPS-incorporation showed remarkable salt stability due to the anti-polyelectrolyte effect.

Water contact angle measurements conducted on DMAPS-containing polymer films indicated that DMAPS chains remained stable at the film-air interface. These films exhibited heightened mechanical reinforcement and reduced water absorption. These positive outcomes are attributed to the formation of a strong and rigid ionically complex network, as substantiated by AFM investigations. However, during annealing, the network dissolved, leading to a decrease in film properties. Additionally, DMAPS films displayed superior barrier performance due to the presence of this sturdy ionic network. Notably, at elevated temperatures, this property was further enhanced by increased mobility of polymer chains within the film. This mobility resulted in improved ionic complexation with zwitterions, further enhancing the film's performance. Furthermore, the removal of water-soluble components yielded favorable enhancements in the polymer film properties.

The DMAPS-containing films displayed decreased hydrophilicity, rougher textures, and notably reduced fouling tendencies compared to reference film. Particularly intriguing was the behavior of the film containing 5% DMAPS, which exhibited minimal fouling despite having a lower water content. This exceptional outcome was attributed to a combination of electrostatic interactions and the textured surface, intensifying the strong bonding of the limited water present. The impressive attributes showcased by the zwitterionic monomer DMAPS in MMA/n-BA polymer coating films introduce fresh possibilities and alternatives for colloidal stabilization beyond conventional surfactants.

In Chapter 4, high solids content, entirely surfactant-free polymer dispersion were created by employing various ZMs featuring sulfonate groups. Various approaches were employed to produce surfactant-free seeds. This was achieved by introducing a more hydrophobic monomer, BMA, which led to a reduction of water-soluble species and consequently, this approach resulted in the successful synthesis of well-defined seeds with a satisfactory particle size devoid of any charges.

This study focused on understanding how the structural differences of these ZMs influenced their incorporation into latex particles, a decisive factor affecting both colloidal stability and overall polymer

performance. This time, four sulfobetaine ZMs were investigated: DMAPS and M3295 with methacrylic functionality, A3367 with acrylic functionality, and A3361 with acrylamide functionality. The study's findings highlighted the considerable impact of ZMs' relative hydrophilicity and their reactivity ratios with MMA on their incorporation rate into polymer particles. ZM M3295, with an extra methylene group, showed higher incorporation (61%) than DMAPS (42%), indicating a slight hydrophilicity reduction. Remarkably, ZM A3361, featuring acrylamide functionality, exhibited the highest incorporation rate (74%). Nevertheless, at higher solids content, incorporation decreased due to excessive water-soluble species. Conversely, ZM A3367, an acrylic-functional ZM, had the lowest incorporation rate (28%) due to unfavorable reactivity ratios with MMA and n-BA, leading to increased coagulation. The substantial incorporation of ZMs, especially A3361, resulted in improved salt and freeze-thaw stability of the polymer particles.

Furthermore, this chapter delved into the anti-polyelectrolyte properties of ZMs. The presence of salt within the dispersion resulted in an increase in particle size, as determined by DLS measurements. This size expansion was linked to chain elongation due to the anti-polyelectrolyte effect. Interestingly, TEM examinations showcased similar particle sizes for both scenarios. However, TEM studies unveiled a remarkable change: the previously distinct boundary between the core and shell of the particles became blurred, nearly erasing the particle's original identity. This transformation can be attributed to the elongation of DMAPS polymer chains on the particle surface. Despite being in a collapsed state, some chains managed to extend further away from the core, leading to a distinctive corrugated appearance of the shell.

The films produced from these ZM-containing latexes demonstrated substantial mechanical reinforcement through water evaporation, surpassing conventionally stabilized films. This strengthening was attributed to the creation of a rigid network composed of polymer chains rich in ZM units and this distinctive network structure, characterized by multiple ionic bonds, contributed to

diminished water absorption and significantly heightened humidity barrier performance of the ZM films. Additionally, the presence of extra counter ions in A3361 system extended this network, enabling increased ionic interactions among zwitterionic units, thereby further enhancing the properties. Moreover using A3361 ZM high solids content polymer latex (50%) was produced too.

Chapter 5 of this thesis delved into a genuine and earnest effort to synthesize thermo-responsive waterborne adhesives, utilizing only ZMs as the stabilizing agent. The driving force behind this undertaking was the idea that by dissolving the rigid ionic network surrounding particles at higher temperatures, it could lead to the development of effective thermo-responsive Pressure-Sensitive Adhesives (PSAs). The initial part of the chapter focused on the successful synthesis of PSAs using petroleum-based monomers n-BA/MMA. This particular endeavor proved to be fruitful, with the ZM A3361-based PSA exhibiting considerably improved properties in comparison to the reference PSA. The utilization of AFM further validated that the aggregation of ZM units at elevated temperature was pivotal in bestowing the PSA with its thermo-responsive characteristics.

Taking a step forward, bio based monomers 2-OA and IBOMA were introduced into the process. The aim was to create a fully surfactant- free bio based PSA. However, the high hydrophobicity of P-IBOMA posed a challenge, impeding the synthesis of a completely bio based latex. Nevertheless, by incorporating more hydrophilic MMA, the incorporation of additional ZM units for dispersion stabilization was facilitated. Two different ZMs, namely DMAPS and A3361, were employed, resulting in the development of high solids content PSAs. Unfortunately, coagulum was present, negatively affecting the PSA properties. The thermo-responsive effect was evident in all three PSAs, including the reference. For the ZM-based PSA, AFM images indicated the aggregation of ZM units, which contributed to the phase separation. In contrast, for the reference, it appeared to be linked to the migration of the Dowfax 2A1 surfactant. This chapter introduces the potential applications of ZMs while emphasizing the significance of fine-tuning formulations and conducting further research to enhance these possibilities.

In Chapter 6, comparative analysis of latexes with varying polymer compositions, all stabilized with a small proportion of the ZM DMAPS, were conducted and compared to reference binders from Synthomer that were stabilized using conventional surfactants or surfmer. The latex performance was evaluated across diverse attributes within enamel paint formulations.

DMAPS-containing paint formulations fell short of attaining the required viscosity. This discrepancy suggested lower incorporation of DMAPS units on polymer particles and or may be potential lack of compatibility with the employed thickening agent. Overall, the all paints exhibited satisfactory storage stability over a month, with occasional phase separation that could be easily resolved through agitation prior to use. DMAPS-containing paints displayed commendable gloss properties comparable to reference paints, barring those integrating functional monomers HEMA and AA. The latter exhibited diminished gloss due to heightened surface roughness. Film properties, including whitening index and contrast ratio, proved satisfactory across all paints, although rubout performance was notable primarily in the surfmer-stabilized paint. The incorporation of DMAPS exhibited a favorable influence on film hardness and blocking resistance, likely attributable to the establishment of an ionic network within the film and plausible ionic interactions within this network. Notably, DMAPS-based paints demonstrated robust stability under UV exposure, excluding the styrene-containing variant, which displayed sensitivity due to its aromatic structure. Regarding stain resistance, DMAPS paints excelled, especially the styrene-containing latex, which demonstrated optimal stain removal. However, stain removal from writing products was consistent across all paints. Water absorption and permeability characteristics in DMAPS and reference paints were akin, indicating that water-soluble oligomers impacted water resistance similarly to conventional surfactants. Accelerated weathering trials revealed comparable performance for most paints, except the styrene-containing version, which displayed heightened UV sensitivity owing to its aromatic composition. To sum up, DMAPS-stabilized paints demonstrated parallel properties to traditional paints and even exhibited slight superiority in snail trail

performance. The influence of DMAPS incorporation on paint attributes was evident, with the primary monomer composition significantly shaping paint performance. Future investigations could explore latexes with heightened DMAPS (or alternative zwitterionic monomers) content, offering a comparative analysis against standard paints. These findings deepen our comprehension of the potential of zwitterionic monomers as stabilizers in paint formulations and their implications for paint properties.

This research has highlighted that incorporating ZM into common coating formulations can eliminate the necessity for surfactants and their associated effects. The introduction of an ionically complex network has bestowed distinctive properties upon waterborne dispersions, thereby unlocking new application possibilities for these coatings.

7.1. Future perspectives

The culmination of this thesis opens the door to various future directions that can expand upon the achieved outcomes. The journey of utilizing ZMs to create surfactant-free polymer dispersions and the resulting ionically complex network holds promise for further advancements and applications.

Notably, the study did not delve into the mechanism of particle nucleation and reactivity ratios of ZMs, leaving room for future investigations in this area. Such inquiries could yield insights crucial for refining the synthesis of small particle size surfactant-free seeds and polymer latex.

In terms of application possibilities, the antifouling studies predominantly revolved around DMAPS. A promising avenue for future research involves exploring other ZMs with potentially heightened fouling resistance to comprehensively assess their efficacy.

By using different ZMs and refining formulations with bio-based monomers, exciting opportunities can emerge, leading to creative solutions that are in line with eco-friendly practices.

Conclusiones

El surfactante juega un papel muy importante en la polimerización en emulsión, principalmente en la nucleación de las partículas, así como en la estabilidad durante la polimerización y el almacenaje. Sin embargo, dado que el surfactante está adsorbido físicamente sobre las partículas de polímero se puede desorber y por consiguiente desestabilizar el sistema. Añadido a lo anterior, cuando estas dispersiones poliméricas (látex) se aplican como recubrimientos sobre diferentes sustratos, durante el proceso de secado el surfactante puede migrar tanto a la superficie superior (polímero/aire) como a la inferior (polímero/sustrato) reduciendo las propiedades de la película (brillo, sensibilidad al agua, adhesión...). Con el fin de superar los efectos adversos derivados del uso del surfactante se han empleado diferentes estrategias como el uso de surfactantes reactivos (surfmers) o la polimerización en emulsión libre de surfactante, donde la estabilidad viene dada única y exclusivamente por el iniciador o por el uso de monómeros funcionales. Recientemente se ha visto que mediante el empleo de sulfonato de estireno de sodio como monómero funcional se pueden obtener látex estables libres de surfactante con alto contenido en sólidos (>60%), sin embargo, debido a la hidrofilidad del monómero el polímero resulta más sensible al agua. En la misma línea, se ha visto que mediante la incorporación de monómeros funcionales aniónicos y catiónicos se puede obtener una buena resistencia al agua además de unas mejores propiedades mecánicas derivadas de las interacciones entre los grupos iónicos de cargas opuestas.

Los monómeros zwitteriónicos son monómeros que presentan el mismo número de cargas positivas (catiónicas) y negativas (aniónicas) en la misma molécula dando como resultado una molécula neutra. Los polímeros zwitteriónicos se caracterizan entre otras por su efecto antipolielectrolito y su resistencia

al ensuciamiento. Es por ello que el empleo de monómeros zwitteriónicos puede ser una buena alternativa a los surfactantes convencionales ya que se espera obtener la estabilidad coloidal y una mejora de las propiedades de la película (sensibilidad al agua, resistencia mecánica...) simultáneamente.

El objetivo de esta tesis doctoral es el de sintetizar dispersiones poliméricas acuosas (látex) libres de surfactante, coloidalmente estables, con alto contenido en sólidos y capaces de formar películas mediante la incorporación química de monómeros zwitteriónicos en las partículas de polímero.

Para lograr este objetivo, se utilizó una formulación de revestimiento típica MMA/n-BA (50/50 en peso) y una variedad de monómeros zwitteriónicos. Sin embargo, la implementación de esta idea no fue sencilla y presentaba una serie de retos. A causa de la baja solubilidad y carácter hidrofóbico de los monómeros principales empleados (MMA y n-BA) éstos principalmente se encuentran en la fase orgánica (gotas y/o partículas). Por el contrario, los monómeros zwitteriónicos son altamente solubles en agua y por consiguiente residen principalmente en la fase acuosa. Para asegurar la estabilidad de los látex durante el proceso de síntesis y almacenamiento, y evitar los efectos adversos de las especies hidrófilas migratorias en las propiedades de la película, es imprescindible que el monómero zwitteriónico esté químicamente unido a las partículas de polímero, y a su vez reducir la fracción que permanece en la fase acuosa. Estos látex fueron sintetizados mediante polimerización en emulsión semicontinua sembrada dado que es el método más empleado en la industria para obtener una calidad consistente del producto y un mejor control de la eliminación del calor y de la nucleación.

Con la finalidad de encontrar el monómero zwitteriónico más adecuado, se llevaron a cabo polimerizaciones en emulsión en discontinuo con diferentes monómeros zwitteriónicos. La principal diferencia entre los monómeros zwitteriónicos fue el grupo aniónico que presentaban (carboxilato, fosfato y sulfonato) (Capítulo 2). 2-(Methacryloyloxy) ethyl dimethyl-(3-sulfopropyl) ammonium hydroxide (DMAPS) con el grupo sulfonato resultó ser el mejor candidato debido principalmente a su insensibilidad al pH. Tras seleccionar el monómero zwitteriónico se estudió el efecto del iniciador en la

incorporación de DMAPS en las partículas de polímero mediante el empleo de cinco iniciadores: persulfato de potasio (KPS), iniciador soluble en agua que genera radicales hidrofílicos y negativamente cargados en la fase acuosa y azobisisobutironitrililo (AIBN), iniciador soluble en fase orgánica que forma principalmente radicales hidrofóbicos en la fase orgánica, como iniciadores térmicos. Además, se utilizaron tres pares de iniciadores redox: peróxido de hidrógeno/ ácido ascórbico (HPO/As.Ac), un sistema soluble en agua que produce radicales neutros e hidrofílicos; hidroperóxido de terc-butilo/ ácido ascórbico (TBHP/As.Ac) e hidroperóxido de terc-butilo/Bruggolite FF7 (TBHP/FF7), ambos generando radicales neutros e hidrofóbicos en la fase acuosa. El nivel de hidrofobicidad exhibido por los radicales desempeñó un papel crucial en la incorporación de DMAPS en las partículas de polímero MMA/n-BA. En presencia de radicales hidrofílicos, la incorporación de unidades DMAPS dentro de las cadenas de polímero se vio reducida, dando lugar a la formación de oligómeros solubles en agua y por consiguiente en una menor incorporación. Por el contrario, los radicales terc-butoxi que son lo suficientemente hidrófobos como para entrar directamente en las partículas de polímero, presentaron el grado más alto de incorporación de DMAPS, especialmente cuando se combinó con FF7. Este efecto se puede atribuir al consumo de radicales más lento asociado con este par redox en particular. Obviamente, la elección del iniciador influyó significativamente tanto en las propiedades del látex como en la de las películas resultantes. Los látex sintetizados empleando el iniciador TBHP/FF7, con la máxima incorporación de DMAPS, mostraron una mejor estabilidad en medio salino, mientras que los látex sintetizados con el iniciador KPS exhibieron mayor resistencia a los ciclos de congelación y descongelación debido posiblemente a la presencia de los grupos sulfatos provenientes tanto del iniciador KPS como del surfactante convencional, SDS, empleado en la síntesis de la siembra.

En el Capítulo 3, se estudió el efecto de la concentración del monómero zwitteriónico DMAPS en la incorporación de las partículas de polímero. Para ello se sintetizaron diferentes látex de MMA/n-BA (50% C.S.) en los cuales se varió la concentración de DMAPS (0.5-5%). Al mismo tiempo y para fines

comparativos, se sintetizó un látex de referencia estabilizado con SDS. A partir de este estudio, se encontró que la concentración de DMAPS afectaba significativamente la estabilidad coloidal. Por un lado, una baja concentración de DMAPS dio lugar a un número de unidades estabilizantes insuficiente que resultó en una cantidad de coágulo importante. De igual manera, la alta concentración de DMAPS también resultó en una gran cantidad de coágulo, sin embargo, en este caso probablemente debido a la presencia de un gran número de oligómeros solubles en agua. Por el contrario, mediante el empleo de concentraciones de DMAPS intermedias (1-3%) se logró sintetizar látex con alto contenido en sólidos y libres de coágulo. Desde luego, la incorporación de DMAPS en las partículas de polímero fue fundamental para obtener la estabilidad coloidal, y se observó que cuanto mayor era la concentración de DMAPS, mayor era su incorporación en las partículas de polímero dando lugar a látex de menor tamaño de partícula. La alta incorporación de DMAPS mostró una notable estabilidad en medio salino debido seguramente al efecto antipolielectrolito muy característico entre los monómeros zwitteriónicos.

Las medidas del ángulo de contacto realizadas con agua sobre las películas poliméricas que contenían DMAPS indicaron que no había migración de las especies hidrofílicas a la superficie de la película, a su vez, estas películas resultaron ser menos hidrofílicas que la película de referencia. Añadido, estas películas mostraron un refuerzo mecánico superior y una menor sensibilidad al agua (menor cantidad de agua absorbida). Estas mejoras se atribuyen a la formación de una red iónica fuerte y rígida entre los grupos zwitterionónicos que se encuentran principalmente en la superficie de las partículas, tal y como se pudo observar mediante AFM. Las imágenes del AFM obtenidas de la sección transversal de las películas mostraron que en las películas obtenidas a partir de los látex sintetizados con DMAPS las partículas formaban una estructura tipo colmena donde los límites entre las partículas estaban llenos de polímero rico en DMAPS. Sin embargo, tras el recocido a 80 °C las propiedades mecánicas cayeron como resultado de la destrucción de la red iónica. Estas películas también presentaron una menor permeabilidad al vapor de agua, una vez más, posiblemente debido a la presencia de esta red iónica. Por

otro lado, tras someter a los látex a un proceso de diálisis, se observó que las películas preparadas a partir de estos látex dializados presentaban todavía mejores propiedades, indicando claramente el efecto adverso de la presencia de las especies solubles en agua. Por si esto fuera poco, las películas que contenían DMAPS resultaron ser más hidrófobas, rugosas y con mayor resistencia al ensuciamiento que la película de referencia. Cabe destacar el comportamiento de la película con un contenido de 5% de DMAPS, que mostró un ensuciamiento mínimo a pesar de tener un menor contenido de agua asociada.

En el Capítulo 4, se intentó ir un paso más allá sintetizando látex de MMA/n-BA completamente libres de surfactante con un alto contenido en sólidos mediante el empleo de varios monómeros zwitteriónicos. Con el fin de sintetizar siembras completamente libres de surfactante se emplearon diferentes estrategias y finalmente el empleo de BMA como monómero principal y la adición de FF7 y TBHP por separado a lo largo de la reacción resultó ser la mejor estrategia. La introducción de un monómero más hidrófobo, BMA, llevó a una reducción del número de especies solubles en agua y, en consecuencia, resultó en una siembra totalmente libre de surfactante, únicamente estabilizada por el monómero zwitteriónico correspondiente con un tamaño de partícula razonable para posteriormente ser utilizada en la síntesis del látex de alto contenido en sólidos y completamente libre de surfactante.

La idea de utilizar diferentes monómeros zwitteriónicos no fue otra que la de tratar de comprender cómo las diferencias estructurales de estos monómeros zwitteriónicos, presentando el mismo grupo aniónico podían influir en su incorporación en las partículas de polímero, un factor decisivo que afecta tanto a la estabilidad coloidal como al rendimiento general del polímero. En esta ocasión, se investigaron cuatro monómeros zwitteriónicos los cuales tenían en común el mismo grupo aniónico, un sulfonato: DMAPS y M3295 con funcionalidad metacrílica, A3367 con funcionalidad acrílica y A3361 con funcionalidad acrilamida. Los hallazgos del estudio destacaron el impacto de la hidrofilicidad relativa de los monómeros zwitteriónicos y sus relaciones de reactividad con MMA en su incorporación en las partículas de polímero. El monómero zwitteriónico M3295, con un grupo metileno adicional con

respecto al DMAPS, mostró una mayor incorporación (61%) que DMAPS (42%), probablemente porque M3295 es ligeramente menos hidrófilo. Sorprendentemente, el ZM A3361, con funcionalidad acrilamida, exhibió la máxima incorporación (74%). Sin embargo, cuando la misma reacción fue repetida en contenido de sólidos más altos (50%), su incorporación disminuyó posiblemente a causa un mayor número de especies solubles en agua. Por el contrario, el A3367, el monómero zwitteriónico con funcionalidad acrílica, tuvo la tasa de incorporación más baja (28%) probablemente debido a sus relaciones de reactividad desfavorables con MMA y n-BA y por consiguiente el látex presentó una cantidad de coágulo considerable. El aumento de la incorporación del monómero zwitteriónico, especialmente el de A3361, resultó en una mejora de la estabilidad frente a la sal y a los procesos de congelación y descongelación del látex.

Las películas creadas a partir de estos látex que contenían diferentes monómeros zwtteriónicos presentaron un refuerzo mecánico sustancial superando a las películas obtenidas a partir de los látex estabilizados con surfactante convencional, SDS. Este fortalecimiento se atribuyó, una vez más, a la creación de una red rígida compuesta por cadenas de polímero ricas en unidades de monómero zwitteriónico caracterizada por múltiples enlaces iónicos, que a su vez resultó en películas menos sensibles al agua (menor absorción de agua) y a una mejora de las propiedades de barrera frente a la humedad reduciendo su permeabilidad.

Por otro lado, este capítulo exploró el efecto antipolieléctrolito para el caso del monómero zwitteriónico DMAPS. Para ello, se sintetizaron dos látex estabilizados con DMAPS en presencia y ausencia de NaCl y posteriormente se analizó el tamaño de partícula. El TEM mostró tamaños de partícula muy similares mientras que el tamaño de partícula determinado mediante DLS fue considerablemente mayor para las partículas sintetizadas en presencia de NaCl como resultado de la extensión de las cadenas enriquecidas en DMAPS localizadas principalmente en la superficie de las partículas. A su vez, las imágenes del TEM revelaron que las partículas sintetizadas en presencia de sal presentaban una mayor rugosidad.

El Capítulo 5 de esta tesis exploró la posibilidad de sintetizar adhesivos sensibles a la presión (del inglés pressure sensitive adhesive, PSA) termo sensibles en fase acuosa empleando monómeros zwitteriónicos como agente estabilizante. La fuerza impulsora detrás de esta idea fue lo observado para los recubrimientos en los capítulos anteriores en los que, tras el proceso de recocido, las propiedades mecánicas caían debido a la destrucción de la red iónica. Esta idea podría conducir al desarrollo de PSAs termo sensibles para su empleo en etiquetas removibles. La parte inicial del capítulo se centró en la síntesis de PSAs utilizando monómeros derivados del petróleo n-BA/MMA. El PSA sintetizado en presencia del mómero zwitteriónico A3361 exhibió un comportamiento termo sensible y las propiedades adhesivas fueron considerablemente mejores que las del PSA de referencia. Sin embargo, con la intención de avanzar un poco más, se sustituyeron los monómeros derivados del petróleo por monómeros de origen biológico concretamente, 2-OA e IBOMA, con el objetivo de sintetizar PSAs empleando en su totalidad monómeros de origen biológico y completamente libres de surfactante. Sin embargo, no fue posible la síntesis de un PSA completamente libre de surfactante y de origen biológico debido a la alta hidrofobicidad de IBOMA. La incorporación de un monómero más hidrófilo (MMA, a pesar de no tener origen biológico) promovió la incorporación de unidades de monómero zwitteriónicos dando lugar a un látex estable. Siguiendo esta estrategia se sintetizaron 3 PSAs, dos de ellos en los cuales se emplearon diferentes monómeros zwitteriónicos; DMAPS y A3361 y un tercero en el que se empleó un surfactante convencional para de ser utilizado como referencia. Desafortunadamente, los adhesivos sintetizados empleando monómeros zwitteriónicos presentaron un poco de coágulo (siendo mayor para el caso de DMAPS) lo que afectaron negativamente a las propiedades del PSA. El efecto termosensible fue evidente en los tres PSAs, incluido el de referencia. Para los PSAs basados en el monómero zwitteriónico, las imágenes de AFM indicaron la agregación de unidades de monómero zwitteriónico, lo que contribuyó a la disolución de la red. En contraste, en el caso del PSA de referencia, parecía estar vinculado a la migración del surfactante Dowfax 2A1.

En el capítulo 6, se evaluó el rendimiento de los látex de MMA/n-BA estabilizados con DMAPS libres de surfactante como aglutinantes en formulaciones de pintura de esmalte, y se comparó con aglutinantes de referencia (proporcionados por Synthomer) que fueron estabilizados mediante surfactantes convencionales o surfmers. Las formulaciones de pintura que contenían DMAPS no lograron alcanzar la viscosidad requerida. Esta discrepancia sugirió una menor incorporación de unidades de DMAPS en las partículas de polímero y/o la falta de compatibilidad con el agente espesante empleado. En general, todas las pinturas mostraron una estabilidad de almacenamiento satisfactoria durante un mes.

Las pinturas que contenían DMAPS mostraron propiedades de brillo admirables y comparables a las pinturas de referencia, a excepción de aquellas que integraban monómeros funcionales como HEMA y AA. Estas últimas exhibieron menor brillo debido a una mayor rugosidad superficial. Las propiedades de la película, incluidos el índice de blancura y el de contraste, resultaron satisfactorios en todas las pinturas, aunque el rendimiento al frotar fue notable principalmente en la pintura estabilizada con el surfmer. La incorporación de DMAPS ejerció una influencia favorable en la dureza de la película y la resistencia al bloqueo, probablemente atribuible al establecimiento de una red iónica dentro de la película y posibles interacciones iónicas dentro de esta red. Cabe destacar que las pinturas basadas en DMAPS mostraron una gran estabilidad a la radiación UV, excluyendo la variante que contenía estireno, que mostró sensibilidad debido a su estructura aromática. En cuanto a la resistencia a las manchas, las pinturas con DMAPS presentaron los mejores resultados, especialmente el látex que contenía estireno, que demostró una eliminación óptima de las manchas. Sin embargo, la eliminación de manchas de productos de escritura fue similar en todas las pinturas. Las características de absorción y permeabilidad al agua en las pinturas con DMAPS y en las de referencia fueron similares, lo que indica que los oligómeros solubles en agua afectaron de manera similar a la resistencia al agua en comparación con los surfactantes convencionales. Las pruebas aceleradas de envejecimiento revelaron un rendimiento comparable para la mayoría de las pinturas, excepto la versión que contenía estireno, que mostró una

mayor sensibilidad a la radiación UV debido a su composición aromática. En resumen, las pinturas estabilizadas con DMAPS presentaron propiedades similares a las pinturas tradicionales e incluso exhibieron una ligera superioridad en el rendimiento contra las manchas. La influencia de la incorporación de DMAPS en las propiedades de la pintura fue evidente, y la composición primaria del monómero influyó significativamente en el rendimiento de la pintura.

Parts of this thesis have been presented in conferences, workshops, and Industrial Liaison Program (ILP) meetings, both as oral or poster presentation. In addition, parts of the work described in this thesis have been published or are planned to be published.

In the following, an overview of the oral and poster presentation is given, and a list of the publications is presented. The title and authors of planned publications may change.

Oral presentations

Murali, S.; Agirre, A.; Tomovska, R. **"Incorporation of zwitterionic monomers into waterborne polymer dispersions"** 9th PhD workshop on Polymer Reaction Engineering (Online), 2021.

Murali, S.; Agirre, A.; Tomovska, R. **"Incorporation of zwitterionic monomers into waterborne polymer dispersions"** Oral presentation in the Industrial Liason Meeting of POLYMAT, Donostia-San Sebastián (Spain). 2019-2022.

Poster presentations

Murali, S.; Agirre, A.; Tomovska, R. **"Use of zwitterionic monomers into waterborne polymer dispersions"** Poster presentation (Best poster award) GEP-SLAP, San-Sebastian, Spain, 2022.

List of publications

Zwitterionic monomers as stabilizers for high solids content polymer colloids for high-performance coatings applications. **Murali, Sumi, Agirre, Amaia and Tomovska, Radmila.** s.l. : Elsevier, 2022, Progress in Organic Coatings, Vol. 173, p. 107196.

Chemical structure of zwitterionic monomers as a tool to produce colloidally stable (meth)acrylic polymer colloids. **Murali, Sumi, Agirre, Amaia, Irusta, Lourdes González, Alba and Tomovska, Radmila.** s.l. : Elsevier, 2023, Polymer, Vol.287,p. 126421.

Zwitterionic stabilized water-borne polymer colloids for antifouling coatings. **Murali, Sumi, Agirre, Amaia, Arrizabalaga, Jon, Rafaniello, Iliane, Schäfer, Thomas, and Tomovska, Radmila-***Submitted*

Exploiting Acrylamide-based Zwitterionic Monomers as Colloidal Stabilizers for High Solids Content Waterborne Systems. **Murali, Sumi, Agirre, Amaia and Tomovska, Radmila-** *Under preparation*

Effect of initiator type on chemical incorporation of DMAPS onto polymer colloids- **Murali, Sumi, Agirre, Amaia and Tomovska, Radmila-** *Under preparation.*

Thermo –Responsive Waterborne Pressure-Sensitive Adhesives stabilized with Zwitterionic Monomers- **Murali, Sumi, Agirre, Amaia and Tomovska, Radmila-** *Under preparation.*

Appendix I. Materials and Polymerization Processes

I.1. Materials

Monomers methyl methacrylate (MMA, purity 99.9 %, Quimidroga), n-butyl acrylate (n-BA, purity 99.5 %, 10–20 ppm MEHQ, Quimidroga) butyl methacrylate (BMA, purity 99%, 10 ppm MEHQ, Sigma Aldrich) zwitterionic monomers, 2-(methacryloxy) ethyl 2-(trimethylammonio) ethyl phosphate (M 2005)(purity ≥ 96.01%, TCI chemicals), 3-[[2-(methacryloxy)ethyl]dimethylammonio] propionate (M-2359)(purity ≥ 98%, TCI chemicals), 2-[(methacryloyloxy) ethyl] dimethyl-(3 sulfopropyl) ammonium hydroxide (DMAPS)(purity≥95.0% Sigma-Aldrich), 4-[[2-(methacryloyloxy) ethyl] dimethylammonio] butane-1-sulfonate (M3295)(purity ≥ 97%, TCI chemicals), 3-[[2-(acryloyloxy) ethyl] dimethylammonio] propane-1-sulfonate (A3367))(purity ≥ 98%, TCI chemicals), and 3-[(3-acrylamidopropyl) dimethylammonio] propane-1-sulfonate (A3361) (purity ≥ 97.0%, TCI chemicals) were used. Bio-based monomer 2-octyl acrylate (2OA) was kindly supplied by Arkema (France) while Evonik Industries (Essen, Germany) kindly supplied isobornyl methacrylate (Visiomer® Terra IBOMA).

The initiator potassium persulfate (KPS, Aldrich), azobisisobutyronitrile (AIBN, purity 98%, Sigma-Aldrich), tert-butyl hydroperoxide (TBHP, 70 wt% aqueous solution, Luperox Sigma-Aldrich), hydrogen peroxide (HPO, 30 wt% aqueous solution, Sigma-Aldrich), ascorbic acid (As.Ac, Sigma-Aldrich purity ≥ 99%), Bruggolite (FF7,Bruggemann)) were used without further purification.

Conventional surfactant sodium dodecyl sulfate (SDS, Sigma-Aldrich), alkyldiphenyloxide disulfonate (Dowfax 2A1), kindly provided by Dow Chemical, chain transfer agent 2-ethylhexyl thioglycolate (2EHTG, Sigma-Aldrich) were used as received. Distilled water was utilized in all the reactions. Hydroquinone (HQ, purity, 99 %, Panreac) was employed to stop the reactions.

Technical grade tetrahydrofuran (THF, Scharlab) and High-Performance Liquid Chromatography (HPLC) grade THF (Scharlab) were used for soxhlet extraction and Size Exclusion Chromatography (SEC) measurements, respectively. Hydrochloric acid (HCl, 1M,Sigma Aldrich) was used to decrease the pH of A3361 latex dispersions. NaCl (synthesis grade, Scharlab) and $CaCl_2$ (synthesis grade, Scharlab) were used for salt stability analysis.

For the paints formulations and binders synthesized in Chapter 6, monomers styrene (St), acrylic acid (AA), hydroxyl ethyl methyl acrylate (HEMA), initiator sodium persulfate (NaPS), pH modifier 10% sodium hydroxide (NaOH), biocide CIT/MIT 1.5%, antifoaming agent BIT 20-D, reagent Omyacarbyl 40 (97% calcium carbonate powder) were kindly provided by Synthomer. Reductant Bruggolite FF6 (Bruggemann) were used as received. Treated water from the plant was utilized for all reactions.

For the paint formulation, thickener Natrosol 250 HBR (Ashland), dispersant Additol VXW 6200 (Allnex), defoamer Agitan E256 (Muzing) and biocide preventol (Lanxess) were employed.

For characterization of paints, colors DB.BE (blue), DB.NO, SF.NH (black), oversaturated solution of ammonium dihydrogen phosphate ($NH_4H_2PO_4$) were kindly provided by Synthomer. Pigment Tiona RCL 535 (Tronox), co-solvent propylene glycol, coalescing solvent Texanol, pH modifier 10% NaOH (Synthomer) were utilized

I.2. Synthesis processes

I.2.1. Homopolymerization of zwitterionic monomers

Zwitterionic monomers were subjected to homopolymerization within a small vial, utilizing KPS as the thermal initiator at a concentration of 1% wbm. The free radical homopolymerization of these ZMs was conducted in aqueous medium for 3 hours. The polymerization reaction took place at a temperature of 70 °C and the target solids content was 3%. Following the polymerization process, the

resulting polymer conversion was evaluated by ^{1}H NMR analysis. In this analysis, the vinyl hydrogen peaks were quantitatively integrated to determine the extent of monomer conversion. The glass transition temperatures (Tg) of the homopolymers were determined through Differential Scanning Calorimetry (DSC) analysis.

I.2.2. Surfactant-free batch emulsion polymerizations in the tumbler

The monomers, n-BA, MMA and ZM, water and initiator were placed in a 50 ml tumbler bottle. The mixture was magnetically stirred and purged with N_2 for 20 minutes prior to be introduced in the tumbler. The reactions were allowed to polymerize for 3 hours at 70°C. The amount of ZM was varied from 0.5 to 3 % wbm. Thermal initiator KPS, redox initiators TBHP/As.Ac and TBHP/FF7 were employed with different concentrations (0.5-1 wbm %). The reactions were carried out both above and below the pKa of the anionic group presented in the ZM as shown in Table I.1.

Table I.1. Studied conditions in the surfactant-free batch emulsion polymerizations carried out in the tumbler (10 % S.C.).

ZM	ZM (wbm %)	Initiator	Initiator (wbm %)	pH
M-2005		KPS	1	
M-2359	0.5-3	TBHP/As.Ac	0.5 & 1	2-4,6-8 &8-9
DMAPS		TBHP/FF7	0.5 & 1	

I.2.3. Synthesis of the seed

The recipe used to synthesize the seed stabilized with conventional surfactant SDS is given in Table I.2. 1 L jacketed glass reactor equipped with reflux condenser, N_2 inlet, temperature probe, stainless steel agitator and a sampling tube was used. The reactor was first charged with water, SDS and MMA/n-BA mixture and stirred at a rate of 200 rpm under N_2 atmosphere. When the temperature reached the desired value (70 °C), the initiator KPS was added as a shot. The system was allowed to react

batch-wise for 3 hours. Afterwards, the temperature of the reactor was increased to 90 °C and left to react for additional 2 hours in order to reach full conversion. The target solids content was 10%.

Table I.2. Recipe for the seed stabilized with SDS (10 % S.C.).

Ingredients	Amount (g)
n-BA	39.94
MMA	40
SDS[a]	0.81
KPS[a]	0.80
Water	720

[a] **1% wbm**

I.2.4. Synthesis of polymer latex using ZMs

Polymer latexes using ZMs were synthesized using a seeded semi-continuous emulsion polymerization. The polymerization reactions took place in a glass jacketed reactor with capacities of 250 ml. The reactor was equipped with a reflux condenser, a sampling device, an inlet for introducing nitrogen gas (N_2), and a sturdy anchor-type stirrer that rotated at 200 rpm. In the semi-continuous approach, the temperature and inlet flow rates of the feeding materials were under the control of an automated system called Camile TG, developed by CRW Automation Solutions. This system ensured precise management of the reaction conditions. Regular sampling of the reaction mixture was performed at specific time intervals to monitor the progress of the reaction.

An appropriate quantity of seeds was introduced into the reactor, followed by a N_2 purging process that continued until the end of the reaction. A standard coating formulation consisting of MMA/n-BA in a 1:1 weight ratio was employed.

In reactions with different type of initiators, initiator concentration of 1 wbm % was used. This was kept constant while keeping the DMAPS quantity (2 wbm %) and the target solids content (50%) constant across all the reactions under investigation.

In the reactions where thermal initiators were used, the initiators were added as a shot when the temperature reached the desired temperature 70 °C. KPS was dissolved in water while AIBN was dissolved in n-BA. Additional reaction was carried out with KPS but this time the KPS was included in the pre-emulsion and fed during the reaction. In the case where redox pairs were employed the oxidant, HPO or TBHP were added as a shot after the reactor reached the desired temperature (50 °C). The reductant, As.Ac or FF7 was placed in the pre-emulsion that was composed of MMA and n-BA mixture (1:1 weight ratio) and zwitterionic monomer that was fed during the reaction.

Once desired temperature achieved, initiator was added as shot, followed by the feeding of pre-emulsion containing MMA/n-BA mixture (1:1 weight ratio), ZM, distilled water and FF7 (reductant) at a uniform feeding rate, during 3.5 hr. Following the completion of feeding, the reaction underwent an additional batch-wise during of 1.5 hours at the same temperature to ensure full conversion of any residual unreacted monomers.

The formulations employed throughout this study are summarized in the following tables. Formulations involving different initiators are presented in detail within Table I.3. Table I.4 outlines formulations that encompass varying quantities of ZM DMAPS, spanning from 0.5 to 5 wbm %. Table I.5 presents the formulations including different ZMs, which are distinctively combined with completely surfactant-free seeds. In order to investigate the influence of the anti-polyelectrolyte behavior of ZM with acrylamide functionality (A3361), an additional reaction was conducted at a lower pH of 3-4 by adding a small amount of 0.01 M HCl. With ZM A3361, a higher solids content latex with a more industrial-like composition (50% S.C.) was produced as well.

In Chapter 5, a petroleum-based acrylic Pressure Sensitive Adhesive (PSA) was synthesized using a 90/10 ratio of n-BA/MMA. For the sake of comparison, another PSA was prepared by substituting ZM A3361 with SDS. The formulation employed for synthesizing the petroleum-based PSA with A3361 is given in Table I.6.

Table I.3. The recipe for seeded semi-continuous emulsion polymerization reactions with different initiator systems. The feeding rate in all reactions was 0.76g/min.

	KPS-Shot	KPS-Feed	AIBN	HPO/As.Ac	TBHP/As.Ac	TBHP/FF7
Initial Charge (g)						
Seed	40.06	40.05	40.09	40.03	40.02	40.03
KPS	1.88	---	---	---	---	---
AIBN	---	---	1.85	---	---	---
HPO	---	---	---	2.57	---	---
TBHP	---	---	---	---	2.58	2.57
n-BA	---	---	30.03	---	---	---
Water	20.16	---	---	---	---	---
Feed						
n-BA	90.03	90.02	60.55	90.08	90.05	90.1
MMA	90.02	90.03	90.02	90.05	90.01	90.06
DMAPS	3.61	3.62	3.63	3.62	3.61	3.62
KPS	---	1.86	---	---	---	---
As.Ac	---	---	---	1.82	1.82	---
FF7	---	---	---	---	---	1.8
Water	100.23	120.1	120.5	120.03	120.4	120.2

Table I.4. The representative recipe for seeded semi-continuous reactions by 2% DMAPS. The feeding rate of the reaction was 0.76g/min.

Ingredients	Initial charge (g)	Feed
Seed [a]	40.03	
n-BA	---	90.1
MMA	---	90.06
DMAPS/SDS [b]	---	3.62
TBHP	2.57	---
FF7	---	1.8
Water	---	120.2

[a] Seed stabilized by SDS [b] amount of DMAPS varied from 0.5-5% wbm

Table I.5. Representative recipe for completely surfactant-free seeded semi-continuous emulsion polymerization reactions using 2% wbm A3361 (30% S.C.). The feeding rate of the reaction was 0.53g/min.

Ingredients	Initial charge (g)	Feed (g)
Seed	30	---
n-BA	---	27.1
MMA	---	26.7
A3361 /SDS	---	1.1
TBHP	0.81	---
FF7	---	0.54
Water	---	98.3

Table I.6. The representative recipe for seeded semi-continuous reactions of petroleum based PSA by using 2% A3361 (pet-PSA-A3361). The feeding rate of the reaction was 0.76 g/min.

Ingredients	Initial charge (g)	Feed (g)
Seed	40.03	
n-BA	---	162.26
MMA	---	18.2
A3361/SDS	---	3.68
TBHP	2.6	---
FF7	---	1.89
Water	---	121

Appendix II. General Characterization Methods

II.1. Latex characterization

II.1.1. Solids content and monomer conversion

The monomer to polymer conversion (X_m) was determined using a gravimetric method, involving the measurement of the non-volatile portion of the dispersion. In the experimental process, around 2 mL of latex samples were extracted from the reactor. The free radical polymerization was promptly stopped by adding roughly 0.1 mL of a hydroquinone (HQ) solution in water, with a concentration of 1 wt %. The obtained samples were left to dry in aluminum caps at 60 °C until a constant weight was reached. The solids content (S.C.), also known as the non-volatile fraction of the dispersions, was calculated by establishing a weight ratio between the dry solid and the latex, as indicated in equation II.1 below.

$$S.C. = Dry\ solid\ (g)\ /\ Latex\ (g) \qquad \textbf{(eq.II.1)}$$

Subsequently, the monomer conversion was calculated based on the solids content of the dispersions, following equation II.2. This Equation includes terms such as NPF (non-polymeric solid fraction such amount of initiator, surfactant, HQ etc.) m_{latex} is the weight of the latex and m_{mon} is the amount of monomer. In semi-continuous polymerization processes two different conversions can be defined: the instantaneous conversion (X_i), which takes into account the monomer fed at each time to reactor; and

the overall conversion (X_t), which considers the whole monomer amount that is going to be fed into the reactor.

$$\boldsymbol{Xm} = \frac{\boldsymbol{mass\ of\ polymer}}{\boldsymbol{mass\ of\ monomer}} = \frac{\boldsymbol{S.C.{*}m_{latex}{-}NPF}}{\boldsymbol{m_{monomer}}} \qquad \textbf{(eq.II.2)}$$

The conversion of ZMs in the polymer dispersions (latexes) was determined by using ^{1}H NMR Spectroscopy (Bruker Avance-400), using 450 µL of latex dissolved in 50 µL D_2O. For that, aim the characteristic shift at 5.7 ppm corresponding to the vinyl peak of ZMs was used as can be seen in Figure II.I, which presents the ^{1}H-NMR spectra of latex samples, withdrawn at different time intervals during the emulsion polymerization performed in the presence of 2% of DMAPS.

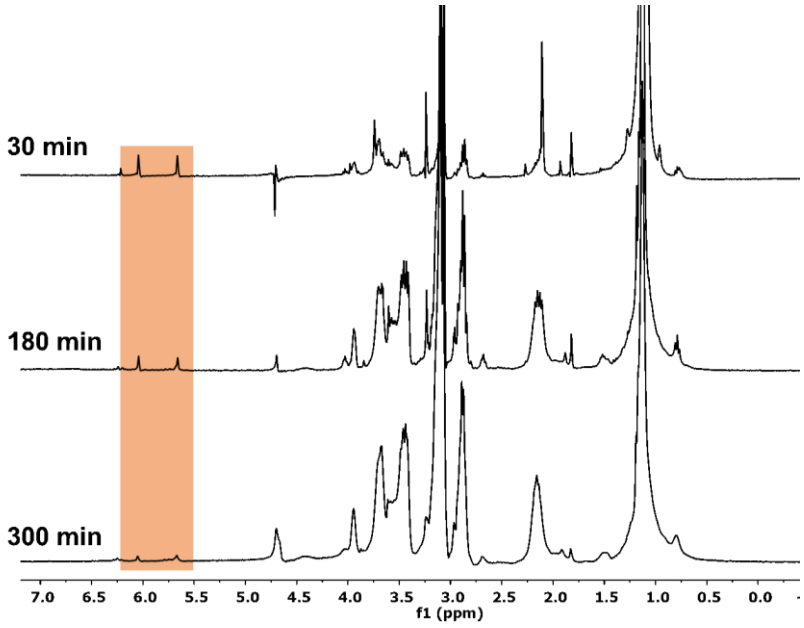

Figure II.1 ^{1}H-NMR spectra of 2% DMAPS (50% S.C.) latex at different reaction times (30,180 and 300 min).

II.1.2. Coagulum amount

To determine the coagulum content, the final latex was filtered through a polyamide mesh (85 µm), and the amount was calculated based on the total solids content of the latex.

II.1.3. Average particle size and particle size distribution

II.1.3.1. Dynamic Light Scattering (DLS)

The average particle diameter was assessed at a temperature of 25 °C, employing dynamic light scattering (DLS) with a Malvern ZetaSizer Nano-S instrument. This instrument was equipped with a 633 nm red laser and operated with a 173° backscatter angle. The samples used for the measurements were prepared by diluting a portion of latex with deionized water. Each measurement run entailed a 2-minute period for temperature stabilization. The reported values were the Z-average of three repeated measurements.

Results obtained from DLS were used to determine the number of particles (Np). Np was determined following equation II.3.

$$\boldsymbol{Np = \frac{Vp}{Vt} = \frac{6\left(\frac{W_{pol}}{\rho_{pol}}\right)X}{\pi d_p^3}} \qquad \textbf{(eq.II.3.)}$$

In this case, W_{pol} corresponds to the amount of polymer (g) at each time, and it was calculated from the monomer conversion (X). p_{pol} refers to the polymer density (1.11 g cm^{-3}) and dp to the z-average particle size. Np involved some uncertainty because the third power of dp was used in their calculation.

The theoretical growth of the particles was calculated using equation II.4 , where Dp_{seed}, $mass_{seed}$, and $S.C._{seed}$ represent the z-average particle size, mass, and solids content of the seed, respectively, and Dp_t, $mass_t$, and $S.C._t$ denote the z-average particle size, mass, and solids content of the latex at a specific time.

These calculations assumed the absence of secondary nucleation, meaning that all the monomer added in the semi-batch stage was utilized for particle growth.

$$DP_t = DP_{seed}\left(\frac{mass_t * S.C._t}{mass_{seed} * S.C._{seed}}\right)^{1/3} \quad \textbf{(eq.II.4)}$$

II.1.3.2. Capillary Hydrodynamic Fractionation (CHDF)

The determination of average particle size and particle size distribution in Chapter 3 and 4 was also measured using capillary hydrodynamic fractionation (CHDF) technique. The CHDF-3000 instrument from Matec Applied Science was employed, operating with a flow rate of 1.4 mL min^{-1} at a temperature of 35 °C and a detector wavelength of 220 nm. The carrier fluid used was 1X-GR500 from Matec. For analysis, the samples were appropriately diluted to a concentration of 0.5% S.C. using the carrier fluid. The analysis of the samples was carried out using Matec software version 2.3.

II.1.3.3. Transmission Electronic Microscopy (TEM)

The particle size of DMAPS latex for anti-polyelectrolyte study in Chapter 4 was analyzed by transmission electron microscopy (TEM) using a Jeol TM-1400 Plus series 120 kV electron microscope.

II.1.4. Gel content

The gel content of the polymers (GC %) was assessed through Soxhlet extraction utilizing tetrahydrofuran (THF) as the solvent. This measurement determines the weight fraction of the polymer that remaines insoluble in THF. To perform this measurement, small drops of the latex were placed on glass fiber pads (for PSAs, cartridge were employed) (filter weight W_0) and the samples were oven dried at 60 °C overnight. Subsequently, these pads (dry polymer weight W_1) were introduced into the Soxhlet extractor, and a continuous extraction process was initiated using THF under reflux conditions for 24

hours. During the course of extraction, the polymer chains that were soluble dissolved into the THF, while the polymer fraction that was insoluble (referred to as the "gel") remained embedded within the pad. After the extraction process, the pads were dried (gel weight W_2), and the gel content of the polymers was determined through the application of equation II.5:

$$\textbf{\textit{Gel content}}\ (\%) = \frac{W_2 - W_0}{W_1 - W_0} * \mathbf{100} \qquad \textbf{(eq.II.5)}$$

II.1.5. Molar mass distribution (MMD) of the soluble fraction (sol molar mass)

The molar mass of the soluble fraction (obtained after Soxhlet extraction) was determined using Size Exclusion Chromatography (SEC). The setting constisted on a pump (LC-20A, Shimadzu), an auto sampler (Waters 717 plus), a differential refractometer (Waters 2410), and a guard column (styragel guard column) followed by three columns in series (Styragel HR2, HR4, and HR6 with varying pore sizes ranging from 10^2 to 10^6 Å) and the analyses were performed at 35 °C and THF was used as the mobile phase at a rate of 1 mL min^{-1}. Calibration was relative to PS standards. A series of PS standards in the range of 575-3,848,000 g mol^{-1} were used to prepare a universal calibration.

The solution of the polymer in THF recovered from the Soxhlet extraction was left to evaporate and afterwards was re-dissolved at approximately 1 mg ml^{-1}. Prior to injection into the SEC instrument, the solution was filtered through a polyamide filter with a pore size of 45μm.

In Chapter 3, the molar mass of whole polymer was measured in an Agilent PL-GPC 50 integrated Gel Permeation Chromatography system using DMF (0.05M LiBr) as mobile phase at 50 °C and a flow rate of 1 mL/min was utilized. The column employed was KD-806M (Shodex) and all the measurements were performed at 50 °C. Polystyrene standards were used for column calibration. The samples were dissolved

in the mobile phase at approximately 1 mg/ml and prior to injection they were filtered with a 0.45um pore size Nylon filter.

II.1.6. Amount of water-soluble species

To determine the amount of water-soluble species in the latexes, a small quantity of each latex was ultracentrifugated in pollyallomer tubes using a TFT 70.38 fixed angle rotator in Centrikon T-2190 centrifuge (Kontron Instruments). To do so, the latexes were diluted (12.5 wt% S.C.) and ultracentrifugated at 30,000 rpm for 2 hours at 4 °C. The serums were carefully taken with a syringe and dried at room temperature for 2 days under air purge and the dry residues were assigned as water-soluble species. For each latex, an average of 3 measurements was reported.

II.1.7. Incorporation of zwitterionic monomers

The incorporation of ZMs was calculated by Fourier-Transform Infrared Spectroscopy (FTIR) analysis using films casted from original and dialysed latex with Bruker Alpha FTIR spectrometer with Attenuated Total Reflection (ATR) mode. Films of similar thickness were introduced in the sample holder and an average of five measurements were taken. Spectra were recorded in transmission mode in the spectral region from 3000 to 400 cm^{-1} with a resolution of 0.9 cm^{-1}. The area of the peak of sulfonate group (1030cm^{-1}) was determined and by the use of a calibration curve, the incorporation of ZMs was calculated. The calibration curve was prepared by integrating the area of the sulfonate group (1030cm^{-1}) of films casted from latexes with different but known amounts of ZM DMAPS.

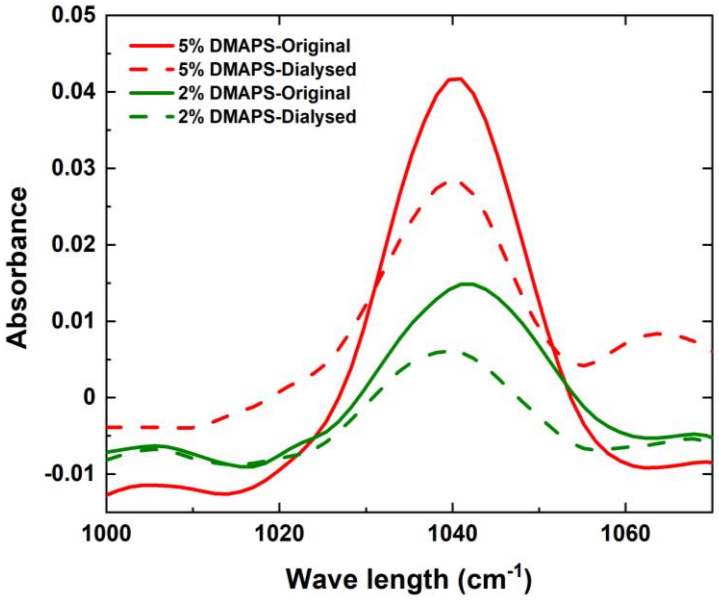

Figure II.2. FTIR spectra of 2% and 5% DMAPS films prepared from original and dialysed films, sulfonate peak is shown at peak 1030 cm^{-1}.

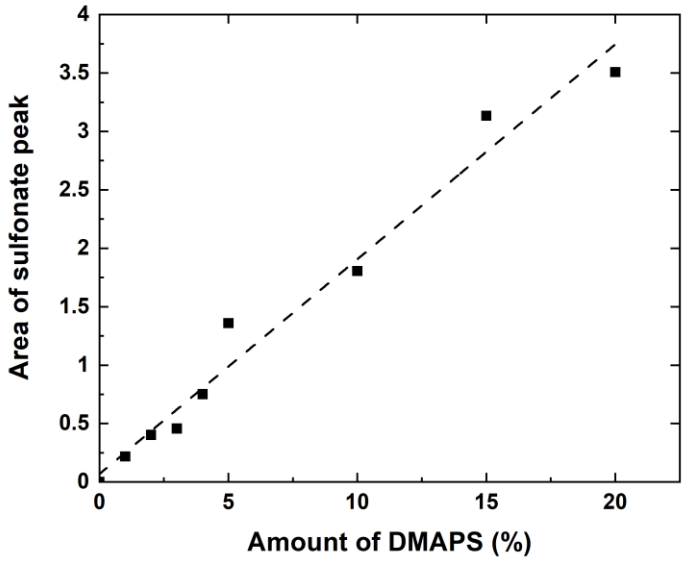

Figure II.3. Calibration curve used for determining the incorporation of different ZMs.

II.1.8. Salt stability of the latex

Salt tolerance experiments were conducted to examine the stability of the latex samples when exposed to electrolytes. This was achieved by adding equal amount of saline solution to equal amount of latex and after gently stirring were left to rest for 24 hours at room temperature. The particle size was measured prior and after.

II.1.9. Freeze-thaw stability

Latexes were subjected to different numbers of freeze-thaw cycles. Each freeze-thaw cycle consisted in freezing the latex at -20 °C for 24 hours followed by thawing at room temperature for 24 hours.

II.2. Polymer film characterization methods

II.2.1. Water contact angle (CA)

The standard sessile drop method was utilized for static water contact angle measurements, employing the Data Physics OCA 20 model goniometer. Films with a thickness of 120 µm (wet thickness) were formed from latexes on glass substrates and then air-dried for 24 hours at 23 °C and 55% relative humidity. A volume of 3 µL of deionized water was deposited onto the film surfaces, and a minimum of 10 measurements were taken from various positions on the surface to calculate an average value. Then, the films were rinsed with deionized water, followed by another 24-hour drying period under the same conditions. The contact angle measurements were repeated to assess any potential changes.

II.2.2. Differential Scanning Calorimetry (DSC)

The glass transition temperature (Tg) was determined by Differential Scanning Calorimeter (DSC, Q1000, TA instruments). About 3-5 mg of samples were placed into aluminum hermetic pans, were first heated to 150 °C with a heating rate of 10 °C min^{-1} and kept isothermal for 2 minutes. Then, they were cooled down to -50 °C with a cooling rate of 10 °C min^{-1} and kept isothermal for 2 minutes. The second heating run was carried out at 10 °C min^{-1} to determine the Tg of the polymers.

II.2.3. Mechanical properties -tensile test

For determination of mechanical properties, all the latexes were diluted to same solids content prior to cast the films, to eliminate the effect of the solids content on the film formation. As prepared films (from original and dialyzed latexes) and annealed films (80 °C for 3 days) were tested. Tensile test measurements were conducted using a TA.HD plus Texture Analyser. The tests were performed under controlled conditions of 23 ± 2 °C and 55 ± 5% relative humidity. The tests were carried out with a crosshead speed of 25 mm/min on approximately 0.6 mm wet thick films. To prepare the films for

characterization, the latexes were cast in silicone molds and were dried at 23 °C and 55% relative humidity until constant weight. Each sample was prepared in at least 6 replicates, and the resulting average values were reported.

II.2.4. Water uptake

In order to evaluate the water sensitivity of the films, films with approximately 0.6 mm thickness (wet) were prepared by casting the latex into silicone molds and dried at 23 ± 2 °C and 55 ± 5 % of relative humidity during 7 days until a constant weight for the film was achieved. To determine the water absorption of the films, water uptake test was performed. To check the reproducibility of the results, three films were used and each films were introduced in to a closed flask containing 100 ml deionized water. At some time intervals, the films were taken out from the flasks, smoothly blotted with paper and weighted. The water uptake was calculated with respect to the initial weight of the dried film.

II.2.5. Atom Force Microscopy (AFM)

To determine the morphology of the films, AFM measurements were performed. AFM images were obtained using a Bruker dimension icon atomic force microscope equipped with the NanoScope V Controller (Bruker), operating in tapping mode. An integrated silicon tip/cantilever (TESP-V2, Bruker) with a resonance frequency of 320 kHz and nominal constant of 37 N/m was used. For the analysis of the cross-section of the films, the samples were cut on a Leica FC6 cryo ultra microtome. The cut-off temperature was -25 ° C.

II.2.6. Moisture permeability

The water vapour (moisture) permeability (P) of the films was measured by a gravimetric cell (Sartorius BP210D). The cell, made of Teflon, was partially filled with water and sealed using a polymeric membrane. Subsequently, 300 μm thick films were then attached to the open mouth of the gravimetric

cell containing water so that the film is exposed to water vapour (100% RH). The cell was well sealed so that the water could only scape by permeating through the film and it was placed on a balance within a temperature and humidity-controlled chamber set at 25 °C and 40% of RH to measure the loss of weight over time. The moisture permeability (P) (g.mm/m^2 day) was calculated from the slope of the weight loss (water loss) versus time plot, utilizing Equation II.6:

$$\boldsymbol{P = \frac{m.l}{A.(a_{int} - a_{ext})}} \qquad \textbf{(eq.II.6)}$$

Where *m (mass flux)* is the slope of the curve, *l* is the film thickness, *A* is the area of contact between the film and water vapour (2.54 cm^2), a_{int} is the water vapour activity in the headspace of the cell (considered 1) and a_{ext} is the water vapour activity in the chamber (about 0.4). Three samples of each film were tested and the reported values is an average of the three measurements.

II.2.7. Quartz Crystal Microbalance with Dissipation monitoring (QCM-D)

To detect the antifouling ability of the films, QCM-D was used, using bovine serum albumin (BSA) as model foulant. QCM-D measurements were performed on a Q-SENSE E1 system operating at 23 °C. The latexes were deposited by means of drop coating with 2 µL pipette and dried at room temperature for three days. Prior to the measurements, the samples were stabilized overnight under a constant PBS buffer flux of 100 µL /min. Subsequently, they were put in contact with different concentrations of BSA in aqueous buffer (PBS) solution up to a maximum of 1000 mg BSA/L. QCM-D technique detects changes in the resonance frequency (Δf), and dissipation (ΔD). During the adsorption/desorption cycle, the resonance frequency of the crystal changes according to changes in the mass. If the mass forms an evenly distributed, rigid layer whose mass is small compared to that of the crystal, then the mass per unit area can be calculated from the Sauerbrey Equation II.7.

$$\boldsymbol{\Delta m = -C \cdot \Delta f / n} \qquad \textbf{(eq.II.7)}$$

In this equation, C is a constant (17.7 ng $cm^{-2}s^{-1}$ for this equipment) and n is the resonance overtone number (n=5 was used here). Where appropriate, a 2nd order data noise smoothing was applied for better visualization of the data.

II.2.8. Multi-Parametric Surface Plasmonic Resonance (MP-SPR)

Prior to carrying out surface plasmonic resonance measurements, the MP-SPR SiO_2 sensor was first introduced in an ozone cleaner for 10 minutes. Then, the sensor was placed in a sensor holder and introduced in a beaker with Milli-Q water for at least another 10 minutes. Afterwards, the sensor was dried with nitrogen and placed in the support for SPR sensors. Then a measurement of 30 seconds was carried out (in gas range) in order to get the reference peak minimum angle of the SPR curve. Afterwards, the sensor was placed on the spin coater (kept in place by applying vacuum) and 5 µl of the latex (0.03 wt%) were deposited on the sensor and left to dry in the oven (50 °C) overnight. Once the film was completely dry it was stabilized with a PBS solution for several hours (at least 5h). Once the sensor was stabilized adsorption measurement were carried out. First, 10 minutes baseline was made as reference with PBS solution. Then, BSA 1000 ppm solution was passed over the sensor for 65 minutes (adsorption) and finally, PBS buffer was injected for at least another 60 minutes (desorption).

II.3. Evaluation of adhesive films (Chapter 5)

The Pressure Sensitive Adhesive (PSA) films were prepared by casting the latex (previously diluted to 40% S.C.) over a flame treated polyethylene terephthalate (PET) sheet (29 µm thick) using a 250 µm thick applicator. Films protected from dust were dried at 23 °C and 55% humidity overnight. The thickness of dry films was around 100 µm. The films for the probe tack measurements were prepared in the same way but on a glass substrate instead of on PET substrate.

II.3.1. 180° Peel strength

The 180° peel strength assessment was conducted on stainless steel panels following ASTM-D3330 guidelines. PSA tape, with a width of 25 mm, were applieded to the panel, ensuring the adhesive side was in contact with the panel. Subsequently, a 2 kg rubber-coated roller was used to apply pressure by rolling over the tape specimens five times. The applied tapes were left to dwell for 10 minutes. The tapes were carefully peeled off at a crosshead speed of 5 mm/s. The resulting peel strength value in newtons per centimeter (N/cm) was determined by averaging the measurements obtained from peeling 6 cm of the tape specimens.

II.3.2. Loop tack

Loop tack test was performed on a 25 mm wide stainless steel plate in accordance with ASTM-D6195. 10 cm long PSA tape specimens with a width of 25 mm were attached in as loop to the upper grip of the equipment. The loop was allowed to move downward at a speed of 0.1 mm/s until it was brought in full contact with the plate (25 mm x 25 mm). After letting it in contact for 0.1 s it was moved upward at 0.055 mm/s. The force required to peel off the loop was measured in N/25mm and the average of four measurements was reported.

II.3.3. Probe tack

The probe tack assessments were executed on glass plates as the substrate. Latex films (with a final thickness of 100 μm in order to eliminate substrate influence) were directly applied onto the glass plate and air-dried for 6 hours prior to the test. Subsequently, a stainless steel ball probe was gradually lowered at a speed of 0.1 mm/s until it came into contact with the adhesive test panel surface, exerting a compressive force of 4.5 N. Immediately after the contact period (1 second), the crosshead was started to move upward at a speed of 0.055 mm/until the probe was entirely separated from the adhesive. The

area under the curve represents the work of adhesion (W_{adh}) and was reported in J/m^2. The same experiment was also performed with the PSA films at 60 °C using a temperature controller chamber during analysis.

II.3.4. Shear Adhesion Failure Temperature (SAFT)

Shear Adhesion Failure Temperature (SAFT) tests were performed on stainless steel panels using SAFT equipment (Sneep Industries) in accordance with ASTM-D4498. The PSA tape specimens were applied to the panel with a contact area of 25 mm × 25 mm and pressed 4 times with a 2 kg rubber-coated roller. Afterwards, the tapes were dwelled for 10 min. The test panel (with the tapes) was held by the test stand at an angle of about 1°C relative to the vertical. Once the weights of 1 kg were held from the free ends of the tapes the temperature was increased from 23 °C to 200 °C at 1°C/min rate. For this test, the temperature of failure in °C was reported. The same experiment was performed but with the PSA films previously annealed at 80 °C overnight.

II.4. Evaluation of latex and paints (Chapter 6)

This segment outlines the characterization methods employed for the latex and paints developed during the internship at Synthomer.

II.4.1. Latex characterization

II.4.1.1.Particle size

Z-average particle diameter was measured at 25 °C by using a dynamic light scattering (DLS) Nano Brook 90 Plus instrument. The latex sample was diluted with distilled water to prevent multiple scattering.

II.4.1.2. Solids content (S.C.)

The solids content of the latexes/paints was determined gravimetrically. The sample was weighed in a steel pan and put into an oven at 140°C for 20/60 minutes to dry. The S.C. was determined by the ratio between the weight of the dry sample and the wet sample.

II.4.1.3. Viscosity

Brookfield Dial Reading LVT model viscometer was utilized to measure the viscosity of the as-produced latexes. The measurements were performed by using LV-1, LV-2, or LV-3 spindle at a speed of 20 rpm for 18 seconds at room temperature.

II.4.1.4. Minimum film forming temperature (MFFT)

MFFT of the latex was measured in the MFFT-60 instrument (Rhopoint) at a temperature range of 5-23 °C. 150 µm wet thick films were cast on the MFFT bar.

II.4.1.5. Water resistance test

Films of 150 µm wet thickness were cast onto glass substrates, and dried at room temperature for one day in the climate room (23°C & 50% RH). The substrates were immersed in a water tank at 23 °C up to half of their height. The observations, such as, blistering, wrinkling, and discoloration were recorded in certain time intervals (5, 10, 15, 30 (min), 1, 4, 24 (hrs.))

II.4.1.6. Thermo-mechanical resistance (RTM)

Latex was mixed with calcium carbonate powder (Omyacarb 40) in a stainless cup and stirred gently using a spatula. Then the mixture was homogenized using a high-speed disperser at 1000 rpm for 1 minute. After that, the speed was increased to 3000 rpm and agitated for 30 minutes. The stirring was

stopped if the mixture was coagulated during this time or soon after 30 minutes. The time and temperature of the mixture were recorded.

II.4.2. Paint characterization

Before any measurement, the paints were slightly mixed with a spatula to obtain a smooth and homogeneous mixture.

II.4.2.1. Viscosity

Krebs unit (KU) viscosity by Stormer-type viscometer

Sheen 480 Krebs viscometer was used to measure the Stormer viscosity (consistency) of the paints. It resembles to pouring the paint.

Cone & plate viscosity (ICI)

ICI type cone & plate analogue viscometer was used to measure the viscosity of the paints under high shear to mimic the shear conditions applied during brushing, rolling or spraying.

Brookfield Viscosity

Brookfield Dial Reading LVT model viscometer was used to measure the viscosity of the paints. The measurements were carried out by using LV-1, LV-2 or LV-3 spindle at a speed of 20 rpm for 18 seconds at room temperature.

II.4.2.2. Storage stability at 50 °C

This test is an accelerated test for the storage stability of the paints. In addition, it gives an idea about the resistance of the paint to high temperatures encountered during transport and storage, especially in hot climates. 50g of paints were taken into containers and put into an oven at 50°C. The changes in the appearance and condition of the paints (such as yellowing, phase separation,

coagulation) were checked after 28 days. In addition, viscosities and pH of the paints were also measured and compared with the initial values.

II.4.2.3. Specific gravity (S.G)

The density of coatings were determined by using reference ISO method 2811-1:2018. The weight of an empty pycanometer and pycanometer with 100 ml of paint were measured and density was calculated using equation II.8

$$\mathbf{S.G= PC-PV/V} \qquad \mathbf{(eq.II.8)}$$

Where, PC is the weight of the pycanometer filled with the sample (g), PV corresponds to the weight of the empty pycanometer (g) and V is the pycanometer capacity (cm^3).

II.4.3. Paint film properties

All the tested films were dried in a climate room at 23 °C & 50% RH.

II.4.3.1. CIE L*a* b* parameters

The color of coated objects was visualized and quantified by using the CIELAB color space (International commission on illumination), using the X-Rite spectrophotometer. Each color is represented by a color point (L*, a*, b*) in the color space; L*, a*, and b* are the color coordinates of the color point (Figure II.4). The L*axis gives the lightness: a white object has an L* value of 100 and the L* value of a black object is 0. Chromatic (real) colors are described by using the two axes in the horizontal plane. The a* axis is the green-red axis and the b*axis goes from blue (-b*) to yellow (+b*). Δb represents the yellowing difference and ΔE is the color difference of the two colors. A small ΔE value implies that the colors are close to one another. The color difference can be calculated by using mathematical theorem of Pythagoras given in equation II.9.

$$\mathbf{2\Delta E} = \sqrt{(\mathbf{\Delta L}*^{\mathbf{2}}) + (\mathbf{\Delta a}*^{\mathbf{2}}) + (\mathbf{\Delta b}*^{\mathbf{2}})} \qquad \mathbf{(eq.II.9)}$$

These properties were determined on 300 µm wet paint films, cast onto a glass plate, and dried in the climate room for 1 day. The spectrophotometer was calibrated using white and black background and all parameters were determined. To carry out the measurements, the instrument was placed on the film, and lower the body of the equipment is pressed down until the measurement is complete. Additional two measurements were taken at different positions.

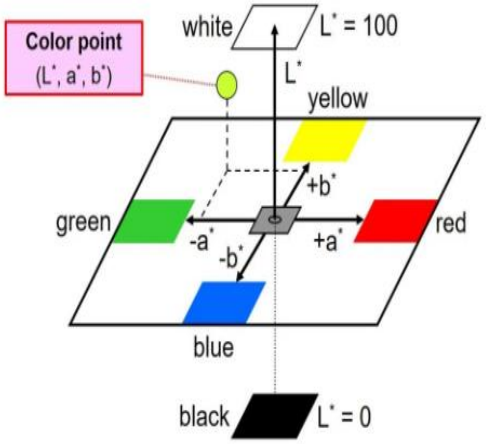

Figure II.4. The 3-dimensional CIE L*a*b color space.

II.4.3.2. Contrast ratio (CR)

Opacity was measured directly by the contrast ratio formula. The contrast ratio will help to determine how much paint is required per m² or to put, in other words, it illustrates the ability of a paint to hide a contrasting substrate. Throughout the paint industry, the terms hiding, opacity, and contrast ratio have frequently been used interchangeably. CR is calculated by taking the ratio of Y tristimulus value of the specimen on black background to that on white background using an X-Rite spectrophotometer (equation II.10)

$$CR = Y_{black} / Y_{white} * 100 \qquad \textbf{(eq.II.10)}$$

CR was determined on 100 µm wet thickness paint films, cast onto polyester film dried in the climate room for 1 day. The spectrophotometer was calibrated using white and black opacity and sample opacity were measured in black and white zones three times.

II.4.3.3. Gloss

The term gloss refers to the visual appearance of a finish with respect to its gloss level. Glossy paints reflect most light in the specular (mirror-like) direction and they provide a bright sheen when they are dried. For gloss paints, low PVC (below 25%) is usually used to prevent particles from disrupting the surface and so reducing the gloss of the film. Gloss is measured on a scale from 0 to 100, with 0 being no gloss and 100 being perfectly mirror-like. These gloss levels are measured at different angles i.e. 20°, 60°, or 85° depending on the gloss level to be achieved. This is based on the angle of sight that these paints would normally be seen. In the present work, 21% PVC has been employed; therefore expecting a gloss finish for coatings and gloss units (gu) should be above 60 gu at 60° angle.

300 µm wet thick films were cast onto standard glass substrates and dried for 1 day in the climate room. Gloss measurements were carried out by using Elcometer 408 at three angles (20°, 60°, and 85°). The average of three measurements was reported.

If the paint and colorant are not compatible, the colorant may not disperse well in the paint and poor color development is observed. This results in the loss of colorant value and unexpected final color. Moreover, paint with poor color development can display color differences when subjected to different shear forces during application.

80 g of paints were weighed in a plastic cup and colors DB.BE (3%), DB.NO (1.5%), and SF.NH (2.5%) were added. After mixing them manually they were mixed in the homogenizer for 5 minutes at 750 rpm. Two films with a 300 µm wet thickness were applied crosswise on an opacity chart and dried for 15 minutes in the climate room.

II.4.3.4. Colour rubout

Out of two films, one is divided into two zones (zone 1 and zone 2), other film as whole will create zone 3 (Figure II.5.). The test was performed firstly by gently rubbing zone1 with a fingertip until resistance was felt and the film was left to dry for 24 hours in the climate room. The next day, in zone 2 a drop of paint was added and spread circularly (100 times), and a paint drop was placed in order to identify the rubbed part. The same procedure was repeated in zone 3, but this time drop of the coat was spread 10 times longitudinally (across 7 or 8 cm). After that, again zone 1 was rubbed circularly 100 times.

The results are given by the classification of rubout, in terms of color difference between the areas subject to spreading and the remaining film according to a scale from 0 to 2, where 0 corresponds to no difference and 2 corresponds to a big difference.

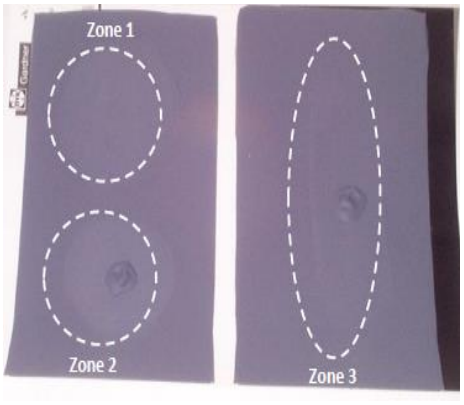

Figure II.5. Scheme of color rubout test.

II.4.3.5. *König* pendulum hardness

The hardness of the material can be defined as the resistance of the coating against the mechanical force such as scratch and rubbing.[1] A *König* pendulum tester (Byk Gardner) weighs 200±0.2 g, consists of a triangular open framework with an adjustable counterpoise weight, and two spherical bearings with a diameter of 5 mm were utilized to monitor the pendulum hardness values of coatings. The period of the pendulum's oscillation was 1.40 ± 0.02 s. The pendulum hardness test is based on the principle that the harder the measured surface, the longer the oscillation time of the pendulum. Pendulum hardness is generally measured with respect to the pendulum's oscillation time from 6° to 3° position at climatic conditions.

A 100 µm wet thickness coating film was applied on a glass plate and dried for 24 hours in the climate room. The equipment was calibrated using a plain glass plate when the amplitude of the pendulum decreases from 6° to 3° position. The number of oscillations should be between 172-185, which adds up to a time of 250 ± 10 s. Hardness was determined for each paint film by registering the total number of oscillations. This was executed after 24, 48, and 72 hours, as well as 7 and 14 drying days.

II.4.3.6. Exposure to UV

The aim of this method is to evaluate changes in coatings after exposure to UV rays. 300 µm wet thickness film was applied on a glass plate and dried for 24 hours in the climate room. L*a*b* parameters of paints were determined before and after 5 days placed in a UV chamber (UVA 340 lamps; Novasol Test, radiation info: distance 500 mm, intensity 800 W/m^2 at a wavelength < 800 nm). The colour variation (ΔE) and yellowing (Δb) were also determined.

II.4.3.7. Blocking resistance

The paint can be applied on surfaces in contact, such as a door and a frame. When a freshly painted door is closed, it may stick shut if the blocking resistance is poor. 60 µm wet thickness paints were cast onto cardboard paper using a spiral applicator and left to dry for 1 day under climatic conditions.

Substrates with (76 mm x 26 mm x 1 mm) dimensions were cut, using a glass sheet. The glass sheet was stacked on the base plate of the device, overlapping faces covered with two sheets to obtain an angle of 90° (Figure II.6. (a)) between the two sheets with the support of a wood piece, a steel piston is positioned on the stacked test slides so that the base of the piston covers completely the contact surface (6.76 cm^2) and is kept in contact for 1 hour (Figure II.6., (b)). To determine the blocking resistance, each sample was placed between two wooden plates for support, a wood piston was placed vertically over the top wooden support and the entire system was centered (Figure II.6. (c)). On the wooden piston, a 2L glass beaker was placed and water was added from a dropper funnel. When the two-coated slides were separated, the tap was immediately turned off, the water added with the superior wooden block, and the wood piston was weighed. The experiments in which the glass sheets were broken were not taken into account. The blocking (g/cm^2) was determined by the following expression (equation II.11)

$$\mathbf{B = WT / A} \qquad \mathbf{(eq.II.11.)}$$

where WT is the total weight of the glass beaker with added water and the top wooden block (g) and A corresponds to the area of contact between the coatings films (6.76 cm^2). Paints presenting a blocking above 300 g/cm^2 (WT> 2030 g) are considered as high block coatings.

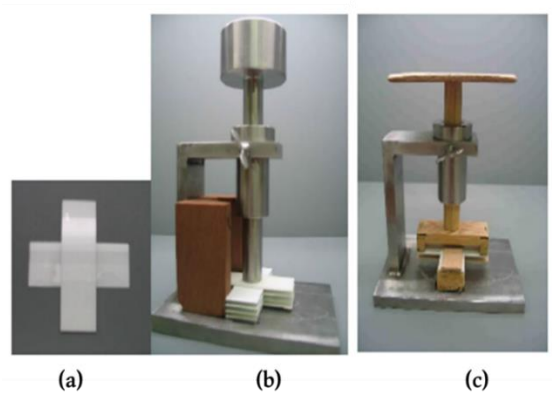

Figure II.6. Assembly of test sample for blocking resistance.

II.4.3.8. Snail Trial

Snail trail is described, as a change of appearance of paints that happens over the first days or weeks of exposure to the exterior environment (low temperature and high humidity). It is also known by other names, such as, water staining, water streaking, or surfactant leaching. White paints were pigmented with 3% of blue paste coloris DB.BE and manually homogenized until the pigment was incorporated, followed by 5 minutes of mixing in the homogenizer at 750 rpm.

200 µm wet thickness films were applied onto three separate leneta sheets and dried for one day in the climate room. The next day, two transversal films with a wet thickness of 200 µm were applied to the films, known as zone 1 and zone 2 of the films (Figure II.7). Immediately after applying the crossed films, the first sheet was kept in a climate chamber at 5 °C for 16 hours. The second and third sheets were dried for 4 and 8 hours in the climate room and afterwards kept inside the climate chamber at 5°C for 16 hours. The dried sheets were positioned vertically and in zone 1 a drop of water in four different places were added and dried for 5 minutes. Over zone 2, about 0.5 ml of water were added with a pipette in three different places while keeping the sheets horizontally and dried for 10 minutes at room temperature.

The sheets were again positioned vertically to drain the excess of water and kept in the climate room for 24 hrs.

The final results were given by the classification of the snail effect carried out according to a scale from 0 to 5, where 0 corresponds to an optimal value (no mark) and 5 corresponds to a bad value (total mark) in both zones.

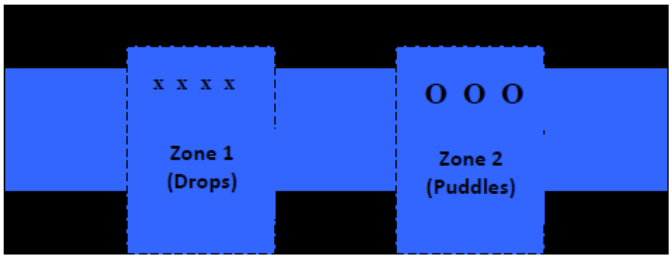

Figure II.7. Scheme of snail trail effect.

II.4.3.9. Stain resistance

Stain resistance is the paint's ability to withstand discoloration but also how easy is to clean. 200 µm wet thickness paints were cast on glass plates and left at climate room for one week. A small quantity of the household products to be tested was applied to three different areas of the film and covered them with a watch glass. After exposure, products were removed with a paper towel, damp cleaning cloth, and cleaning product (ammonium) with soft circular movements for 10 seconds. Stain zones were compared before and after removal. The final results are given by the classification of the degree of staining of the original stain, the stain subjected to washing with water, and the stain subjected to washing with water/cleaning product carried out according to a scale of 0 to 5, where 0 corresponds to an optimal value (no stain) and 5 corresponds to a poor value (staining of the same intensity as the product used).

Determination of stain resistance to writing products

200 µm wet thickness paints were cast on a leneta sheet and left in climate room for one week. Once the coated leneta sheets were ready, a line with the writing products to be tested was applied longitudinally and waited for 2 hours. Leneta sheets were submitted to the wet rub resistance test for 100 cycles, allowed to dry for one night in climatic conditions, and again submitted for additional 400 cycles. Stain zones were compared before and after removal. The classification of the degree of staining with writing products is carried out according to a scale of 0 to 2, where 0 corresponds to an optimal value (absence of the stain) and 2 corresponds to a terrible value (non-removal of the stain).

II.4.3.10. Cyclic water absorption and weight loss

Films of 150 µm wet thicknesses were cast on Teflon substrate, dried at 50°C for 30 minutes, and then cooled down to 23°C in a climate room. Using a cutting press, two test pieces (4 cm x 4 cm) were cut and each sample was left in a vial containing 200 mL water in the climate room. After 24 hours of immersion, films were smoothly blotted with paper and weighed. Subsequent weighing of samples were continued after 3 and 7 days of immersion. After each cycle of immersion, samples were dried as long as necessary (minimum period of 2 days), until the constant weight of the test piece was reached and weight loss was calculated. The water uptake was calculated in relation to the initial dry weight of the sample. The water absorption (AA) and weight loss (PP) expressed in percentage (%), were determined using the following equations II.12 and II.13:

$$\boldsymbol{AA = \frac{A_n - P_0}{P_0} * 100} \qquad \textbf{(eq.II.12)}$$

$$\boldsymbol{PP = \frac{P_n - P_0}{P_0} * 100} \qquad \textbf{(eq.II.13)}$$

P_0 – Initial weight of the test piece (g)

A_n – Weight of the test piece after n day(s) of water immersion (g)

P_n – Weight of the test piece after n day(s) of water immersion, and at least, 2 days of drying (g)

II.4.3.11. Water vapour permeability (WVP)

Films of 150 µm wet thicknesses were cast on a cardboard substrate, dried at 50°C for 30 min, and then cooled down to 23°C in the climate room. 9 cm diameter circles were coated cardboards and fixed to the lid using the silicone sealer. This wet cup method used 50 g of the oversaturated solution of ammonium dihydrogen phosphate ($NH_4H_2PO_4$) in order to attain desired humidity (93%) and the container was closed tight and kept in a climate room. The water vapour permeability (WVP) in g/ (m^2·d) was given by the following Equation II.14.

$$\boldsymbol{WVP = \frac{P_0 - P_d}{A} * n} \qquad \textbf{(eq.II.14.)}$$

Where, P_0 corresponds to the initial weight of the container (g), P_d is the weight of the container after d days (g) and A the area of the filmarea (0.00502 m^2).

The results were given by averaging all the values and water vapour permeability of coatings were classified according to the obtained values. If the value was above 150, the coatings were highly permeable, if it was below 15, the permeability of coatings was low, if the permeability is between 15-150, and it fall under the medium category.

II.4.3.12. QUV accelerated ageing (weathering cycle test)

The aim of this test is to evaluate the resistance of coatings to accelerated ageing resulting from a set number of condensation and UV rays in a QUV tester. 300 µm wet thickness paints were cast on an aluminum plate and left at climate room for one week. The films were exposed to UV for a period of 4 hours at approximately 60 °C (UVA 340 lamps), followed by a condensation period of 4 hours at approximately 45 °C. For the accelerated ageing test, 84 cycles were used, which corresponded to 28

days (672 hours). After this period, gloss and Lab parameters were measured and surface defects were noted.

II.5. References

1. **G. Sward** and **J. V. Koleske**, "Paint and coating testing manual 15th edition of the Gardner-Sward handbook," *ASTM International West Conshohocken PA*, vol. 1026, p. 13–20, 2012.

Appendix III. List of Acronyms and Abbreviations

^{1}H NMR	Proton nuclear magnetic resonance
2-OA	2-Octyl acrylate
A3361	3-[(3-Acrylamidopropyl) dimethylammonio] propane-1-sulfonate
A3367	3-[[2-(Acryloyloxy) ethyl] dimethylammonio] propane-1-sulfonate
AA	Acrylic acid
AFM	Atomic force microscopy
AIBN	Azobisisobutyronitrile
APMH	N-(3-Aminopropyl) methacrylamide hydrochloride
As.Ac	Ascorbic acid
ATRP	Atom transfer radical polymerization
BMA	Butyl methacrylate
BSA	Bovine serum albumin
CA	Contact angle
$CaCl_2$	Calcium chloride
CB	Polycarboxybetaines
CHDF	Capillary hydrodynamic fractionation
CSL	Carbon spacer length
CTA	Chain transfer agent
Đ	Dispersity
DABCO	1,4-diazabicyclo[2.2.2]octane
DLS	Dynamic light scattering
DMAPS	[2-(Methacryloyloxy) ethyl] dimethyl-(3 sulfopropyl) ammonium hydroxide
DMF	Dimethylformamide
Dowfax-2A1	Disodium lauryl phenyl ether disulfonate
DP	Degree of polymerization
Dp	Average particle size
DSC	Differential scanning calorimetry
EDL	Electrical double layer

EHTG	2-Ethyl hexyl thioglycolate
Fe^{2+}	Ferrous ion
FF6	Bruggolite FF6
FF7	Brugolitte FF7
FTIR	Fourier transform infrared
GPC	Gel permeation chromatography
HCl	Hydrochloric acid
HEMA	2-hydroxyethyl methacrylate
HPO	Hydrogen peroxide
IA	Itaconic acid
IBOMA	Isoboryl methacrylate
IEP	Isoelectric point
KPS	Potassium persulfate
LiBr	Lithium bromide
M-2005	2-(methacryloxy) ethyl 2-(trimethylammonio)ethyl phosphate
M-2359	3-[[2-(methacryloxy)ethyl]dimethylammonio] propionate
M3295	4-[[2-(Methacryloyloxy) ethyl] dimethylammonio] butane-1-sulfonate
MAA	Methacrylic acid
MFFT	Minimum film forming temperature
MMA	Methyl methacrylate
MMD	Molar mass distribution
MMT	Montmorillonite
MPC	2-methacryloyloxyethyl phosphoryl choline
MP-SPR	Multi-parametric surface plasmon resonance
MT	Metoprolol tartrate
$\overline{M_w}$	Weight average molar mass
Na_2CO_3	Sodium carbonate
Na_2HPO_4	Disodium phosphate
NaCl	Sodium chloride
$NaHCO_3$	Sodium bicarbonate
NaOH	Sodium hydroxide
NaPS	Sodium persulfate

NaSS	Sodium styrene sulfonate
n-BA	n-Butyl acrylate
$NH_4H_2PO_4$	Ammonium dihydrogen phosphate
Np	Number of particles
NSP	Non-spherical polymer particles
PC	Polyphosphobetaines
PEG	Polyethylene glycol
pH	Potense hydrogen
PHFBA	Poly (hexafluorobutyl methacrylate)
Pka	Acid dissociation constant
PSA	Pressure sensitive adhesive
PS-co-DVB	Polystyrene copolymer divinyl benzene
PSD	Particle size distribution
PSPP	Poly [3-(methacryloylamino) propyl]-dimethyl (3-sulfopropyl) ammonium hydroxide
QCM-D	Quartz crystal microbalance with dissipation monitoring
RAFT	Reversible addition-fragmentation chain transfer technique
RTM	Thermo mechanical resistance
S.C.	Solids content
SAFT	Shear Adhesion Failure Temperature
SB	Sulfobetaines
SDS	Sodium dodecyl sulfate
SEC	Size exclusion chromatography
SEM	Scanning electron microscope
SFEP	Surfactant-free emulsion polymerization
S.G	Specific gravity
St	Styrene
T_{room}	Room temperature
TBHP	Tert-butyl hydroperoxide
TEM	Transmission electron microscopy
TFMA	2,2,2-trifluoroethyl methacrylate
Tg	Glass transition temperature

THF	Tetrahydrofuran
UCST	Upper critical solution temperature
VOC	Volatile organic compounds
WSO	Water-soluble oligomer fraction
W_{adh}	Work of adhesion
wbm	Weight based on main monomers
wt	Total weight
WVTR	Water vapour transmission rate
Xi	Instantenous monomer conversion
X_t	Total monomer conversion
ZM	Zwitterionic monomer
ZP	Zwitterionic polymer

Thesis in 2 minutes

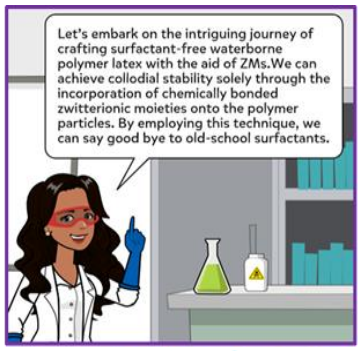

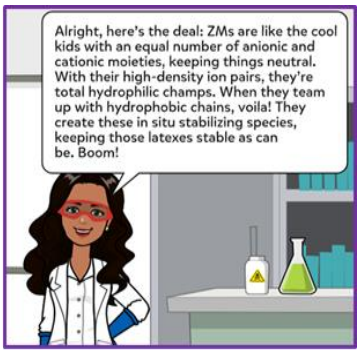

BEFORE

AFTER